INFORMATION TO USERS

This manuscript has been reproduced from the microfilm master. UMI films the text directly from the original or copy submitted. Thus, some thesis and dissertation copies are in typewriter face, while others may be from any type of computer printer.

The quality of this reproduction is dependent upon the quality of the copy submitted. Broken or indistinct print, colored or poor quality illustrations and photographs, print bleedthrough, substandard margins, and improper alignment can adversely affect reproduction.

In the unlikely event that the author did not send UMI a complete manuscript and there are missing pages, these will be noted. Also, if unauthorized copyright material had to be removed, a note will indicate the deletion.

Oversize materials (e.g., maps, drawings, charts) are reproduced by sectioning the original, beginning at the upper left-hand corner and continuing from left to right in equal sections with small overlaps.

Photographs included in the original manuscript have been reproduced xerographically in this copy. Higher quality 6" x 9" black and white photographic prints are available for any photographs or illustrations appearing in this copy for an additional charge. Contact UMI directly to order.

Bell & Howell Information and Learning
300 North Zeeb Road, Ann Arbor, MI 48106-1346 USA
800-521-0600

Université d'Ottawa · University of Ottawa

Effects of Rotational Elastic Edge Supports on Buckling and Free Vibration of Thin Rectangular Plates

Thesis Submitted to the School of Graduate Studies
as partial fulfilment of the requirements for the
Degree of Master of Applied Science.

© **Hari Kishan Koduru**

Ottawa-Carleton Institute for Mechanical and Aerospace Engineering
University of Ottawa
Ottawa, Ontario, Canada, K1N 5N6

May 1999

To my love ***Jaya***

ABSTRACT

Rectangular plates are found in most structures of modern industry. Their two-dimensional structural action results in lighter structures and therefore offers numerous economic advantages. Recently interest in rectangular plates increased due to rapid growth in electronic technology where electronic circuit boards in the form of thin rectangular plates are employed.

It is well known that while a clamped boundary condition along the edge of thin rectangular plates is easy to formulate mathematically, it is difficult to achieve, even under laboratory conditions. This is due in part to the fact that some rotational elasticity is likely to be found in such supports, whether it is introduced intentionally or inadvertently. In this study, the effects of such elasticity on the free vibration and buckling of plates subjected to uniform in-plane loading are examined. Loading is applied in a direction perpendicular to a pair of opposite edges where lateral displacement is forbidden and edge rotation is opposed by a moment proportional to the degree of edge rotation. The edges running parallel to the in-plane loading are free. Highly accurate solutions are obtained by the method of superposition. Two plates are analysed; one with rotational elastic support at one edge, the other edge being simply supported and, a second plate with rotational elastic support at the pair of opposite edges. Free vibration eigenvalues and buckling loads are computed for various plate geometries, dimensionless rotational stiffnesses with various in-plane loads. It is observed that in limiting cases, eigenvalues and buckling loads agree well in comparison with those of classical cases such as pinned and clamped boundary conditions. It is also found that the edges can be given any desired value of the rotational stiffness.

Acknowledgements

I would like to express my gratitude to my supervisor, Dr. D. J Gorman, for his time, ideas and guidance, which he supplied throughout the course of my thesis work. In addition, I thank him for sharing his wealth of experience with me.

I wish to express my appreciation to the academic members and staff of the department of mechanical engineering, especially Solange Lamontagne, Marie Rainville, and Lise Ouellet for their help.

I would also like to thank my friends and colleagues for their suggestions and encouragement.

Finally, I would like to thank my parents for their sound advice, and continual support and encouragement.

Table of Contents

Page No.

List of Tables

List of Figures

Nomenclature

a	Plate dimension along x - direction
b	Plate dimension along y - direction, in-plane loaded edge
D	$= E h^3 / \{12(1- \nu^2)\}$, Plate flexural rigidity
E	Young's modulus of elasticity of plate material
h	Plate thickness
ν	Poisson's ratio of plate material
K	Basic rotational elastic stiffness
K_{2R}	Dimensionless rotational elastic stiffness along edge $\xi = 1$
K_{4R}	Dimensionless rotational elastic stiffness along edge $\xi = 0$
k	Number of Fourier terms in a series solution
M	Bending moment

M^*	Dimensionless bending moment
M^*_1	Dimensionless bending moment along edge $\xi = 1$
M^*_2	Dimensionless bending moment along edge $\xi = 0$
S_ξ	Slope along edges parallel to ξ - axis
S_η	Slope along edges parallel to η - axis
V_ξ	Shear force along edges parallel to ξ - axis
V_η	Shear force along edges parallel to η - axis
P/b	Plate edge loading per unit length
N_x	$= P_x / b$, distributed In-plane load
P_x	Total in-plane load
P_ξ	$= - P_x \ b / D$
w	Plate lateral displacement
W	Plate lateral displacement divided by "a"
x, y	Plate spatial co-ordinates
ξ, η	Spatial co-ordinates divided by a, and b, respectively

ϕ	Plate aspect ratio, b / a
λ^2	$= \omega a^2 \sqrt{(\rho / D)}$
ω	Circular frequency of vibration
ρ	Mass of plate per unit area

Chapter 1

Introduction

1.1 Problem Definition

Rectangular plates are one of the most commonly used structures in the industrial world. They are used to carry lateral loads, in-plane loads, and sometimes both.

In recent years, for example, an interest has arisen in the dynamic behaviour of thin rectangular plates used as electronic circuit boards. Typically these plates support attached electronic components and may rest on point supports. Since these electronic circuit boards are often installed in moving vehicles, such as aircraft, it is essential to obtain a foreknowledge of their natural frequencies so that conditions of resonance can be avoided during their service life.

The dynamic behaviour of thin rectangular plates depends on plate geometry, plate material, and edge support conditions. It is known that plate natural frequencies are dependent on plate stiffness. The apparent plate stiffness, and hence its free vibration frequencies can be altered by the presence of static in-plane loads.

Compressive in-plane loads cause a reduction in natural frequencies while tensile loads have the opposite effect, i.e., they lead to an increase in these frequencies. Vibration analysis of plates with in-plane loading did not get much attention until the late 1960's.

The present thesis is mainly an extension of the work conducted by Michelussi[4]. He concentrated mainly on plates with in-plane loads and with classical, simply supported, clamped, or free edge conditions.

It is known that in the real world a true condition of clamping is almost never achieved. This is true, even though such edge conditions are easy to formulate mathematically. In fact, there will always be some rotational elasticity along a nominally clamped edge.

In this thesis the effects of edge rotational elasticity on the free vibration and buckling of

rectangular plates subjected to in-plane loading are investigated analytically. The loading runs in a direction perpendicular to a pair of opposite edges where lateral displacement is forbidden and edge rotation is opposed by a moment proportional to the degree of edge rotation. Edges running parallel to the in-plane loading are free.

Free vibration eigenvalues and buckling loads are computed for various plate geometries, with various levels of in-plane loading and various dimensionless edge stiffnesses.

1.2 Literature Review

Plate vibration problems are solved by various methods; however these methods fall into two categories. They are,

1. Numerical Methods,
2. Analytical Methods.

Examples of numerical methods are the finite element method, finite difference methods, and the boundary element method.

Examples of analytical (continuum mechanics) methods are the Rayleigh-Ritz[7] method and the superposition method.

1.2.1 Rayleigh - Ritz Method

The Rayleigh-Ritz method is an energy method based on the principle of minimization of the total potential energy of the system. An inherent advantage of this energy method is that you do not need to solve the governing differential equation. A disadvantage, when compared with the superposition method, lies in the fact that suitable series of functions must be chosen in advance to represent displacement of the structure of interest. No such functions need to be selected when utilizing the superposition method.

A basic requirement of the functions utilised in the Rayleigh-Ritz method is that each function must satisfy exactly the prescribed geometric boundary conditions of the problem. "Forced" or

"natural" boundary conditions may be ignored. It is characteristic of the Rayleigh-Ritz method that computed eigenvalues obtained for structures undergoing free vibration will always be greater than the actual eigenvalues, though, in most problems this deviation from actual eigenvalues can be made arbitrarily small by taking sufficient terms in the series. In fact, the eigenvalues computed by this method are essential upper limits for the actual eigenvalues.

1.2.2 Advantages of Superposition Method over Rayleigh-Ritz Method

In employing the Rayleigh-Ritz[7] method it is customary to express plate lateral displacement as a series of functions composed of crossed beam free vibration eigenfunctions. Unfortunately, these beam functions must satisfy certain boundary conditions. In the case of the completely free plate, for example, the crossed free-free beam eigenfunctions do not fully satisfy the plate free edge boundary conditions. This is because of the existence of mixed derivatives appearing in the formulation of plate free edge conditions.

In utilisation of the superposition method no such function selection is required. Furthermore, unlike the Rayleigh-Ritz[7] method, solutions obtained by the superposition method satisfy exactly the governing differential equation throughout the entire domain of the plate. Boundary conditions are satisfied to any desired degree by utilising more terms in the solution.

1.3 Method of Solution

In the present work solutions for buckling loads and free vibration eigenvalues have been obtained by the superposition method. A through description of the method and its utilisation for solving plate vibration problems has been provided by Gorman[2].

This thesis studies the effect of rotational elastic edge support on the buckling and free vibration eigenvalues of rectangular isotropic plates with one-directional in-plane loading. The analysis is based on classical thin plate theory or Kickoff plate theory. A value of 0.333 is used throughout for the Poisson ratio.

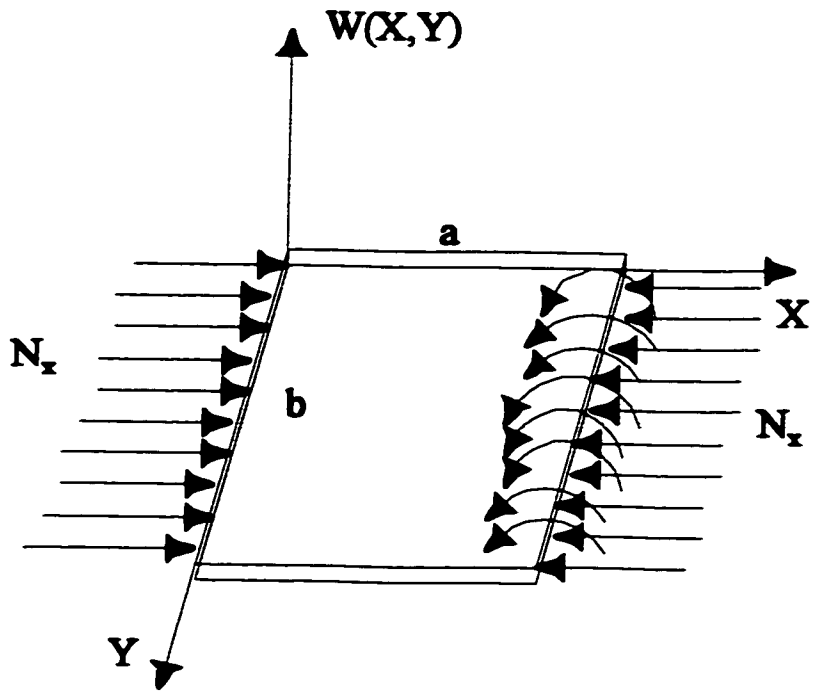

Figure 1.1 A thin rectangular plate with torsional edge subjected to uniform in-plane loads.

A thin rectangular plate with torsional edge support along one boundary is shown in Figure 1.1. Uniform in-plane force N_x is applied in 'x' direction as indicated in the figure.

Chapter 2.

The Underlying Theory and Analysis

It is necessary to conduct an accurate free vibration analysis of rectangular plates, if the designer is concerned with possible resonance between the plate and support system. In vibration problems considered here, we do not allow for energy dissipation; in other words, we make no allowance for the existence of damping forces. Small damping forces have very little effect on the natural frequencies of the system.

2.1 Governing Differential Equation

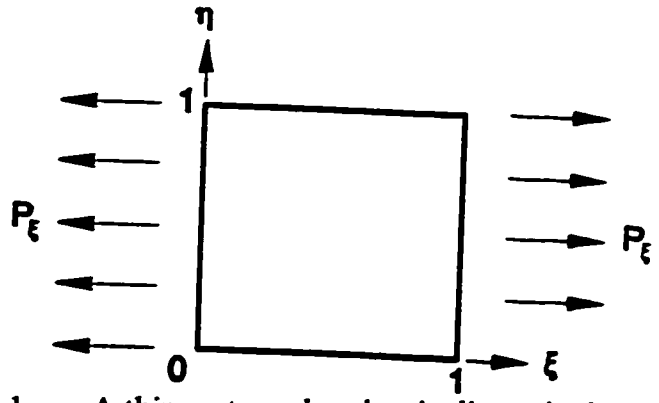

Figure 2.1 A thin rectangular plate in dimensionless coordinates.

The following assumptions are made regarding the plate of interest, in keeping with Kirkhoff plate theory.

1. The plate thickness is small in comparison to its lateral dimensions and the distance between nodal lines. (Lines along which, no vibratory displacement occurs).
2. The maximum lateral displacement of the plate is small in comparison to its thickness.
3. The effects of transverse shear and rotary inertia are neglected.

These assumptions apply in many practical situations. The uniform in-plane load is constant and evenly distributed along edges $\xi = 0$ and $\xi = 1$, as shown in Figure 2.1. A dimensionless coordinate

system is utilised in the solutions. The advantage of doing this becomes evident in the generation of data, where families of plates are analysed instead of a single plate, permitting an efficient presentation of the results. The dimensionless free vibration equation[4] is

$$\frac{\partial^4 W(\xi,\eta)}{\partial \eta^4} + 2\Phi^2 \frac{\partial^4 W(\xi,\eta)}{\partial \xi^2 \partial \eta^2} + \Phi^4 \frac{\partial^4 W(\xi,\eta)}{\partial \xi^4}$$
$$+ P_\xi \Phi^2 \frac{\partial^2 W(\xi,\eta)}{\partial \xi^2} - \lambda^4 \Phi^4 W(\xi,\eta) = 0 \qquad (2.1)$$

where symbols are as defined in the nomenclature. The dimensionless in-plane load parameter P_ξ is positive in compression and negative in tension. Hence P_ξ shown in Figure 2.1 is negative. An analytical solution is desired for $W(\xi,\eta)$ which will exactly satisfy both equation(2.1) and the specified boundary conditions for each plate.

2.2 Boundary Conditions

Boundary conditions are defined by combinations of prescribed edge displacement, slope, bending moment, and shear force. Expressions for these have been derived by Timoshenko[1] and translated into dimensionless coordinates by Gorman[2], and are reviewed here for convenience. Note that all quantities are expressed in terms of the plate displacement $W(\xi,\eta)$. The mathematical formulation for the slope is

$$S_\xi = \frac{\partial W(\xi,\eta)}{\partial \xi} \qquad (2.2)$$

for lines parallel to the ξ - axis, and,

$$S_\eta = \frac{\partial W(\xi,\eta)}{\partial \eta} \tag{2.3}$$

for lines parallel to the η - axis. The distributed bending moment is

$$M_\xi = -\frac{D}{a}\left[\frac{\partial^2 W(\xi,\eta)}{\partial \xi^2} + \frac{\upsilon}{\Phi^2}\frac{\partial^2 W(\xi,\eta)}{\partial \eta^2}\right] \tag{2.4}$$

about edges perpendicular to the ξ - axis, and,

$$M_\eta = -\frac{D}{b\Phi}\left[\frac{\partial^2 W(\xi,\eta)}{\partial \eta^2} + \upsilon\Phi^2\frac{\partial^2 W(\xi,\eta)}{\partial \xi^2}\right] \tag{2.5}$$

about edges perpendicular to the η - axis. The distributed shear force is

$$V_\xi = -\frac{D}{a^2}\left[\frac{\partial^3 W(\xi,\eta)}{\partial \xi^3} + \frac{(2-\upsilon)}{\Phi^2}\frac{\partial^3 W(\xi,\eta)}{\partial \xi \partial \eta^2} + \frac{P_\xi}{\Phi^2}\frac{\partial W(\xi,\eta)}{\partial \xi}\right] \tag{2.6}$$

for edges perpendicular to the ξ - axis, and,

$$V_\eta = -\frac{D}{b^2\Phi}\left[\frac{\partial^3 W(\xi,\eta)}{\partial \eta^3} + (2-\upsilon)\phi^2\frac{\partial^3 W(\xi,\eta)}{\partial \eta \partial \xi^2}\right] \tag{2.7}$$

for edges perpendicular to the η - axis. When used, these equations are usually equated to zero, and constants outside of the large parentheses can be omitted.

2.2.1 Pinned Edge

A pin forbids displacements yet permits rotation. These characteristics indicate that a state

of zero displacement and zero bending moment must exist along a simply supported or pinned edge. Knowing this, contributions from equations (2.4) and (2.5) for bending moment may be simplified. The pinned edge is defined by

$$W(\xi,\eta) = \frac{\partial^2 W(\xi,\eta)}{\partial \xi^2} = 0 \tag{2.8}$$

for edges perpendicular to the ξ - axis, and,

$$W(\xi,\eta) = \frac{\partial^2 W(\xi,\eta)}{\partial \eta^2} = 0 \tag{2.9}$$

for edges perpendicular to the η - axis.

2.2.2 Clamped Edge

A clamp or fixed support restrains the plate from both displacing and rotating. These characteristics indicate that a state of zero displacement and zero slope must exist along the edge. Contributions for slope are given by equations (2.2) and (2.3). The clamped edge is defined by

$$W(\xi,\eta) = \frac{\partial W(\xi,\eta)}{\partial \xi} = 0 \tag{2.10}$$

for edges perpendicular to the ξ - axis, and,

$$W(\xi,\eta) = \frac{\partial W(\xi,\eta)}{\partial \eta} = 0 \tag{2.11}$$

for edges perpendicular to the η - axis.

2.2.3 Free Edge

As the name indicates, a free edge is not restrained and may both displace and rotate. These

characteristics indicate that a state of zero bending moment and zero shear force must exist along the edge. Contributions for bending moment and shear force are given by equations (2.4), (2.5), (2.6) and (2.7). The free edge is defined by

$$\frac{\partial^2 W(\xi,\eta)}{\partial \xi^2} + \frac{\upsilon}{\Phi^2}\frac{\partial^2 W(\xi,\eta)}{\partial \eta^2} = \frac{\partial^3 W(\xi,\eta)}{\partial \xi^3} + \frac{(2-\upsilon)}{\Phi^2}\frac{\partial^3 W(\xi,\eta)}{\partial \xi \partial \eta^2} + \frac{P_\xi}{\Phi^2}\frac{\partial W(\xi,\eta)}{\partial \xi} = 0 \quad (2.12)$$

for edges perpendicular to the ξ - axis, and,

$$\frac{\partial^2 W(\xi,\eta)}{\partial \eta^2} + \upsilon\Phi^2\frac{\partial^2 W(\xi,\eta)}{\partial \xi^2} = \frac{\partial^3 W(\xi,\eta)}{\partial \eta^3} + (2-\upsilon)\Phi^2\frac{\partial^3 W(\xi,\eta)}{\partial \eta \partial \xi^2} = 0 \quad (2.13)$$

for edges perpendicular to the η - axis.

2.2.4 Slip Shear Edge

A fourth condition of interest, slip shear, though rarely encountered along actual plate edges, provides a useful mathematical entity. Slip shear is identified by zero slope and zero shear force. Contributions for slope and shear force are given by equations (2.2) and (2.7) respectively. Slip shear edge conditions become,

$$\frac{\partial W(\xi,\eta)}{\partial \xi} = \frac{\partial^3 W(\xi,\eta)}{\partial \xi^3} = 0 \quad (2.14)$$

for edges perpendicular to the ξ - axis, and,

$$\frac{\partial W(\xi,\eta)}{\partial \eta} = \frac{\partial^3 W(\xi,\eta)}{\partial \eta^3} = 0 \quad (2.15)$$

for edges perpendicular to the η - axis.

2.3 Levy-Type Solution

Of the four classical boundary conditions described above, only the pinned and slip shear edges properly accommodate the trigonometric functions in a Levy-type solution. The Levy-type solution is a series solution involving Fourier sine or cosine series running in one coordinate direction, where the associated coefficients are functions of the other coordinate. The trigonometric series is appropriately chosen so that the prescribed boundary conditions at two opposing extremities of the plate are automatically satisfied. It is very important that, upon substitution into the governing equation, derivatives of the trigonometric terms form linear multiples of themselves, permitting the separation of variables to occur. A plate will be given a specific form of solution based upon the type of edge conditions present;

$$W(\xi,\eta) = \sum_{m=1,2,3}^{\infty} Y_m(\eta)\sin(m\pi\xi) \tag{2.16}$$

for simply supported condition along both $\xi = 0$ and $\xi = 1$ edges,

$$W(\xi,\eta) = \sum_{m=0,1,2}^{\infty} Y_m(\eta)\cos(m\pi\xi) \tag{2.17}$$

for slip shear conditions along both $\xi = 0$ and $\xi = 1$edges,

$$W(\xi,\eta) = \sum_{m=1,3,5}^{\infty} Y_m(\eta)\sin(m\pi\xi/2) \tag{2.18}$$

for simply supported conditions along $\xi = 0$ and slip shear condition along $\xi = 1$ edges,

$$W(\xi,\eta) = \sum_{m=1,3,5}^{\infty} Y_m(\eta)\cos(m\pi\xi/2) \tag{2.19}$$

for slip shear conditions along $\xi = 0$ and simply supported conditions along $\xi = 1$ edges,

$$W(\xi,\eta) = \sum_{n=1,2,3}^{\infty} Y_n(\xi)\sin(n\pi\eta) \tag{2.20}$$

for simply supported conditions along both $\eta = 0$ and $\eta = 1$ edges,

$$W(\xi,\eta) = \sum_{n=0,1,2}^{\infty} Y_n(\xi)\cos(n\pi\eta) \tag{2.21}$$

for slip shear conditions along both $\eta = 0$ and $\eta = 1$ edges,

$$W(\xi,\eta) = \sum_{n=1,3,5}^{\infty} Y_n(\xi)\sin(n\pi\eta/2) \tag{2.22}$$

for simply supported conditions along $\eta = 0$ and slip shear conditions along $\eta = 1$ edges, and

$$W(\xi,\eta) = \sum_{n=1,3,5}^{\infty} Y_n(\xi)\cos(n\pi\eta/2) \tag{2.23}$$

for slip shear conditions along $\eta = 0$ and simply supported conditions along $\eta = 1$ edges.

2.4 Method of Superposition

It is over two decades since Gorman[2] began a fairly systematic exploitation of the superposition method for obtaining of solutions to rectangular plate free vibration problems.

This method was subsequently successfully applied to thick Mindlin plates, laminated rectangular plates, plates with point supports and with local attached masses. In the present thesis this method is successfully utilised for plates with elastic edge supports and uniform in-plane loading.

2.4.1 Details of the Method

A simple Levy-type solution cannot be derived for plates not meeting the minimum requirement of two opposite edges having pinned or slip shear conditions. Instead, two or more appropriate plate problems (or building blocks), whose Levy-type solutions can be obtained, are superimposed. Each building block possesses a harmonically varying boundary condition, either slope or bending moment. By properly adjusting these in the superimposed solution, the prescribed boundary conditions of the original plate are satisfied to any desired degree of accuracy.

The terminology used to describe the boundary conditions of the plates considered in this thesis is now introduced. It follows a system adopted by Leissa[3] where the boundary conditions of

each side are listed in a standard order, namely $\xi = 0$, $\eta = 0$, $\xi = 1$ and $\eta = 1$. This is equivalent to labelling the left side of the plate first and proceeding in a counter-clockwise manner conforming to the axis orientation used in this paper. Each side is assigned a single letter which, according to Table 2.1, identifies the type of edge present.

Label	Edge Type	Boundary Conditions
C	Clamped	Displacement (W) = 0 and Slope (S) = 0
F	Free	Moment (M) = 0 and Shearing Force (V) = 0
R	Slip Shear	Slope (S) = 0 and Shearing Force (V)= 0
S	Simply Supported	Displacement (W) = 0 and Moment (M) = 0
V	Zero shear force	V = 0, and slope expressed in Fourier series
W	Zero displacement	W = 0, and Moment expressed Fourier series

Table 2.1 Boundary Conditions and Symbols Summary.

Pinned and slip shear edge conditions permit an immediate Levy-type solution, as explained in section 2.3. Hence, the method of superposition is usually employed in the presence of either a clamped or free edge.

Chapter 3

Derived Analytical Solutions

Chapter 2 discussed fundamental equations and theory used in the analysis of plate vibration. The concepts developed are exploited in this chapter to derive analytic solutions using the superposition method. Mainly, two plates are analysed, SFTF and TFTF. As mentioned earlier, boundary conditions are written in standard order, namely $\xi = 0$, $\eta = 0$, $\xi = 1$ and $\eta = 1$. Here boundary condition 'T' represents elastic rotational edge support.

Analytical solutions for SFTF and TFTF plates are obtained by modifying coefficient matrices of SFCF and CFCF plates respectively. The building blocks used for analysing the SFCF(in fact SFTF) plates are SRSV, SVSR and SRWR, while the WRSR building block is added to the above building blocks for the analysis of CFCF (in fact TFTF) plates.

First of all, analytical solutions for SRSV, SVSR SRWR and WRSR building blocks are derived. These building blocks are then exploited in getting solutions for SFCF and CFCF plates. The derivations of all the building blocks and their utilisation in obtaining the total solution of SFCF and CFCF plates, which are taken from work of D. J. Michelussi[4], are presented here for completeness and convenience. Once coefficient matrices are obtained for SFCF and CFCF plates, they can be modified to incorporate rotational stiffness along edges $\xi = 0$, $\xi = 1$, wherever applicable, to get analytical solutions for SFTF and TFTF plates.

Clamped edges are modelled by first enforcing zero vertical edge displacement in all building blocks and then adjusting a harmonic bending moment about that edge to properly achieve the zero slope condition. This is accomplished by superimposing a zero displacement edge(W) on a number of pinned edges(S).

Similarly, a free edge is modelled by first enforcing zero vertical edge reaction in all building blocks and then adjusting a harmonic slope about the edge to properly achieve the zero bending moment condition. This is accomplished by superimposing a zero shear force edge (V) on one of slip

shear (R).

The building blocks superimposed for solutions are depicted in Figure 3.1

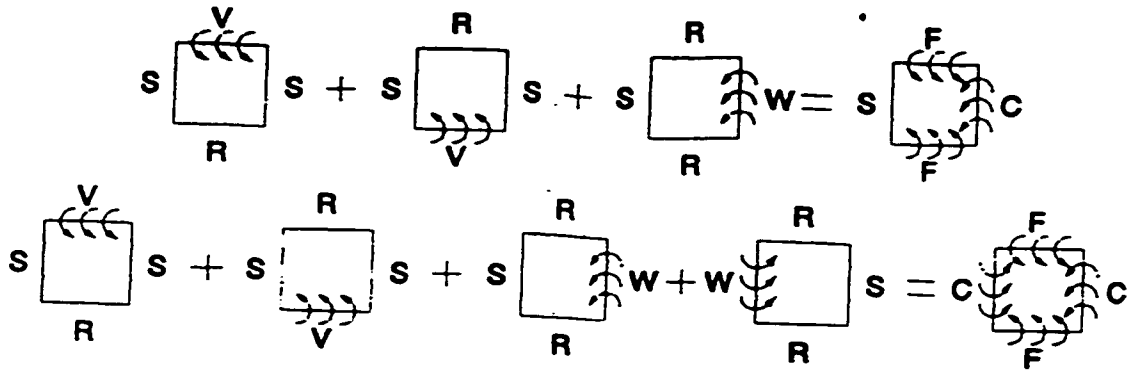

Figure 3.1 Building blocks for SFCF and CFCF plates[4].

3.1 The SRSV Building Block

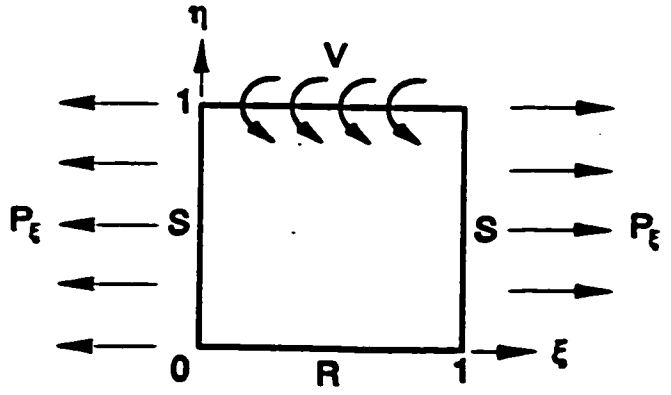

Figure 3.2 SRSV building block under unilateral in-plane load.

Levy-type solution (2.16) automatically satisfies the pinned edge boundary conditions at ξ=0 and ξ = 1 of the SRSV building block shown in Figure 3.2. The explicit solution is derived by substituting the Levy-type solution, equation (2.16), into the governing equation of motion (2.1), giving,

$$\sum_{m=1,2,3}^{\infty}\left[Y_m''''(\eta)-2(\phi m\pi)^2 Y_m''(\eta)+\left((\phi m\pi)^4-(\phi\lambda)^4-P_c(\phi m\pi)^2\right)Y_m(\eta)\right]\sin(m\pi\xi)=0 \quad (3.1)$$

Equation (3.1) is a product of two independent functions which equals zero. Since $\sin(m\pi\xi)$ cannot equal zero for all values of ξ, the function of η within the square brackets must equal zero for any value of m. The ξ and η variables in equation (2.1) are separated to produce the following equation, a fourth order ordinary homogeneous differential equation in η.

$$Y_m''''(\eta)-2\phi^2\delta_m Y_m''(\eta)+\phi^4\Delta_m Y_m(\eta)=0 \quad (3.2)$$

Where

$$\delta_m=m\pi^2$$

and

$$\Delta_m=m\pi^4-\lambda^4-P_c(m\pi/\phi)^2.$$

The four characteristic roots of equation (3.2) are defined as,

$$r=\pm\phi\sqrt{\delta_m\pm\sqrt{\delta_m^2-\Delta_m}} \quad (3.3)$$

Real, imaginary and complex roots can be obtained from equation (3.3) depending upon the values of δ_m and Δ_m parameters. Consequently, three different harmonic general solutions exist for $Y_m(\eta)$ which satisfy the governing equation of motion.

The four arbitrary constants within a general solution for $Y_m(\eta)$ are determined by enforcing four boundary conditions. The slip shear condition at $\eta = 0$ and the zero shear force boundary condition at edge $\eta = 1$ provide the expressions needed for determining the four arbitrary constants. Since there are three general solutions to be examined, expressing the boundary relations in terms of $Y_m(\eta)$ would be convenient. This is accomplished by separating the variables in the boundary condition equations. The Levy-type solution, equation(2.16), is first substituted into equations (2.15) and evaluated at $\eta = 0$, giving,

$$\sum_{m=1,2,3}^{\infty} Y_m'(0)\sin(m\pi\xi)=0$$

and

$$\sum_{m=1,2,3}^{\infty} Y_m^{'''}(0)\sin(m\pi\xi) = 0$$

Since $\sin(m\pi\xi)$ cannot be equal to zero for all values of ξ in the above equations, the evaluated functions of $Y_m(\eta)$ must equal zero for any value of m. The above equations become,

$$Y_m' = 0 \tag{3.4}$$

and

$$Y_m''' = 0 \tag{3.5}$$

which are used to enforce the slip shear edge condition at $\eta = 0$. The zero shear force edge at $\eta = 1$ is examined next. Levy-type solution (2.16) is substituted into the zero shear force equation

$$\frac{\partial^3 W(\xi,\eta)}{\partial\eta^3} + (2-\upsilon)\phi^2\frac{\partial^3 W(\xi,\eta)}{\partial\eta\partial\xi^3} = 0$$

and is substituted into harmonic slope function,

$$\frac{\partial W(\xi,\eta)}{\partial\eta} = \sum_{m=1,2,3}^{\infty} E_m\sin(m\pi\xi).$$

Note that the harmonic slope function is a Fourier sine series; same type of series as the Levy-type solution. The resulting equations evaluated at $\eta = 1$ and rearranged giving,

$$\sum_{m=1,2,3}^{\infty} Y_m'''(1)\sin(m\pi\xi) - \sum_{m=1,2,3}^{\infty} Y_m'(1)(2-\upsilon)(m\pi\phi)^2\sin(m\pi\xi) = 0,$$

and

$$\sum_{m=1,2,3}^{\infty} Y_m'(1)\sin(m\pi\xi) = \sum_{m=1,2,3}^{\infty} E_m\sin(m\pi\xi).$$

The preceding two equations are true if and if only if the coefficients in the Fourier sine series are equivalent. This allows us to simplify the equations to

$$Y_m(1) = E_m \tag{3.6}$$

and

$$\bar{Y}_m(1) = E_m(2-\upsilon)(m\pi\phi)^2 \tag{3.7}$$

Equations (3.2) to (3.7) are exploited in the following sections to specifically obtain solutions for $Y_m(\eta)$ of SRSV building block. The reader should take note that the original partial differential equation problem has been significantly reduced to an ordinary differential equation problem.

3.1.1 Case 1 Solution

Four distinct complex roots result when $\delta_m^2 < \Delta_m$ in equation (3.3). The roots are defined by, $\pm\beta_m \pm\gamma_m i$, giving general solution of the form

$$\begin{aligned} Y_m(\eta) = {} & A_m \sinh(\beta_m\eta)\sin(\gamma_m\eta) + B_m \sinh(\beta_m\eta)\cos(\gamma_m\eta) \\ & + C_m \cosh(\beta_m\eta)\sin(\gamma_m\eta) + D_m \cosh(\beta_m\eta)\cos(\gamma_m\eta) \end{aligned} \tag{3.8}$$

where,

$$\beta_m = \phi\sqrt{\frac{\sqrt{\Delta_m} + \delta_m}{2}}$$

and

$$\gamma_m = \phi\sqrt{\frac{\sqrt{\Delta_m} - \delta_m}{2}}$$

The first and last terms are even, while the two middle terms are odd.

Constants A_m, B_m, C_m and D_m are determined by enforcing equations (3.4) to (3.7). Substituting solution (3.8) into equations (3.4) and (3.5) yields

$$B_m\beta_m + C_m\gamma_m = 0$$

and

$$B_m\beta_m(\beta_m^2 - 3\gamma_m^2) + C_m\gamma_m(\gamma_m^2 - 3\beta_m^2) = 0$$

Thus, constants B_m and C_m, which are associated with the odd terms in equation (3.8), are zero. One may intuitively conclude that only even terms will satisfy the constraints set by equations (3.4) and (3.5). In the remaining case solutions, the odd terms will simply be removed to enforce the slip shear edge at $\eta = 0$. Next, the simplified solution is substituted into equations (3.6) and (3.7). The resulting algebraic equations evaluated at $\eta = 1$ are,

$$A_m(\beta_m\cosh(\beta_m)\sin(\gamma_m) + \gamma_m\sinh(\beta_m)\cos(\gamma_m))$$
$$+D_m(\beta_m\sinh(\beta_m)\cos(\gamma_m) - \gamma_m\cosh(\beta_m)\sin(\gamma_m)) = E_m$$

and

$$A_m(\beta_m(\beta_m^2 - 3\gamma_m^2)\cosh(\beta_m)\sin(\gamma_m) + \gamma_m(3\beta_m^2 - \gamma_m^2)\sinh(\beta_m)\cos(\gamma_m))$$
$$+D_m(\beta_m(\beta_m^2 - 3\gamma_m^2)\sinh(\beta_m)\cos(\gamma_m) - \gamma_m(3\beta_m^2 - \gamma_m^2)\cosh(\beta_m)\sin(\gamma_m)) = (2-\upsilon)(m\pi\phi)^2 E_m.$$

Expressed in matrix form, and solved for A_m and D_m in terms of E_m, the above equations lead to;

$$A_m = E_m\left[\frac{\beta_m(\beta_m^2 - 3\gamma_m^2)\sinh(\beta_m)\cos(\gamma_m) - \gamma_m(3\beta_m^2 - \gamma_m^2)\cosh(\beta_m)\sin(\gamma_m)}{-2\beta_m\gamma_m(\beta_m^2 + \gamma_m^2)(\sinh^2(\beta_m) + \sin^2(\gamma_m))}\right]$$
$$- E_m\left[\frac{(2-\upsilon)(m\pi\phi)^2(\beta_m\sinh(\beta_m)\cos(\gamma_m) - \gamma_m\cosh(\beta_m)\sin(\gamma_m))}{-2\beta_m\gamma_m(\beta_m^2 + \gamma_m^2)(\sinh^2(\beta_m) + \sin^2(\gamma_m))}\right] \qquad (3.9)$$

and

$$D_m = E_m\left[\frac{(2-\upsilon)(m\pi\phi)^2(\beta_m\cosh(\beta_m)\sin(\gamma_m)+\gamma_m\sinh(\beta_m)\cos(\gamma_m))}{-2\beta_m\gamma_m(\beta_m^2+\gamma_m^2)(\sinh^2(\beta_m)+\sin^2(\gamma_m))}\right]$$
$$-E_m\left[\frac{\beta_m(\beta_m^2-3\gamma_m^2)\cosh(\beta_m)\sin(\gamma_m)+\gamma_m(3\beta_m^2-\gamma_m^2)\sinh(\beta_m)\cos(\gamma_m)}{-2\beta_m\gamma_m(\beta_m^2+\gamma_m^2)(\sinh^2(\beta_m)+\sin^2(\gamma_m))}\right] \quad (3.10)$$

slope parameter E_m controls the building block's amplitude.

3.1.2 Case 2 Solution

Two imaginary and two real roots result when $\delta_m^2 > \Delta_m$ and $\Delta_m < 0$ in equation (3.3), The roots are defined by, $\pm\beta_m$ and $\pm\gamma_m i$, giving general solution of the form

$$Y_m(\eta) = A_m\sinh(\beta_m\eta) + B_m\cosh(\beta_m\eta) + C_m\sin(\gamma_m\eta) + D_m\cos(\gamma_m\eta) \quad (3.11)$$

where

$$\beta_m = \phi\sqrt{\sqrt{\delta_m^2 - \Delta_m} + \delta_m}$$

and

$$\gamma_m = \phi\sqrt{\sqrt{\delta_m^2 - \Delta_m} - \delta_m}$$

The first and third terms of the solution are odd, while the second and fourth terms are even.

The procedure used to determine the constants A_m, B_m, C_m and D_m in section 3.1.1 is repeated here. As we already discussed in the previous section, to satisfy the slip shear boundary condition, the odd terms A_m and C_m are set to zero. The remaining even terms are substituted into equations (3.6) and (3.7) resulting two algebraic equations, which are evaluated at $\eta = 1$ are,

$$B_m\beta_m\sinh(\beta_m) - D_m\gamma_m\sin(\gamma_m) = E_m$$

and

$$B_m \beta_m^3 \sinh(\beta_m) + D_m \gamma_m^3 \sin(\gamma_m) = (2-\upsilon)(m\pi\phi)^2 E_m.$$

Solving for B_m and D_m gives,

$$B_m = E_m \left[\frac{\gamma_m^2 + (2-\upsilon)(m\pi\phi)^2}{\beta_m (\beta_m^2 + \gamma_m^2) \sinh(\beta_m)} \right] \tag{3.12}$$

and

$$D_m = -E_m \left[\frac{\beta_m^2 - (2-\upsilon)(m\pi\phi)^2}{\gamma_m (\beta_m^2 + \gamma_m^2) \sinh(\gamma_m)} \right] \tag{3.13}$$

3.1.3 Case 3 Solution

Four distinct real roots result when $\delta_m^2 > \Delta_m$ and $\Delta_m > 0$ in equation(3.3). The roots are defined by, $\pm\beta_m$ and $\pm\gamma_m$, giving solution of the form

$$\begin{aligned} Y_m(\eta) = {} & A_m \sinh(\beta_m \eta) + B_m \cosh(\beta_m \eta) \\ & + C_m \sinh(\gamma_m \eta) + D_m \cos(\gamma_m \eta) \end{aligned} \tag{3.14}$$

where

$$\beta_m = \phi \sqrt{\delta_m + \sqrt{\delta_m^2 - \Delta_m}}$$

and

$$\gamma_m = \phi \sqrt{\delta_m - \sqrt{\delta_m^2 - \Delta_m}}$$

The first and third terms of the solution are odd, while the second and fourth terms are even.

Constants A_m and C_m must equal zero in order to satisfy the slip shear boundary conditions at $\eta = 0$. The even terms in equation (3.14) are then substituted into equations (3.6) and (3.7) to enforce the zero shear force edge condition. The resulting equations, evaluated at $\eta = 1$, are

$$B_m \beta_m \sinh(\beta_m) + D_m \gamma_m \sin(\gamma_m) = E_m$$

and

$$B_m \beta_m^3 \sinh(\beta_m) + D_m \gamma_m^3 \sin(\gamma_m) = (2-\upsilon)(m\pi\phi)^2 E_m$$

Solving for constants B_m and D_m gives

$$B_m = E_m \left[\frac{(2-\upsilon)(m\pi\phi)^2 - \gamma_m^2}{\beta_m (\beta_m^2 - \gamma_m^2) \sinh(\beta_m)} \right] \tag{3.15}$$

and

$$D_m = -E_m \left[\frac{\beta_m^2 - (2-\upsilon)(m\pi\phi)^2}{\gamma_m (\beta_m^2 - \gamma_m^2) \sinh(\gamma_m)} \right] \tag{3.16}$$

3.2 SVSR Building Block

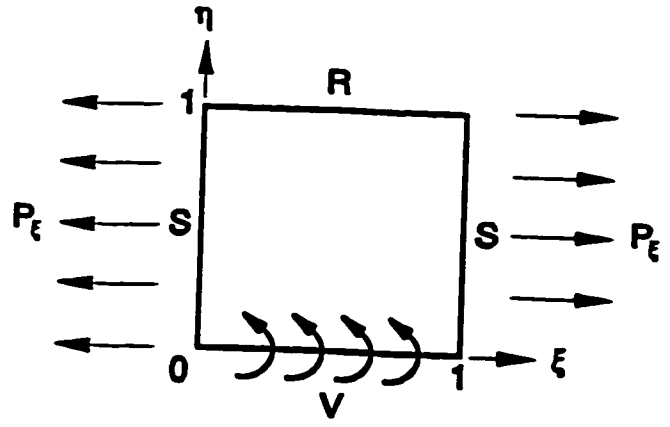

Figure 3.3 SVSR building block under uniform in-plane load

Consider the SVSR building block shown in Figure 3.3. A quick inspection of the SRSV plate

of Figure 3.2 reveals that solution for the SVSR plate is similar, except for the boundary conditions along the edges $\eta = 0$ and $\eta = 1$, which are reversed. Solutions for this plate can be derived from those presented in section 3.1 by simply replacing coordinate η by $1 - \eta$. The Levy-type solution in this situation becomes,

$$W(\xi,\eta) = \sum_{p=1,2,3}^{\infty} Y_p(1-\eta)\sin(p\pi\xi).$$

This is equation (2.16) with the η coordinate replaced by $1-\eta$. I will present here a brief summary of the individual case solutions for SVSR building block.

3.2.1 Case 1 Solution

The first case solution of the SVSR occurs when $\delta_p^2 < \Delta_p$. It is defined by equation (3.8) of section 3.1.1 where coordinate η replaced by $1 - \eta$. Constants B_p and C_p are zero, while A_p and D_p are defined by equations (3.9) and (3.10) respectively, as shown in 3.1.1, where index m is replaced by p.

3.2.2 Case 2 Solution

The second case solution is considered when $\delta_p^2 > \Delta_p$ and $\Delta_p < 0$. It is defined by equation (3.11) of section 3.1.2, where coordinate η replaced by $1 - \eta$. Constants A_p and C_p are zero, while B_p and D_p are defined by equations (3.12) and (3.13) respectively, as shown in section 3.1.2, where index m is replaced by p.

3.2.3 Case 3 solution

The third case solution arises when $\delta_p^2 > \Delta_p$ and $\Delta_p > 0$ and $\delta_p > 0$. It is defined by the equation (3.14), where coordinate η replaced by $1 - \eta$. Constants A_p and C_p are zero, while B_p and D_p are defined by equations (3.15) and (3.16) respectively, as shown in section 3.1.3, where index m is replaced by p.

3.3 SRWR Building Block

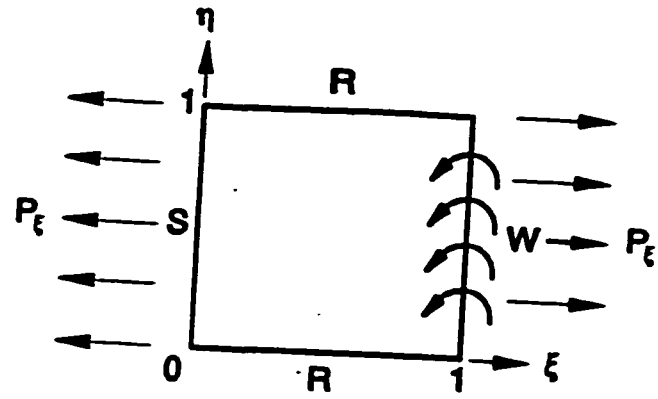

Figure 3.4 SRWR building block under uniform in-plane loading.

The SRWR building block is shown in Figure 3.4. Levy-type solution (2.21) satisfies the slip-shear boundary condition at $\eta = 0$ and $\eta = 1$. Substituting equation (2.21) into governing differential equation of motion, equation (2.1), gives,

$$\sum_{n=0,1,2}^{\infty}\left[\phi^4 Y_n''''(\xi) - 2\phi^2\left((n\pi)^4 - \frac{P_\xi}{2}\right)Y_n''(\xi) + \left((n\pi)^2 - \lambda^4\phi^4\right)Y_n(\xi)\right]\cos(n\pi\eta) = 0 \qquad (3.17)$$

It is obvious that equation (3.17) is a product of two independent functions which equal zero, and $\cos(n\pi\eta)$ cannot equal zero for all values of η. Therefore the function of ξ within the square brackets must equal zero for any value of n. Separating the variables in equation (2.1) and dividing through by Φ^4 produces,

$$Y_n''''(\xi) - \frac{2\delta_n}{\phi^2}Y_n''(\xi) + \frac{\Delta_n}{\phi^4}Y_n(\xi) = 0 \qquad (3.18)$$

where

$$\delta_n = (n\pi)^2 - \frac{P_\xi}{2}$$

and,

$$\Delta_n = (n\pi)^4 - \lambda^4\phi^4$$

Equation (3.18) is an ordinary homogeneous differential equation. General solutions for $Y_n(\xi)$ are easily obtained by the method of undetermined coefficients. Each general solution will contain four terms of the form

$$Ce^{r\xi}$$

where C is an undetermined coefficient and r is a characteristic root. The four characteristic roots are defined by

$$r = \pm\frac{1}{\phi}\sqrt{\delta_n \pm \sqrt{\delta^2 - \Delta_n}}. \tag{3.19}$$

Real, imaginary and complex roots can be obtained from equation (3.19), depending upon the values of δ_n and Δ_n. Consequently four different harmonic general solutions exist for $Y_n(\xi)$ which satisfy the governing equation of motion.

The arbitrary coefficients within a general solution for $Y_n(\xi)$ are determined by enforcing four boundary conditions at $\xi = 0$, and $\xi = 1$. The boundary conditions, initially functions of $W(\xi,\eta)$, are expressed in terms of $Y_n(\xi)$. This is accomplished by separation of variables and allows the direct application of boundary conditions to the general solutions.

The Levy-type solution, equation (2.21), is first substituted into equation (2.8) and evaluated at $\xi = 0$, giving,

$$\sum_{n=0,1,2}^{\infty} Y_n(0)\cos(n\pi\eta) = 0$$

and,

$$\sum_{n=0,1,2}^{\infty} Y_n''(0)\cos(n\pi\eta) = 0 \quad .$$

$\cos(n\pi\eta)$ cannot be zero for all values of η in the above equations. Therefore the above equations become,

$$Y_n(0) = 0 \tag{3.20}$$

and,

$$Y_n''(0) = 0 \tag{3.21}$$

And are the reduced boundary conditions of the simply supported edge at $\xi = 0$.

Next we will proceed to the boundary condition at $\xi = 1$. The zero displacement and moment driven edge conditions at $\xi = 1$ are defined by,

$$W(\xi, \eta) = 0$$

and,

$$-\frac{D}{a}\left[\frac{\partial^2 W(\xi,\eta)}{\partial \xi^2} + \frac{\upsilon}{\phi^2}\frac{\partial^2 W(\xi,\eta)}{\partial \eta^2}\right] = \sum_{n=0,1,2}^{\infty} E_n \cos(n\pi\eta)$$

The trigonometric terms used for the harmonic moment function are identical to those used in the Levy-type solution. The left hand side of the moment condition is given by equation (2.4) and is simplified in two stages. First, the constant, -D/a is absorbed into the Fourier coefficient E_n. Then, the zero displacement condition is used to eliminate the term $\partial^2 W(\xi,\eta)/\partial\eta^2$. Note that $\partial^2 W(1,\eta)/\partial\eta^2$ and $\partial W(1,\eta)/\partial\eta$ will equal zero if $W(1,\eta)$ equals zero. This is equivalent to stating that the slope and concavity of a horizontal line are zero. Separating the variables begins by substituting Levy-type solution (2.21) into the reduced equations. Evaluating the resulting equations at $\xi = 1$ and rearranging gives,

$$\sum_{n=0,1,2}^{\infty} Y_n(1)\cos(n\pi\eta) = 0$$

and,

$$\sum_{n=0,1,2}^{\infty} Y_n''(1)\cos(n\pi\eta) = \sum_{n=0,1,2}^{\infty} E_n \cos(n\pi\eta).$$

The preceding two equations are further simplified (for a particular value of n) to,

$$Y_n(1) = 0 \tag{3.22}$$

and,

$$Y_n''(1) = E_n \tag{3.23}$$

Equations (3.20) , (3.21), (3.22), and (3.23) are utilised in the following sections to specifically obtain solutions for $Y_n(\xi)$.

3.3.1 Case 1 Solution

The similarities between equations (3.19) and (3.3) indicate that the first three case solutions of the current plate will correspond to those derived in section 3.1. Four distinct complex roots are obtained when $\delta_n^2 < \Delta_n$ in equation (3.19). These roots are defined by $\pm\beta_n \pm\gamma_n i$, which give a general solution of the form,

$$\begin{aligned} Y_n(\xi) = {} & A_n\sinh(\beta_n\xi)\sin(\gamma_n\xi) + B_n\sinh(\beta_n\xi)\cos(\gamma_n\xi) \\ & + C_n\cosh(\beta_n\xi)\sin(\gamma_n\xi) + D_n\cosh(\beta_n\xi)\cos(\gamma_n\xi) \end{aligned} \tag{3.24}$$

where

$$\beta_n = \frac{1}{\phi}\sqrt{\frac{\sqrt{\Delta_n} + \delta_n}{2}}$$

and,

$$\gamma_n = \frac{1}{\phi}\sqrt{\frac{\sqrt{\Delta_n} - \delta_n}{2}}$$

The first and last terms of the solution are even, while the two middle terms are odd.

Constants A_n, B_n, C_n and D_n are determined by enforcing equations (3.20) to (3.23). Substituting solution (3.24) into conditions (3.20) and (3.21) yields,

$$D_n = 0$$

and

$$D_n\left(\beta^2 - \gamma^2\right) + 2A_n\beta_n\gamma_n = 0$$

Thus, constants A_n and D_n, which are associated with the even terms in equation (3.24), are zero. Next, the simplified solution is substituted into equation (3.22) and (3.23). The resulting

homogeneous algebraic equations are,

$$B_n\sinh(\beta_n)\cos(\gamma_n) + C_n\cosh(\beta_n)\sin(\gamma_n) = 0$$

and

$$B_n\left[\left(\beta_n^2 - \gamma_n^2\right)\sinh(\beta_n)\cos(\gamma_n) - 2\beta_n\gamma_n\cosh(\beta_n)\sin(\gamma_n)\right]$$
$$+C_n\left[\left(\beta_n^2 - \gamma_n^2\right)\cosh(\beta_n)\sin(\gamma_n) + 2\beta_n\gamma_n\sinh(\beta_n)\cos(\gamma_n)\right] = E_n$$

Solving for B_n and C_n gives,

$$B_n = E_n\left[\frac{\cosh(\beta_n)\sin(\gamma_n)}{2\beta_n\gamma_n(\cos^2(\gamma_n) - \cosh^2(\beta_n))}\right] \tag{3.25}$$

$$C_n = -E_n\left[\frac{\sinh(\beta_n)\cos(\gamma_n)}{2\beta_n\gamma_n(\cos^2(\gamma_n) - \cosh^2(\beta_n))}\right] \tag{3.26}$$

Note that bending moment parameters E_n control the building block's amplitude in all case solutions.

3.3.2 Case 2 Solution

Two imaginary and two real roots are obtained when $\delta_n^2 > \Delta_n$ and $\Delta_n < 0$ in equation (3.19). These roots are defined by $\pm\beta_n$, and $\pm\gamma_n i$, which give a general solution

$$Y_n(\xi) = A_n\sinh(\beta_n\xi) + B_n\cosh(\beta_n\xi) + C_n\sin(\gamma_n\xi) + D_n\cos(\gamma_n\xi) \tag{3.27}$$

where

$$\beta_n = \frac{1}{\phi}\sqrt{\sqrt{\delta_n^2 - \Delta_n} + \delta_n}$$

and,

$$\gamma_n = \frac{1}{\phi}\sqrt{\sqrt{\delta_n^2 - \Delta_n} - \delta_n}$$

The first and third terms of the solution are odd, while the second and fourth terms are even.

The procedure used to determine constants A_n, B_n, C_n and D_n in section 3.3.1 is repeated here. Setting B_n and D_n equal to zero eliminates the even terms and satisfies the pinned edge boundary condition at $\xi = 0$. The remaining odd terms in equation (3.27) are substituted into equations (3.22) and (3.23) to enforce zero displacement along the edge at $\xi = 1$. The resulting algebraic equations are,

$$A_n \sinh(\beta_n) + C_n \sin(\gamma_n) = 0$$

and,

$$A_n \beta_n^2 \sinh(\beta_n) - C_n \gamma_n^2 \sin(\gamma_n) = E_n$$

This leads to,

$$A_n = \frac{E_n}{(\beta_n^2 + \gamma_n^2)\sinh(\beta_n)} \tag{3.28}$$

and

$$C_n = -\frac{E_n}{(\beta_n^2 + \gamma_n^2)\sin(\gamma_n)} \tag{3.29}$$

3.3.3 Case 3 Solution

Four distinct real roots result when $\delta_n^2 > \Delta_n$ and $\Delta_n > 0$ and $\delta_n > 0$ in equation (3.19). These roots are defined by $\pm\beta_n$, and $\pm\gamma_n$, which give a general solution

$$Y_n(\xi) = A_n \sinh(\beta_n \xi) + B_n \cosh(\beta_n \xi) + C_n \sinh(\gamma_n \xi) + D_n \cosh(\gamma_n \xi) \tag{3.30}$$

where

$$\beta_n = \frac{1}{\phi}\sqrt{\delta_n + \sqrt{\delta_n^2 - \Delta_n}}$$

and

$$\gamma_n = \frac{1}{\phi}\sqrt{\delta_n - \sqrt{\delta_n^2 - \Delta_n}}$$

The first and third terms of the solution are odd while the second and fourth terms are even.

Constants B_n and D_n must equal zero in order to satisfy the pinned edge boundary conditions at $\xi = 0$. The remaining odd terms in equation (3.30) are substituted into equations (3.22) and (3.23) to enforce the zero displacement edge condition at $\xi = 1$. The resulting algebraic equations are,

$$A_n \sinh(\beta_n) + C_n \sinh(\gamma_n) = 0$$

and

$$A_n \beta_n^2 \sinh(\beta_n) + C_n \gamma_n^2 \sinh(\gamma_n) = E_n$$

Solving these equations for A_n and C_n leads to,

$$A_n = \frac{E_n}{\left(\beta_n^2 - \gamma_n^2\right)\sinh(\beta_n)} \tag{3.31}$$

and

$$C_n = -\frac{E_n}{\left(\beta_n^2 - \gamma_n^2\right)\sinh(\gamma_n)} \tag{3.32}$$

3.3.4 Case 4 Solution

As expected, the first three general solutions of this plate are comparable to those SRSV plate (equations (3.8), (3.11), (3.14)). The following differences exist between the two sets of general solutions. Coordinate η is replaced by ξ, index m is replaced by n, and plate aspect ratio ϕ is replaced by $1/\phi$. In the new fourth case, four distinct imaginary roots are obtained when $\delta_n^2 > \Delta_n$ and $\Delta_n > 0$

and $\delta_n < 0$ in equation (3.19). These roots are defined by $\pm\beta_n i$, and $\pm\gamma_n i$, giving a general solution of the form

$$Y_n(\xi) = A_n\sin(\beta_n\xi) + B_n\cos(\beta_n\xi) + C_n\sin(\gamma_n\xi) + D_n\cos(\gamma_n\xi) \tag{3.33}$$

where

$$\beta_n = \frac{1}{\phi}\sqrt{-\delta_n - \sqrt{\delta_n^2 - \Delta_n}}$$

and

$$\gamma_n = \frac{1}{\phi}\sqrt{-\delta_n + \sqrt{\delta_n^2 - \Delta_n}}$$

The first and third terms of the solution are odd while the second and fourth terms are even.

Constants B_n and D_n must equal zero in order to satisfy the pinned edge boundary conditions at $\xi = 0$. The remaining odd terms in equation (3.33) are substituted into equations (3.22) and (3.23) to enforce the zero displacement edge condition at $\xi = 1$. The resulting algebraic equations are,

$$A_n\sin(\beta_n) + C_n\sin(\gamma_n) = 0$$

and

$$-A_n\beta_n^2\sin(\beta_n) - C_n\gamma_n^2\sin(\gamma_n) = E_n$$

Expressing this system of equations in matrix form and using Cramer's rule to solve for constants A_n and C_n gives,

$$A_n = \frac{E_n}{\left(\gamma_n^2 - \beta_n^2\right)\sin(\beta_n)} \tag{3.34}$$

and

$$C_n = -\frac{E_n}{\left(\gamma_n^2 - \beta_n^2\right)\sin(\gamma_n)} \tag{3.35}$$

3.4 WRSR Building Block

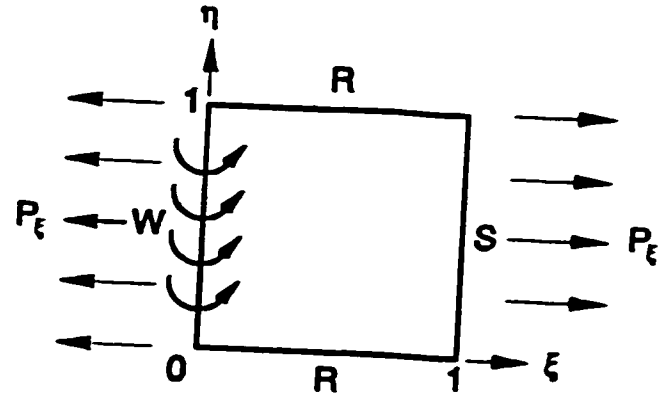

Figure 3.5 WRSR building block under uniform in-plane load.

The WRSR building block is shown in Figure 3.5. A close look at the SRWR plate, shown in Figure 3.4, reveals that solutions for WRSR plate can be derived from those presented in section 3.3 simply by replacing coordinate ξ by 1 - ξ. The Levy-type solution would be

$$W(\xi,\eta) = \sum_{q=0,1,2}^{\infty} Y_q(1-\xi)\cos(q\pi m).$$

This is equivalent to equation (2.21) with the coordinate ξ replaced with 1- ξ. The individual case solutions are as follows with constants δ_q and Δ_q as defined in section 3.3.

3.4.1 Case 1 Solution

When $\delta_q^2 < \Delta_q$, the solution is given by equation (3.24) of section 3.3.1, with coordinate ξ replaced by 1- ξ. Constants A_q and D_q are zero, while B_q and C_q are defined by equations (3.25) and (3.26), respectively.

3.4.2 Case 2 Solution

The second case solution is considered when $\delta_q^2 > \Delta_q$ and $\Delta_q < 0$. It is given by equation (3.27) of section 3.3.2, with coordinate ξ replaced by 1- ξ. Constants B_q and D_q are zero, while A_q and C_q are defined by equations (3.28) and (3.29), respectively.

3.4.3 Case 3 Solution

The third case solution arises when $\delta_q^2 > \Delta_q$ and $\Delta_q > 0$ and $\delta_q > 0$. It is expressed by equation (3.30) of section 3.3.3, with coordinate ξ replaced by 1- ξ. Constants B_q and D_q are zero, while A_q and C_q are defined by equations (3.31) and (3.32), respectively.

3.4.4 Case 4 Solution

The fourth case solution is encountered when $\delta_q^2 > \Delta_q$ and $\Delta_q > 0$ and $\delta_q < 0$. It is defined by equation (3.33) of section 3.3.4, with coordinate ξ replaced by 1- ξ. Constants B_q and D_q are zero, while A_q and C_q are defined by equations (3.34) and (3.35), respectively.

3.5 The SFTF Plate

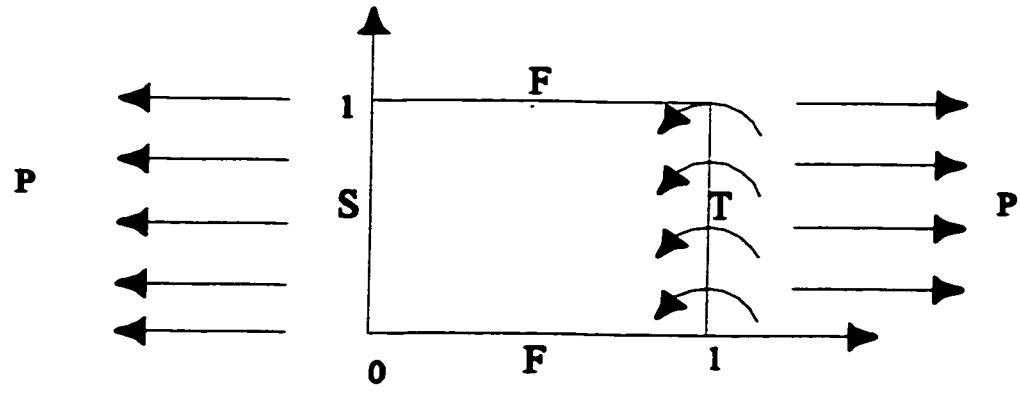

Figure 3.6 The SFTF plate under unilateral in-plane load.

Boundary Condition of specified edge				
PLATE	$\xi = 0$	$\eta = 0$	$\xi = 1$	$\eta = 1$
SRSV	W=0, $M_\xi = 0$	$S_\eta = 0$, $V_\eta = 0$	W=0, $M_\xi = 0$	$S_\eta \propto E_m$, $V_\eta = 0$
SVSR	W=0, $M_\xi = 0$	$S_\eta \propto E_p$, $V_\eta = 0$	W=0, $M_\xi = 0$	$S_\eta = 0$, $V_\eta = 0$
SRWR	W=0, $M_\xi = 0$	$S_\eta = 0$, $V_\eta = 0$	W=0, $M_\xi \propto E_n$	$S_\eta = 0$, $V_\eta = 0$
SFCF	W=0, $M_\xi = 0$	$S_\eta = 0$, $V_\eta = 0$	W=0, $M_\xi = 0$	$S_\eta = 0$, $V_\eta = 0$

Table 3.1 Boundary conditions summary of SFCF plate and its building blocks[4].

By the name itself, the superposition method indicates that it is a procedure of positioning something over something else. Here, in this section we will present the solution of SFCF plate by utilising this method. An analytical-type solution for the SFCF plate is obtained by superimposing the SRSV(section 3.1), SVSR(section 3.2), and SRWR (section 3.3) building blocks, as shown in Figure 3.1. This is a very economical approach as the required analytical solutions for the building blocks are already available. Hence, the SFCF solution becomes the sum of its building block solutions as follows,

$$W(\xi,\eta) = W_{SRSV}(\xi,\eta) + W_{SVSR}(\xi,\eta) + W_{SRWR}(\xi,\eta)$$

or

$$W(\xi,\eta) = \sum_{m=1,2,3}^{\infty} Y_m(\eta)\sin(m\pi\xi) + \sum_{p=1,2,3}^{\infty} Y_p(1-\eta)\sin(p\pi\xi) + \sum_{n=0,1,2}^{\infty} Y_n(\xi)\cos(n\pi\eta). \tag{3.36}$$

Expressions for $Y_m(\eta)$ (of SRSV plate), $Y_p(1-\eta)$ (of SVSR plate) and $Y_n(\xi)$ (of SRWR plate) are summarised in Table 3.2. All coefficients in the building block solutions are linearly proportional to

their respective plate amplitude (E) factors. Only three of the eight boundary conditions required for the SFCF plate have yet to be satisfied in the superimposed solution given by equation (3.36). Each building block's factor is properly adjusted to enforce one of the three remaining conditions. In reviewing Table 3.1, the following conclusions can be made :

E_m (of the SRSV plate) must neutralise the bending moment at $\eta = 1$,

E_p (of the SVSR plate) must neutralise the bending moment at $\eta = 0$, and

E_n (of the SRWR plate) must neutralise the slope at $\xi = 1$.

The zero bending moment conditions are enforced by substituting equation (3.36) into equation (2.5), and simplifying, to obtain,

$$\sum_{m=1,2,3}^{\infty}\left[Y_m''(1)-\upsilon(m\pi\phi)^2 Y_m(1)\right]\sin(m\pi\xi)+\sum_{p=1,2,3}^{\infty}\left[Y_p''(0)-\upsilon(p\pi\phi)^2 Y_p(0)\right]\sin(p\pi\xi)$$
$$+\sum_{n=0,1,2}^{\infty}\left[-(n\pi)^2 Y_n(\xi)+\upsilon\phi^2 Y_n''(\xi)\right]\cos(n\pi)=0 \qquad (3.37)$$

and

$$\sum_{m=1,2,3}^{\infty}\left[Y_m''(0)-\upsilon(m\pi\phi)^2 Y_m(0)\right]\sin(m\pi\xi)+\sum_{p=1,2,3}^{\infty}\left[Y_p''(1)-\upsilon(p\pi\phi)^2 Y_p(1)\right]\sin(p\pi\xi)$$
$$+\sum_{n=0,1,2}^{\infty}\left[-(n\pi)^2 Y_n(\xi)+\upsilon\phi^2 Y_n''(\xi)\right]=0 \qquad (3.38)$$

It is important to properly express equations (3.37) and (3.38) so that the influence of building block amplitude factors in the superimposed solution can be determined. This is accomplished by eliminating the ξ variable. By observing the above equation we note that m and p indices consist of the same sequence of numbers. Hence, they can be associated with a single summation sign. The $Y_n(\xi)$ and $Y_n''(\xi)$ terms under the second summation are expanded into sine series. With some simplification, equations (3.37) and (3.38) become

$$\sum_{\substack{m,p=1,2,3\\n=0,1,2}}^{\infty}\Big\{Y_m''(1)-\upsilon(m\pi\phi)^2Y_m(1)+Y_p''(0)-\upsilon(p\pi\phi)^2Y_p(0)$$

$$-2(n\pi)^2(-1)^n\int_0^1 Y_m(\xi)\sin(m\pi\xi)d\xi+2\upsilon\phi^2(-1)^n\int_0^1 Y_n''(\xi)\sin(m\pi\xi)d\xi\Big\}\sin(m\pi\xi)=0 \qquad (3.39)$$

and

$$\sum_{\substack{m,p=1,2,3\\n=0,1,2}}^{\infty}\Big\{Y_m''(0)-\upsilon(m\pi\phi)^2Y_m(0)+Y_p''(1)-\upsilon(p\pi\phi)^2Y_p(1)$$

$$-2(n\pi)^2\int_0^1 Y_m(\xi)\sin(m\pi\xi)d\xi+2\upsilon\phi^2\int_0^1 Y_n''(\xi)\sin(m\pi\xi)d\xi\Big\}\sin(m\pi\xi)=0 \qquad (3.40)$$

respectively. $\sin(m\pi\xi)$ cannot be zero for all values of ξ. Hence, parenthesized quantities must equal zero for each value of m or p. These quantities are expressed in terms of E factors(or building block amplitudes). Equation (3.39) becomes,

$$\sum_{\substack{m,p=1,2,3\\n=0,1,2}}^{\infty}\left[a_mE_m+c_pE_p+b_mE_n\right]=0 \qquad (3.41)$$

while equation (3.40) becomes

$$\sum_{\substack{m,p=1,2,3\\n=0,1,2}}^{\infty}\left[i_mE_m+k_pE_p+j_mE_n\right]=0\ . \qquad (3.42)$$

With the bending moment conditions fulfilled, attention is focussed on satisfying the zero slope condition at $\xi = 1$. This is done by substituting the superimposed solution (3.36) in the slope equation (2.2). The resulting expression is equated to zero, simplified, and evaluated at $\xi = 1$, giving

$$\sum_{m=1,2,3}^{\infty}(m\pi)Y_m(\eta)\cos(m\pi\xi)+\sum_{p=1,2,3}^{\infty}(p\pi)Y_p(1-\eta)\cos(p\pi\xi)$$
$$+\sum_{n=0,1,2}^{\infty}Y_n'(1)\cos(n\pi\eta)=0. \tag{3.43}$$

Building Block	Case	Equation	Equal-to-Zero	Non-zero
SRSV	1	(3.8)	B_m, C_m	A_m (3.9), D_m (3.10)
Section 3.1	2	(3.11)	A_m, C_m	B_m (3.12), D_m (3.13)
$Y_m(\eta)$	3	(3.14)	A_m, C_m	B_m (3.15), D_m (3.16)
SVSR	1	(3.8)*	B_p, C_p	A_p(3.9), D_p (3.10)
Section 3.2	2	(3.11)*	A_p, C_p	B_p (3.12), D_p (3.13)
$Y_p(1-\eta)$	3	(3.14)*	A_p, C_p	B_p (3.15), D_p (3.16)
SRWR	1	(3.24)	A_n, D_n	B_n (3.25), C_n (3.26)
Section 3.3	2	(3.27)	B_n, D_n	An (3.28), C_n (3.29)
$Y_n(\xi)$	3	(3.30)	B_n, D_n	A_n (3.31), C_n (3.32)
	4	(3.33)	B_n, D_n	A_n (3.34), C_n (3.35)

Table 3.2 Summary of building block solutions of SFCF plate[4].

* Replace coordinate η with $1-\eta$.

The dependence of the above equation on coordinate η is handled by expanding $Y_m(\eta)$ and $Y_p(\eta)$ in cosine series. Following this procedure yields,

$$\sum_{m,p=1,2,3}^{\infty}\left\{m\pi(-1)^m\int_0^1 Y_m(\eta)d\eta+p\pi(-1)^p\int_0^1 Y_p(1-\eta)d\eta+Y_n'(1)\right\}=0$$

for n = 0 and

$$\sum_{\substack{m,p=1,2,3\\n=1,2}}^{\infty}\left\{2m\pi(-1)^m\int_0^1 Y_m(\eta)\cos(n\pi\eta)d\eta\right.$$
$$\left.+2p\pi(-1)^p\int_0^1 Y_p(1-\eta)\cos(n\pi\eta)d\eta+Y_n^{\cdot}(1)\right\}\cos(n\pi\eta)=0 \tag{3.44}$$

for $n \neq 0$. The coefficients of this Fourier series must be zero for each value of n. Equation (3.44) is expressed as,

$$\sum_{\substack{m,p=1,2,3\\n=0,1,2}}^{\infty}\left[e_{mn}E_m+g_{pn}E_p+f_nE_n\right]=0. \tag{3.45}$$

where,

$$\begin{array}{l} \\ (3.41) \\ \\ \\ (3.42) \\ \\ \\ (3.45) \\ \\ \end{array}\left|\begin{array}{ccccccccc} \multicolumn{3}{c}{\text{SRSV}} & \multicolumn{3}{c}{\text{SVSR}} & \multicolumn{3}{c}{\text{SRWR}} \\ a_1 & 0 & 0 & c_1 & 0 & 0 & b_{10} & b_{11} & b_{12} \\ 0 & a_2 & 0 & 0 & c_2 & 0 & b_{20} & b_{21} & b_{22} \\ 0 & 0 & a_3 & 0 & 0 & c_3 & b_{30} & b_{31} & b_{32} \\ i_1 & 0 & 0 & k_1 & 0 & 0 & j_{10} & j_{11} & j_{12} \\ 0 & i_2 & 0 & 0 & k_2 & 0 & j_{20} & j_{21} & j_{22} \\ 0 & 0 & i_3 & 0 & 0 & k_3 & j_{30} & j_{31} & j_{32} \\ e_{10} & e_{11} & e_{12} & g_{10} & g_{11} & g_{12} & f_1 & 0 & 0 \\ e_{20} & e_{21} & e_{22} & g_{20} & g_{21} & g_{22} & 0 & f_2 & 0 \\ e_{30} & e_{31} & e_{32} & g_{30} & g_{31} & g_{32} & 0 & 0 & f_3 \end{array}\right| \begin{Bmatrix} E_{m=1} \\ E_{m=2} \\ E_{m=3} \\ E_{p=1} \\ E_{p=2} \\ E_{p=3} \\ E_{n=0} \\ E_{n=1} \\ E_{n=2} \end{Bmatrix} = \begin{Bmatrix} 0 \\ 0 \\ 0 \\ 0 \\ 0 \\ 0 \\ 0 \\ 0 \\ 0 \end{Bmatrix}$$

Figure 3.7 Three term expansion of algebraic equations of the SFCF plate[4].

Equations (3.41), (3.42), and (3.45) are expanded by k terms, producing 3k linear homogeneous equations with 3k unknown E factors. Figure 3.7 portrays the system of equations, in matrix form, which is expanded in three terms. Coefficients preceding E factors are building block contributions and are defined in Appendix B.

Until now we have developed equations for the SFCF plate which has been taken from the work done by D. J. Michelussi[4]. To incorporate rotational elastic stiffness along edge $\xi = 1$, to convert the clamped edge to a rotational elastic edge, the above coefficient matrix (Figure 3.7) is modified. To achieve this end, we have to concentrate on the equations which represent the boundary conditions along the edge $\xi = 1$. Consider the third set of equations in the above matrix, i.e., the equations represented by equation (3.45), and consider the case in which a torsional spring is placed along the edge $\xi = 1$. We know that the moment is proportional to the slope. So we can write,

$$M = K\frac{dw}{dx} \tag{3.46}$$

This equation is dimensional, converting it into dimensionless form we get,

$$\frac{dw}{dx} = a.\frac{\partial(W/a)}{\partial(x/a)} = \frac{\partial W}{\partial \xi} \tag{3.47}$$

where W = (displacement)/a ; ξ = x/a.

Following the same method we can convert moment 'M' into dimensionless form as

$$M^{*} = \frac{Ma}{D} \tag{3.48}$$

where M^{*} is the dimensionless moment. Therefore we can write equation (3.46) as,

$$M^{*} = \frac{Ma}{D} = \frac{Ka}{D}\frac{\partial W}{\partial \xi}$$

Representing Ka/D as K_{2r}. Then the above equation can be written as,

$$M^{*} - K_{2r}\frac{\partial W}{\partial \xi} = 0/_{\xi=1}$$

Alternatively, it can be written as

$$K_{2r}\frac{\partial W}{\partial \xi} - M^{*} = 0. \tag{3.49}$$

Observing the above matrix, it is obvious that we already have $\partial W/\partial \xi$ in the third set of equations (equation (3.45)). Therefore multiplying these equations with K_{2r} we get $K_{2r}.\partial W/\partial \xi$. The first two segments of the third set of equations (terms with e_{mn} and g_{pn}) represent only slope of simply supported edges along $\xi = 1$. Therefore moment exists only in the third block of this equation set. Subtracting the moment amplitude $M^{*} = 1$ from the diagonal elements of this block, we will exactly fulfill the requirements of equation (3.49).

Thus after all changes have been made to incorporate rotational elasticity, the above coefficient matrix becomes,

	SRSV			SVSR			SRWR				
	a_1	0	0	c_1	0	0	b_{10}	b_{11}	b_{12}	E_{m-1}	0
(3.41)	0	a_2	0	0	c_2	0	b_{20}	b_{21}	b_{22}	E_{m-2}	0
	0	0	a_3	0	0	c_3	b_{30}	b_{31}	b_{32}	E_{m-3}	0
	i_1	0	0	k_1	0	0	j_{10}	j_{11}	j_{12}	E_{p-1}	0
(3.42)	0	i_2	0	0	k_2	0	j_{20}	j_{21}	j_{22}	E_{p-2}	= 0
	0	0	i_3	0	0	k_3	j_{30}	j_{31}	j_{32}	E_{p-3}	0
	$e_{10}K_{2r}$	$e_{11}K_{2r}$	$e_{12}K_{2r}$	$g_{10}K_{2r}$	$g_{11}K_{2r}$	$g_{12}K_{2r}$	$f_1K_{2r}-1$	0	0	E_{n-0}	0
(3.45)	$e_{20}K_{2r}$	$e_{21}K_{2r}$	$e_{22}K_{2r}$	$g_{20}K_{2r}$	$g_{21}K_{2r}$	$g_{22}K_{2r}$	0	$f_2K_{2r}-1$	0	E_{n-1}	0
(modified)	$e_{30}K_{2r}$	$e_{31}K_{2r}$	$e_{32}K_{2r}$	$g_{30}K_{2r}$	$g_{31}K_{2r}$	$g_{32}K_{2r}$	0	0	$f_3K_{2r}-1$	E_{n-2}	0

Figure 3.8 Coefficient matrix equation resulting from three term expansion of algebraic equations of the SFTF plate.

Eigenvalues are found by requiring that the determinant of this coefficient matrix be zero. Appropriate eigenvalues are acquired by examining eigenvalue versus determinant value graphs, which are plotted from generated data. Exact eigenvalues are calculated by refining these appropriate roots using a numerical bisection method. Once an eigenvalue is determined, the associated eigenvector, whose elements are the amplitudes of the superimposed building blocks, is calculated. The mode shape is created by back-substituting these amplitudes into the original building block solutions. The above procedure is the same for all superimposed solutions.

3.6 The TFTF Plate

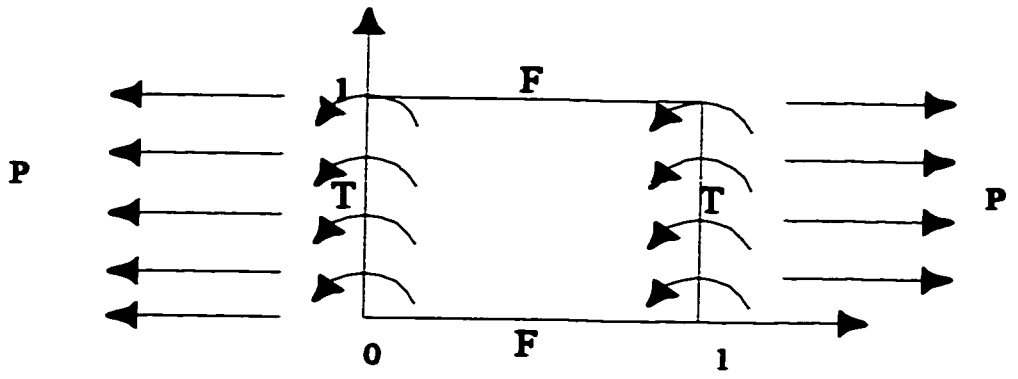

Figure 3.9 The TFTF thin rectangular plate under unilateral in-plane load.

Consider the plate presented in Figure 3.9, where none of the edges are given simple or slip shear supports. Obviously, the method of superposition must be utilised. A superimposed solution consisting of SRSV, SVSR, SRWR, and WRSR building blocks, is shown in Figure 3.1. The building block solutions are derived in sections 3.1 through 3.4 respectively. The CFCF plate solution becomes

$$W(\xi,\eta) = W_{srsv}(\xi,\eta) + W_{svsr}(\xi,\eta) + W_{srwr}(\xi,\eta) + W_{wrsr}(\xi,\eta)$$

PLATE	$\xi = 0$	$\eta = 0$	$\xi = 1$	$\eta = 1$
SRSV	W=0, $M_\xi = 0$	$S_\eta = 0$, $V_\eta = 0$	W=0, $M_\xi = 0$	$S_\eta \propto E_m$, $V_\eta = 0$
SVSR	W=0, $M_\xi = 0$	$S_\eta \propto E_p$, $V_\eta = 0$	W=0, $M_\xi = 0$	$S_\eta = 0$, $V_\eta = 0$
SRWR	W=0, $M_\xi = 0$	$S_\eta = 0$, $V_\eta = 0$	W=0, $M_\xi \propto E_n$	$S_\eta = 0$, $V_\eta = 0$
WRSR	W=0, $M_\xi \propto E_q$	$S_\eta = 0$, $V_\eta = 0$	W=0, $M_\xi = 0$	$S_\eta = 0$, $V_\eta = 0$
CFCF	W=0, $M_\xi = 0$	$S_\eta = 0$, $V_\eta = 0$	W=0, $M_\xi = 0$	$S_\eta = 0$, $V_\eta = 0$

Table 3.3 Boundary conditions summary of CFCF plate and its building blocks[4]

or

$$W(\xi,\eta) = \sum_{m=1,2,3}^{\infty} Y_m(\eta)\sin(m\pi\xi) + \sum_{p=1,2,3}^{\infty} Y_p(1-\eta)\sin(p\pi\xi) + \sum_{n=0,1,2}^{\infty} Y_n(\xi)\cos(n\pi\eta) + \sum_{q=0,1,2}^{\infty} Y_q(1-\xi)\cos(q\pi\eta). \quad (3.46)$$

Table 3.4 summarises the building block solutions. Each building block possesses a distinct boundary condition which regulates its amplitude. The final solution is achieved once the harmonic rotations and moments are adequately adjusted to enforce the four remaining boundary conditions. According to Table 3.2, these include zero bending moment for the free edges at $\eta = 1$ and $\eta = 0$, and zero slope for the clamped edges at $\xi = 1$ and $\xi = 0$.

Bending moments defined by equation (2.5) along the free edges are equated to zero. Equation (3.46) for $W(\xi,\eta)$ is substituted into the expression. Evaluation at $\eta = 1$ and $\eta = 0$ gives

Building Block	Case	Equation	Coefficients: Equal-to-Zero	Coefficients: Non-zero
SRSV	1	(3.8)	B_m, C_m	A_m (3.9), D_m (3.10)
Section 3.1	2	(3.11)	A_m, C_m	B_m (3.12), D_m (3.13)
$Y_m(\eta)$	3	(3.14)	A_m, C_m	B_m (3.15), D_m (3.16)
SVSR	1	(3.8)*	B_p, C_p	A_p(3.9), D_p (3.10)
Section 3.2	2	(3.11)*	A_p, C_p	B_p (3.12), D_p (3.13)
$Y_p(1-\eta)$	3	(3.14)*	A_p, C_p	B_p (3.15), D_p (3.16)
SRWR	1	(3.24)	A_n, D_n	B_n (3.25), C_n (3.26)
Section 3.3	2	(3.27)	B_n, D_n	An (3.28), C_n (3.29)
$Y_n(\xi)$	3	(3.30)	B_n, D_n	A_n (3.31), C_n (3.32)
	4	(3.33)	B_n, D_n	A_n (3.34), C_n (3.35)
WRSR	1	(3.24)**	A_q, D_q	B_q (3.25), C_q (3.26)
Section 3.4	2	(3.27)**	B_q, D_q	A_q(3.28), C_q (3.29)
$Y_q(1-\xi)$	3	(3.30)**	B_q, D_q	A_q (3.31), C_q (3.32)
	4	(3.33)**	B_q, D_q	A_q (3.34), C_q (3.35)

Table 3.4 Summary of building block solution of the CFCF plate[4].

* Replace coordinate η with $1 - \eta$, ** Replace coordinate ξ with $1 - \xi$

$$\sum_{m=1,2,3}^{\infty}\left[\ddot{Y}_m(1)-\upsilon(m\pi\phi)^2 Y_m(1)\right]\sin(m\pi\xi)+$$
$$\sum_{p=1,2,3}^{\infty}\left[\ddot{Y}_p(0)-\upsilon(p\pi\phi)^2 Y_p(0)\right]\sin(p\pi\xi)+$$
$$\sum_{n=0,1,2}^{\infty}\left[-(n\pi)^2 Y_n(\xi)+\upsilon\phi^2\ddot{Y}_n(\xi)\right]\cos(n\pi)+ \qquad (3.47)$$
$$\sum_{q=0,1,2}^{\infty}\left[-(q\pi)^2 Y_q(1-\xi)+\upsilon\phi^2\ddot{Y}_q(1-\xi)\right]\cos(q\pi)=0$$

and

$$\sum_{m=1,2,3}^{\infty}\left[Y_m''(0)-\upsilon(m\pi\phi)^2 Y_m(0)\right]\sin(m\pi\xi)+$$
$$\sum_{p=1,2,3}^{\infty}\left[Y_p''(1)-\upsilon(p\pi\phi)^2 Y_p(1)\right]\sin(p\pi\xi)+$$
$$\sum_{n=0,1,2}^{\infty}\left[-(n\pi)^2 Y_n(\xi)+\upsilon\phi^2 Y_n''(\xi)\right]+ \qquad (3.48)$$
$$\sum_{q=0,1,2}^{\infty}\left[-(q\pi)^2 Y_q(1-\xi)+\upsilon\phi^2 Y_q''(1-\xi)\right]=0$$

respectively. Indices m and p are assigned to a single summation sign since they consist of the same sequence of numbers. The same is done with indices n and q. The $Y_n(\xi)$, $Y_n''(\xi)$, $Y_q(1-\xi)$ and $Y_q''(1-\xi)$ terms in equations (3.47) and (3.48) are expanded into Fourier sine series, giving

$$\sum_{\substack{m,p=1,2,3\\ n,q=0,1,2}}^{\infty}\Big\{Y_m''(1)-\upsilon(m\pi\phi)^2 Y_m(1)+Y_p''(0)-\upsilon(p\pi\phi)^2 Y_p(0)$$
$$-2(n\pi)^2(-1)^n\int_0^1 Y_n(\xi)\sin(m\pi\xi)d\xi+2\upsilon\phi^2(-1)^n\int_0^1 Y_n''(\xi)\sin(m\pi\xi)d\xi \qquad (3.49)$$
$$-2(q\pi)^2(-1)^q\int_0^1 Y_q(1-\xi)\sin(m\pi\xi)d\xi+2\upsilon\phi^2(-1)^q\int_0^1 Y_q''(1-\xi)\sin(m\pi\xi)d\xi\Big\}\sin(m\pi\xi)=0$$

and

$$\sum_{\substack{m,p=1,2,3\\n,q=0,1,2}}^{\infty}\Big\{Y_m''(0)-\upsilon(m\pi\phi)^2Y_m(0)+Y_p''(1)-\upsilon(p\pi\phi)^2Y_p(1)$$

$$-2(n\pi)^2\int_0^1 Y_n(\xi)\sin(m\pi\xi)d\xi+2\upsilon\phi^2\int_0^1 Y_n''(\xi)\sin(m\pi\xi)d\xi \qquad (3.50)$$

$$-2(q\pi)^2\int_0^1 Y_q(1-\xi)\sin(m\pi\xi)d\xi+2\upsilon\phi^2\int_0^1 Y_q''(1-\xi)\sin(m\pi\xi)d\xi\Big\}\sin(m\pi\xi)=0$$

respectively. Note that the $\sin(m\pi\xi)$ function cannot be equal to zero for all values of ξ. Equations (3.49) and (3.50) are restated in terms of E factors as

$$\sum_{\substack{m,p=1,2,3\\n,q=0,1,2}}^{\infty}\left[a_{mn}E_{mn}+c_{pq}E_{pq}+b_{mn}E_{mn}+d_{pq}E_{pq}\right]=0 \qquad (3.51)$$

and

$$\sum_{\substack{m,p=1,2,3\\n,q=0,1,2}}^{\infty}\left[i_{mn}E_{mn}+k_{pq}E_{pq}+j_{mn}E_{mn}+l_{pq}E_{pq}\right]=0 \qquad (3.52)$$

respectively. The coefficient preceding each E factor which is plate amplitude is defined in appendix A and can be described as a building block contribution in the superimposed solution.

Slope along the clamped edges is defined by equation (2.2) and is set equal to zero. Once again, the superimposed solution, given by equation (3.46), is used for $W(\xi,\eta)$ in the expression. Evaluation results in

$$\sum_{m=1,2,3}^{\infty}(m\pi)Y_m(\eta)\cos(m\pi)+\sum_{p=1,2,3}^{\infty}(p\pi)Y_p(1-\eta)\cos(p\pi)$$

$$+\sum_{n=0,1,2}^{\infty}Y_n'(1)\cos(n\pi\eta)-\sum_{q=0,1,2}^{\infty}Y_q'(0)\cos(q\pi\eta)=0. \qquad (3.53)$$

for $\xi = 1$ and

$$\sum_{m=1,2,3}^{\infty} (m\pi)Y_m(\eta) + \sum_{p=1,2,3}^{\infty} (p\pi)Y_p(1-\eta) + \sum_{n=0,1,2}^{\infty} \dot{Y}_n(0)\cos(n\pi\eta) - \sum_{q=0,1,2}^{\infty} \dot{Y}_q(1)\cos(q\pi\eta) = 0. \tag{3.54}$$

for $\xi = 0$. The first and third terms in both of the above equations are expanded into Fourier cosine series. Equations (3.53) becomes

$$\sum_{m,p=1,2,3}^{\infty} \left\{ m\pi(-1)^m \int_0^1 Y_m(\eta)d\eta + p\pi(-1)^p \int_0^1 Y_p(1-\eta)d\eta + \dot{Y}_n(1) - \dot{Y}_q(0) \right\} = 0$$

for $n = 0$ and

$$\sum_{\substack{m,p=1,2,3 \\ n,q=1,2}}^{\infty} \left\{ 2m\pi(-1)^m \int_0^1 Y_m(\eta)\cos(n\pi\eta)d\eta + 2p\pi(-1)^p \int_0^1 Y_p(1-\eta)\cos(n\pi\eta)d\eta + \dot{Y}_n(1) - \dot{Y}_q(0) \right\} \cos(n\pi\eta) = 0 \tag{3.55}$$

for $n \neq 0$. While the equation (3.54) becomes

$$\sum_{m,p=1,2,3}^{\infty} \left\{ m\pi \int_0^1 Y_m(\eta)d\eta + p\pi \int_0^1 Y_p(1-\eta)d\eta + \dot{Y}_n(0) - \dot{Y}_q(1) \right\} = 0$$

for $n = 0$ and

$$\sum_{\substack{m,p=1,2,3 \\ n,q=1,2}}^{\infty} \left\{ 2m\pi \int_0^1 Y_m(\eta)\cos(n\pi\eta)d\eta + 2p\pi \int_0^1 Y_p(1-\eta)\cos(n\pi\eta)d\eta + \dot{Y}_n(0) - \dot{Y}_q(1) \right\} \cos(n\pi\eta) = 0 \tag{3.56}$$

for n ≠ 0. The final forms of equations (3.96) and (3.97) are

$$\sum_{\substack{m,p=1,2,3\\ n,q=0,1,2}}^{\infty}\left[e_{mn}E_{an}+g_{pn}E_{pq}+f_{nq}E_{an}+h_{nq}E_{sq}\right]=0 \tag{3.57}$$

and

$$\sum_{\substack{m,p=1,2,3\\ n,q=0,1,2}}^{\infty}\left[s_{mn}E_{an}+u_{pn}E_{pq}+t_{nq}E_{an}+v_{nq}E_{sq}\right]=0 \tag{3.58}$$

respectively. Once again, the building block contributions are listed in appendix A.

Figure 3.10 is a matrix representation of the linear equations resulting from a three term expansion of equations (3.51), (3.52), (3.57) and (3.58).

$$\begin{array}{l}
\\
(3.51)\\
\\
\\
(3.52)\\
\\
\\
(3.57)\\
\\
\\
(3.58)\\
\\
\\
\end{array}
\begin{array}{|c|}\hline\end{array}
\begin{bmatrix}
\overset{SRSV}{a_1} & 0 & 0 & c_1 & 0 & 0 & b_{10} & b_{11} & b_{12} & d_{10} & d_{11} & d_{12}\\
0 & a_2 & 0 & 0 & c_2 & 0 & b_{20} & b_{21} & b_{22} & d_{10} & d_{11} & d_{12}\\
0 & 0 & a_3 & 0 & 0 & c_3 & b_{30} & b_{31} & b_{32} & d_{10} & d_{11} & d_{12}\\
i_1 & 0 & 0 & k_1 & 0 & 0 & j_{10} & j_{11} & j_{12} & l_{10} & l_{11} & l_{12}\\
0 & i_2 & 0 & 0 & k_2 & 0 & j_{20} & j_{21} & j_{22} & l_{10} & l_{11} & l_{12}\\
0 & 0 & i_3 & 0 & 0 & k_3 & j_{30} & j_{31} & j_{32} & l_{10} & l_{11} & l_{12}\\
e_{10} & e_{11} & e_{12} & g_{10} & g_{11} & g_{12} & f_1 & 0 & 0 & h_1 & 0 & 0\\
e_{20} & e_{21} & e_{22} & g_{20} & g_{21} & g_{22} & 0 & f_2 & 0 & 0 & h_2 & 0\\
e_{30} & e_{31} & e_{32} & g_{30} & g_{31} & g_{32} & 0 & 0 & f_3 & 0 & 0 & h_3\\
s_{10} & s_{11} & s_{12} & u_{10} & u_{11} & u_{12} & t_1 & 0 & 0 & v_1 & 0 & 0\\
s_{20} & s_{21} & s_{22} & u_{20} & u_{21} & u_{22} & 0 & t_2 & 0 & 0 & v_2 & 0\\
s_{30} & s_{31} & s_{32} & u_{30} & u_{31} & u_{32} & 0 & 0 & t_3 & 0 & 0 & v_3
\end{bmatrix}
\begin{Bmatrix}
E_{a=1}\\ E_{a=2}\\ E_{a=3}\\ E_{p=1}\\ E_{p=2}\\ E_{p=3}\\ E_{s=0}\\ E_{s=1}\\ E_{s=2}\\ E_{s=0}\\ E_{s=1}\\ E_{s=2}
\end{Bmatrix}
=
\begin{Bmatrix}
0\\0\\0\\0\\0\\0\\0\\0\\0\\0\\0\\0
\end{Bmatrix}$$

Figure 3.10A three term expansion of the algebraic equations for the CFCF plate[4].

Until now we were working on equations for the CFCF plate which was the work done by D. J. Michelussi[4]. To incorporate rotational elasticity along edges $\xi = 0$ and $\xi = 1$, we will follow exactly the same procedure which we followed for SFCF plate (for edge condition along $\xi = 1$) at the end of section 3.5.

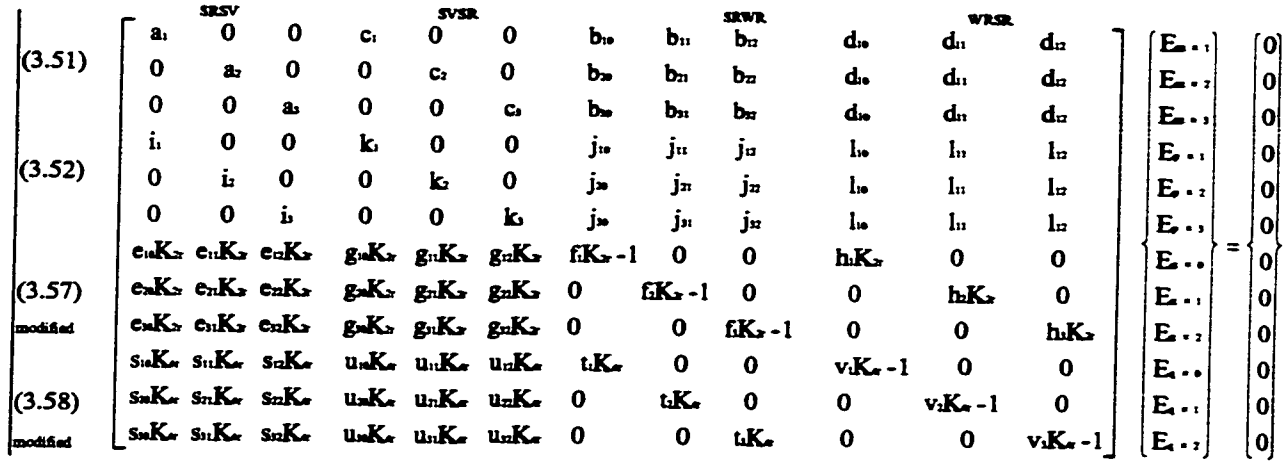

Figure 3.11 Coefficient matrix equation resulting three term expansion of algebraic equations of the TFTF plate.

Consequently, we need to modify two sets of equations of the above matrix. These are equation sets from equations (3.57) and (3.58), which represent slopes along edges $\xi = 1$ and $\xi = 0$ respectively. The modified equations following the procedure in section 3.5, can be written as,

$$M_1^* - K_{2r}\frac{\partial W}{\partial \xi} = 0/_{\xi=1} \qquad \text{and} \qquad M_2^* - K_{4r}\frac{\partial W}{\partial \xi} = 0/_{\xi=0}$$

The above equations can be rewritten as,

$$K_{2r}\frac{\partial W}{\partial \xi} - M_1^* = 0/_{\xi=1} \qquad \text{and} \qquad K_{4r}\frac{\partial W}{\partial \xi} - M_2^* = 0/_{\xi=0}$$

as described in section 3.5, the modified coefficient matrix becomes,

Eigenvalues and mode shapes are obtained by following the procedure described at the end of section (3.5).

Chapter 4

Presentation of Results

Free vibration analysis results are presented for thin rectangular plates subjected to evenly distributed uniform in-plane loads having torsional rotational edge supports. Plate stability is analysed prior to free vibration. The magnitude of each in-plane load used is a specific percentage of critical buckling load for the plate being analysed. Critical buckling loads are computed for both SFTF and TFTF plates, where 'T' stands for rotational elastic edge support as mentioned in the third chapter. Buckling loads for the above plates are calculated for 10 different rotational stiffnesses : 0.5, 1.0, 2.0, 3.0, 4.0, 5.0, 7.5, 10.0, 20.0, 30.0, and for 9 different aspect ratios: 1/3.0, 1/2.5, 1/2.0, 1/1.5, 1/1, 1.5/1, 2.0/1, 2.5/1, 3.0/1.

The reason for selecting these particular stiffness values is due to the fact that, for zero rotational stiffness, the edge acts as a pinned edge while for infinite rotational stiffness it acts as a clamped edge. Critical buckling loads and eigenvalues are already available for pinned and clamped edge boundary conditions and it was found that by gradually increasing the rotational stiffness of an edge, the clamped edge conditions are almost achieved for dimensionless stiffness values 30 and above. This behaviour can be observed from the graphs shown in Figures 4.1, 4.2, 4.5 and 4.6 which depict that the buckling load curve becomes almost horizontal for the dimensionless stiffness values around 30 and the reason for selecting these many stiffness values is to obtain smooth plots.

Coming to the aspect ratios, the most common plate used in the industry is the square plate. Other plates that can be found in the industries are plates with aspect ratios 1/1.5, 1.5/1, 2.0/1. The reason for selecting these many aspect ratios is to study the trend and behaviour of a plate at different aspect ratios.

Eigenvalues and associated eigenvectors are then presented for the first four modes of vibration. Free vibration analysis is also performed for all the above mentioned, rotational stiffnesses and aspect ratios.

Equal stiffnesses are considered for TFTF along the torsional edge supports. All results computed are accurate to 4 digits and are presented in dimensionless form.

4.1 Buckling Analysis Results

As mentioned, first we analyse the stability of each plate. Equation (2.1) can be modified to analyse plate buckling due to in-plane loads. Setting the parameter λ^2 equal to zero, eliminates the dynamic characteristics of free vibration from the governing equation. The resulting equation is,

$$\frac{\partial^4 W(\xi,\eta)}{\partial\eta^4} + 2\varphi^2\frac{\partial^4 W(\xi,\eta)}{\partial\eta^2\partial\xi^2} + \varphi^4\frac{\partial^4 W(\xi,\eta)}{\partial\xi^4} + P_\xi\varphi^2\frac{\partial^2 W(\xi,\eta)}{\partial\xi^2} = 0 \qquad (4.1)$$

and is used to determine buckling loads. The first value of P_ξ to satisfy equation (4.1) is the critical

$\phi\backslash K_{2r}$	0.5	1.0	2.0	3.0	4.0	5.0	7.5	10.0	20.0	30.0
1/3.0	1.091	1.178	1.319	1.426	1.508	1.573	1.686	1.759	1.895	1.949
1/2.5	1.5771	1.704	1.907	2.062	2.181	2.274	2.44	2.546	2.744	2.823
1/2.0	2.481	2.679	3.998	3.24	3.428	3.576	3.837	4.005	4.319	4.445
1/1.5	4.458	4.811	5.381	5.814	6.15	6.416	6.885	7.187	7.756	7.982
1/1	10.20	11.00	12.29	13.27	14.03	14.63	15.70	16.39	17.69	18.21
1.5/1	23.32	25.12	28.02	30.23	31.95	33.32	35.74	37.30	40.25	41.43
2.0/1	41.83	45.03	50.19	54.13	57.20	59.64	63.96	66.74	72.013	74.11
2.5/1	65.73	70.71	78.80	84.96	89.76	93.58	100.34	104.71	112.96	116.27
3.0/1	95.01	102.21	113.84	122.72	129.64	135.15	144.89	151.19	163.11	167.88

Table 4.1 Critical buckling loads of SFTF rectangular plate

buckling load for a given plate. The free vibration solution presented in chapter 3 can be used to obtain buckling loads. Thus for plate buckling, λ^2 is set equal to zero and the effect of P_ξ on the determinant is examined instead.

Dimensionless critical buckling loads are presented in the following Tables 4.1 and 4.2 for plates SFTF and TFTF respectively, for above specified aspect ratios and rotational stiffness values. Obtained results are also analysed graphically.

$\phi \backslash K_{2r}$	0.5	1.0	2.0	3.0	4.0	5.0	7.5	10.0	20.0	30.0
1/3.0	1.199	1.389	1.715	1.983	2.205	2.388	2.735	2.973	3.455	3.658
1/2.5	1.733	2.007	2.478	2.864	3.184	3.451	3.953	4.299	4.999	5.296
1/2.0	2.73	3.15	3.89	4.496	4.997	5.42	6.21	6.75	7.86	8.33
1/1.5	4.891	5.65	6.97	8.05	8.94	9.69	11.11	12.08	14.07	14.91
1/1	11.18	12.89	15.85	18.29	20.31	22.01	25.21	27.42	31.94	33.86
1.5/1	25.51	29.38	36.05	41.54	46.10	49.93	57.16	62.17	72.39	76.75
2.0/1	45.73	52.60	64.46	74.24	62.36	89.17	102.05	110.98	129.22	136.99
2.5/1	71.82	82.56	101.09	116.38	129.03	139.73	159.88	173.86	202.41	214.58
3.0/1	103.78	119.25	145.94	167.95	186.26	201.61	230.65	250.80	291.96	309.52

Table 4.2 Critical buckling loads of TFTF rectangular plate

Figures 4.1, 4.2, 4.5 and 4.6 show changes in critical buckling load with the change in rotational elastic stiffness while Figures 4.3, 4.4, 4.7 and 4.8 show changes in critical buckling load with respect to aspect ratio of the plate for both SFTF and TFTF plates respectively. Similar trends are observed in the behaviour of both SFTF and TFTF plates.

Figure 4.1 **Buckling load Vs. Dimensionless rotational stiffness, SFTF plate, Φ = 1/3.0, 1/2.5, 1/2.0, 1/1.5**

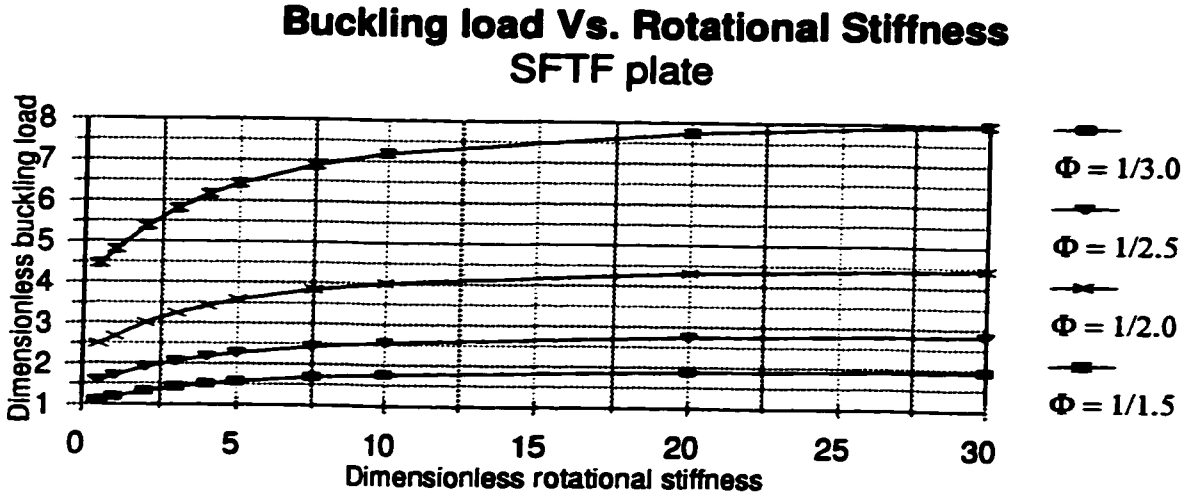

Figure 4.2 **Buckling load Vs. Dimensionless rotational stiffness, SFTF plate, Φ = 1/1, 1.5/1, 2.0/1, 2.5/1, 3.0/1**

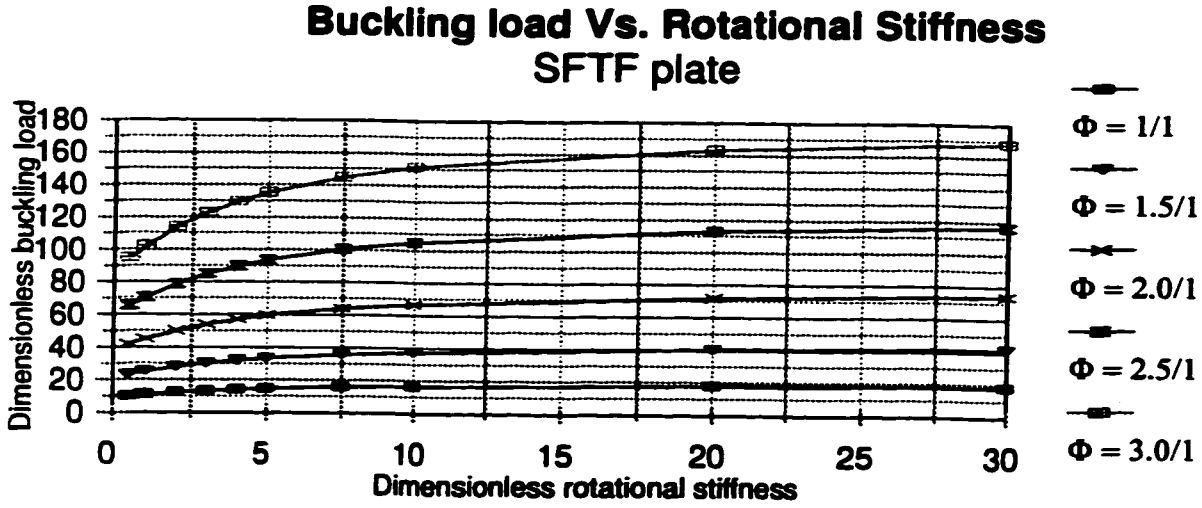

Figure 4.3 **Buckling load Vs. Aspect ratio, SFTF plate, K_{2r} = 0.5, 1.0, 2.0, 3.0, 4.0 (here K = K_{2R})**

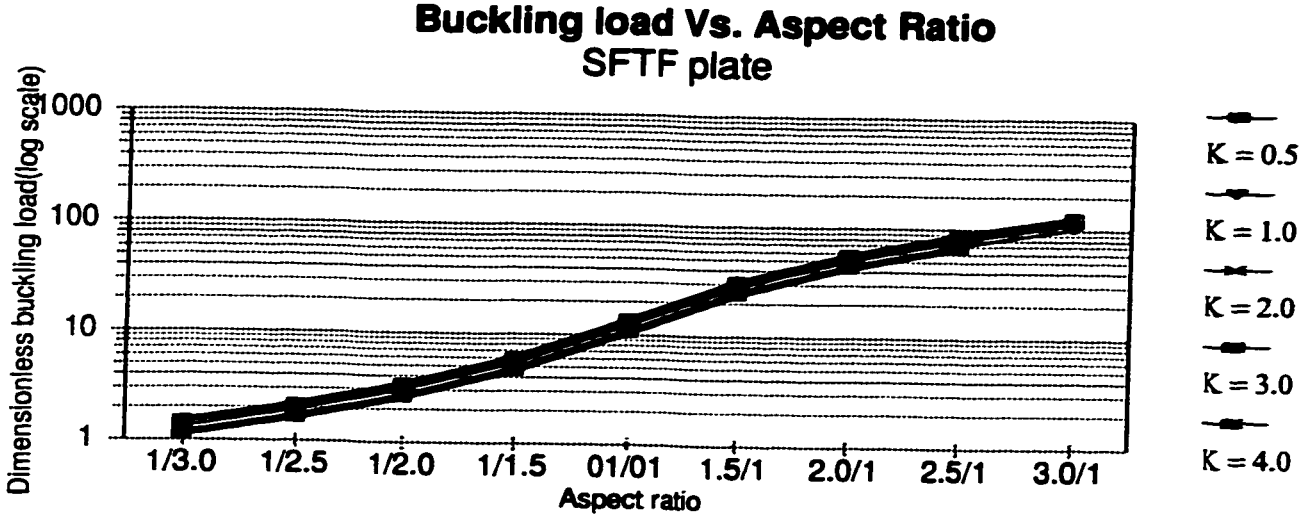

Figure 4.4 **Buckling load Vs. Aspect ratio, SFTF plate, K_{2r} = 5.0, 7.5, 10.0, 20.0, 30.0 (here K = K_{2R})**

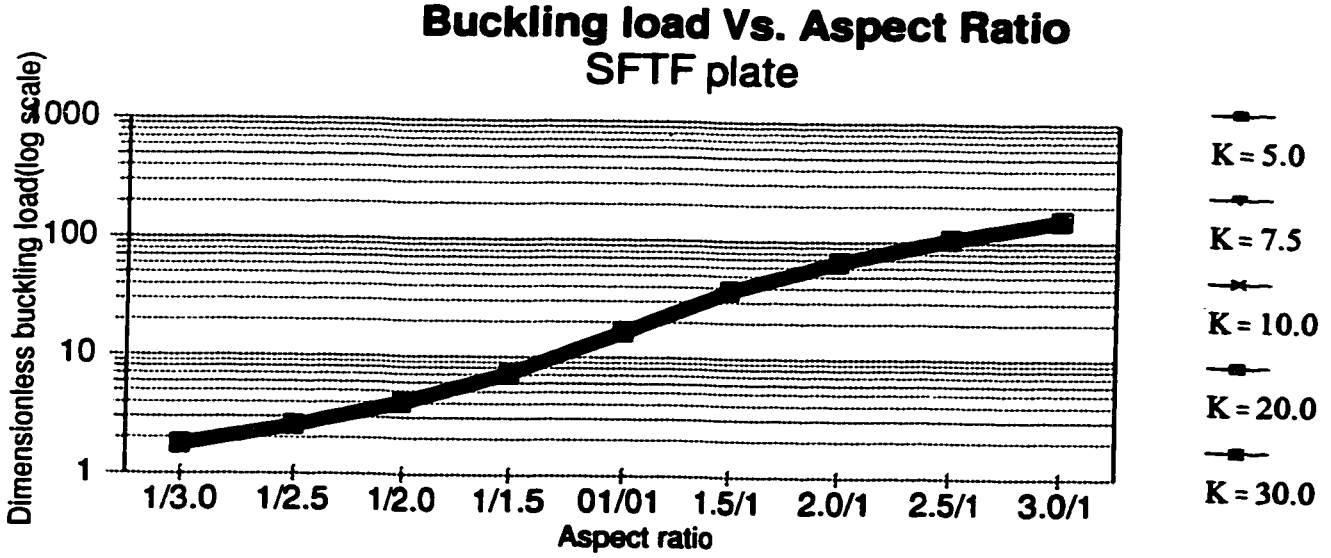

Figure 4.5 **Buckling load Vs. Dimensionless rotational stiffness, TFTF plate, Φ = 1/3.0, 1/2.5, 1/2.0, 1/1.5**

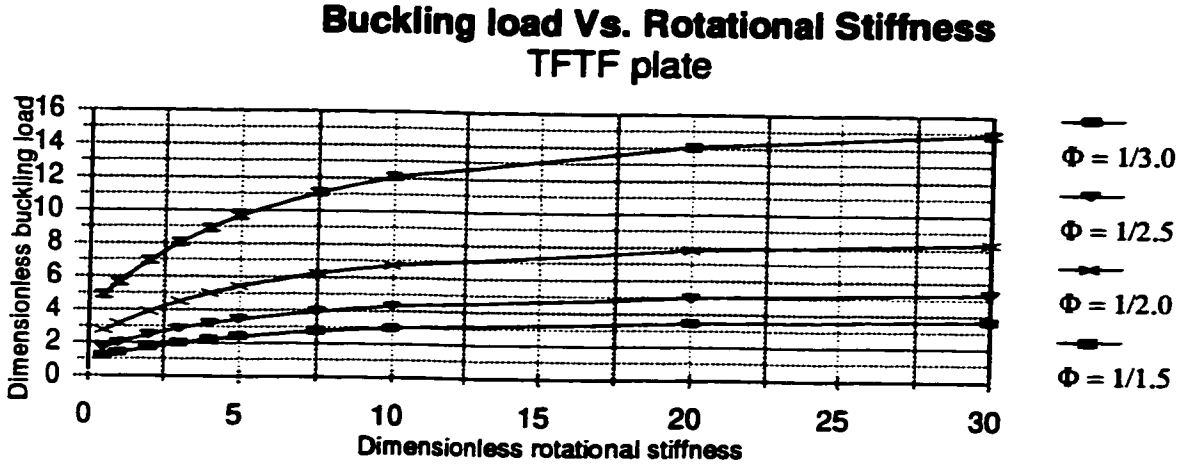

Figure 4.6 **Buckling load Vs. Dimensionless rotational stiffness, TFTF plate, Φ = 1/1, 1.5/1, 2.0/1, 2.5/1, 3.0/1**

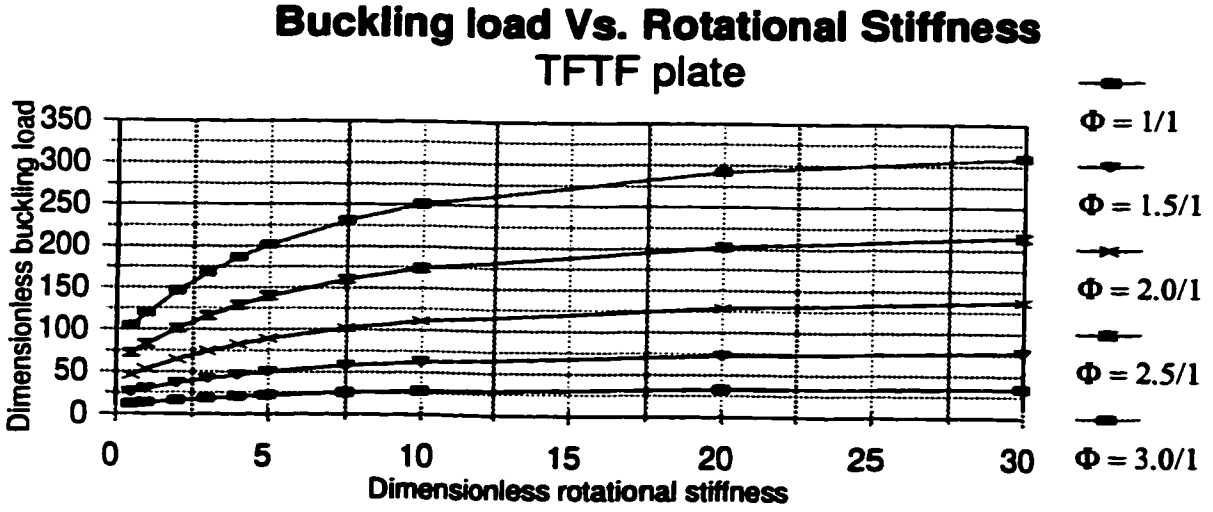

Figure 4.7 **Buckling load Vs. Aspect ratio, TFTF plate, K_{2r} = 0.5, 1.0, 2.0, 3.0, 4.0 (here $K = K_{2R} = K_{4R}$)**

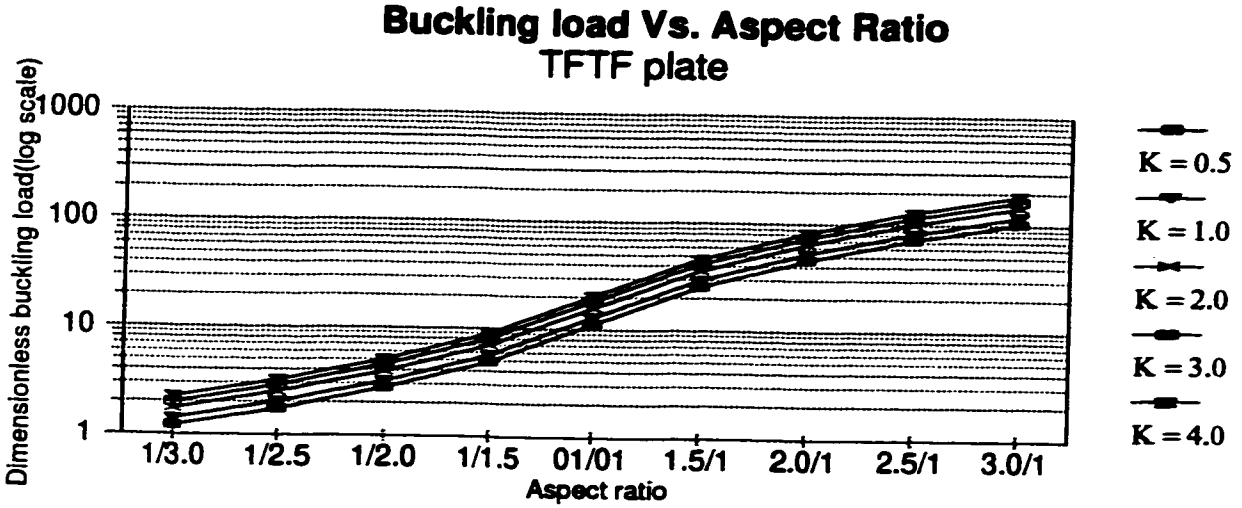

Figure 4.8 **Buckling load Vs. Aspect ratio, TFTF plate, K_{2r} = 5.0, 7.5, 10.0, 20.0, 30.0 (here $K = K_{2R} = K_{4R}$)**

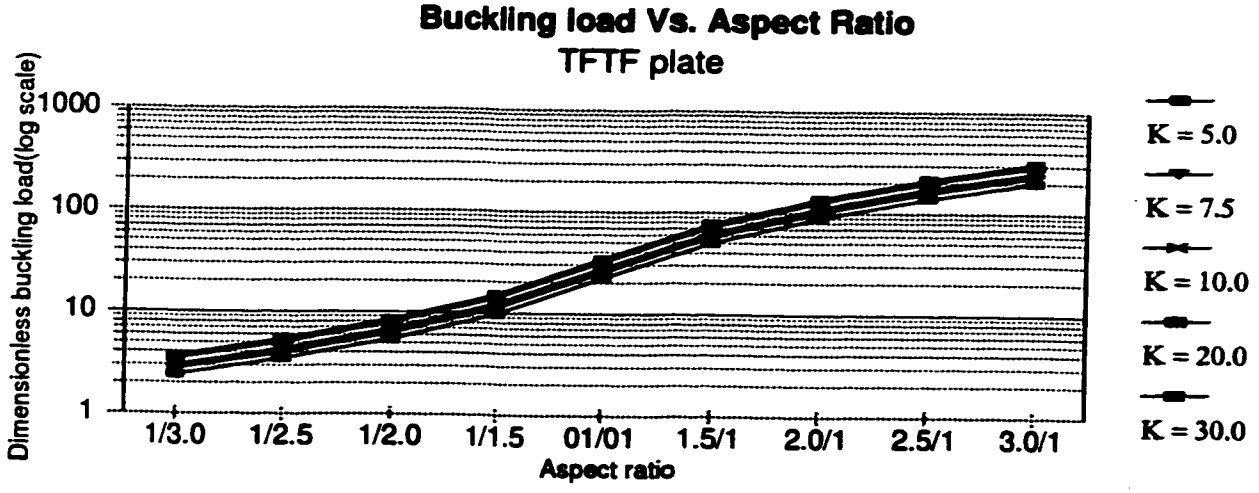

4.2 Free Vibration Analysis Results

In the free vibration analysis, natural frequencies are determined by examining the effect of λ^2 on the determinant of a coefficient matrix comprised of building block contributions. The λ^2 value which makes the determinant of matrices zero, of Figures 3.8 and 3.11, is a dimensionless natural frequency. Results were obtained for the first four modes of vibration with the help of a Fortran program. Quite often it is sufficient to know the value of only a limited number of lowest frequencies rather than all the frequencies. The higher frequencies cannot be taken too seriously, even if an exact solution of the eigenvalue problem is obtained, because the nature of the assumptions employed in defining the models in most elementary theories restricts the validity of the solutions only to the lower modes.

Eigenvalues are calculated for SFTF and TFTF plates for nine different aspect ratios(1/3.0, 1/2.5, 1/2.0, 1/1.5, 1/1, 1.5/1, 2.0/1, 2.5/1, 3.0/1) and for ten different rotational stiffness values(0.5, 1.0, 2.0, 3.0, 4.0, 5.0, 7.5, 10.0, 20.0, 30.0) and for various in-plane loads as a percentage of critical buckling load for each combination of aspect ratio and rotational stiffness values. The percentages of critical buckling loads considered for computations are (-100%. -50%, 0%, 20%, 40%, 60%, 80%, 90%, 99%)

Eigenvalues, eigenvalue curves and mode shapes are presented for plates, both SFTF and TFTF, having aspect ratios 1/1, 1.5/1 in Figures 4.9 through 4.26 and Tables 4.3 through 4.42 and the values for plates with remaining aspect ratios are presented in Appendix A. Eigenvalue curves are presented and mode shapes are illustrated for specific plate combinations. All mode shapes shown are for zero in-plane load , unless specified.

Tables 4.3 - 4.7 Eigenvalues, SFTF Plate, $\phi = 1 / 1$

[4.3] $K_g = 0.5$, $\Phi = 1/1.0$ In-plane load as a percentage of buckling load (0.26)

Mode	-100%	-50%	0%	20%	40%	60%	80%	90%	99%
1	14.20	12.29	10.04	8.980	7.777	6.351	4.493	3.179	1.0192
2	19.03	17.66	16.17	15.54	14.88	14.18	13.45	13.07	12.72
3	37.90	37.23	36.55	36.27	35.99	35.71	34.94	34.36	33.83
4	44.11	41.77	39.28	38.24	37.17	36.08	35.43	35.29	35.16

[4.4] $K_g = 1.0$, $\Phi = 1/1.0$ In-plane load as a percentage of buckling load (0.52)

Mode	-100%	-50%	0%	20%	40%	60%	80%	90%	99%
1	14.75	12.78	10.44	9.334	8.084	6.601	4.668	3.301	1.046
2	19.46	18.01	16.43	15.75	15.05	14.31	13.52	13.12	12.74
3	38.12	37.40	36.67	36.37	36.07	35.77	35.09	34.46	33.89
4	44.86	42.37	39.73	38.62	37.48	36.30	35.46	35.31	35.17

[4.5] $K_g = 2.0$, $\Phi = 1/1.0$ In-plane load as a percentage of buckling load (1.04)

Mode	-100%	-50%	0%	20%	40%	60%	80%	90%	99%
1	15.64	13.55	11.07	9.900	8.575	7.002	4.951	3.499	1.094
2	20.15	18.58	16.86	16.12	15.34	14.52	13.66	13.20	12.78
3	38.49	37.70	36.88	36.55	36.21	35.88	35.4	34.71	34.08
4	46.13	43.42	40.52	39.31	38.05	36.75	35.54	35.37	35.21

[4.6] $K_g = 3.0$, $\Phi = 1/1.0$ In-plane load as a percentage of buckling load (1.57)

Mode	-100%	-50%	0%	20%	40%	60%	80%	90%	99%
1	16.31	14.13	11.55	10.33	8.951	7.311	5.171	3.655	1.143
2	20.69	19.03	17.20	16.41	15.59	14.71	13.78	13.29	12.84
3	38.79	37.94	37.06	36.70	36.34	35.98	35.61	35.00	34.32
4	47.14	44.27	41.20	39.91	38.57	37.19	35.75	35.43	35.26

[4.7] $K_g = 4.0$, $\Phi = 1/1.0$ In-plane load as a percentage of buckling load (2.09)

Mode	-100%	-50%	0%	20%	40%	60%	80%	90%	99%
1	16.83	14.59	11.93	10.67	9.249	7.557	5.347	3.782	1.192
2	21.12	19.39	17.49	16.66	15.80	14.88	13.90	13.38	12.90
3	39.04	38.14	37.22	36.84	36.46	36.08	35.69	35.30	34.59
4	47.98	44.99	41.79	40.43	39.04	37.59	36.08	35.50	35.32

Tables 4.8 - 4.12 Eigenvalues, SFTF Plate, $\phi = 1 / 1$

[illegible]

Mode	-100%	-50%	0%	20%	40%	60%	80%	90%	99%
1	17.25	14.96	12.23	10.95	9.491	7.761	5.493	3.889	1.25
2	21.47	19.69	17.72	16.87	15.97	15.02	14.00	13.46	12.95
3	39.26	38.32	37.36	36.96	36.57	36.17	35.76	35.54	34.85
4	48.68	45.60	42.30	40.90	39.46	37.96	36.40	35.62	35.37

[illegible]

Mode	-100%	-50%	0%	20%	40%	60%	80%	90%	99%
1	18.01	15.63	12.79	11.45	9.933	8.122	5.752	4.072	1.294
2	22.13	20.25	18.17	17.27	16.32	15.30	14.21	13.63	13.08
3	39.67	38.67	37.64	37.22	36.76	36.36	35.92	35.70	35.44
4	50.03	46.80	43.32	41.85	40.33	38.75	37.11	36.26	35.53

[illegible]

Mode	-100%	-50%	0%	20%	40%	60%	80%	90%	99%
1	18.53	16.08	13.17	11.80	10.23	8.369	5.928	4.196	1.331
2	22.58	20.64	18.49	17.56	16.57	15.51	14.37	13.76	13.19
3	39.97	38.92	37.85	37.41	36.97	36.52	36.06	35.83	35.62
4	50.995	47.67	44.09	42.58	41.01	39.38	37.68	36.80	35.99

[illegible]

Mode	-100%	-50%	0%	20%	40%	60%	80%	90%	99%
1	19.57	17.01	13.94	12.49	10.84	8.874	6.291	4.453	1.404
2	23.53	21.47	19.18	18.18	17.11	15.97	14.74	14.08	13.45
3	40.65	39.52	38.36	37.89	37.40	36.91	36.42	36.16	35.94
4	53.14	49.65	45.88	44.28	42.63	40.90	39.10	38.18	37.32

[illegible]

Mode	-100%	-50%	0%	20%	40%	60%	80%	90%	99%
1	20.03	17.41	14.28	12.80	11.11	9.092	6.446	4.564	1.436
2	23.96	21.85	19.50	18.47	17.37	16.19	14.91	14.23	13.58
3	40.99	39.83	38.62	38.13	37.63	37.12	36.61	36.35	36.11
4	54.17	50.60	46.76	45.13	43.44	41.68	39.84	38.89	38.01

Figure 4.9 Eigenvalue curves, SFTF plate, K_{2R}=0.5, ϕ = 1/1,

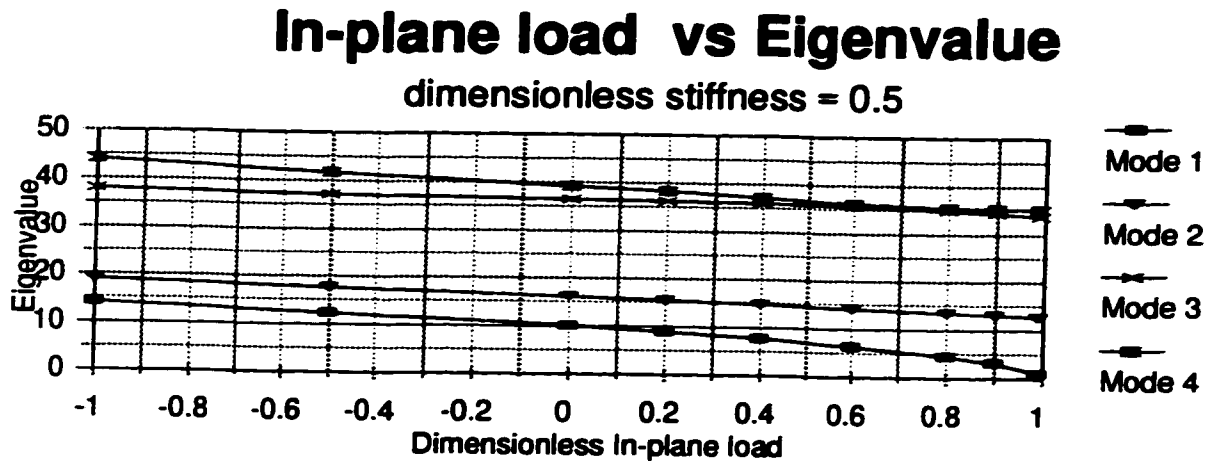

Figure 4.10 Eigenvalue curves, SFTF plate, K_{2R}=1.0, ϕ = 1/1,

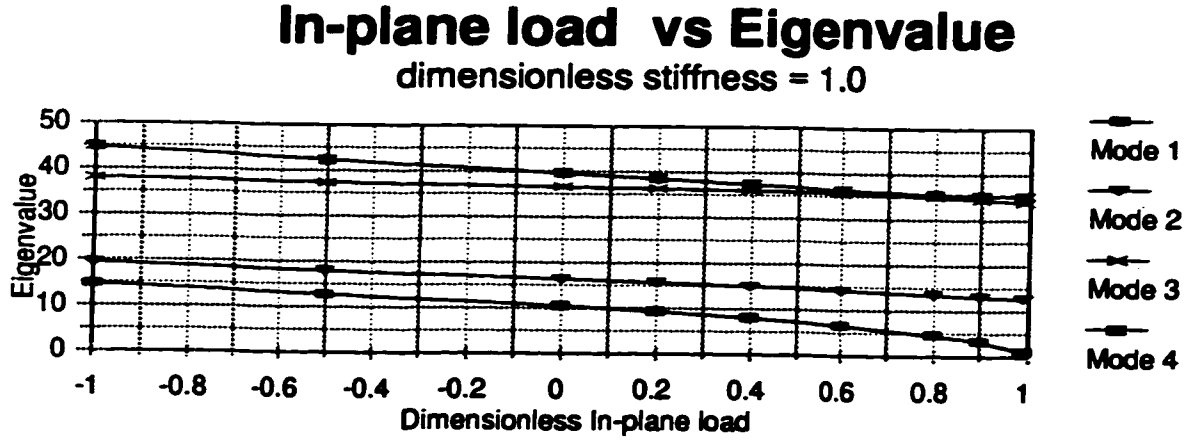

Figure 4.11, SFTF Plate, $K_{2r} = 0.5$, $\Phi = 1/1$

In-plane load = -100% of buckling load

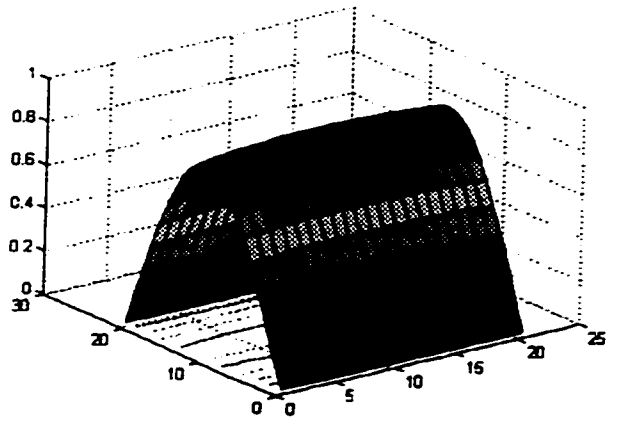

Mode 1

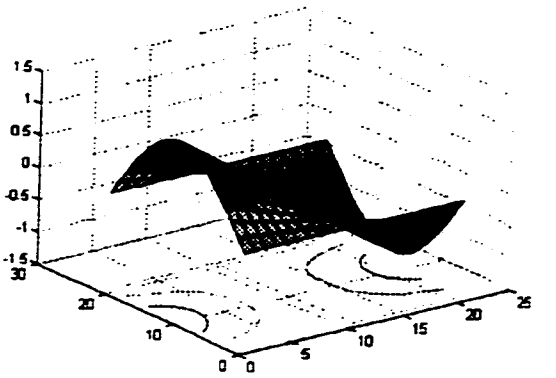

Mode 2

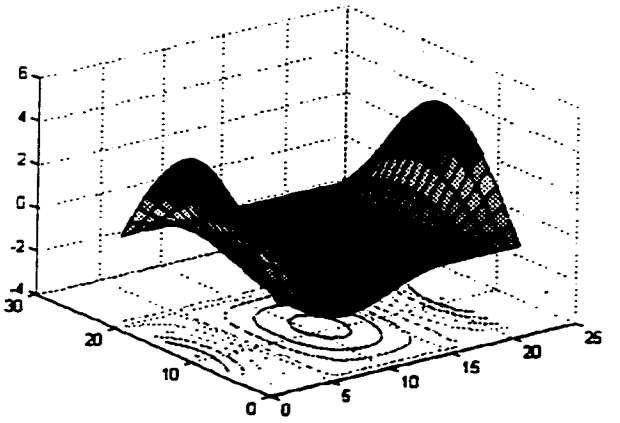

Mode 3

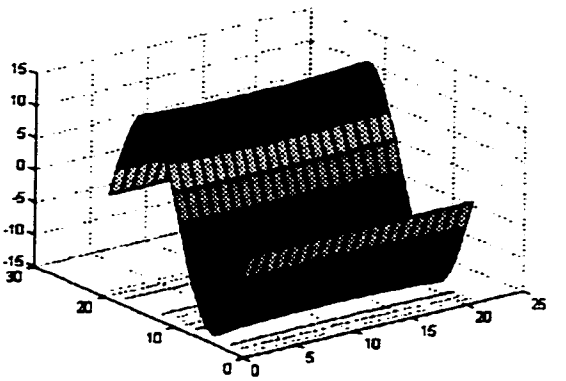

Mode 4

Figure 4.12, SFTF Plate, $K_{2r} = 0.5$, $\Phi = 1/1$

In-plane load = 99% of buckling load

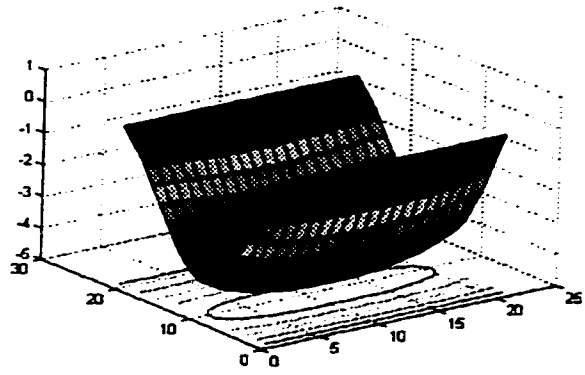

Mode 1

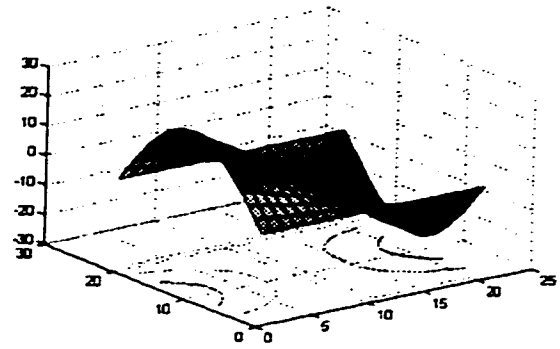

Mode 2

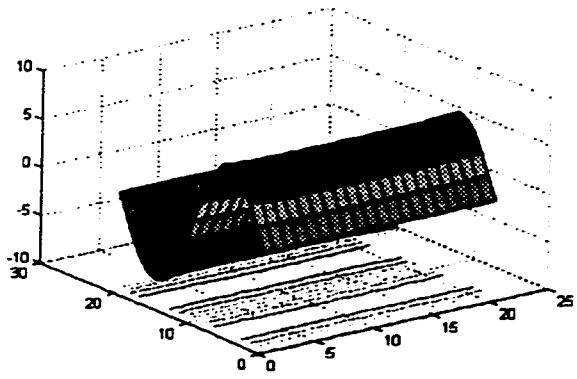

Mode 3

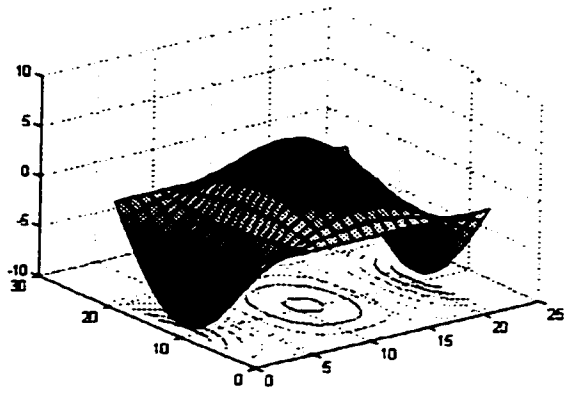

Mode 4

Figure 4.13, SFTF Plate, $K_{2r} = 30.0$, $\Phi = 1/1$

In-plane load = 99% of buckling load

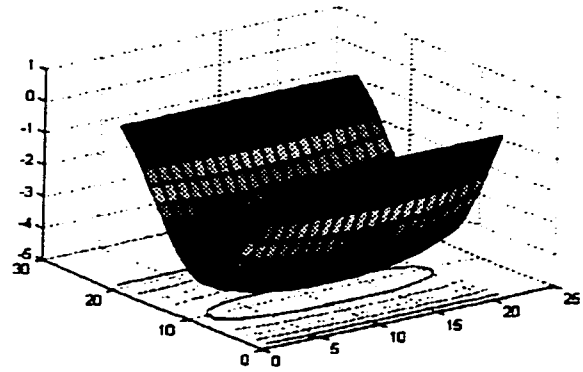

Mode 1

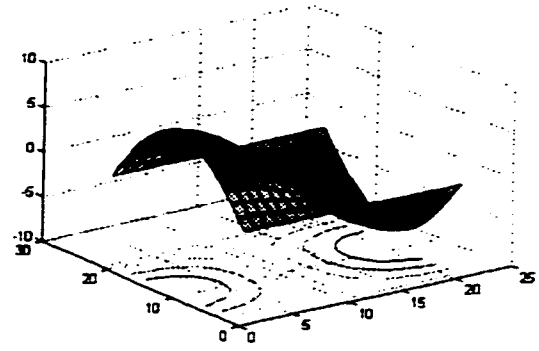

Mode 2

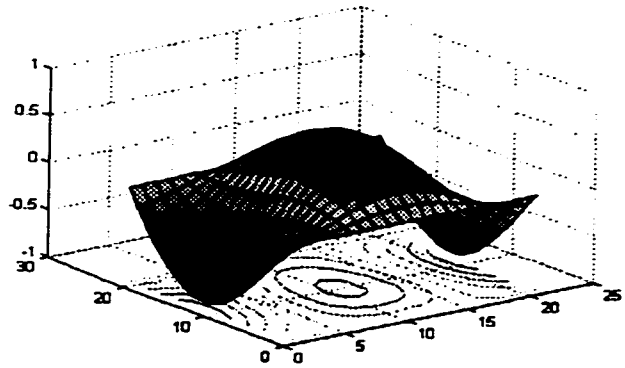

Mode 3

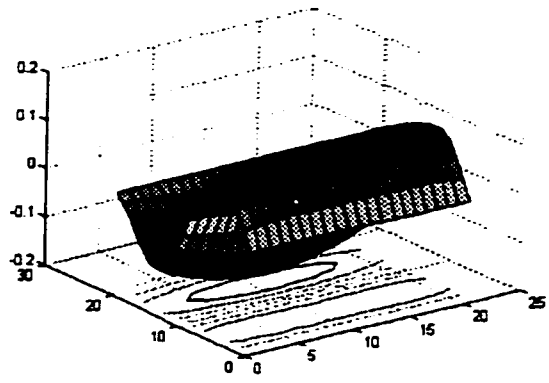

Mode 4

Tables 4.13 - 4.17 **Eigenvalues, SFTF Plate,** $\phi = 1.5 / 1$

[4.13]									
Mode	-100%	-50%	0%	20%	40%	60%	80%	90%	99%
1	14.31	12.39	10.12	9.050	7.838	6.400	4.526	3.201	1.015
2	16.62	15.00	13.19	12.39	11.53	10.60	9.595	9.046	8.522
3	25.08	24.04	22.95	22.50	22.04	21.57	21.09	20.85	20.62
4	41.51	40.89	40.26	40.01	39.75	39.49	38.88	38.35	37.86

[4.14]									
Mode	-100%	-50%	0%	20%	40%	60%	80%	90%	99%
1	14.86	12.87	10.51	9.403	8.143	6.649	4.701	3.324	1.046
2	17.10	15.41	13.50	12.65	11.75	10.77	9.687	9.098	8.535
3	25.41	24.30	23.14	22.65	22.16	21.66	21.14	20.88	20.64
4	41.71	41.05	39.93	38.81	37.65	36.46	35.23	34.60	34.02

[4.15]									
Mode	-100%	-50%	0%	20%	40%	60%	80%	90%	99%
1	15.74	13.64	11.14	9.966	8.632	7.050	4.986	3.526	1.112
2	17.88	16.06	14.00	13.09	12.11	11.04	9.851	9.200	8.572
3	25.95	24.73	23.45	22.92	22.38	21.82	21.24	20.95	20.68
4	42.05	41.31	40.56	39.49	38.22	36.91	35.56	34.86	34.22

[4.16]									
Mode	-100%	-50%	0%	20%	40%	60%	80%	90%	99%
1	16.41	14.22	11.62	10.40	9.007	7.358	5.206	3.682	1.167
2	18.48	16.57	14.40	13.44	12.40	11.26	9.993	9.294	8.617
3	26.38	25.08	23.72	23.15	22.56	21.96	21.34	21.03	20.74
4	42.33	41.53	40.73	40.09	38.74	37.34	35.89	35.15	34.46

[4.17]									
Mode	-100%	-50%	0%	20%	40%	60%	80%	90%	99%
1	16.93	14.68	12.00	10.73	9.305	7.603	5.381	3.808	1.212
2	18.95	16.97	14.72	13.72	12.64	11.45	10.12	9.380	8.662
3	26.73	25.37	23.94	23.34	22.72	22.09	21.44	21.102	20.80
4	42.56	41.72	40.87	40.52	39.21	37.74	36.23	35.44	34.72

Tables 4.18 - 4.22 Eigenvalues, SFTF Plate, $\phi = 1.5 / 1$

[illegible]

Mode	-100%	-50%	0%	20%	40%	60%	80%	90%	99%
1	17.35	15.04	12.30	11.01	9.546	7.802	5.523	3.909	1.243
2	19.33	17.30	14.99	13.95	12.83	11.60	10.22	9.455	8.706
3	27.02	25.61	24.13	23.50	22.86	22.20	21.52	21.17	20.86
4	42.75	41.88	40.99	40.63	39.62	38.11	36.54	35.73	34.98

[illegible]

Mode	-100%	-50%	0%	20%	40%	60%	80%	90%	99%
1	18.11	15.72	12.86	11.52	9.988	8.166	5.784	4.094	1.300
2	20.04	17.91	15.48	14.39	13.21	11.91	10.43	9.611	8.802
3	27.57	26.08	24.49	23.83	23.15	22.44	21.71	21.33	20.99
4	43.13	42.20	41.25	40.86	40.47	38.90	37.24	36.38	35.59

[illegible]

Mode	-100%	-50%	0%	20%	40%	60%	80%	90%	99%
1	18.63	16.17	13.24	11.86	10.29	8.415	5.962	4.222	1.344
2	20.52	18.33	15.83	14.70	13.48	12.12	10.59	9.729	8.881
3	27.96	26.41	24.77	24.07	23.36	22.62	21.86	21.46	21.10
4	43.41	42.44	41.45	41.04	40.63	39.53	37.81	36.93	36.11

[illegible]

Mode	-100%	-50%	0%	20%	40%	60%	80%	90%	99%
1	19.67	17.09	14.02	12.56	10.90	8.922	6.326	4.481	1.427
2	21.52	19.21	16.55	15.35	14.04	12.59	10.93	9.997	9.069
3	28.80	27.14	25.37	24.62	23.85	23.05	22.22	21.79	21.40
4	44.04	42.99	41.92	41.48	41.03	40.58	39.24	38.30	37.44

[illegible]

Mode	-100%	-50%	0%	20%	40%	60%	80%	90%	99%
1	20.13	17.50	14.35	12.87	11.17	9.142	6.484	4.594	1.464
2	21.96	19.60	16.87	15.64	14.30	12.80	11.09	10.12	9.162
3	29.19	27.49	25.66	24.89	24.09	23.26	22.40	21.96	21.55
4	44.36	43.27	42.06	41.70	41.24	40.78	39.97	39.02	38.13

Figure 4.14 Eigenvalue curves, SFTF plate, K_{2R}=0.5, ϕ = 1.5/1,

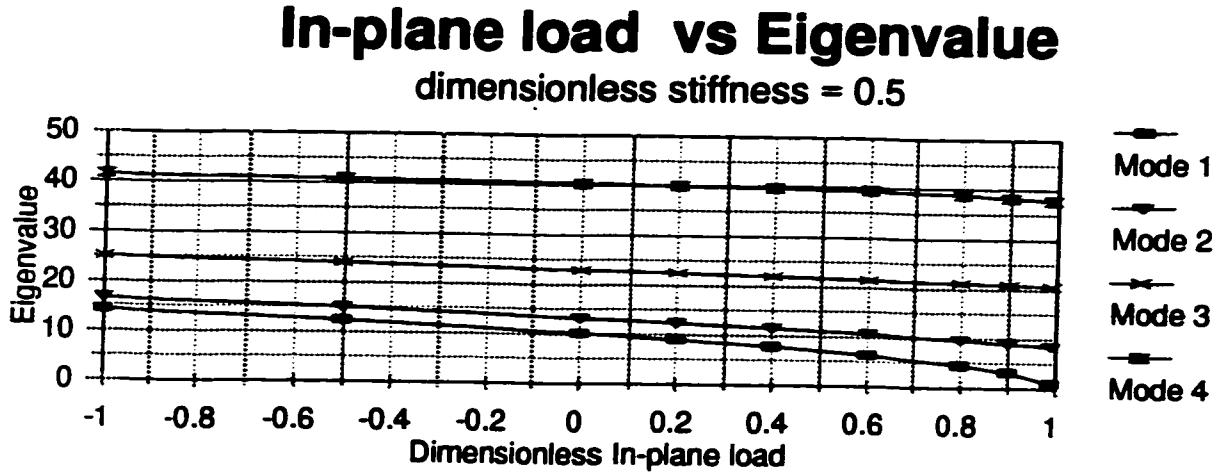

Figure 4.15 Eigenvalue curves, SFTF plate, K_{2R}=1.0, ϕ = 1.5/1,

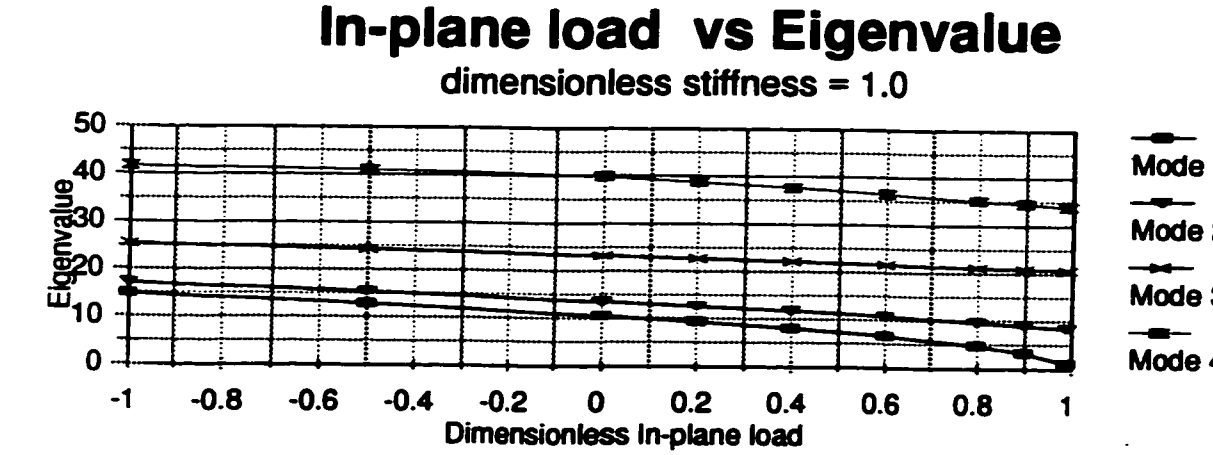

Figure 4.16, SFTF Plate, $K_{2r} = 0.5$, $\Phi = 1.5/1$

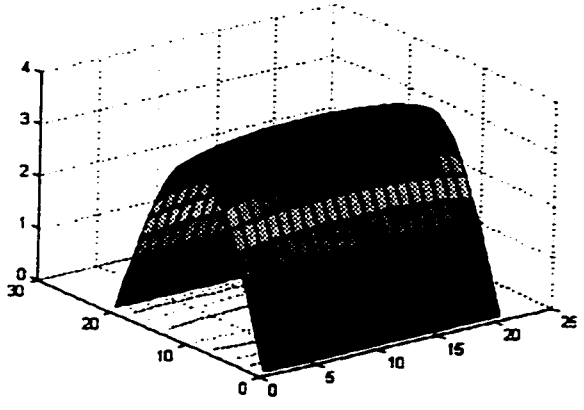

Mode 1

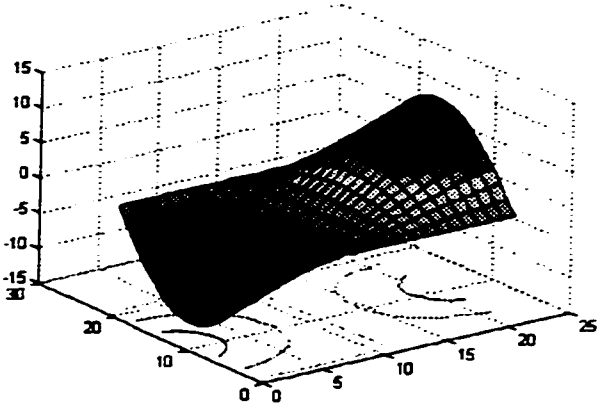

Mode 2

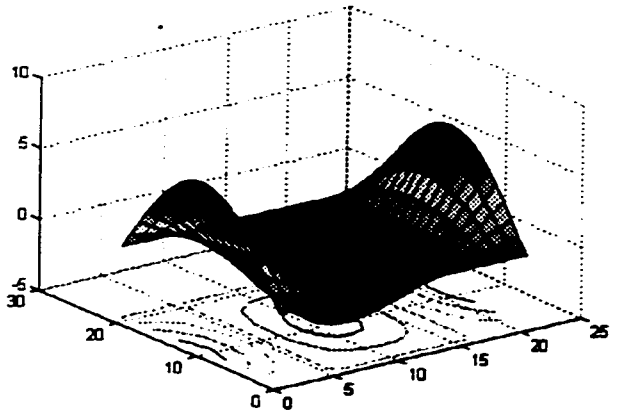

Mode 3

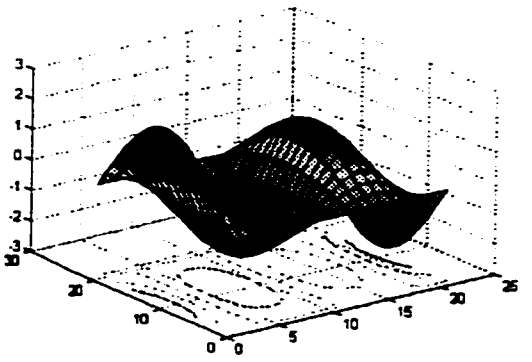

Mode 4

Figure 4.17, SFTF Plate, K_{2r} =1.0, Φ = 1.5/1

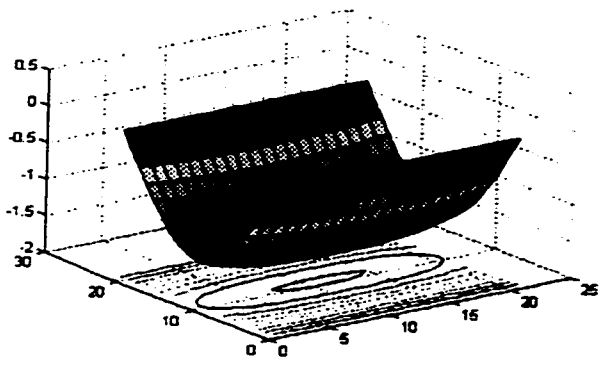

Mode 1

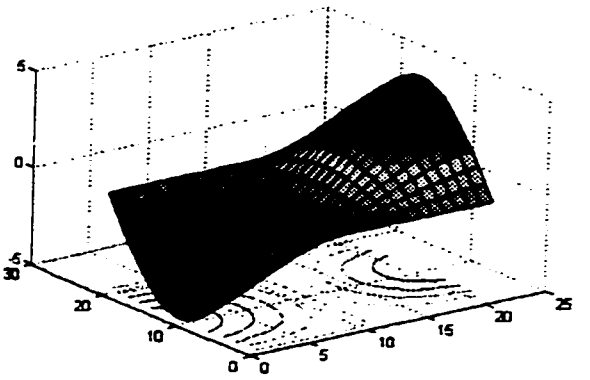

Mode 2

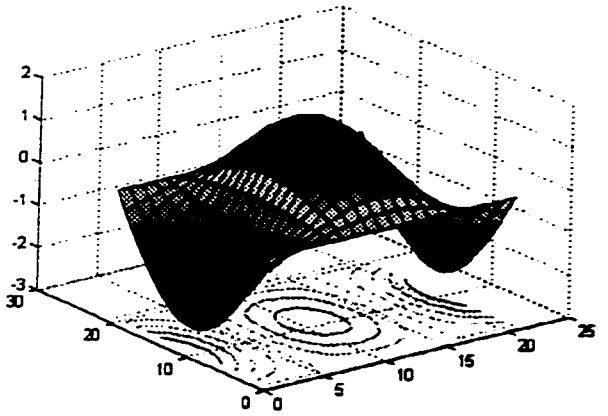

Mode 3

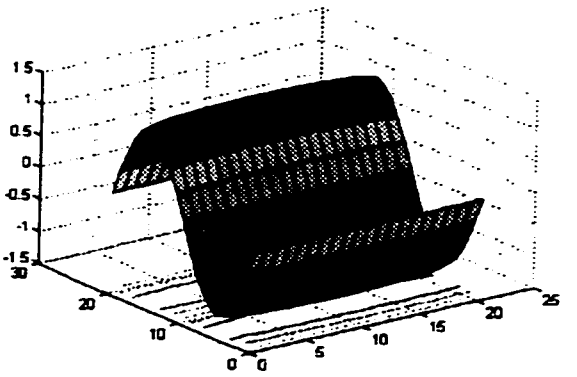

Mode 4

Table 4.23 - 4.27 Eigenvalues, TFTF Plate, $\phi = 1 / 1$

[4.23]	$K_{x,y} = 8.5$, $\phi = 1/1$ In-plane load as a percentage of Buckling load (1.0)								
Mode	-100%	-50%	0%	20%	40%	60%	80%	90%	99%
1	14.86	12.87	10.51	9.37	8.137	6.644	4.696	3.319	1.037
2	19.53	18.06	16.46	15.78	15.07	14.31	13.52	13.11	12.72
3	38.15	37.42	36.68	36.37	36.07	35.77	35.05	34.49	33.83
4	44.97	42.45	39.76	38.64	37.48	36.28	35.46	35.30	35.15

[4.24]	$K_{x,y} = 12$, $\phi = 1/1$ In-plane load as a percentage of Buckling load (1.0)								
Mode	-100%	-50%	0%	20%	40%	60%	80%	90%	99%
1	15.97	13.83	11.28	10.10	8.749	7.145	5.054	3.577	1.148
2	20.39	18.76	16.98	16.22	15.41	14.50	13.66	13.18	12.74
3	38.61	37.77	36.92	36.57	36.22	35.87	35.29	34.56	33.89
4	46.50	43.67	40.65	39.38	38.06	36.71	35.52	35.33	35.80

[4.25]	$K_{x,y} = 16.5$, $\phi = 1/1$ In-plane load as a percentage of Buckling load (1.0)								
Mode	-100%	-50%	0%	20%	40%	60%	80%	90%	99%
1	17.75	15.38	12.55	11.23	9.729	7.946	5.621	3.977	1.273
2	21.83	19.94	17.86	16.96	16.01	15.00	13.91	13.33	12.79
3	39.39	38.39	37.35	36.93	36.51	36.07	33.64	34.90	34.09
4	49.09	45.78	42.20	40.71	39.14	37.50	35.79	35.41	35.21

[4.26]	$K_{x,y} = 24$, $\phi = 1/1$ In-plane load as a percentage of Buckling load (1.0)								
Mode	-100%	-50%	0%	20%	40%	60%	80%	90%	99%
1	19.13	16.57	13.53	12.11	10.49	8.568	6.060	4.287	1.360
2	22.97	20.90	18.59	17.58	16.51	15.37	14.13	13.47	12.84
3	40.07	38.92	37.72	37.25	36.76	36.26	35.76	35.28	34.34
4	51.21	47.55	43.56	41.86	40.09	38.24	36.30	35.50	35.27

[4.27]	$K_{x,y} = 48$, $\phi = 1/1$ In-plane load as a percentage of Buckling load (1.0)								
Mode	-100%	-50%	0%	20%	40%	60%	80%	90%	99%
1	20.22	17.53	14.32	12.82	11.10	9.072	6.419	4.543	1.451
2	23.91	21.69	19.19	18.11	16.94	15.69	14.33	13.59	12.90
3	40.63	39.37	38.06	37.53	36.99	36.44	35.88	35.60	34.65
4	52.99	49.04	44.72	42.89	40.96	38.93	36.80	35.68	35.33

Table 4.28 - 4.32 Eigenvalues, TFTF Plate, $\phi = 1 / 1$

[4.28] $K_{x,c} = -5.8$, $\phi = 1/1$, buckled out of a plane [illegible]

Mode	-100%	-50%	0%	20%	40%	60%	80%	90%	99%
1	21.13	18.32	14.97	13.40	11.61	9.487	6.712	4.748	1.500
2	24.64	22.35	19.71	18.59	17.31	15.97	14.51	13.72	12.97
3	41.13	39.77	38.36	37.79	37.20	36.60	36.00	35.69	34.96
4	54.50	50.32	45.74	43.78	41.73	39.57	37.28	36.07	35.41

[4.29] $K_{x,c} = -7.5$, $\phi = 1/1$, buckled out of a plane [illegible]

Mode	-100%	-50%	0%	20%	40%	60%	80%	90%	99%
1	22.82	19.80	16.20	14.50	12.57	10.27	7.274	5.146	1.625
2	26.19	23.62	20.72	19.43	18.05	16.55	14.89	13.99	13.13
3	42.10	40.57	38.97	38.32	37.65	36.96	36.27	35.91	35.59
4	57.44	52.85	47.81	46.54	43.35	40.94	38.38	37.09	35.77

[4.30] $K_{x,c} = -10.3$, $\phi = 1/1$, buckled out of a plane [illegible]

Mode	-100%	-50%	0%	20%	40%	60%	80%	90%	99%
1	24.00	20.83	17.06	15.28	13.25	10.83	7.616	5.435	1.732
2	27.26	24.54	21.45	20.08	18.60	15.99	15.21	14.22	13.28
3	42.86	41.18	39.45	38.74	38.01	37.27	36.51	36.12	35.77
4	59.57	54.72	49.38	47.07	44.64	42.07	39.32	37.88	36.52

[4.31] $K_{x,c} = -20.8$, $\phi = 1/1$, buckled out of a plane [illegible]

Mode	-100%	-50%	0%	20%	40%	60%	80%	90%	99%
1	26.51	23.05	18.91	16.95	14.71	12.04	8.540	6.047	1.912
2	29.59	26.56	23.11	21.56	19.88	18.03	15.96	14.81	13.68
3	44.54	42.64	40.63	39.80	38.94	38.07	37.18	36.72	36.30
4	64.43	59.07	53.14	50.57	47.86	44.97	41.87	40.23	38.70

[4.32] $K_{x,c} = -34.8$, $\phi = 1/1$, buckled out of a plane [illegible]

Mode	-100%	-50%	0%	20%	40%	60%	80%	90%	99%
1	27.66	24.07	19.76	17.72	15.39	12.60	8.942	6.334	2.004
2	30.69	27.53	23.91	22.28	20.51	18.56	16.35	15.12	13.91
3	45.41	43.38	41.26	40.37	39.46	38.53	37.56	37.07	36.62
4	66.83	61.25	55.07	52.39	49.55	46.54	43.30	41.58	39.97

Figure 4.18 Eigenvalue curves, TFTF plate, $K_{2R}=K_{4R}=0.5$, $\phi = 1/1$,

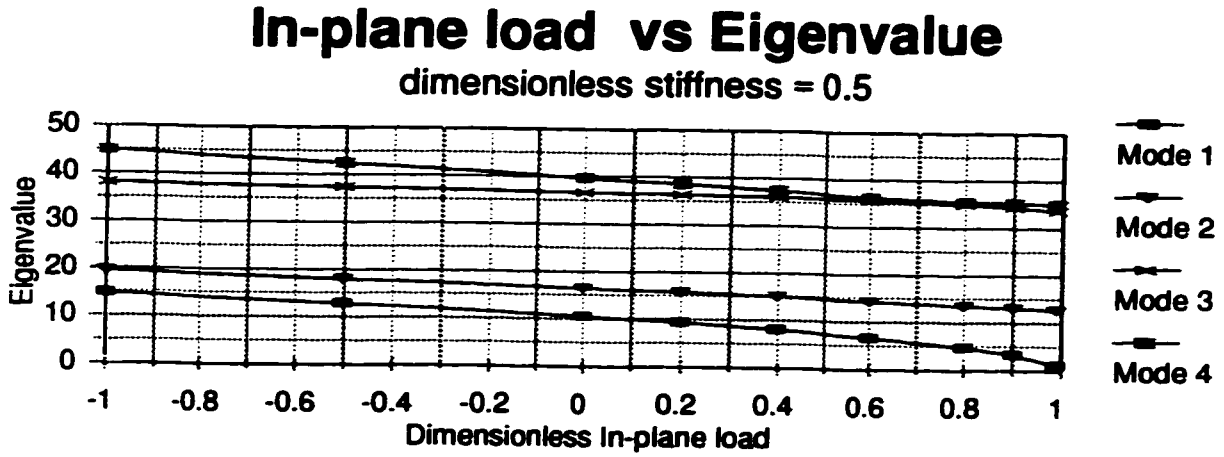

Figure 4.19 Eigenvalue curves, TFTF plate, $K_{2R}=K_{4R}=1.0$, $\phi = 1/1$,

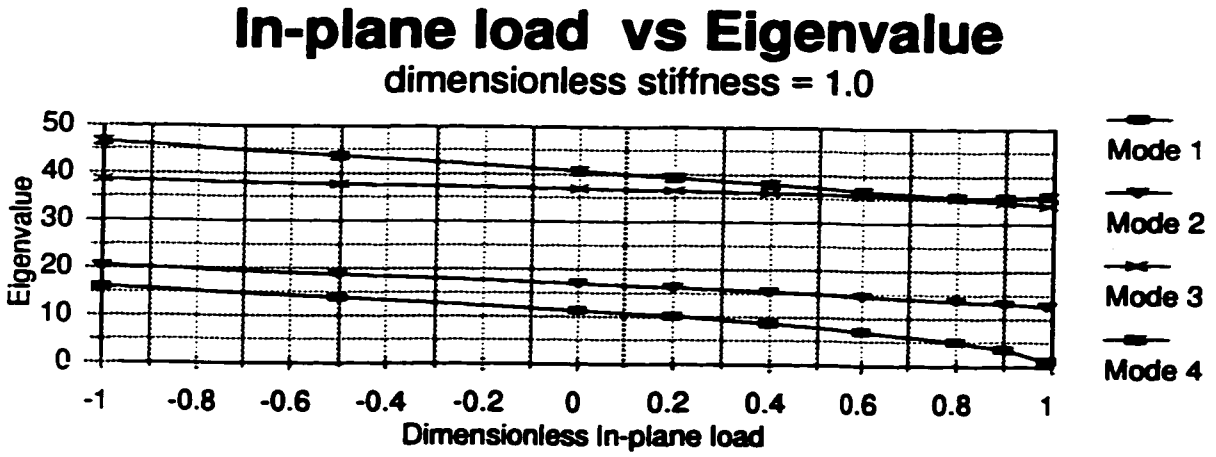

Figure 4.20, TFTF Plate, $K_{2r/4r} = 0.5$, $\Phi = 1/1$

In-plane Load = -100% of Buckling load

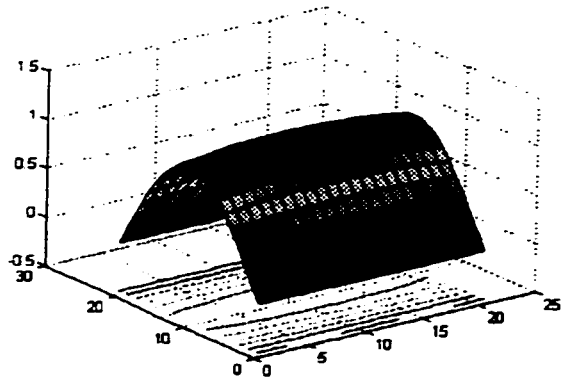

Mode 1

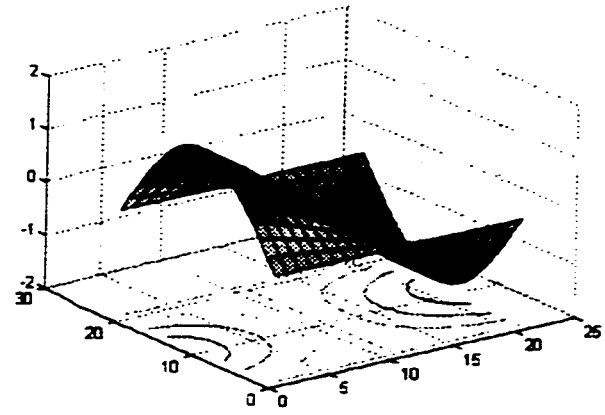

Mode 2

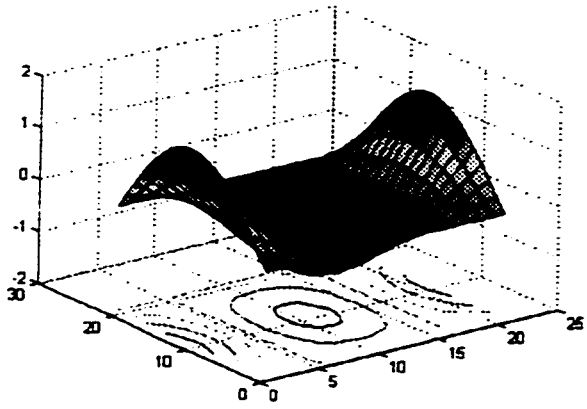

Mode 3

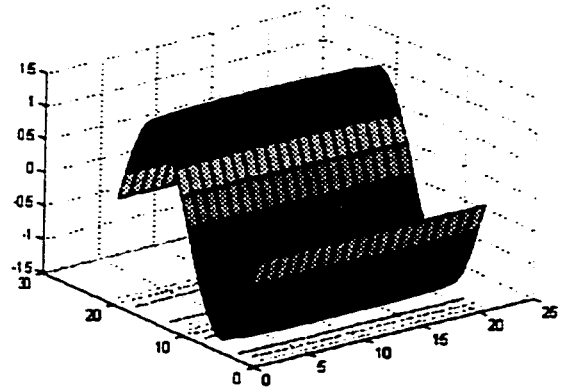

Mode 4

Figure 4.21, TFTF Plate, $K_{2r/4r} = 0.5$, $\Phi = 1/1$

In-plane Load = 99% of Buckling load

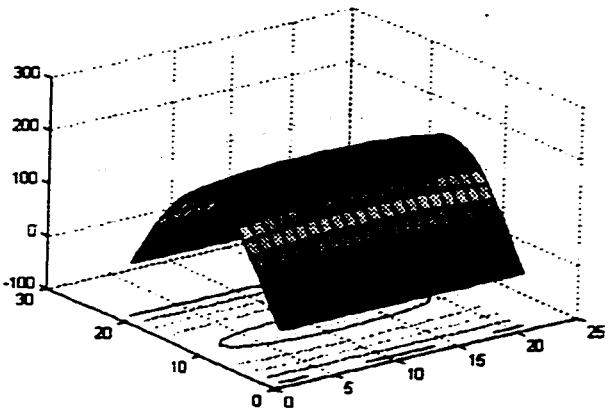

Mode 1

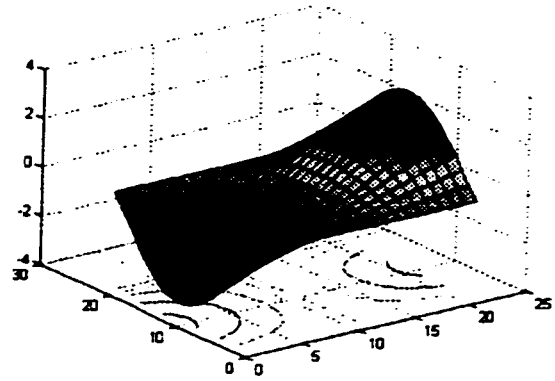

Mode 4

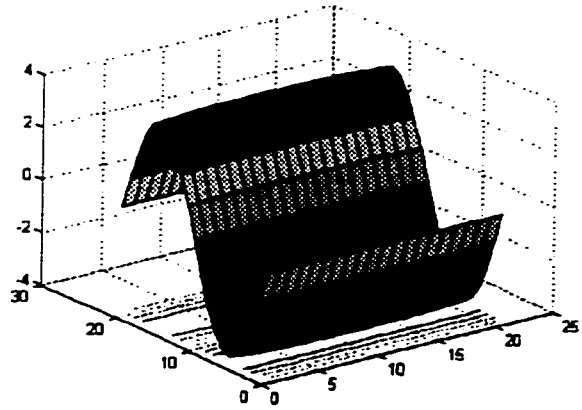

Mode 3

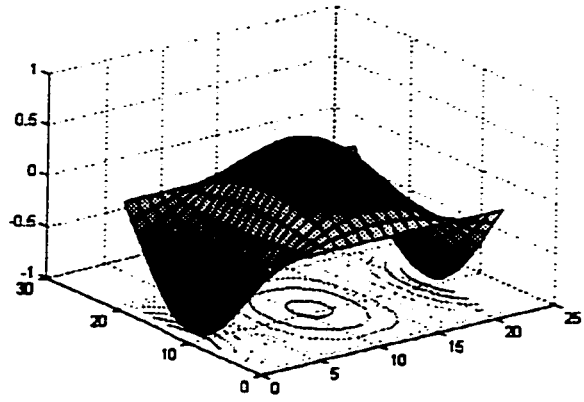

Mode 4

Figure 4.22, TFTF Plate, $K_{2r/4r} = 30.0$, $\Phi = 1/1$

In-plane Load = 99% of Buckling load

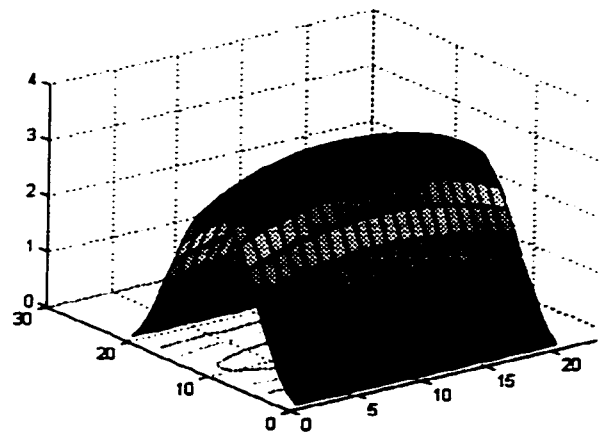

Mode 1

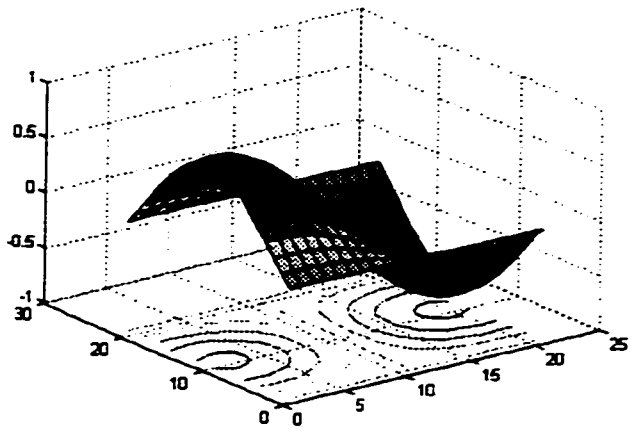

Mode 2

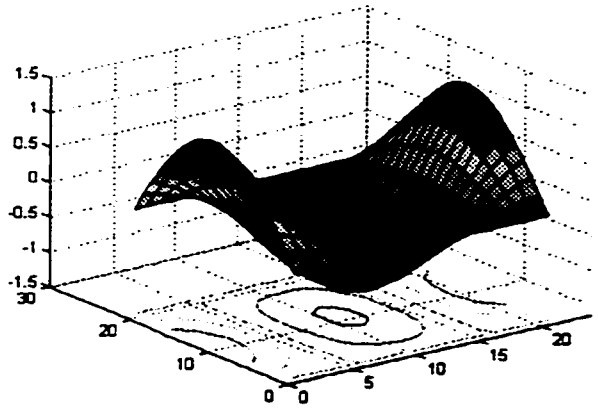

Mode 3

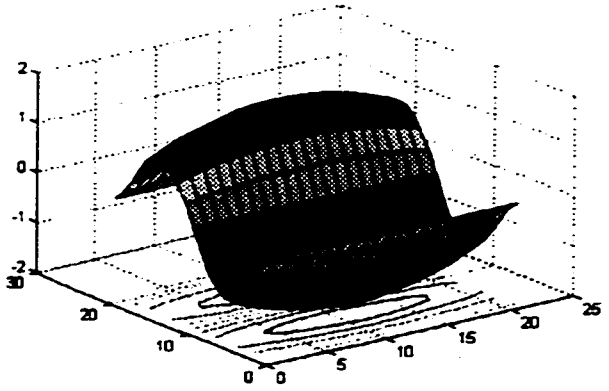

Mode 4

Table 4.33 - 4.37 Eigenvalues, TFTF Plate, $\phi = 1.5 / 1$

[4.33] $K_{y,c} = 0.5$, $\phi = 1.5/1$ In-plane load as a percentage of buckling load ($K_{y,c} = 0.5$)

Mode	-100%	-50%	0%	20%	40%	60%	80%	90%	99%
1	14.96	12.96	10.58	9.465	8.197	6.693	4.733	3.348	1.064
2	17.19	15.47	13.55	12.69	11.78	10.79	9.694	9.098	8.526
3	25.46	24.34	23.16	22.67	22.17	21.66	21.14	20.87	20.63
4	41.74	41.07	39.96	38.83	37.66	36.45	35.20	34.50	33.97

[4.34] $K_{y,c} = 1.0$, $\phi = 1.5/1$ In-plane load as a percentage of buckling load ($K_{y,c} = 1.0$)

Mode	-100%	-50%	0%	20%	40%	60%	80%	90%	99%
1	16.07	13.92	11.36	10.16	8.803	7.188	5.082	3.593	1.134
2	18.16	16.29	14.17	13.23	12.21	11.10	9.873	9.196	8.541
3	26.13	24.87	23.53	22.98	22.41	21.83	21.23	20.92	20.64
4	42.16	41.38	40.60	39.56	38.24	36.86	35.44	34.70	34.03

[4.35] $K_{y,c} = 2.0$, $\phi = 1.5/1$ In-plane load as a percentage of buckling load ($K_{y,c} = 2.0$)

Mode	-100%	-50%	0%	20%	40%	60%	80%	90%	99%
1	17.84	15.45	12.62	11.29	9.778	7.984	5.646	3.991	1.255
2	19.75	17.63	15.21	14.12	12.94	11.65	10.19	9.378	8.579
3	27.27	25.78	24.19	23.52	22.84	22.13	21.40	21.03	20.68
4	42.88	41.95	40.99	40.60	39.31	37.66	35.93	35.04	34.22

[4.36] $K_{y,c} = 3.0$, $\phi = 1.5/1$ In-plane load as a percentage of buckling load ($K_{y,c} = 3.0$)

Mode	-100%	-50%	0%	20%	40%	60%	80%	90%	99%
1	19.21	16.65	13.60	12.17	10.53	8.606	6.087	4.305	1.360
2	21.01	18.69	16.04	14.84	13.54	12.10	10.47	9.542	8.626
3	28.21	26.53	24.74	23.99	23.21	22.40	21.57	21.14	20.74
4	43.49	42.43	41.33	40.89	40.26	38.40	36.44	35.42	34.47

[4.37] $K_{y,c} = 4.0$, $\phi = 1.5/1$ In-plane load as a percentage of buckling load ($K_{y,c} = 4.0$)

Mode	-100%	-50%	0%	20%	40%	60%	80%	90%	99%
1	20.31	17.60	14.38	12.87	11.15	9.109	6.444	4.559	1.447
2	22.02	19.55	16.72	15.44	14.04	12.49	10.70	9.690	8.675
3	28.99	27.17	25.22	24.39	23.54	22.65	21.72	21.25	20.81
4	44.02	42.84	41.64	41.14	40.64	39.08	36.94	35.81	34.77

Table 4.38 - 4.42 Eigenvalues, TFTF Plate, $\phi = 1.5 / 1$

[illegible]

Mode	-100%	-50%	0%	20%	40%	60%	80%	90%	99%
1	21.21	18.39	15.03	13.45	11.66	9.524	6.739	4.767	1.507
2	22.86	20.28	17.30	15.94	14.47	12.81	10.91	9.822	8.724
3	29.65	27.72	25.63	24.75	23.83	22.87	21.87	21.25	20.87
4	44.47	43.21	41.91	41.37	40.83	39.71	37.41	36.21	35.09

[illegible]

Mode	-100%	-50%	0%	20%	40%	60%	80%	90%	99%
1	22.90	19.87	16.26	14.55	12.62	10.31	7.300	5.165	1.632
2	24.45	21.65	18.40	16.92	15.29	13.46	11.34	10.10	8.842
3	30.94	28.79	26.46	25.46	24.42	23.34	22.19	21.60	21.05
4	45.37	43.94	42.47	41.86	41.24	40.61	38.51	37.15	35.89

[illegible]

Mode	-100%	-50%	0%	20%	40%	60%	80%	90%	99%
1	24.08	20.90	17.12	15.33	13.29	10.87	7.700	5.449	1.724
2	25.58	22.62	19.19	17.62	15.89	13.94	11.66	10.32	8.948
3	31.88	29.58	27.08	26.00	24.88	23.70	22.46	21.81	21.21
4	46.05	44.51	42.90	42.24	41.57	40.89	39.45	38.00	36.64

[illegible]

Mode	-100%	-50%	0%	20%	40%	60%	80%	90%	99%
1	26.59	23.12	18.97	17.00	14.76	12.08	8.569	6.069	1.926
2	28.00	24.74	20.93	19.18	17.24	15.04	12.42	10.87	9.239
3	33.97	31.38	28.53	27.29	25.99	24.63	23.17	22.40	21.68
4	47.64	45.86	43.87	43.22	42.43	41.63	40.80	40.38	38.81

[illegible]

Mode	-100%	-50%	0%	20%	40%	60%	80%	90%	99%
1	27.76	24.15	19.82	17.78	15.44	12.64	8.971	6.354	2.008
2	29.13	25.73	21.76	19.92	17.89	15.56	12.80	11.14	9.398
3	34.99	32.27	29.26	27.95	26.57	25.11	23.55	22.73	21.95
4	48.46	46.56	44.57	43.75	42.90	42.04	41.16	40.71	40.07

Figure 4.23 Eigenvalue curves, TFTF plate, $K_{2R}=K_{4R}=1.0$, $\phi = 1.5/1$,

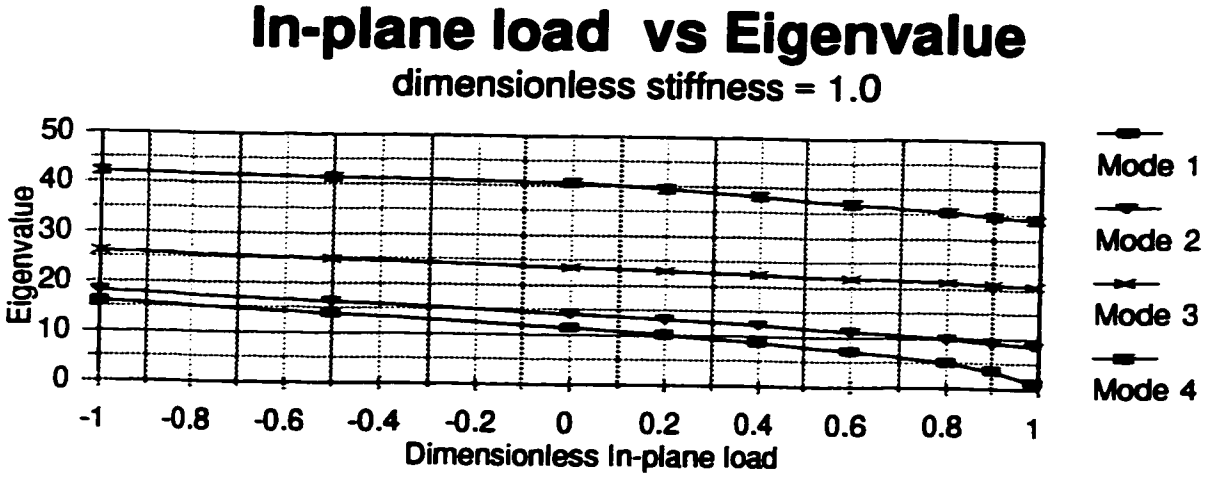

Figure 4.24 Eigenvalue curves, TFTF plate, $K_{2R}=K_{4R}=7.5$, $\phi = 1.5/1$,

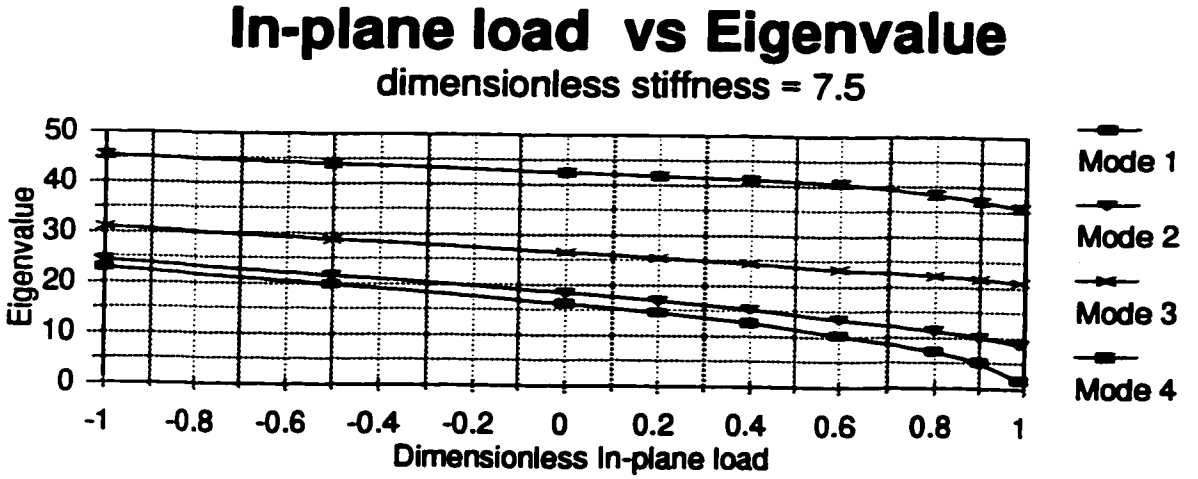

Figure 4.25, TFTF Plate, $K_{2r/4r} = 0.5$, $\Phi = 1.5/1$

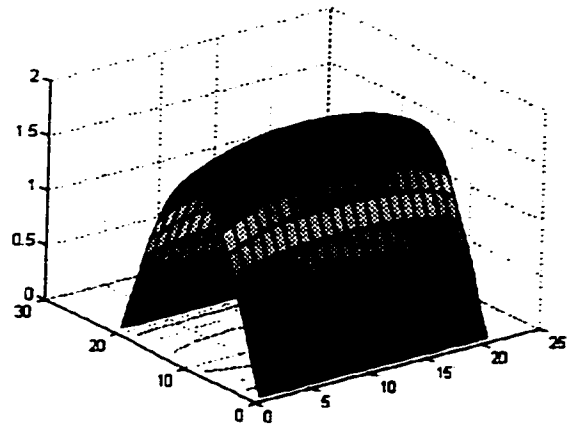

Mode 1

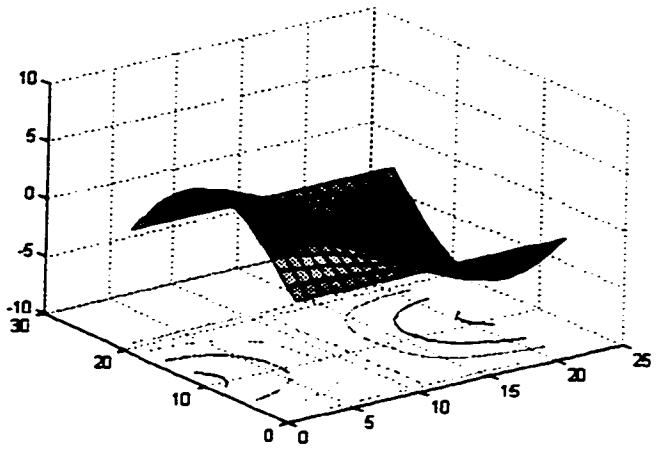

Mode 2

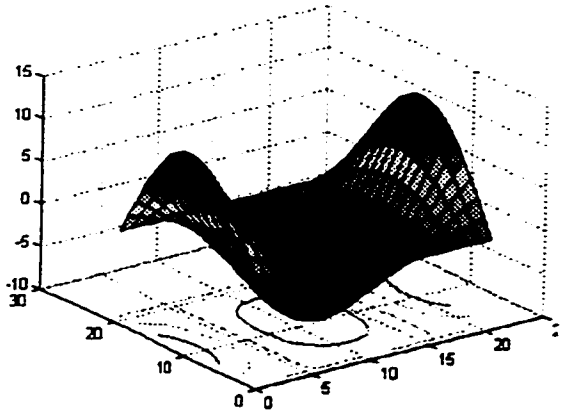

Mode 3

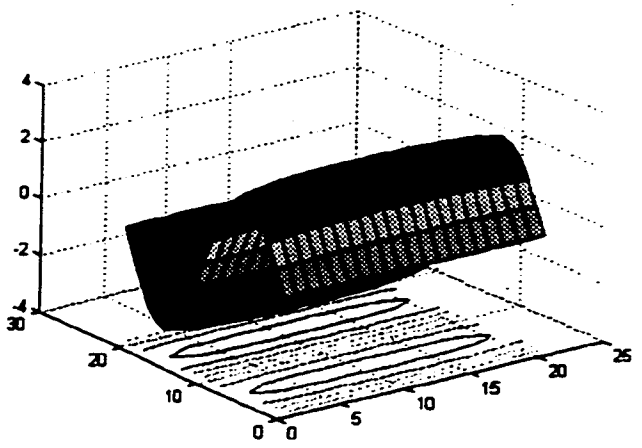

Mode 4

Figure 4.26, TFTF Plate, $K_{2r/4r} = 1.0$, $\Phi = 1.5/1$

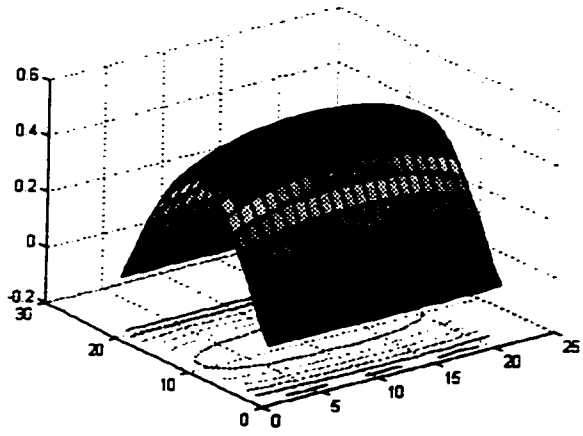

Mode 1

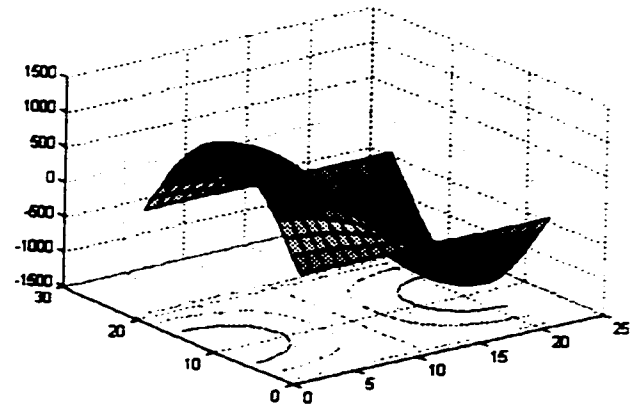

Mode 2

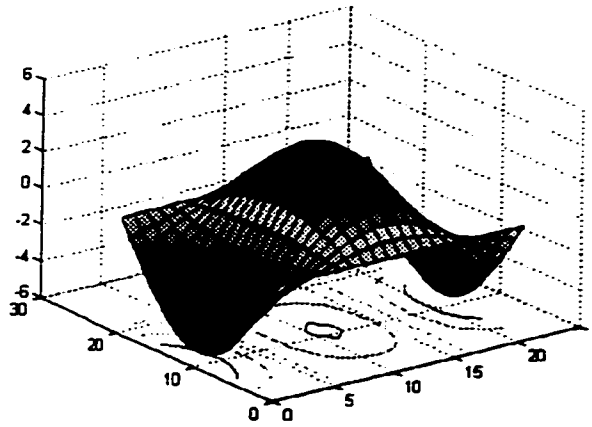

Mode 3

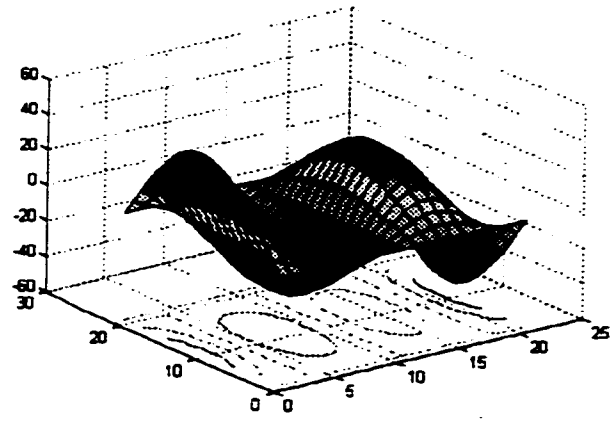

Mode 4

Chapter 5

Discussion of Results and Conclusion

Chapter 4 presents the results of buckling and free vibration analysis of SFTF and TFTF plates with the help of various graphs and mode shapes.

The method of superposition is successfully utilized to obtain highly accurate and convergent results. All results are obtained using a single FORTRAN program (listed in Appendix D) for each plate examined. As mentioned earlier, equal stiffnesses are considered at opposite ends of all TFTF analysed.

5.1 Buckling Analysis Results

It is known that simply supported edges have zero rotational stiffness, hence zero moment at the edge, while ideal clamped edge supports have infinite stiffness, hence, zero slope at the edge. Based on this, as stiffness of the rotational elastic edge (T) is non-zero and finite, buckling loads of the SFTF plate should be greater than the buckling loads of the SFSF plate and less than those of SFCF plate, while limits of the TFTF plate buckling loads are those of SFSF and CFCF plates.

From the Table 5.1, of Michelussi[4], and Tables 5.2 and 5.3, it can be stated that, the buckling analysis results are in good agreement.

Buckling load curves indicate that a plate's critical load increases with aspect ratio, which can be explained from the fact that, as the plate aspect ratio increases, the length of its free edge decreases, making the plate more stiff. It is also observed that as the plate aspect ratio approaches zero, plate behaviour approaches the behaviour of a beam with similar boundary conditions. This phenomenon has been well explained and presented by Gorman[2].

Buckling loads of SFSF, SFCF, and CFCF plates									
Plate\ϕ	1/3.0	1/2.5	1/2.0	1/1.5	1/1	1.5/1	2.0/1	2.5/1	3.0/1
SFSF	0.998	1.429	2.249	4.046	9.276	21.235	38.122	59.932	86.665
SFCF	2.073	3.004	4.732	8.502	19.397	44.142	78.963	123.85	178.82
CFCF	4.145	6.005	9.447	16.928	34.451	87.158	155.56	243.67	351.48

Table 5.1 Critical Buckling loads of SFSF, SFCF and CFCF plates[4].

Buckling Loads of SFTF Rectangular Plate										
$\phi\backslash K_{2r}$	0.5	1.0	2.0	3.0	4.0	5.0	7.5	10.0	20.0	30.0
1/1	10.20	11.00	12.29	13.27	14.03	14.63	15.70	16.39	17.69	18.21
1.5/1	23.32	25.12	28.02	30.23	31.95	33.32	35.74	37.30	40.25	41.43
3.0/1	95.01	102.21	113.84	122.72	129.64	135.15	144.89	151.19	163.11	167.88

Table 5.2 Critical Buckling loads of SFTF plate for Φ = 1/1, 1.5/1 and 3.0/1.

Buckling Loads of TFTF Rectangular Plate										
$\phi\backslash K_{2r4r}$	0.5	1.0	2.0	3.0	4.0	5.0	7.5	10.0	20.0	30.0
1/1	11.18	12.89	15.85	18.29	20.31	22.01	25.21	27.42	31.94	33.86
1.5/1	25.51	29.38	36.05	41.54	46.10	49.93	57.16	62.17	72.39	76.75
3.0/1	103.78	119.25	145.94	167.95	186.26	201.61	230.65	250.80	291.96	309.52

Table 5.3 Critical Buckling loads of TFTF plate for Φ = 1/1, 1.5/1 and 3.0/1.

5.2 Free Vibration Analysis Results

Once again, with the same reasoning, given in section 5.1, eigenvalues of SFTF and TFTF

plates can be compared in the limit with eigenvalues of SFSF, SFCF and CFCF plates.

		In-plane load as a percentage of buckling load								
	Mode	-100%	-50%	0%	20%	40%	60%	80%	90%	99%
SFSF	1	13.53	11.72	9.57	8.56	7.41	6.05	4.28	3.03	0.96
	2	18.54	17.26	15.88	15.30	14.68	14.05	13.38	13.03	12.71
	3	37.66	37.04	36.42	36.17	35.91	35.66	34.81	34.28	33.80
	4	43.26	41.09	38.79	37.84	36.86	35.85	35.40	35.27	35.15.
SFCF	1	21.20	18.44	15.13	13.56	11.78	9.64	6.84	4.84	1.53
	2	25.11	2.86	20.84	19.24	18.06	16.79	15.40	14.66	13.95
	3	42.00	40.73	39.42	38.89	38.34	37.79	37.22	36.94	36.68
	4	57.11	53.35	49.30	47.58	45.79	43.94	42.00	40.99	40.07
CFCF	1	30.88	26.89	22.11	19.83	17.23	14.12	10.03	7.11	2.25
	2	33.82	30.27	26.19	24.34	22.32	20.07	17.51	16.06	14.63
	3	48.12	45.78	43.29	42.24	41.16	40.05	38.90	38.31	37.77
	4	74.05	67.87	61.02	58.04	54.88	51.52	47.90	45.98	44.18

Table 5.4 Eigenvalues of square SFSF, SFCF, and CFCF plates[4].

From the Table 5.4, of Michelussi[4] and Table 5.5, it can be stated that, the buckling analysis results are quite comparable to those of Michelussi[4]. Note that the results presented in the Tables 5.4 and 5.5, are for a square plate.

As mentioned earlier, all results obtained are accurate to 4 digits. From the characteristic nature of Fourier series, it is known that the accuracy of results depends upon the number of terms used in the Fourier expansions. More accuracy is obtained with more terms. Eleven terms are used in the FORTRAN program, to obtain results throughout the analysis with a 4 digit accuracy. The accuracy can be confirmed from the results obtained by the previous researchers, particularly from Michelussi[4], who worked on plates with classical boundary conditions.

	Mode	-100%	-50%	0%	20%	40%	60%	80%	90%	99%
SFTF	1	14.20	12.29	10.04	8.980	7.777	6.351	4.493	3.179	1.019
K_{2r}=0.5	2	19.03	17.66	16.17	15.54	14.88	14.18	13.45	13.07	12.72
	3	37.90	37.23	36.55	36.27	35.99	35.71	34.94	34.36	33.83
	4	44.11	41.77	39.28	38.24	37.17	36.08	35.43	35.29	35.16
SFTF	1	20.03	17.41	14.28	12.80	11.11	9.092	6.446	4.564	1.436
K_{2r}=30	2	23.96	21.85	19.50	18.47	17.37	16.19	14.91	14.23	13.58
	3	40.99	39.83	38.62	38.13	37.63	37.12	36.61	36.35	36.11
	4	54.17	50.60	46.76	45.13	43.44	41.68	39.84	38.89	38.01
TFTF	1	14.86	12.87	10.51	9.37	8.137	6.644	4.696	3.319	1.037
$K_{2r}=K_{4r}$	2	19.53	18.06	16.46	15.78	15.07	14.31	13.52	13.11	12.72
=0.5	3	38.15	37.42	36.68	36.37	36.07	35.77	35.05	34.49	33.83
	4	44.97	42.45	39.76	38.64	37.48	36.28	35.46	35.30	35.15
TFTF	1	27.66	24.07	19.76	17.72	15.39	12.60	8.942	6.334	2.004
$K_{2r}=K_{4r}$	2	30.69	27.53	23.91	22.28	20.51	18.56	16.35	15.12	13.91
=30	3	45.41	43.38	41.26	40.37	39.46	38.53	37.56	37.07	36.62
	4	66.83	61.25	55.07	52.39	49.55	46.54	43.30	41.58	39.97

Table 5.5 Eigenvalues of square SFTF and TFTF plates for stiffness values 0.5 and 30.

Eigenvalue curves presented in section 4.2, Figures 4.9, 4.10, 4.18, 4.19, of square plate, demonstrate the fact that compressive in-plane loads decrease the natural frequency of a plate while tensile in-plane loads have the opposite effect. It is also observed that the trends in both SFTF and TFTF plates are equivalent. SFTF plate eigenvalues ranged from SFSF plate to SFCF plate, while TFTF plate eigenvalues ranged from SFSF plate to CFCF plate.

The associated first four mode shapes have been depicted using three-dimensional surface and

contour plots. The mode shapes are presented for only particular plate configurations. All modes shapes are produced using graphical components of MATLAB. In the process of obtaining mode shapes, displacement data was obtained from the FORTRAN program which was stored in a data file. A translator has been written in MATLAB to convert the displacement data into matrix form. The matrix thus obtained is utilised in plotting mode shapes.

It is known that a sine function is odd while, a cosine function is even, both are orthogonal to each other and Fourier series are composed of both of these sine and cosine functions. Mode shapes will be either symmetrical or anti-symmetrical about a point midway between the edges which means that only one set of functions is contributing to the series solutions even though all terms are considered. The rest of the terms in the series will be zero. Gorman[2] avoids this inefficiency in solutions by separating symmetrical and anti-symmetrical modes of vibration for each plate examined. Although fewer terms are required, this procedure is not used here, as more building blocks are needed. This inefficiency can be overcome by high speed computers available nowadays.

5.3 Conclusion and Future Work

The superposition method has been utilized successfully to study the effects of rotational elastic edge support on buckling and free vibration of thin rectangular plates subjected to uniform in-plane loading. Accurate analytical solutions for natural frequencies and mode shapes of various plates have been obtained. Various building blocks are developed and these building blocks are exploited in obtaining solutions for plates considered. Analytical solutions thus developed are also used to obtain critical buckling loads. Effects of in-plane loads are observed in free vibration analysis.

Free vibration eigenvalues and buckling loads are computed for various plate geometries, various dimensionless rotational stiffnesses with various in-plane compressive and tensile loads. Lateral displacement is forbidden along the in-plane loaded edges and these edges may be given any desired level of rotational stiffness.

The results of the analysed plates are in good agreement, in the limit, with those of SFSF, SFCF and CFCF plates and are accurate to 4 digits.

Finally, the superposition method has evolved as a means for obtaining accurate analytical solutions for rectangular plate free vibration problems. All solutions satisfy exactly the equilibrium equations based on continuum mechanics. The method has been alfeady applied successfully to numerous plate problems by Gorman[2]. This analytical procedure can be extended to plates with combinations of elastic edge support combined with uni-direction or bi-directional in-plane loading.

Chapter 6

References

[1] Timoshenko, S. and Woinowsky-Krieger, S., *Theory of Plates and Shells*, McGraw-Hill, Toronto, 1969.

[2] Gorman, D.J., *Free Vibration Analysis of Rectangular Plates*, Elsevier North Holland Inc., New York, 1982.

[3] Leissa, A.W., *Vibration of Plates*, National Aeronautics and Space Administration, SP-160, 1969.

[4] Michelussi, D.J., "Free Vibration and Buckling Analysis of Thin Plate with Classical Boundary Conditions Under Unilateral In-plane Loads", M.A.Sc. Thesis, Dept. of Mechanical Engineering, University of Ottawa, August, 1996.

[5] Yu, S.D. and Gorman, D.J., "Free Vibration of Fully Clamped Rectangular Plates Subjected to Constant In-plane Loads", Proceedings of the CSME Mechanical Engineering **16**, pp 185-199, 1992.

[6] Bassily, S.F and Dickinson, S.M, "Buckling and Vibration of In-plane Loaded Plates Treated by a Unified Ritz Approach", Journal of Sound and Vibration **59**, pp 1-14, 1978.

[7] Bassily, S.F and Dickinson, S.M, "Buckling and Lateral Vibration of Rectangular Plates Subject to In-plane loads - a Ritz Approach", Journal of Sound and Vibration **24**, pp 219-239, 1972.

[8] Gorman, D.J., "A General Solution for the Free Vibration of Rectangular Plate Resting on Uniform Elastic Edge Supports", Journal of Sound and Vibration **139**, pp 325-335, 1990.

[9] Williams, D.G. and Aalami, B., *Thin Plate Design for In-plane Loading*, John Wiley & Sons, New York, 1979.

[10] Werner Soedel, *Vibration of Shells and Plates*, Marcel Dekker Inc., New York and Basel, 1981.

[11] Singiresu, S. Rao, *Mechanical Vibrations*, Addison-Wesley publishing Company, Don Mills Ontario, 1995.

[12] Rudolph Szilard, *Theory and Analysis of plates Classical and Numerical Methods*, Prentice Hall Inc., Englewood Cliffs, New Jersey, 1973.

[13] Erwin Kreyszig, *Advanced Engineering Mathematics*, Fourth Edition, John Wiley & Sons, New York, 1979.

[14] Patrick Marchand, *Graphics and GUIs with MATLAB*, CRC Press, New York, 1996.

Appendix A

Free Vibration Analysis Results

Tables A.1 - A.5 Eigenvalues, SFTF Plate, $\phi = 1 / 3.0$

[A.1] $K_p = 8.5$, $\phi = 1/3.0$ In-plane load as a percentage of buckling load (1.0)

Mode	-100%	-50%	0%	20%	40%	60%	80%	90%	99%
1	13.92	12.06	9.847	8.807	7.627	6.226	4.458	3.109	0.9654
2	40.28	39.67	38.41	37.39	36.34	35.26	34.14	33.57	33.04
3	43.16	40.86	39.06	38.81	38.56	38.31	38.05	37.92	37.81
4	87.29	86.18	85.04	84.59	84.13	83.54	82.49	81.96	81.48

[A.2] $K_p = 10$, $\phi = 1/3.0$ In-plane load as a percentage of buckling load (1.0)

Mode	-100%	-50%	0%	20%	40%	60%	80%	90%	99%
1	14.49	12.55	10.25	9.165	7.936	6.477	4.573	3.223	1.046
2	40.49	39.84	38.87	37.78	36.65	35.49	34.28	33.67	33.10
3	43.93	41.48	39.17	38.90	38.63	38.36	38.09	37.95	37.82
4	87.68	86.48	85.26	84.76	84.27	83.76	82.64	82.07	81.55

[A.3] $K_p = 12$, $\phi = 1/3.0$ In-plane load as a percentage of buckling load (1.0)

Mode	-100%	-50%	0%	20%	40%	60%	80%	90%	99%
1	15.38	13.32	10.88	9.736	8.433	6.886	4.868	3.439	1.106
2	40.84	40.12	39.38	38.48	37.24	35.95	34.62	33.94	33.31
3	45.21	42.53	39.68	39.08	38.78	38.47	38.17	38.01	37.88
4	88.35	87.01	85.65	85.10	84.55	83.99	83.02	82.39	81.81

[A.4] $K_p = 14$, $\phi = 1/3.0$ In-plane load as a percentage of buckling load (1.0)

Mode	-100%	-50%	0%	20%	40%	60%	80%	90%	99%
1	16.06	13.91	11.36	10.16	8.801	7.181	5.062	3.554	1.132
2	41.14	40.36	39.56	39.08	37.76	36.39	34.96	34.23	33.55
3	46.24	43.40	40.37	39.24	38.91	38.59	38.25	38.09	37.94
4	88.91	87.47	86.00	85.41	84.81	84.21	83.43	82.74	82.12

[A.5] $K_p = 16$, $\phi = 1/3.0$ In-plane load as a percentage of buckling load (1.0)

Mode	-100%	-50%	0%	20%	40%	60%	80%	90%	99%
1	16.57	14.36	11.74	10.51	9.102	7.434	5.252	3.703	1.179
2	41.38	40.56	39.73	39.39	38.24	36.81	35.32	34.55	33.84
3	47.08	44.12	40.96	39.62	39.04	38.70	38.35	38.17	38.01
4	89.38	87.87	86.32	85.70	85.07	84.43	83.80	83.15	82.50

Tables A.6 - A.10 Eigenvalues, SFTF Plate, $\phi = 1 / 3.0$

[illegible]

Mode	-100%	-50%	0%	20%	40%	60%	80%	90%	99%
1	16.97	14.72	12.04	10.78	9.351	7.649	5.427	3.857	1.206
2	41.59	40.74	39.87	39.52	38.68	37.20	35.66	34.87	34.14
3	47.76	44.73	41.47	40.10	39.16	38.80	38.44	38.26	38.09
4	89.79	88.21	86.61	85.96	85.31	84.65	83.99	83.58	82.90

[illegible]

Mode	-100%	-50%	0%	20%	40%	60%	80%	90%	99%
1	17.74	15.39	12.60	11.28	9.775	7.986	5.641	3.971	1.286
2	42.02	41.11	40.18	39.80	39.42	37.99	36.36	35.52	34.74
3	49.12	45.93	42.51	41.05	39.55	39.03	38.64	38.44	38.26
4	90.63	88.95	87.22	86.54	85.84	85.13	84.42	84.06	83.79

[illegible]

Mode	-100%	-50%	0%	20%	40%	60%	80%	90%	99%
1	18.24	15.83	12.97	11.62	10.07	8.239	5.834	4.124	1.312
2	42.33	41.39	40.42	40.02	39.63	38.63	36.95	36.09	35.29
3	50.08	46.80	43.28	41.78	40.24	39.23	38.82	38.61	38.43
4	91.25	89.52	87.74	87.02	86.29	85.56	84.82	84.44	84.11

[illegible]

Mode	-100%	-50%	0%	20%	40%	60%	80%	90%	99%
1	19.24	16.72	13.72	12.30	10.68	8.752	6.226	4.438	1.393
2	43.07	42.07	41.03	40.61	40.18	39.75	38.41	37.50	36.66
3	52.18	48.75	45.05	43.49	41.86	40.18	39.31	39.09	38.89
4	92.82	90.96	89.06	88.29	87.51	86.73	85.93	85.53	85.17

[illegible]

Mode	-100%	-50%	0%	20%	40%	60%	80%	90%	99%
1	19.70	17.12	14.04	12.59	10.93	8.943	6.339	4.485	1.428
2	43.48	42.43	41.36	40.93	40.49	40.04	39.13	38.19	37.33
3	53.21	49.70	45.92	44.32	42.66	40.93	39.59	39.36	39.16
4	93.68	91.76	89.81	89.01	88.21	87.40	86.58	86.17	85.80

Figure A.1 Eigenvalue curves, SFTF plate, K_{2R}=0.5, ϕ = 1/3.0,

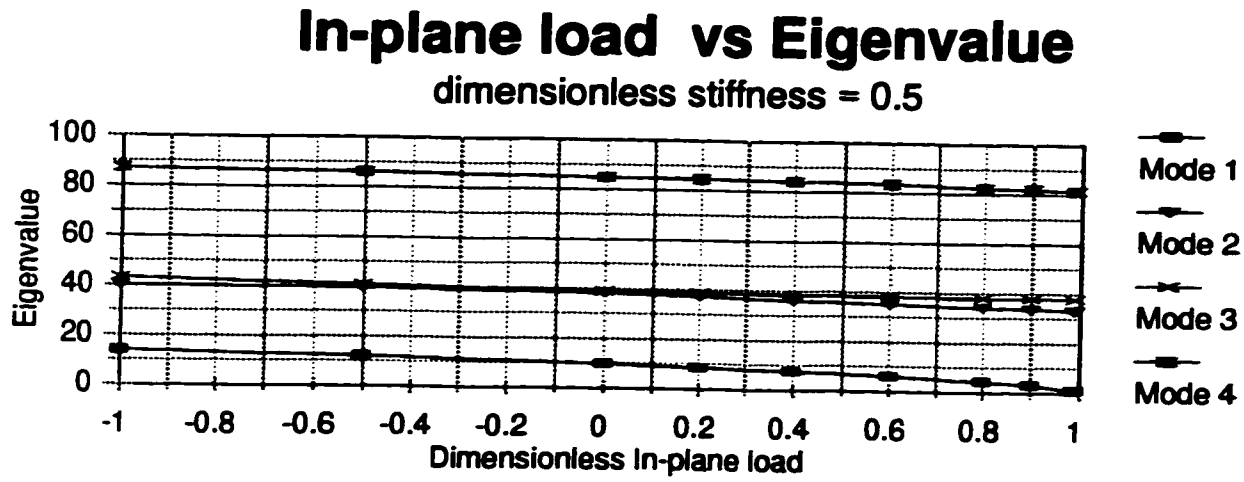

Figure A.2 Eigenvalue curves, SFTF plate, K_{2R}=30.0, ϕ = 1/3.0,

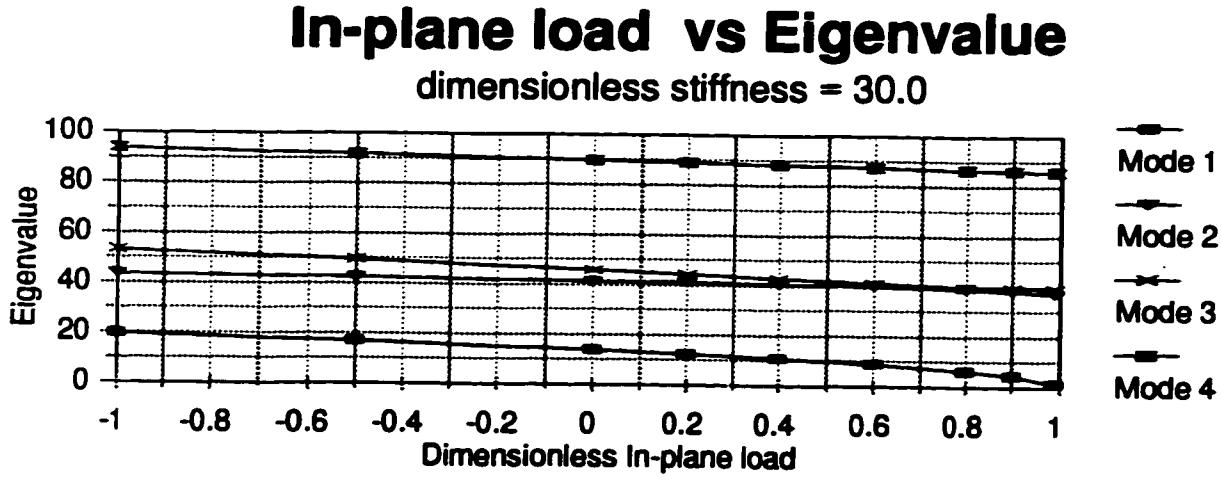

Figure A.3, SFTF Plate, $K_{2r} = 30.0$, $\Phi = 1/3.0$

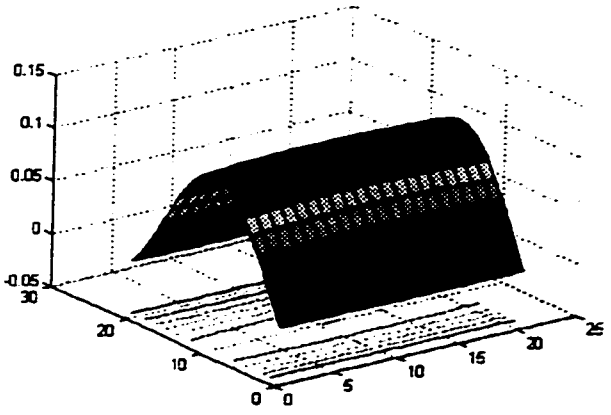

Mode 1

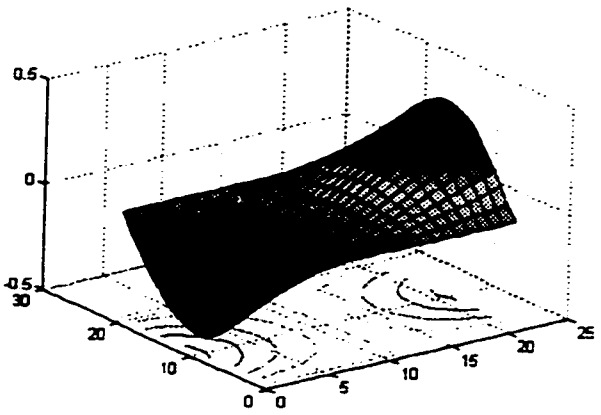

Mode 2

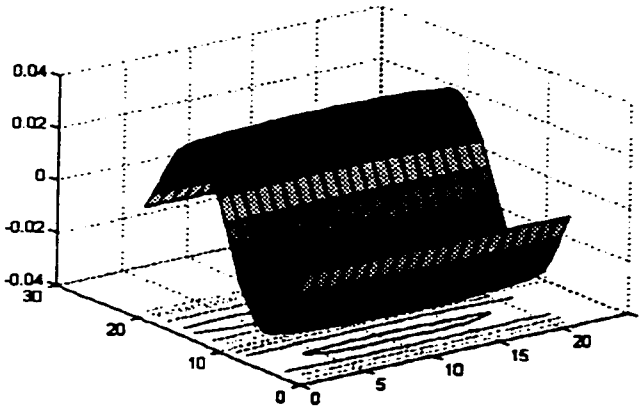

Mode 3

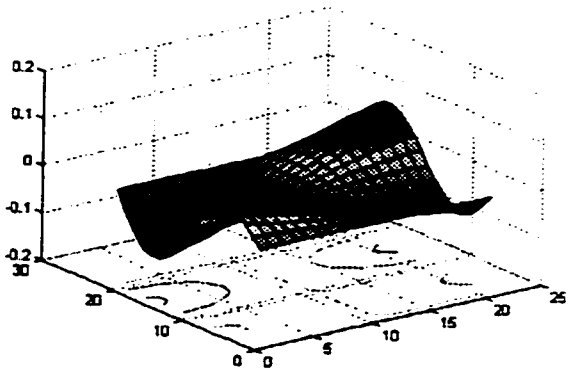

Mode 4

Tables A.11 - A.15 Eigenvalues, SFTF Plate, $\phi = 1 / 2.5$

[A.11] $K_x = 0.5$, $\phi = 1/2.5$ In-plane load as a percentage of Buckling load (1.5710)

Mode	-100%	-50%	0%	20%	40%	60%	80%	90%	99%
1	13.953	12.084	9.867	8.826	7.644	6.241	4.414	3.122	0.987
2	34.47	33.76	33.03	32.73	32.44	32.13	31.83	31.68	31.54
3	43.32	41.01	38.57	37.55	36.50	35.41	34.3	33.72	33.20
4	76.71	75.43	74.13	73.60	73.07	72.54	72.00	71.73	71.48

[A.12] $K_x = 1.0$, $\phi = 1/2.5$ In-plane load as a percentage of Buckling load (3.142)

Mode	-100%	-50%	0%	20%	40%	60%	80%	90%	99%
1	14.51	12.57	10.27	9.188	7.961	6.507	4.615	3.282	1.025
2	34.71	33.95	33.16	32.85	32.52	32.20	31.87	31.71	31.56
3	44.07	41.63	39.03	37.93	36.81	35.65	34.46	33.84	33.28
4	77.14	75.77	74.37	73.81	73.23	72.66	72.08	71.79	71.52

[A.13] $K_x = 2.0$, $\phi = 1/2.5$ In-plane load as a percentage of Buckling load (6.283)

Mode	-100%	-50%	0%	20%	40%	60%	80%	90%	99%
1	15.41	13.35	10.90	9.753	8.446	6.894	4.868	3.432	1.105
2	35.12	34.27	33.40	33.05	32.69	32.32	31.96	31.77	31.60
3	45.37	42.69	39.83	38.63	37.39	36.10	34.77	34.09	33.46
4	77.90	76.38	74.82	74.18	73.54	72.90	72.25	71.92	71.63

[A.14] $K_x = 3.0$, $\phi = 1/2.5$ In-plane load as a percentage of Buckling load (9.425)

Mode	-100%	-50%	0%	20%	40%	60%	80%	90%	99%
1	16.07	13.93	11.39	10.19	8.829	7.214	5.109	3.620	1.127
2	35.45	34.54	33.61	33.23	32.84	32.45	32.06	31.86	31.68
3	46.38	43.55	40.52	39.24	37.92	36.55	35.13	34.40	33.73
4	78.52	76.89	75.21	74.53	73.85	73.15	72.45	72.10	71.78

[A.15] $K_x = 4.0$, $\phi = 1/2.5$ In-plane load as a percentage of Buckling load (12.57)

Mode	-100%	-50%	0%	20%	40%	60%	80%	90%	99%
1	16.60	14.39	11.76	10.53	9.124	7.457	5.279	3.737	1.171
2	35.73	34.78	33.79	33.39	32.98	32.57	32.15	31.94	31.75
3	47.22	44.27	41.11	39.78	38.40	36.96	35.48	34.71	34.00
4	79.05	77.33	75.57	74.85	74.13	73.40	72.66	72.28	71.95

Tables A.16 - A.20 Eigenvalues, SFTF Plate, $\phi = 1 / 2.5$

[A.16] $K_y = 5.6$, $\phi = 1/2.5$ In-plane load as a percentage of Buckling Load (2.74)

Mode	-100%	-50%	0%	20%	40%	60%	80%	90%	99%
1	17.00	14.75	12.07	10.81	9.370	7.665	5.440	3.869	1.234
2	35.97	34.97	33.95	33.53	33.11	32.68	32.25	32.03	31.83
3	47.91	44.88	41.62	40.25	38.83	37.35	35.81	35.02	34.29
4	79.50	77.72	75.89	75.14	74.39	73.63	72.86	72.48	72.13

[A.17] $K_y = 7.5$, $\phi = 1/2.5$ In-plane load as a percentage of Buckling Load (2.74)

Mode	-100%	-50%	0%	20%	40%	60%	80%	90%	99%
1	17.77	15.42	12.62	11.30	9.801	8.014	5.676	4.017	1.270
2	36.43	35.37	34.28	33.83	33.38	32.92	32.45	32.22	32.01
3	49.27	46.08	42.66	41.21	39.70	38.14	36.52	35.68	34.90
4	80.42	78.52	76.56	75.77	74.96	74.15	73.33	72.91	72.54

[A.18] $K_y = 10.0$, $\phi = 1/2.5$ In-plane load as a percentage of Buckling Load (2.74)

Mode	-100%	-50%	0%	20%	40%	60%	80%	90%	99%
1	18.28	15.87	13.00	11.64	10.09	8.249	5.832	4.111	1.305
2	36.78	35.68	34.54	34.07	33.60	33.12	32.63	32.38	32.16
3	50.24	46.96	43.43	41.93	40.38	38.77	37.09	36.22	35.42
4	81.12	79.14	77.10	76.27	75.44	74.59	73.73	73.30	72.91

[A.19] $K_y = 20.0$, $\phi = 1/2.5$ In-plane load as a percentage of Buckling Load (2.74)

Mode	-100%	-50%	0%	20%	40%	60%	80%	90%	99%
1	19.29	16.77	13.75	12.33	10.70	8.765	6.226	4.425	1.397
2	37.56	36.38	35.16	34.66	34.15	33.64	33.11	32.85	32.61
3	52.35	48.91	45.21	43.64	42.01	40.32	38.55	37.63	36.79
4	82.76	80.65	78.48	77.60	76.70	75.80	74.88	74.42	74.00

[A.20] $K_y = 30.0$, $\phi = 1/2.5$ In-plane load as a percentage of Buckling Load (2.74)

Mode	-100%	-50%	0%	20%	40%	60%	80%	90%	99%
1	19.74	17.16	14.08	12.62	10.96	8.976	6.374	4.527	1.431
2	37.95	36.74	35.49	34.97	34.45	33.92	33.37	33.10	32.85
3	53.37	49.86	46.08	44.48	42.82	41.09	39.28	38.35	37.49
4	83.64	81.47	79.24	78.33	77.41	76.48	75.54	75.06	74.63

Figure A.4 Eigenvalue curves, SFTF plate, K_{2R}=0.5, ϕ = 1/2.5,

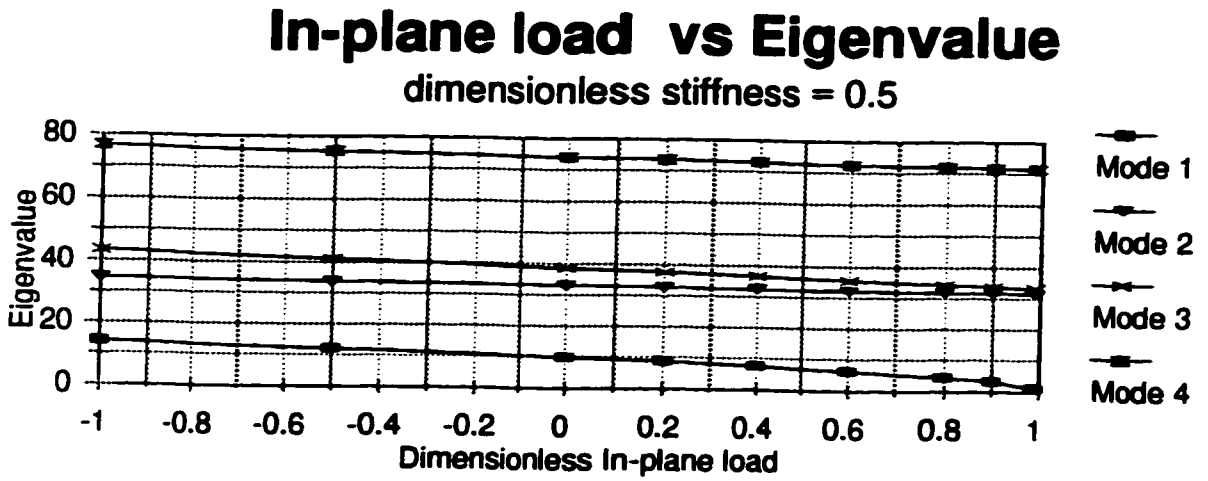

Figure A.5 Eigenvalue curves, SFTF plate, K_{2R}=30.0, ϕ = 1/2.5,

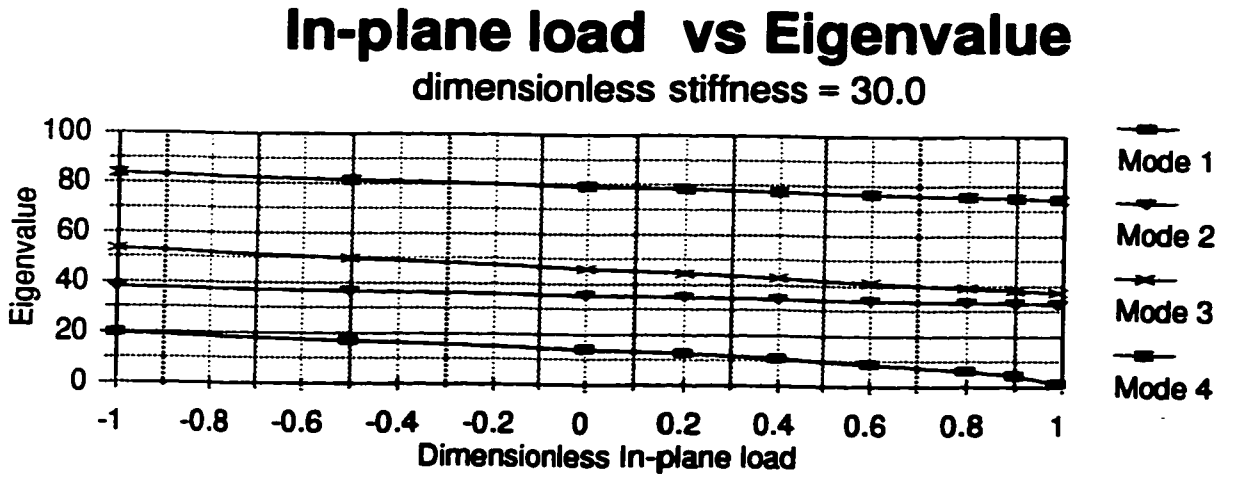

Figure A.6, **SFTF Plate,** **$K_{2r} = 0.5$, $\Phi = 1/2.5$**

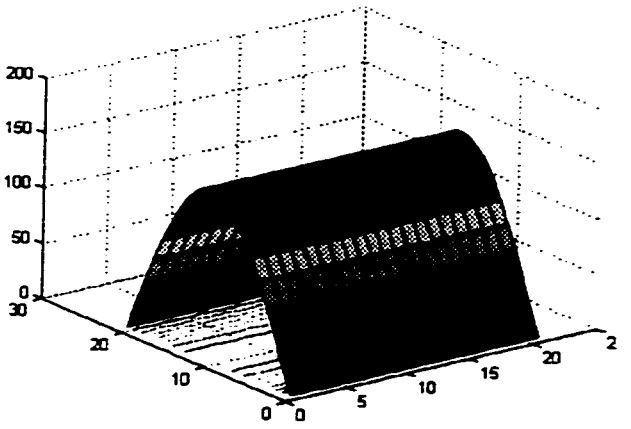

Mode 1

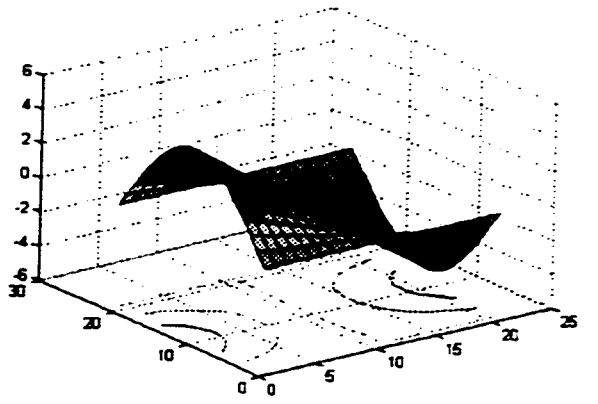

Mode 2

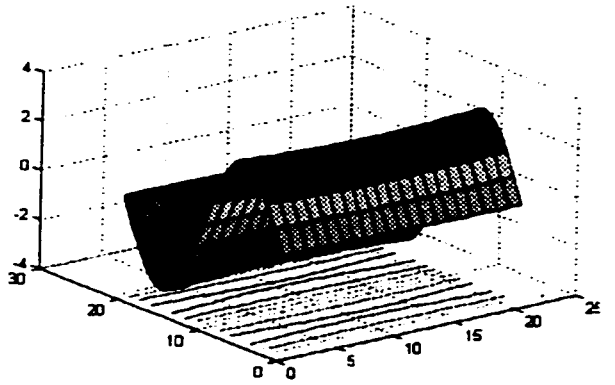

Mode 3

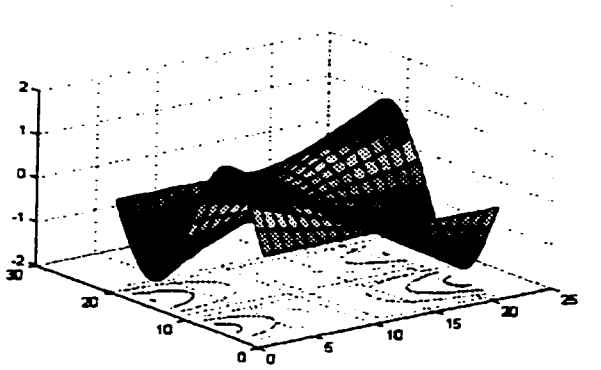

Mode 4

Table A.21 - A.25 Eigenvalues, SFTF Plate, $\phi = 1 / 2.0$

[A.21] $K_x = 0.5$, $\Phi = 1/2.0$ In-plane load as a percentage of buckling load (2.481)

Mode	-100%	-50%	0%	20%	40%	60%	80%	90%	99%
1	14.01	12.13	9.900	8.851	7.659	6.244	4.394	3.078	0.989
2	28.87	28.01	27.13	26.76	26.39	26.01	25.63	25.44	25.26
3	43.54	41.22	38.77	37.74	36.68	35.59	34.47	33.89	33.37
4	66.84	65.35	63.83	63.21	62.59	61.95	61.32	60.99	60.70

[A.22] $K_x = 1.0$, $\Phi = 1/2.0$ In-plane load as a percentage of buckling load (2.57)

Mode	-100%	-50%	0%	20%	40%	60%	80%	90%	99%
1	14.56	12.61	10.30	9.213	7.979	6.515	4.605	3.254	1.034
2	29.16	28.23	27.28	26.89	26.49	26.09	25.68	25.47	25.29
3	44.29	41.83	39.22	38.13	37.00	35.84	34.64	34.02	33.45
4	67.33	65.74	64.11	63.45	62.78	62.10	61.41	61.07	60.75

[A.23] $K_x = 2.0$, $\Phi = 1/2.0$ In-plane load as a percentage of buckling load (2.59)

Mode	-100%	-50%	0%	20%	40%	60%	80%	90%	99%
1	15.45	13.39	10.94	9.783	8.473	6.918	4.890	3.454	1.102
2	29.64	28.62	27.56	27.13	26.68	26.24	25.78	25.55	25.34
3	45.56	42.88	40.02	38.82	37.58	36.30	34.96	34.28	33.65
4	68.19	66.43	64.62	63.88	63.13	62.38	61.61	61.23	60.88

[A.24] $K_x = 3.0$, $\Phi = 1/2.0$ In-plane load as a percentage of buckling load (3.20)

Mode	-100%	-50%	0%	20%	40%	60%	80%	90%	99%
1	16.12	13.97	11.42	10.22	8.852	7.231	5.117	3.620	1.152
2	30.02	28.93	27.80	27.33	26.86	26.38	25.88	25.63	25.41
3	46.58	43.74	40.71	39.43	38.11	36.74	35.31	34.58	33.91
4	68.89	67.01	65.07	64.27	63.47	62.66	61.84	61.42	61.04

[A.25] $K_x = 4.0$, $\Phi = 1/2.0$ In-plane load as a percentage of buckling load (3.83)

Mode	-100%	-50%	0%	20%	40%	60%	80%	90%	99%
1	16.65	14.43	11.80	10.56	9.147	7.472	5.284	3.732	1.183
2	30.34	29.20	28.01	27.51	27.01	26.50	25.98	25.72	25.48
3	47.42	44.47	41.30	39.96	38.58	37.14	35.65	34.88	34.17
4	69.49	67.51	65.47	64.63	63.78	62.92	62.06	61.62	61.22

Tables A.26 - A.30 **Eigenvalues, SFTF Plate,** $\phi = 1 / 2.0$

[A.26]	$K_p = 5.0$, $\phi = 1/2.0$ In-plane load as a percentage of Buckling load (3.570)								
Mode	-100%	-50%	0%	20%	40%	60%	80%	90%	99%
1	17.07	14.80	12.10	10.83	9.387	7.668	5.421	3.826	1.223
2	30.61	29.42	28.18	27.67	27.15	26.62	26.08	25.80	25.55
3	48.13	45.08	41.81	40.43	39.00	37.52	35.97	35.18	34.44
4	70.00	67.94	65.82	64.95	64.07	63.18	62.27	61.82	61.40

[A.27]	$K_p = 7.5$, $\phi = 1/2.0$ In-plane load as a percentage of Buckling load (3.570)								
Mode	-100%	-50%	0%	20%	40%	60%	80%	90%	99%
1	17.83	15.47	12.66	11.33	9.827	8.033	5.684	4.015	1.280
2	31.12	29.86	28.54	28.00	27.44	26.87	26.29	26.00	25.73
3	49.47	46.28	42.84	41.39	39.88	38.32	36.69	35.85	35.07
4	71.00	68.82	66.56	65.64	64.70	63.75	62.78	62.29	61.85

[A.28]	$K_p = 10.0$, $\phi = 1/2.0$ In-plane load as a percentage of Buckling load (3.570)								
Mode	-100%	-50%	0%	20%	40%	60%	80%	90%	99%
1	18.33	15.91	13.03	11.68	10.13	8.290	5.882	4.176	1.311
2	31.49	30.18	28.82	28.25	27.67	27.08	26.47	26.17	25.89
3	50.43	47.14	43.61	42.12	40.57	38.96	37.28	36.41	35.61
4	71.74	69.48	67.15	66.19	65.21	64.23	63.22	62.71	62.25

[A.29]	$K_p = 20.0$, $\phi = 1/2.0$ In-plane load as a percentage of Buckling load (3.570)								
Mode	-100%	-50%	0%	20%	40%	60%	80%	90%	99%
1	19.36	16.83	13.80	12.36	10.73	8.781	6.225	4.407	1.404
2	32.32	30.92	29.45	28.84	28.22	27.58	26.92	26.59	26.28
3	52.57	49.12	45.40	43.82	42.18	40.48	38.71	37.79	36.94
4	73.51	71.10	68.60	67.57	66.53	65.47	64.39	63.84	63.35

[A.30]	$K_p = 30.0$, $\phi = 1/2.0$ In-plane load as a percentage of Buckling load (3.570)								
Mode	-100%	-50%	0%	20%	40%	60%	80%	90%	99%
1	19.81	17.22	14.13	12.66	11.00	9.005	6.395	4.541	1.429
2	32.72	31.28	29.77	29.14	28.50	27.84	27.17	26.82	26.51
3	53.59	50.06	46.27	44.66	43.00	41.26	39.45	38.51	37.65
4	74.41	71.94	69.37	68.32	67.25	66.16	65.06	64.50	63.99

Figure A.7 Eigenvalue curves, SFTF plate, K_{2R}=0.5, ϕ = 1/2.0,

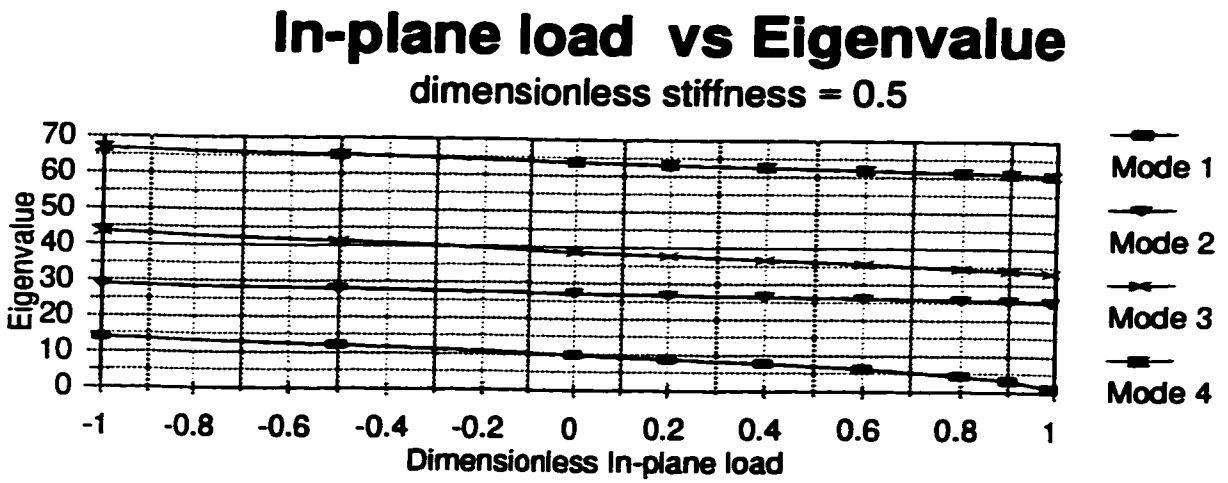

Figure A.8 Eigenvalue curves, SFTF plate, K_{2R}=30.0, ϕ = 1/2.0,

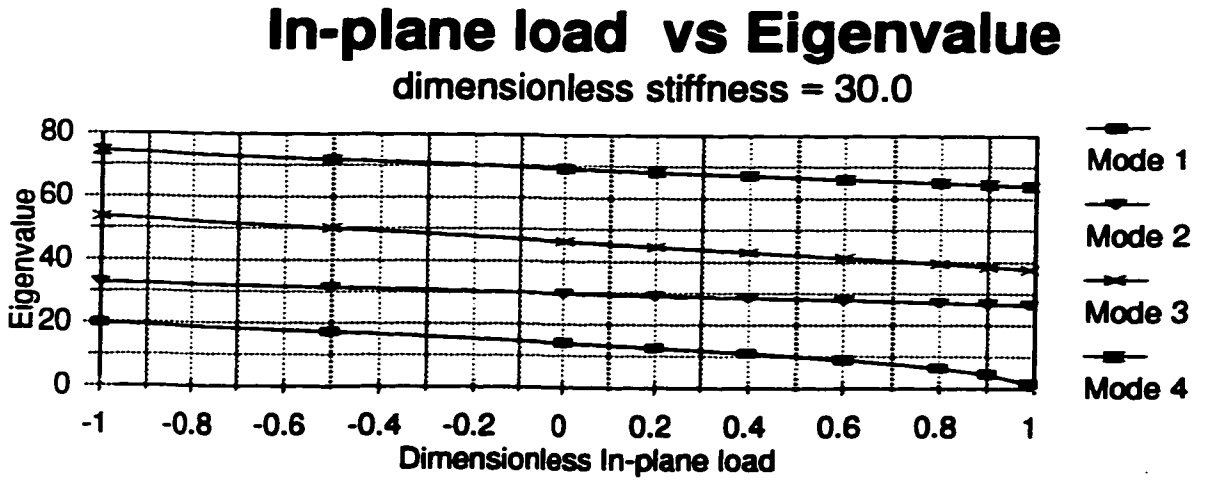

Figure A.9, **SFTF Plate,** **$K_{2r} = 30.0$, $\Phi = 1/2.0$**

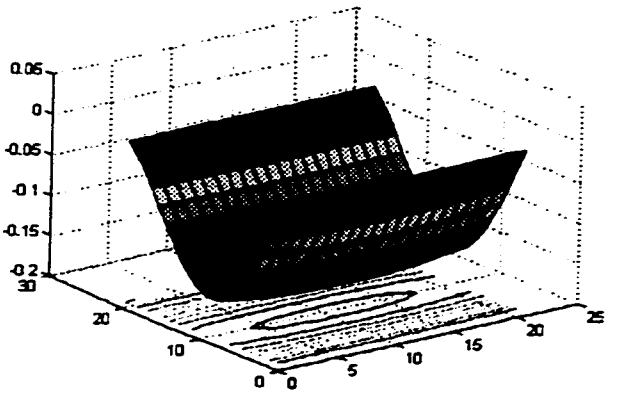

Mode 1

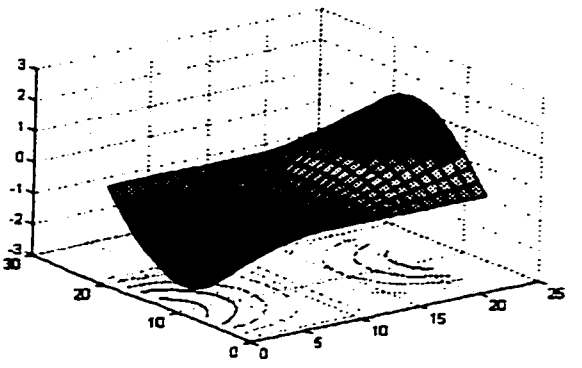

Mode 2

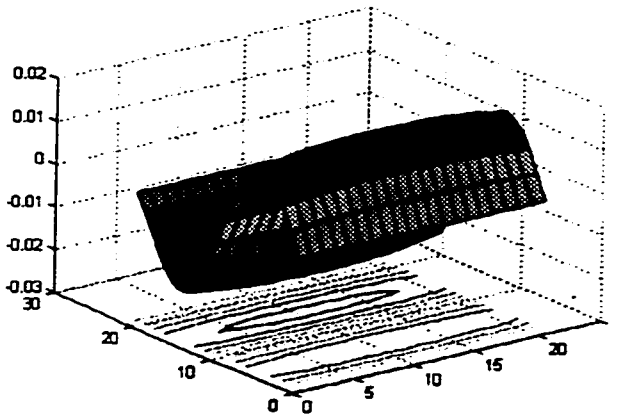

Mode 3

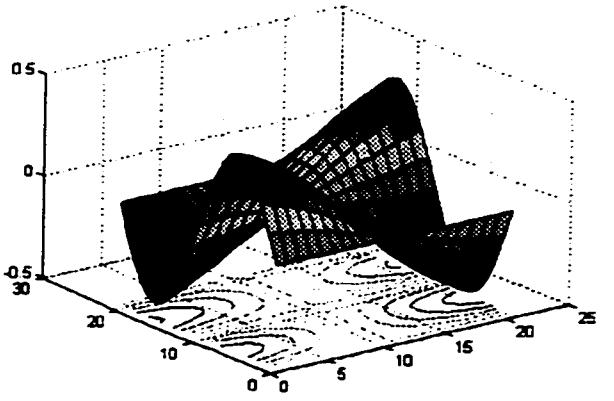

Mode 4

Tables A.31 - A.35 Eigenvalues, SFTF Plate, $\phi = 1 / 1.5$

[A.31] $K_{in} = 0.5$, $\phi = 1/1.5$ In-plane load as a percentage of buckling load (K_{in})

Mode	-100%	-50%	0%	20%	40%	60%	80%	90%	99%
1	14.06	12.18	9.953	8.905	7.715	6.303	4.467	3.172	0.982
2	23.62	22.55	21.42	20.96	20.48	19.99	19.49	19.24	19.00
3	43.78	41.46	39.01	37.98	36.92	35.84	34.72	34.14	33.62
4	58.01	56.29	54.50	53.77	53.03	52.28	51.52	51.13	50.78

[A.32] $K_{in} = 1.0$, $\phi = 1/1.5$ In-plane load as a percentage of buckling load (K_{in})

Mode	-100%	-50%	0%	20%	40%	60%	80%	90%	99%
1	14.64	12.68	10.35	9.260	8.020	6.550	4.633	3.278	1.037
2	23.97	22.82	21.62	21.12	20.61	20.08	19.54	19.27	19.02
3	44.54	42.07	39.45	38.36	37.23	36.06	34.86	34.24	33.67
4	58.60	56.74	54.83	54.04	53.25	52.44	51.62	51.20	50.82

[A.33] $K_{in} = 2.0$, $\phi = 1/1.5$ In-plane load as a percentage of buckling load (K_{in})

Mode	-100%	-50%	0%	20%	40%	60%	80%	90%	99%
1	15.52	13.45	10.99	9.828	8.514	6.953	4.919	3.480	1.098
2	24.54	23.29	21.96	21.41	20.84	20.26	19.66	19.35	19.07
3	45.81	43.12	40.25	39.05	37.80	36.52	35.18	34.50	33.87
4	59.57	57.53	55.41	54.54	53.66	52.76	51.84	51.38	50.96

[A.34] $K_{in} = 3.0$, $\phi = 1/1.5$ In-plane load as a percentage of buckling load (K_{in})

Mode	-100%	-50%	0%	20%	40%	60%	80%	90%	99%
1	16.19	14.03	11.47	10.26	8.892	7.265	5.145	3.645	1.147
2	24.99	23.66	22.24	21.65	21.04	20.41	19.77	19.44	19.14
3	46.83	43.98	40.94	39.65	38.33	36.96	35.53	34.80	34.12
4	60.37	58.19	55.93	54.99	54.04	53.08	52.10	51.60	51.14

[A.35] $K_{in} = 4.0$, $\phi = 1/1.5$ In-plane load as a percentage of buckling load (K_{in})

Mode	-100%	-50%	0%	20%	40%	60%	80%	90%	99%
1	16.72	14.49	11.85	10.60	9.188	7.507	5.313	3.758	1.188
2	25.36	23.97	22.48	21.86	21.22	20.50	19.87	19.52	19.20
3	47.67	44.70	41.53	40.18	38.80	37.36	35.86	35.09	34.38
4	61.04	58.76	56.38	55.39	54.40	53.38	52.34	51.82	51.34

Tables 4.36 - 4.40 Eigenvalues, SFTF Plate, $\phi = 1 / 1.5$

[A.36]	$K_p = 3.0$, $\phi = 1/1.5$								
Mode	-100%	-50%	0%	20%	40%	60%	80%	90%	99%
1	17.14	14.86	12.15	10.88	9.428	7.703	5.449	3.849	1.223
2	25.67	24.23	22.69	22.04	21.37	20.69	19.97	19.60	19.27
3	48.38	45.32	42.04	40.65	39.22	37.73	36.18	35.38	34.65
4	61.61	59.24	56.77	55.76	54.72	53.66	52.58	52.03	51.54

[A.37]	$K_p = 7.5$, $\phi = 1/1.5$								
Mode	-100%	-50%	0%	20%	40%	60%	80%	90%	99%
1	17.90	15.53	12.71	11.38	9.873	8.075	5.725	4.059	1.283
2	26.25	24.72	23.09	22.40	21.69	20.95	20.19	19.80	19.44
3	49.72	46.51	43.07	41.61	40.10	38.53	36.9	36.05	35.28
4	62.72	60.21	57.60	56.51	55.41	54.29	53.14	52.56	52.02

[A.38]	$K_p = 11.4$, $\phi = 1/1.5$								
Mode	-100%	-50%	0%	20%	40%	60%	80%	90%	99%
1	18.41	15.98	13.09	11.72	10.17	8.315	5.888	4.164	1.322
2	26.66	25.07	23.38	22.66	21.92	21.15	20.36	19.94	19.57
3	50.69	47.39	43.84	42.33	40.78	39.16	37.47	36.59	35.79
4	63.54	60.94	58.23	57.11	55.96	54.79	53.60	52.99	52.44

[A.39]	$K_p = 20.4$, $\phi = 1/1.5$								
Mode	-100%	-50%	0%	20%	40%	60%	80%	90%	99%
1	19.44	16.90	13.86	12.42	10.78	8.825	6.262	4.442	1.398
2	27.54	25.85	24.03	23.26	22.47	21.64	20.78	20.33	19.92
3	52.83	49.36	45.62	44.04	42.40	40.69	38.91	37.99	37.14
4	65.42	62.66	59.77	58.58	57.36	56.11	54.83	54.18	53.59

[A.40]	$K_p = 28.4$, $\phi = 1/1.5$								
Mode	-100%	-50%	0%	20%	40%	60%	80%	90%	99%
1	19.90	17.30	14.19	12.72	11.04	9.039	6.413	4.545	1.441
2	27.95	26.22	24.35	23.56	22.73	21.88	20.99	20.52	20.10
3	53.85	50.31	46.50	44.88	43.21	41.46	39.64	38.70	37.83
4	66.36	63.53	60.57	59.35	58.09	56.81	55.50	54.83	54.22

Figure A.12, **SFTF Plate,** $K_{2r} = 1.0$, $\Phi = 1/1.5$

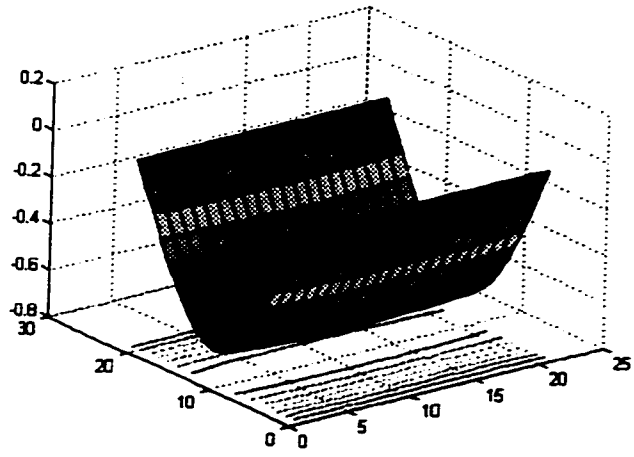

Mode 1

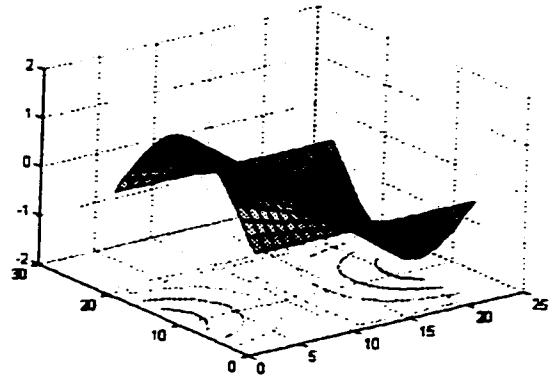

Mode 2

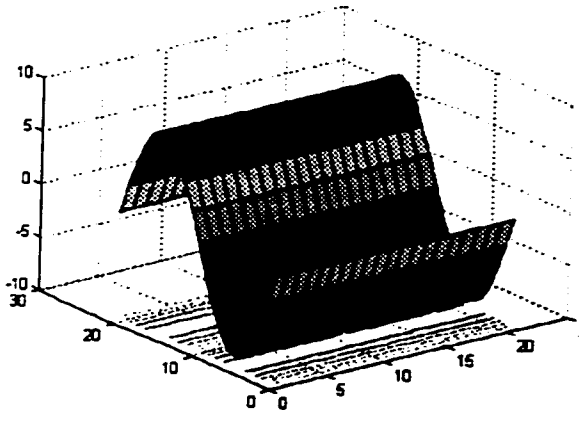

Mode 3

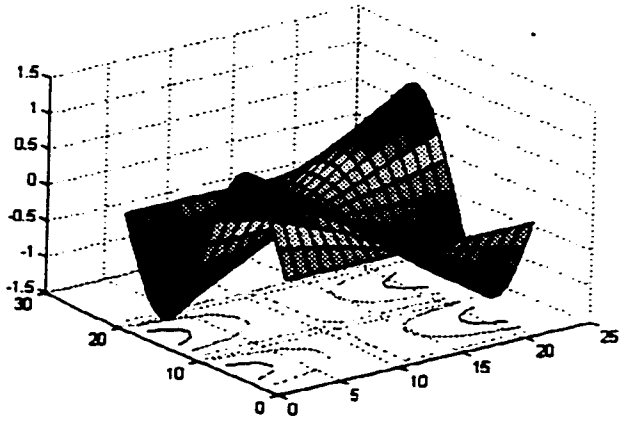

Mode 4

Tables A.41 - A.45 Eigenvalues, SFTF Plate, $\phi = 2.0 / 1$

[A.41]									
Mode	-100%	-50%	0%	20%	40%	60%	80%	90%	99%
1	14.37	12.45	10.16	9.091	7.873	6.429	4.546	3.215	1.019
2	15.71	13.97	11.98	11.08	10.10	9.025	7.797	7.103	6.416
3	20.50	19.20	17.81	17.21	16.60	15.97	15.31	14.97	14.66
4	29.56	28.68	27.76	27.39	27.01	26.62	26.23	26.03	25.86

[A.42]									
Mode	-100%	-50%	0%	20%	40%	60%	80%	90%	99%
1	14.93	12.93	10.56	9.442	8.177	6.677	4.721	3.338	1.051
2	16.21	14.41	12.31	11.37	10.35	9.248	7.905	7.165	6.427
3	20.89	19.52	18.04	17.41	16.75	16.08	15.37	15.01	14.67
4	29.84	28.89	27.91	27.51	27.11	26.69	26.27	26.06	25.87

[A.43]									
Mode	-100%	-50%	0%	20%	40%	60%	80%	90%	99%
1	15.80	13.69	11.18	10.00	8.665	7.077	5.005	3.540	1.120
2	17.03	15.09	12.86	11.85	10.75	9.513	8.094	7.280	6.461
3	21.54	20.05	18.43	17.74	17.03	16.28	15.49	15.09	14.71
4	30.30	29.26	28.18	27.73	27.28	26.82	26.36	26.12	25.90

[A.44]									
Mode	-100%	-50%	0%	20%	40%	60%	80%	90%	99%
1	16.47	14.27	11.66	10.43	9.039	7.384	5.224	3.694	1.169
2	17.65	15.62	13.29	12.23	11.06	9.759	8.250	7.380	6.498
3	22.05	20.47	18.75	18.02	17.25	16.45	15.61	15.17	14.76
4	30.67	29.56	28.40	27.92	27.44	26.94	26.44	26.19	25.95

[A.45]									
Mode	-100%	-50%	0%	20%	40%	60%	80%	90%	99%
1	16.99	14.73	12.04	10.77	9.336	7.627	5.398	3.819	1.210
2	18.14	16.05	13.63	12.53	11.32	9.960	8.383	7.468	6.534
3	22.46	20.81	19.01	18.24	17.44	16.60	15.71	15.25	14.82
4	30.97	29.81	28.59	28.09	27.58	27.05	26.52	26.25	26.01

Tables A.46 - A.50 Eigenvalues, SFTF Plate, $\phi = 2.0 / 1$

[illegible]

Mode	-100%	-50%	0%	20%	40%	60%	80%	90%	99%
1	17.41	15.09	12.344	11.04	9.577	7.827	5.540	3.920	1.243
2	18.54	16.39	13.91	12.78	11.53	10.13	8.495	7.544	6.570
3	22.79	21.09	19.23	18.44	17.61	16.73	15.80	15.32	14.87
4	31.24	30.02	28.75	28.23	27.70	27.15	26.60	26.32	26.06

[illegible]

Mode	-100%	-50%	0%	20%	40%	60%	80%	90%	99%
1	18.17	15.77	12.90	11.55	10.02	8.191	5.801	4.105	1.298
2	19.27	17.03	14.43	13.24	11.93	10.45	8.712	76.96	6.646
3	23.42	21.62	19.66	18.81	17.93	16.99	16.00	15.48	14.99
4	31.72	30.43	29.08	28.52	27.95	27.36	26.77	26.46	26.12

[illegible]

Mode	-100%	-50%	0%	20%	40%	60%	80%	90%	99%
1	18.68	16.22	13.28	11.90	10.32	8.440	5.980	4.234	1.346
2	19.76	17.46	14.78	13.56	12.20	10.67	8.870	7.809	6.709
3	23.85	22.00	19.96	19.08	18.17	17.19	16.15	15.60	15.09
4	32.07	30.73	29.32	28.74	28.14	27.53	26.90	26.59	26.30

[illegible]

Mode	-100%	-50%	0%	20%	40%	60%	80%	90%	99%
1	19.73	17.15	14.06	12.60	10.93	8.948	6.344	4.493	1.427
2	20.78	18.35	15.52	14.22	12.78	11.15	9.207	8.058	6.855
3	24.77	22.80	20.62	19.68	18.68	17.63	16.5	15.90	15.35
4	32.84	31.39	39.87	29.24	28.59	27.93	27.25	26.90	26.58

[illegible]

Mode	-100%	-50%	0%	20%	40%	60%	80%	90%	99%
1	20.19	17.55	14.39	12.90	11.20	9.170	6.505	4.609	1.476
2	21.23	18.75	15.85	14.52	13.04	11.36	9.363	8.175	6.928
3	25.19	23.17	20.93	19.96	18.93	17.84	16.67	16.06	15.48
4	33.20	31.71	30.14	29.49	28.82	28.13	27.42	27.06	26.73

Figure A.13 Eigenvalue curves, SFTF plate, K_{2R}=0.5, ϕ = 2.0/1,

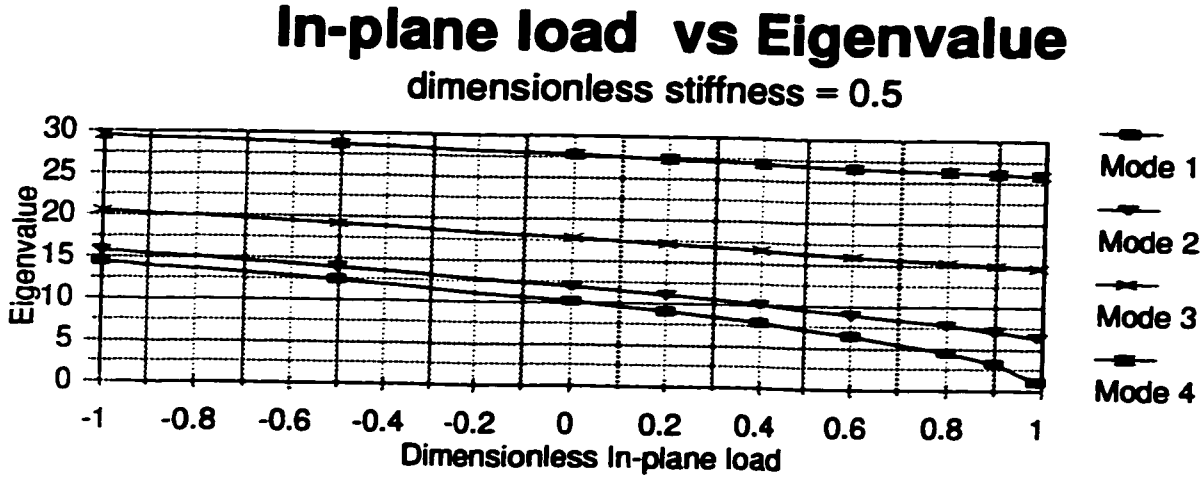

Figure A.14 Eigenvalue curves, SFTF plate, K_{2R}=30.0, ϕ = 2.0/1,

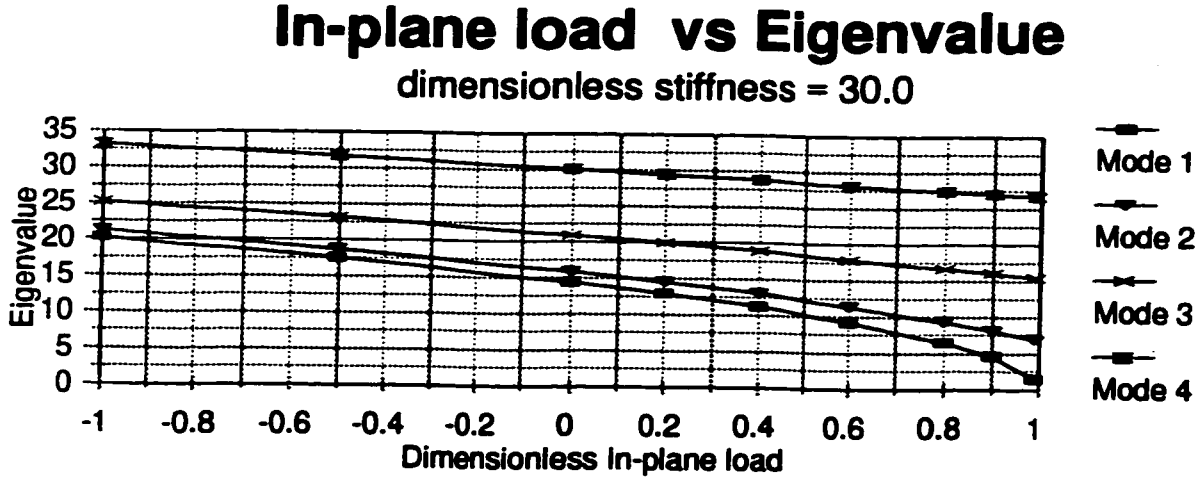

Figure A.15, **SFTF Plate,** **$K_{2r} = 30.0$, $\Phi = 2.0/1$**

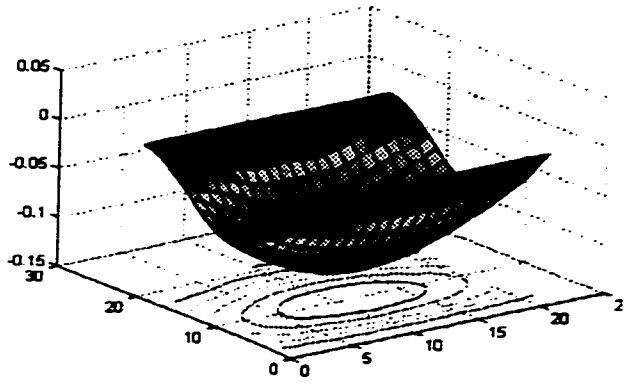

Mode 1

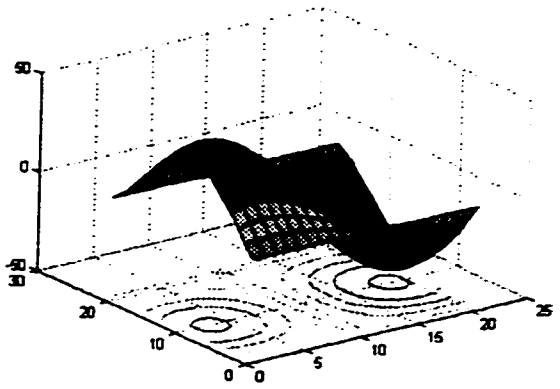

Mode 2

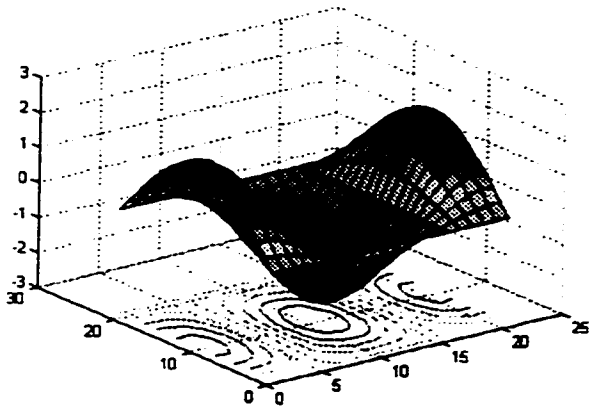

Mode 3

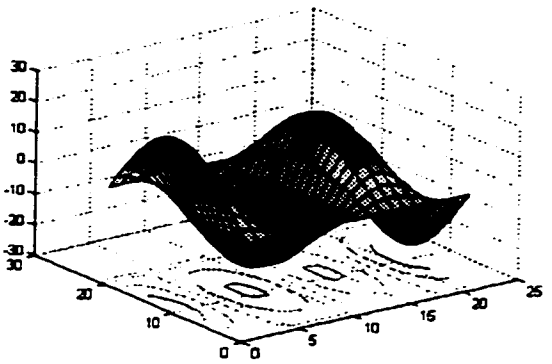

Mode 4

Tables A.51 - A.55 Eigenvalues, SFTF Plate, $\phi = 2.5 / 1$

[A.51]	K_g = 0.5, ϕ = 2.5/1								
Mode	-100%	-50%	0%	20%	40%	60%	80%	90%	99%
1	14.41	12.48	10.19	9.116	7.895	6.446	4.558	3.228	1.019
2	15.27	13.46	11.37	10.42	9.371	8.188	6.802	5.990	5.150
3	18.35	16.88	15.26	14.57	13.84	13.06	12.24	11.81	11.41
4	24.06	22.95	21.79	21.31	20.82	20.31	19.80	19.53	19.29

[A.52]	K_g = 1.0, ϕ = 2.5/1								
Mode	-100%	-50%	0%	20%	40%	60%	80%	90%	99%
1	14.96	12.96	10.58	9.467	8.199	6.696	4.736	3.350	1.068
2	15.79	13.91	11.73	10.73	9.631	8.388	6.925	6.063	5.165
3	18.79	17.24	15.53	14.80	14.02	13.20	12.32	11.86	11.42
4	24.39	23.22	21.98	21.47	20.94	20.40	19.85	19.56	19.30

[A.53]	K_g = 2.0, ϕ = 2.5/1								
Mode	-100%	-50%	0%	20%	40%	60%	80%	90%	99%
1	15.84	13.72	11.21	10.03	8.685	7.093	5.017	3.547	1.119
2	16.63	14.62	12.30	11.23	10.05	8.716	7.131	6.187	5.193
3	19.50	17.83	15.98	15.18	14.33	13.43	12.45	11.94	11.46
4	24.95	23.67	22.31	21.74	21.16	20.56	19.95	19.63	19.34

[A.54]	K_g = 3.0, ϕ = 2.5/1								
Mode	-100%	-50%	0%	20%	40%	60%	80%	90%	99%
1	16.50	14.30	11.69	10.46	9.059	7.400	5.235	3.703	1.171
2	17.26	15.17	12.74	11.62	10.39	8.978	7.300	6.295	5.225
3	20.06	18.29	16.34	15.49	14.58	13.62	12.58	12.03	11.51
4	25.40	24.03	22.58	21.98	21.35	20.71	20.04	19.70	19.39

[A.55]	K_g = 4.0, ϕ = 2.5/1								
Mode	-100%	-50%	0%	20%	40%	60%	80%	90%	99%
1	17.02	14.76	12.06	10.80	9.355	7.644	5.410	3.827	1.214
2	17.76	15.61	13.09	11.94	10.65	9.191	7.441	6.386	5.258
3	20.50	18.67	16.63	15.74	14.79	13.79	12.69	12.11	11.56
4	25.76	24.33	22.81	22.17	21.51	20.84	20.13	19.77	19.44

Tables A.56 - A.60 Eigenvalues, SFTF Plate, $\phi = 2.5 / 1$

[A.56] K_g = 5.8, ϕ = 2.5/1 In-plane load as a percentage of buckling load (A.56)

Mode	-100%	-50%	0%	20%	40%	60%	80%	90%	99%
1	17.44	15.13	12.37	11.07	9.596	7.843	5.552	3.928	1.247
2	18.17	15.96	13.38	12.19	10.87	9.367	7.559	6.465	5.288
3	20.86	18.98	16.87	15.95	14.98	13.93	12.79	12.18	11.61
4	26.06	24.58	23.00	22.34	21.66	20.95	20.22	19.84	19.50

[A.57] K_g = 7.4, ϕ = 2.5/1 In-plane load as a percentage of buckling load (A.57)

Mode	-100%	-50%	0%	20%	40%	60%	80%	90%	99%
1	18.21	15.80	12.93	11.58	10.04	8.207	5.813	4.114	1.304
2	18.91	16.61	13.91	12.67	11.28	9.697	7.784	6.618	5.352
3	21.53	19.55	17.33	16.36	15.32	14.21	12.99	12.34	11.72
4	26.62	25.05	23.38	22.67	21.94	21.18	20.40	19.99	19.62

[A.58] K_g = 10.4, ϕ = 2.5/1 In-plane load as a percentage of buckling load (A.58)

Mode	-100%	-50%	0%	20%	40%	60%	80%	90%	99%
1	18.72	16.25	13.31	11.92	10.34	8.456	5.991	4.240	1.342
2	19.41	17.05	14.28	12.99	11.57	9.927	7.943	6.729	5.403
3	21.99	19.95	17.66	16.65	15.57	14.41	13.14	12.46	11.81
4	27.01	25.39	23.65	22.91	22.15	21.36	20.54	20.12	19.73

[A.59] K_g = 20.8, ϕ = 2.5/1 In-plane load as a percentage of buckling load (A.59)

Mode	-100%	-50%	0%	20%	40%	60%	80%	90%	99%
1	19.77	17.18	14.08	12.62	10.95	8.965	6.356	4.502	1.432
2	20.44	17.95	15.03	13.67	12.15	10.41	8.283	6.972	5.525
3	22.95	20.79	18.35	17.27	16.11	14.86	13.49	12.74	12.03
4	27.86	26.13	24.25	23.46	22.64	21.78	20.88	20.42	19.99

[A.60] K_g = 38.8, ϕ = 2.5/1 In-plane load as a percentage of buckling load (A.60)

Mode	-100%	-50%	0%	20%	40%	60%	80%	90%	99%
1	20.23	17.58	14.42	12.93	11.22	9.186	6.514	4.614	1.467
2	20.89	18.35	15.36	13.97	12.41	10.62	8.435	7.082	5.582
3	23.39	21.17	18.66	17.56	16.36	15.07	13.65	12.88	12.13
4	28.26	26.47	24.54	23.72	22.87	21.99	21.06	20.58	20.13

Figure A.16 Eigenvalue curves, SFTF plate, K_{2R}=0.5, ϕ = 2.5/1,

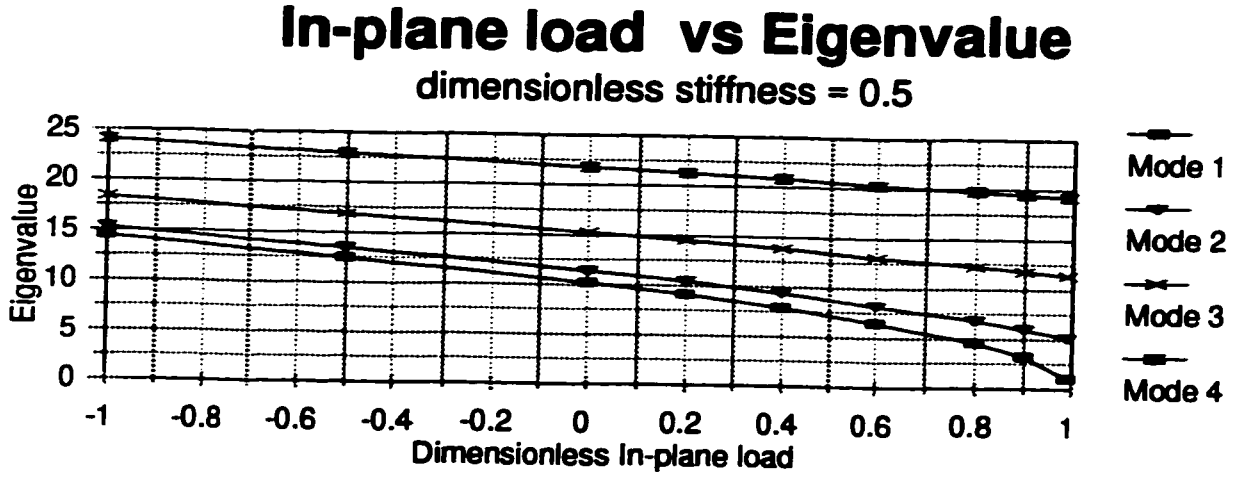

Figure A.17 Eigenvalue curves, SFTF plate, K_{2R}=30.0, ϕ = 2.5/1,

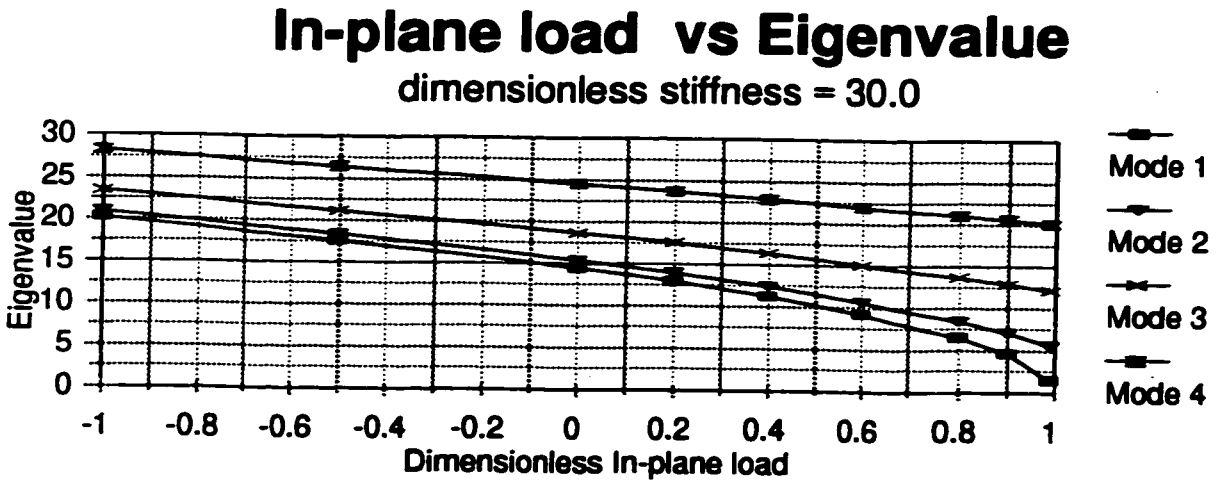

Figure A.18, **SFTF Plate,** **K_{2r} = 0.5, Φ = 2.5/1**

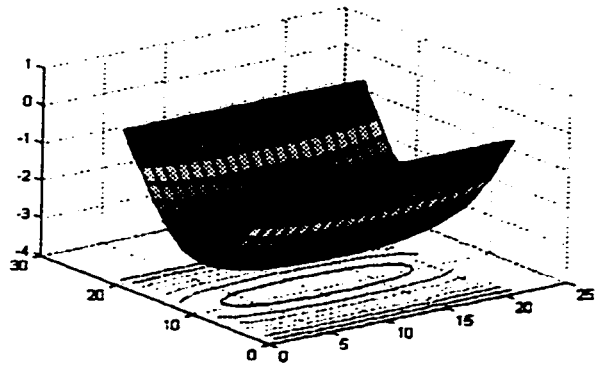

Mode 1

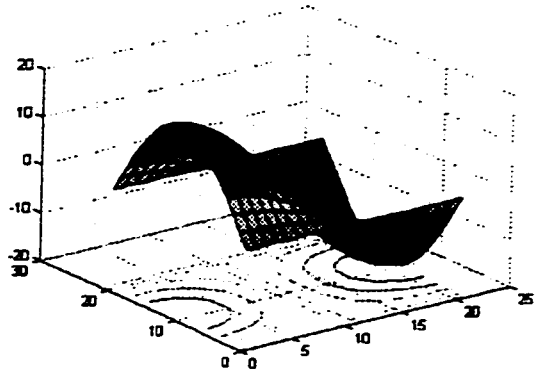

Mode 2

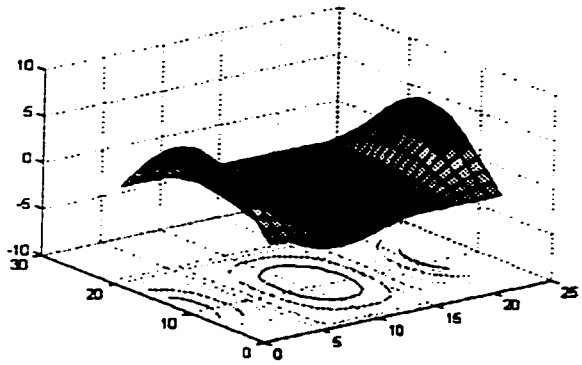

Mode 3

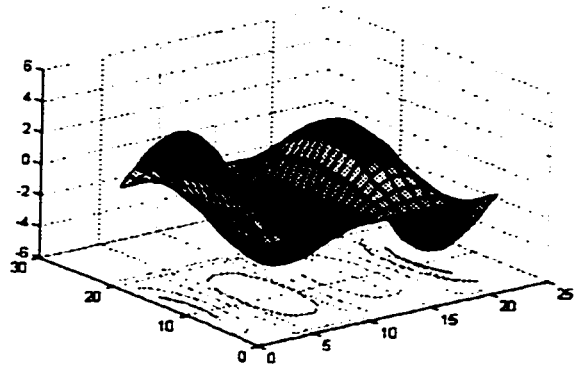

Mode 4

Table A.61 - A.65 Eigenvalues, SFTF Plate, $\phi = 3.0 / 1$

[A.61] $K_x = 0.5$, $\phi = 3.0/1$ In-plane load as a percentage of Buckling load (95.81)

Mode	-100%	-50%	0%	20%	40%	60%	80%	90%	99%
1	14.44	12.51	10.21	9.134	7.910	6.459	4.567	3.230	1.023
2	15.03	13.19	11.04	10.05	8.949	7.696	6.195	5.287	4.309
3	17.18	15.59	13.82	13.04	12.22	11.33	10.37	9.855	9.367
4	21.08	19.81	18.45	17.88	17.28	16.67	16.03	15.70	15.40

[A.62] $K_x = 1.0$, $\phi = 3.0/1$ In-plane load as a percentage of Buckling load (47.91)

Mode	-100%	-50%	0%	20%	40%	60%	80%	90%	99%
1	14.99	12.98	10.60	9.483	8.213	6.706	4.742	3.353	1.057
2	15.56	13.64	11.40	10.37	9.219	7.907	6.327	5.365	4.320
3	17.65	15.98	14.11	13.29	12.42	11.48	10.46	9.904	9.379
4	21.47	20.12	18.68	18.06	17.43	16.78	16.09	15.74	15.41

[A.63] $K_x = 2.0$, $\phi = 3.0/1$ In-plane load as a percentage of Buckling load (15.94)

Mode	-100%	-50%	0%	20%	40%	60%	80%	90%	99%
1	15.86	13.74	11.23	10.04	8.699	7.104	5.025	3.553	1.121
2	16.41	14.37	11.98	10.88	9.659	8.252	6.549	5.502	4.349
3	18.40	16.61	14.60	13.71	12.76	11.74	10.61	10.00	9.415
4	22.10	20.63	19.05	18.38	17.69	16.96	16.21	15.81	15.45

[A.64] $K_x = 3.0$, $\phi = 3.0/1$ In-plane load as a percentage of Buckling load (22.72)

Mode	-100%	-50%	0%	20%	40%	60%	80%	90%	99%
1	16.53	14.32	11.70	10.47	9.073	7.411	5.243	3.708	1.171
2	17.05	14.93	12.44	11.29	10.002	8.524	6.728	5.616	4.379
3	18.99	17.10	14.98	14.05	13.04	11.95	10.74	10.09	9.459
4	22.59	21.04	19.36	18.65	17.90	17.13	16.31	15.89	15.50

[A.65] $K_x = 4.0$, $\phi = 3.0/1$ In-plane load as a percentage of Buckling load (29.64)

Mode	-100%	-50%	0%	20%	40%	60%	80%	90%	99%
1	17.05	14.78	12.08	10.81	9.369	7.655	5.417	3.832	1.213
2	17.50	15.37	12.80	11.61	10.28	8.744	6.874	5.712	4.408
3	19.45	17.50	15.30	14.32	13.27	12.13	10.86	10.17	9.504
4	22.99	21.37	19.62	18.87	18.09	17.27	16.42	15.96	15.55

Table A.66 - A.70 Eigenvalues, SFTF Plate, $\phi = 3.0 / 1$

[A.66] $K_p = 5.0$, $\Phi = 3.0/1$ In-plane load as a percentage of buckling load(35.15)

Mode	-100%	-50%	0%	20%	40%	60%	80%	90%	99%
1	17.47	15.15	12.39	11.09	9.609	7.853	5.559	3.933	1.245
2	17.97	15.72	13.09	11.87	10.502	8.926	6.997	5.792	4.435
3	19.83	17.82	15.55	14.55	13.46	12.28	10.96	10.24	9.548
4	23.32	21.65	19.83	19.06	18.24	17.40	16.50	16.04	15.60

[A.67] $K_p = 7.5$, $\Phi = 3.0/1$ In-plane load as a percentage of buckling load(44.68)

Mode	-100%	-50%	0%	20%	40%	60%	80%	90%	99%
1	18.23	15.82	12.95	11.59	10.05	8.218	5.820	4.119	1.306
2	18.71	16.38	13.63	12.35	10.92	9.264	7.228	5.949	4.492
3	20.52	18.42	16.04	14.98	13.83	12.57	11.17	10.39	9.646
4	23.93	22.17	20.24	19.42	18.55	17.65	16.69	16.18	15.72

[A.68] $K_p = 10.0$, $\Phi = 3.0/1$ In-plane load as a percentage of buckling load(51.39)

Mode	-100%	-50%	0%	20%	40%	60%	80%	90%	99%
1	18.74	16.27	13.33	11.94	10.35	8.467	5.999	4.246	1.346
2	19.219	16.82	13.99	12.68	11.21	9.498	7.391	6.061	4.536
3	21.00	18.84	16.38	15.28	14.09	12.78	11.32	10.51	9.725
4	24.36	22.53	20.54	19.68	18.78	17.84	16.83	16.31	15.82

[A.69] $K_p = 20.0$, $\Phi = 3.0/1$ In-plane load as a percentage of buckling load(63.11)

Mode	-100%	-50%	0%	20%	40%	60%	80%	90%	99%
1	19.79	17.19	14.10	12.64	10.97	8.975	6.363	4.506	1.429
2	20.25	17.73	14.75	13.36	11.80	9.985	7.732	6.300	4.639
3	21.99	19.70	17.09	15.92	14.64	13.24	11.66	10.78	9.917
4	25.26	23.32	21.18	20.26	19.29	18.27	17.17	16.60	16.06

[A.70] $K_p = 30.0$, $\Phi = 3.0/1$ In-plane load as a percentage of buckling load(67.28)

Mode	-100%	-50%	0%	20%	40%	60%	80%	90%	99%
1	20.25	17.61	14.44	12.94	11.23	9.197	6.522	4.620	1.467
2	20.71	18.13	15.09	13.66	12.06	10.20	7.885	6.410	4.689
3	22.43	20.09	17.41	16.21	14.90	13.45	11.82	10.90	10.01
4	25.68	23.68	21.48	20.53	19.53	18.47	17.34	16.75	16.19

Figure A.19 Eigenvalue curves, SFTF plate, K_{2R}=0.5, ϕ = 3.0/1,

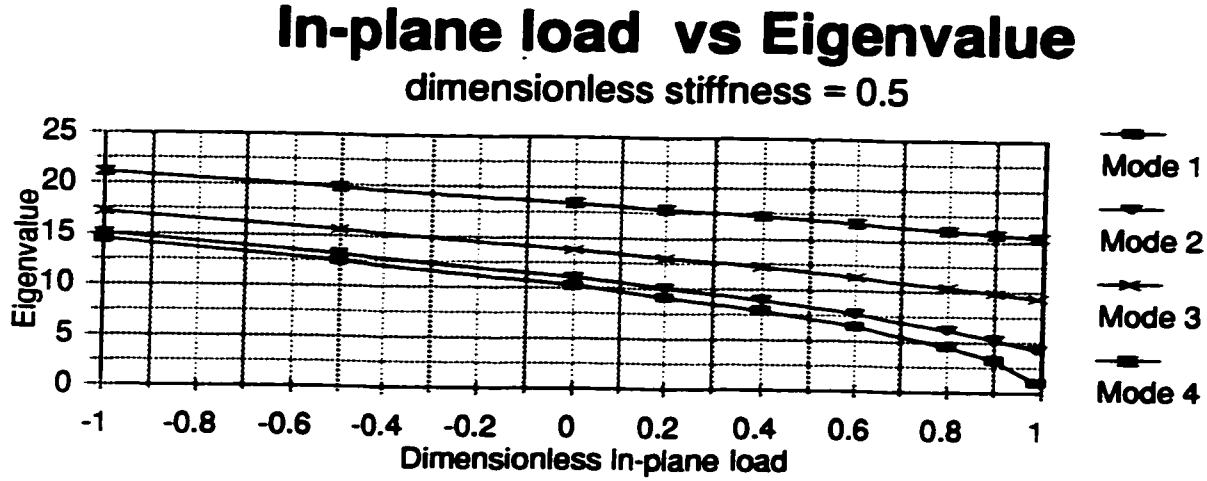

Figure A.20 Eigenvalue curves, SFTF plate, K_{2R}=30.0, ϕ = 3.0/1,

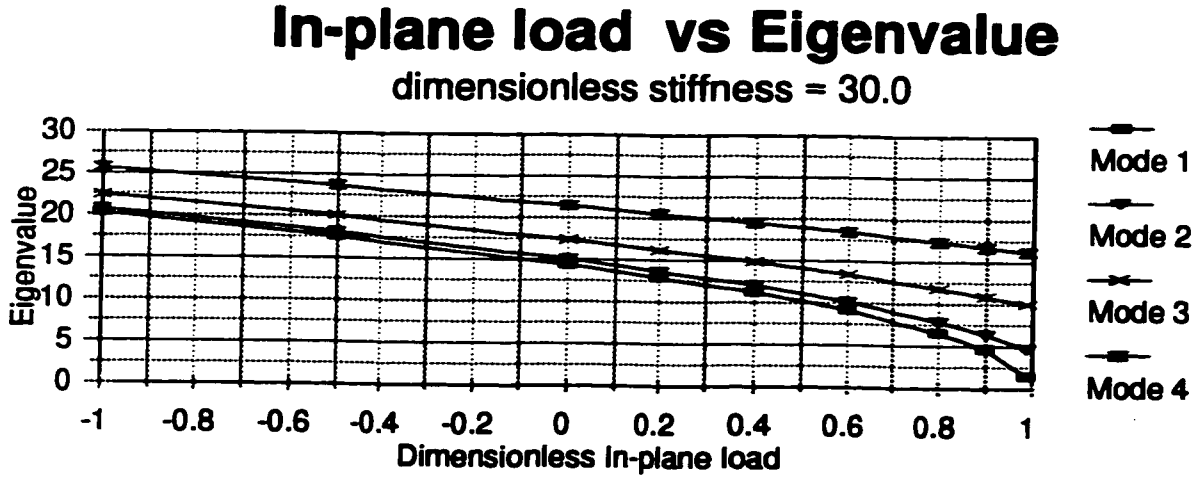

Figure A.21, SFTF Plate, $K_{2r} = 0.5$, $\Phi = 3.0/1$

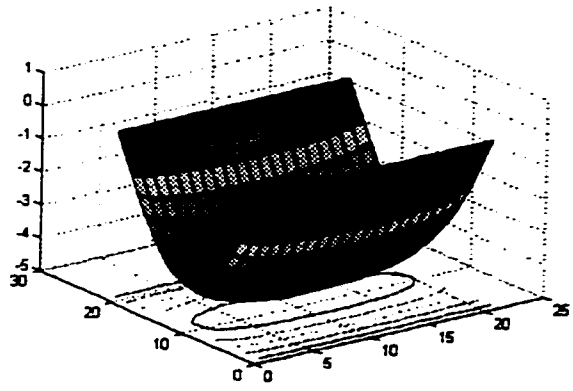

Mode 1

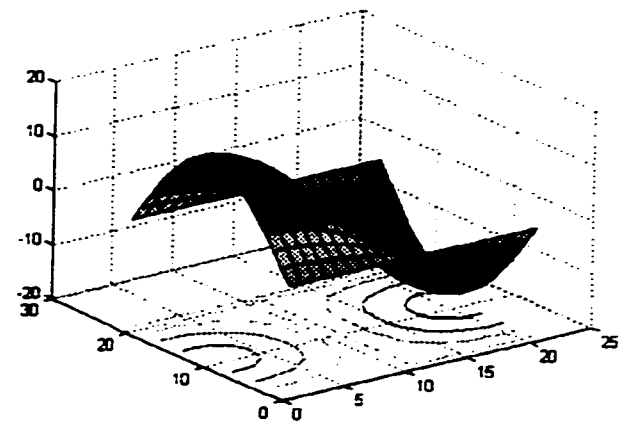

Mode 2

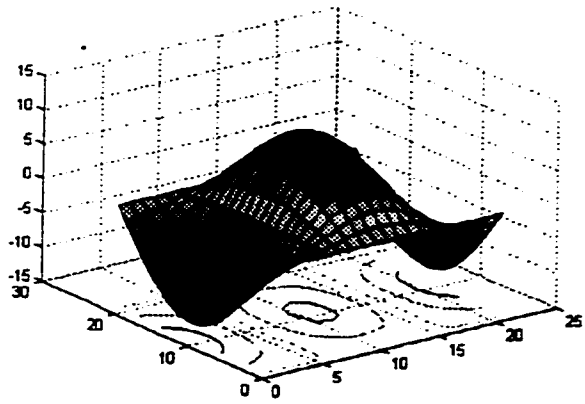

Mode 3

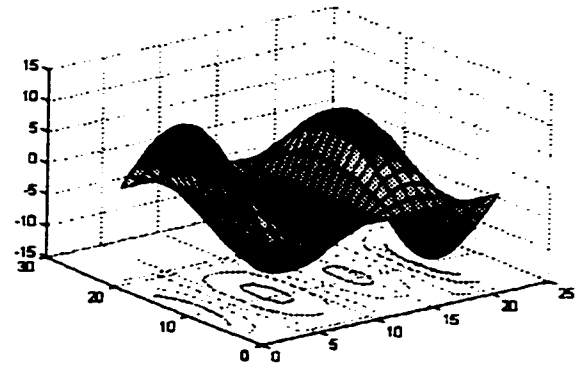

Mode 4

Table A.71 - A.75 Eigenvalues, TFTF Plate, $\phi = 1 / 3.0$

[A.71] $K_{x,cr} = 0.5$, $\phi = 1/3.0$ In-plane load as a percentage of buckling load (1.00)

Mode	-100%	-50%	0%	20%	40%	60%	80%	90%	99%
1	14.60	12.64	10.32	9.232	7.995	6.528	4.615	3.262	1.023
2	40.52	39.85	38.91	37.80	36.65	35.47	34.25	33.62	33.05
3	44.04	41.56	39.18	38.91	38.63	38.36	38.08	37.94	37.81
4	87.73	86.51	85.26	84.77	84.26	83.75	82.60	82.02	81.49

[A.72] $K_{x,cr} = 1.0$, $\phi = 1/3.0$ In-plane load as a percentage of buckling load (1.00)

Mode	-100%	-50%	0%	20%	40%	60%	80%	90%	99%
1	15.73	13.62	11.12	9.945	8.612	7.029	4.966	3.504	1.108
2	40.95	40.19	39.41	38.55	37.25	35.90	34.49	33.77	33.10
3	45.60	42.81	39.81	39.10	38.78	38.46	38.14	37.97	37.83
4	88.53	87.13	85.70	85.12	84.54	83.95	82.86	82.18	81.57

[A.73] $K_{x,cr} = 2.0$, $\phi = 1/3.0$ In-plane load as a percentage of buckling load (1.00)

Mode	-100%	-50%	0%	20%	40%	60%	80%	90%	99%
1	17.53	15.18	12.39	11.08	9.594	7.825	5.515	3.873	1.252
2	41.71	40.78	39.83	39.45	38.34	36.70	35.00	34.11	33.29
3	48.24	44.96	41.41	39.90	39.06	38.66	38.26	38.06	37.88
4	89.96	88.24	86.49	85.78	85.06	84.34	83.44	82.61	81.66

[A.74] $K_{x,cr} = 3.0$, $\phi = 1/3.0$ In-plane load as a percentage of buckling load (1.00)

Mode	-100%	-50%	0%	20%	40%	60%	80%	90%	99%
1	18.89	16.37	13.38	11.97	10.37	8.476	6.006	4.263	1.335
2	42.34	41.29	40.21	39.76	39.317	37.49	35.55	34.54	33.61
3	50.36	46.72	42.77	41.09	39.328	38.87	38.41	38.18	37.97
4	91.16	89.21	87.21	86.39	85.58	84.75	83.91	83.18	82.32

[A.75] $K_{x,cr} = 4.0$, $\phi = 1/3.0$ In-plane load as a percentage of buckling load (1.00)

Mode	-100%	-50%	0%	20%	40%	60%	80%	90%	99%
1	20.00	17.33	14.16	12.67	10.98	8.966	6.340	4.479	1.387
2	42.90	41.74	40.54	40.05	39.56	38.18	36.05	34.93	33.90
3	52.16	48.23	43.95	42.11	40.19	39.06	38.55	38.29	38.06
4	92.22	90.07	87.86	86.95	86.05	85.13	84.20	83.73	82.79

Table A.76 - A.80 Eigenvalues, TFTF Plate, $\phi = 1 / 3.0$

[A.76] $K_{y,c} = 3.0$, $\phi = 1/3.0$ [applied load as a percentage of buckling load (2.78)]

Mode	-100%	-50%	0%	20%	40%	60%	80%	90%	99%
1	20.90	18.12	14.81	13.25	11.48	9.380	6.632	4.684	1.500
2	43.38	42.13	40.84	40.32	39.78	38.82	36.54	35.35	34.23
3	53.68	49.52	44.98	43.03	40.98	39.24	38.69	38.41	38.16
4	93.15	90.83	88.45	87.48	86.50	85.51	84.51	84.00	83.32

[A.77] $K_{y,c} = 7.0$, $\phi = 1/3.0$ [applied load as a percentage of buckling load (2.78)]

Mode	-100%	-50%	0%	20%	40%	60%	80%	90%	99%
1	22.58	19.59	16.03	14.34	12.43	10.15	7.172	5.050	1.605
2	44.36	42.95	41.48	40.88	40.28	39.66	37.66	36.31	35.06
3	56.62	52.06	47.05	44.89	42.62	40.22	39.03	38.71	38.42
4	95.05	92.43	89.73	88.63	87.52	86.38	85.24	84.65	84.14

[A.78] $K_{y,c} = 10.0$, $\phi = 1/3.0$ [applied load as a percentage of buckling load (2.78)]

Mode	-100%	-50%	0%	20%	40%	60%	80%	90%	99%
1	23.73	20.60	16.88	15.12	13.11	10.73	7.610	5.399	1.701
2	45.08	43.57	42.00	41.35	40.70	40.03	38.66	37.22	35.87
3	58.73	53.92	48.63	46.35	43.94	41.38	39.35	39.00	38.69
4	96.49	93.68	90.78	89.60	88.39	87.17	85.94	85.31	84.74

[A.79] $K_{y,c} = 20.0$, $\phi = 1/3.0$ [applied load as a percentage of buckling load (2.78)]

Mode	-100%	-50%	0%	20%	40%	60%	80%	90%	99%
1	26.21	22.79	18.90	16.76	14.54	11.90	8.422	5.942	1.885
2	46.87	45.13	43.32	42.58	41.82	41.04	40.25	39.59	38.06
3	63.57	58.26	52.39	49.84	47.15	44.28	41.21	39.84	39.48
4	100.12	96.91	93.58	92.22	90.83	89.42	87.99	87.26	86.61

[A.80] $K_{y,c} = 30.0$, $\phi = 1/3.0$ [applied load as a percentage of buckling load (2.78)]

Mode	-100%	-50%	0%	20%	40%	60%	80%	90%	99%
1	27.34	23.79	19.54	17.52	15.21	12.46	8.834	6.250	1.989
2	47.80	45.97	44.06	43.27	42.47	41.64	40.80	40.38	39.36
3	65.92	60.41	54.31	51.65	48.85	45.86	42.66	40.96	39.99
4	102.08	98.71	95.21	93.77	92.30	90.82	89.30	88.53	87.84

Figure A.22 Eigenvalue curves, TFTF plate, $K_{2R}=K_{4R}=0.5$, $\phi = 1/3.0$,

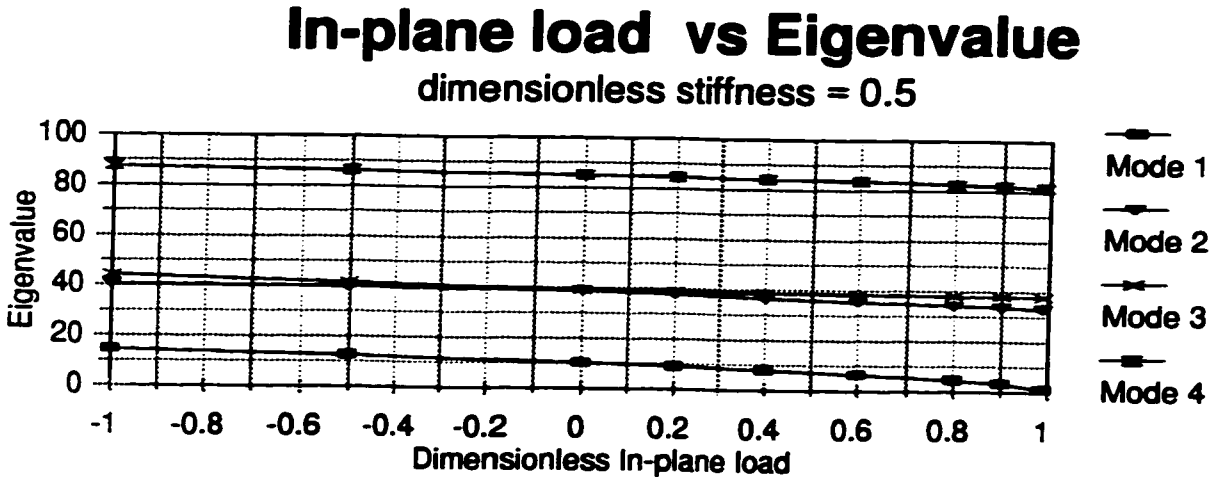

Figure A.23 Eigenvalue curves, TFTF plate, $K_{2R}=K_{4R}=30.0$, $\phi = 1/3.0$,

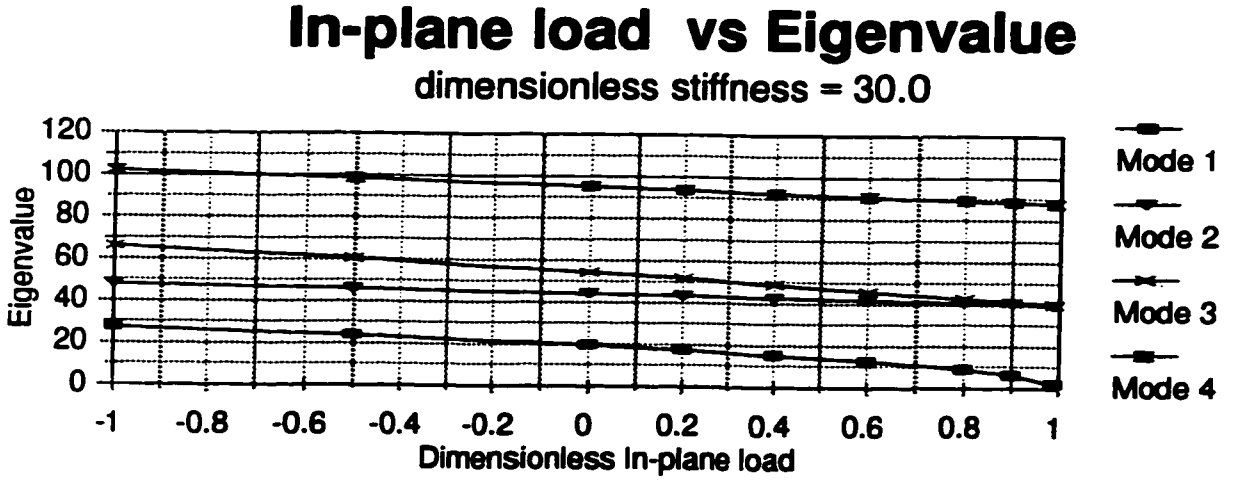

Figure A.24, **TFTF Plate,** $K_{2r/4r} = 30.0, \quad \Phi = 1/3.0$

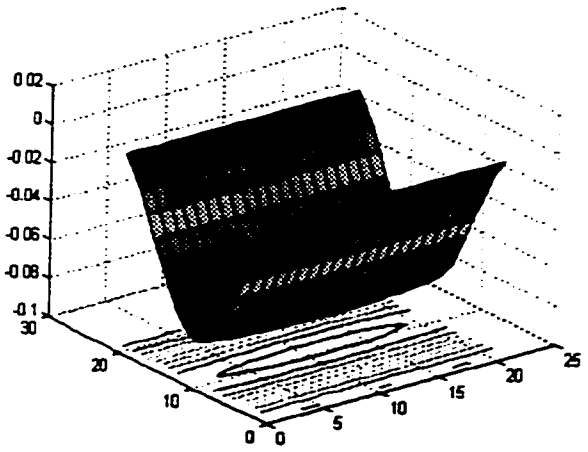

Mode 1

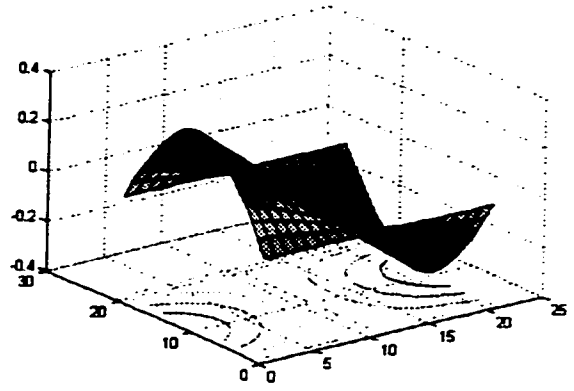

Mode 2

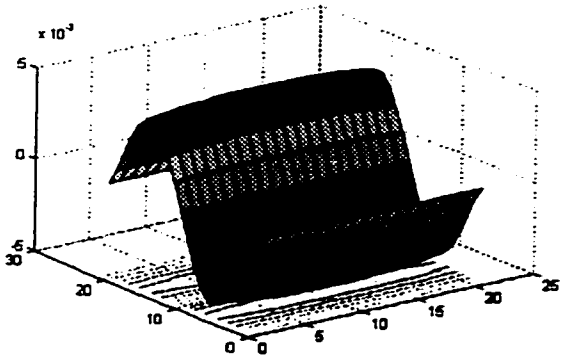

Mode 3

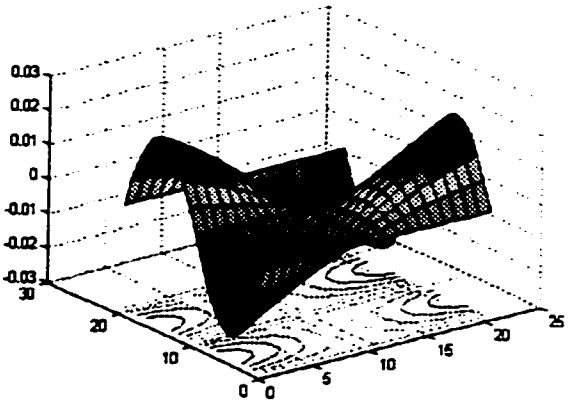

Mode 4

Table A.81 - A.85 Eigenvalues, TFTF Plate, $\phi = 1 / 2.5$

[A.81] $K_{x,a} = 0.5$, $\phi = 1/2.5$ In-plane load as a percentage of buckling load ($N_{x,cr}$)

Mode	-100%	-50%	0%	20%	40%	60%	80%	90%	99%
1	14.62	12.66	10.34	9.253	8.016	6.550	4.641	3.296	1.003
2	34.75	33.97	33.18	32.85	32.53	32.20	31.86	31.69	31.54
3	44.19	41.71	39.06	37.95	36.81	35.63	34.41	33.79	33.21
4	77.20	75.81	74.39	73.81	73.23	72.65	72.06	71.76	71.49

[A.82] $K_{x,a} = 1.0$, $\phi = 1/2.5$ In-plane load as a percentage of buckling load ($N_{x,cr}$)

Mode	-100%	-50%	0%	20%	40%	60%	80%	90%	99%
1	15.76	13.65	11.14	9.962	8.625	7.038	4.967	3.499	1.113
2	35.25	34.36	33.44	33.07	32.69	32.31	31.93	31.73	31.55
3	45.76	42.96	39.97	38.70	37.40	36.05	34.64	33.92	33.26
4	78.12	76.51	74.88	74.21	73.54	72.86	72.18	71.83	71.53

[A.83] $K_{x,a} = 2.0$, $\phi = 1/2.5$ In-plane load as a percentage of buckling load ($N_{x,cr}$)

Mode	-100%	-50%	0%	20%	40%	60%	80%	90%	99%
1	17.55	15.20	12.41	11.10	9.614	7.848	5.544	3.912	1.239
2	36.12	35.04	33.93	33.48	33.01	32.55	32.07	31.83	31.61
3	48.38	45.10	41.56	40.06	38.49	36.86	35.16	34.28	33.46
4	79.72	77.77	75.77	74.96	74.14	73.31	72.47	72.04	71.66

[A.84] $K_{x,a} = 3.0$, $\phi = 1/2.5$ In-plane load as a percentage of buckling load ($N_{x,cr}$)

Mode	-100%	-50%	0%	20%	40%	60%	80%	90%	99%
1	18.92	16.39	13.40	11.99	10.39	8.488	6.015	4.270	1.348
2	36.84	35.62	34.36	33.84	33.31	32.77	32.23	31.95	31.70
3	50.51	46.87	42.92	41.23	39.47	37.63	35.70	34.69	33.76
4	81.06	78.85	76.58	76.65	74.70	73.75	72.79	72.30	71.86

[A.85] $K_{x,a} = 4.0$, $\phi = 1/2.5$ In-plane load as a percentage of buckling load ($N_{x,cr}$)

Mode	-100%	-50%	0%	20%	40%	60%	80%	90%	99%
1	20.02	17.35	14.18	12.69	11.00	8.991	6.371	4.520	1.422
2	37.47	36.13	34.73	34.16	33.58	32.983	32.38	32.07	31.79
3	52.29	48.37	44.09	42.26	40.34	38.33	36.21	35.10	34.07
4	82.24	79.81	77.30	76.27	75.23	74.18	73.11	72.57	72.08

Table A.86 - A.90 Eigenvalues, TFTF Plate, $\phi = 1 / 2.5$

[A.86] $K_{x/c} = -5.0$, $\phi = 1/2.5$ In-plane load as a percentage of Buckling load (-5.65)

Mode	-100%	-50%	0%	20%	40%	60%	80%	90%	99%
1	20.93	18.14	14.83	13.28	11.50	9.401	6.654	4.711	1.488
2	38.01	36.57	35.07	34.45	33.82	33.18	32.53	32.19	31.89
3	53.81	49.66	45.12	43.17	41.12	38.97	36.69	35.50	34.39
4	83.26	80.65	77.95	76.85	75.72	74.58	73.43	72.84	72.31

[A.87] $K_{x/c} = -7.5$, $\phi = 1/2.5$ In-plane load as a percentage of Buckling load (-8.48)

Mode	-100%	-50%	0%	20%	40%	60%	80%	90%	99%
1	22.61	19.61	16.05	14.37	12.46	10.19	7.221	5.119	1.613
2	39.08	37.46	35.77	35.07	34.36	33.62	32.88	32.50	32.15
3	56.74	52.19	47.19	45.04	42.77	40.37	37.82	36.48	35.23
4	85.33	82.39	79.35	78.10	76.82	75.53	74.21	73.54	72.94

[A.88] $K_{x/c} = -10.0$, $\phi = 1/2.5$ In-plane load as a percentage of Buckling load (-11.30)

Mode	-100%	-50%	0%	20%	40%	60%	80%	90%	99%
1	23.78	20.64	16.90	15.14	13.13	10.74	7.606	5.383	1.700
2	39.88	38.15	36.32	35.56	34.79	34.00	33.19	32.77	32.39
3	58.89	54.07	48.77	46.48	44.07	41.51	38.78	37.34	35.99
4	86.91	83.76	80.48	79.12	77.75	76.35	74.92	74.20	73.54

[A.89] $K_{x/c} = -20.0$, $\phi = 1/2.5$ In-plane load as a percentage of Buckling load (-22.59)

Mode	-100%	-50%	0%	20%	40%	60%	80%	90%	99%
1	26.24	22.82	18.73	16.80	14.59	11.95	8.496	6.045	1.907
2	41.76	39.79	37.70	36.83	35.94	35.02	34.07	33.59	33.15
3	63.70	58.40	52.53	49.99	47.30	44.44	41.38	39.76	38.34
4	70.74	87.16	83.42	81.87	80.30	78.69	77.04	76.21	75.45

[A.90] $K_{x/c} = -30.0$, $\phi = 1/2.5$ In-plane load as a percentage of Buckling load (-33.89)

Mode	-100%	-50%	0%	20%	40%	60%	80%	90%	99%
1	27.40	23.84	19.58	17.56	15.25	12.49	8.860	6.277	1.989
2	42.74	40.65	38.44	37.52	36.57	35.59	34.59	34.07	33.60
3	66.09	60.57	54.46	51.80	48.98	46.00	42.79	41.098	39.49
4	92.79	89.02	85.08	83.45	81.78	80.08	78.33	77.45	76.64

Figure A.25 Eigenvalue curves, TFTF plate, $K_{2R}=K_{4R}=0.5$, $\phi = 1/2.5$,

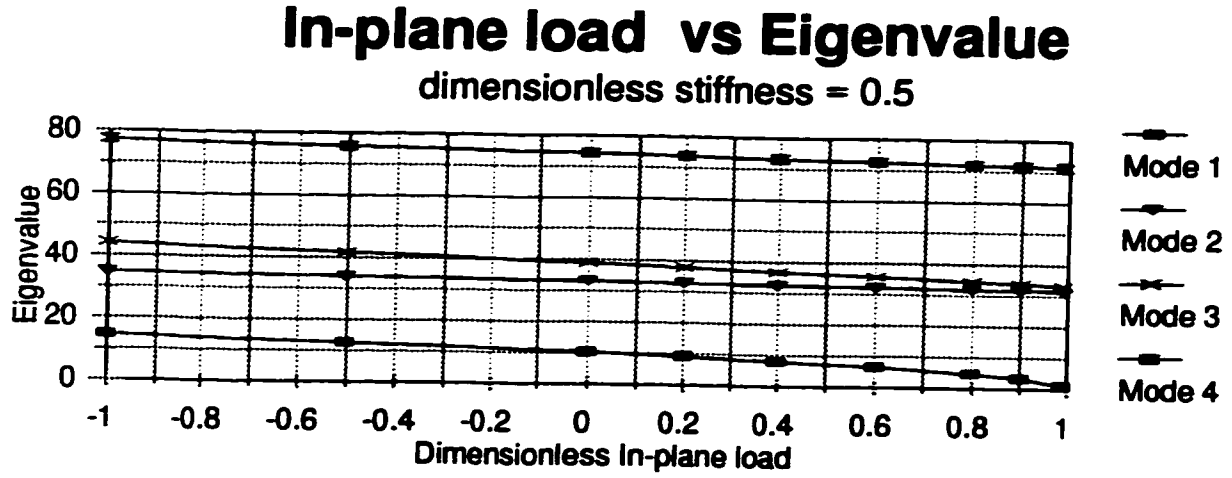

Figure A.26 Eigenvalue curves, TFTF plate, $K_{2R}=K_{4R}=30.0$, $\phi = 1/2.5$,

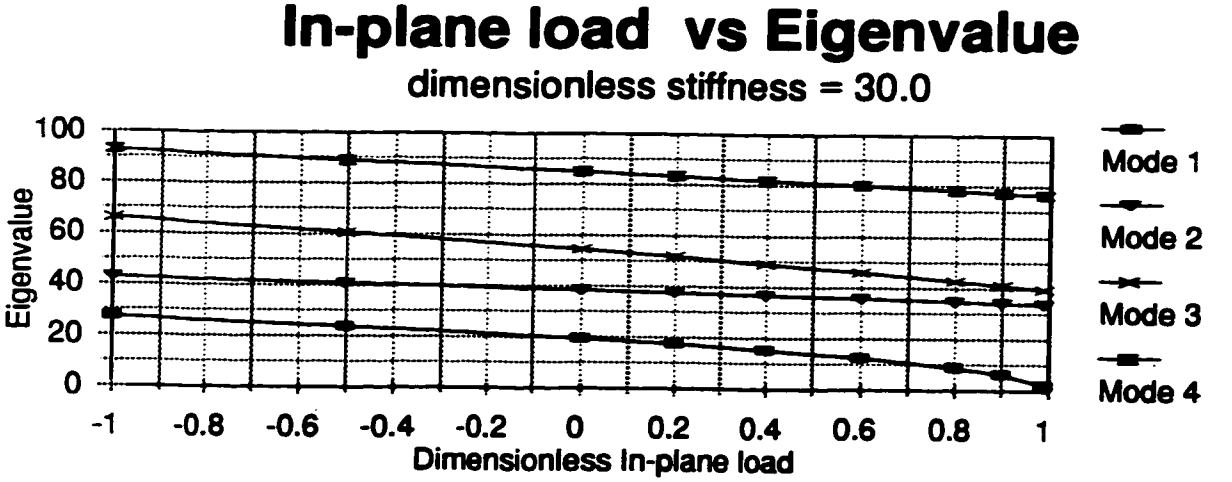

Figure A.27, **TFTF Plate,** $K_{2r/4r} = 0.5$, $\Phi = 1/2.5$

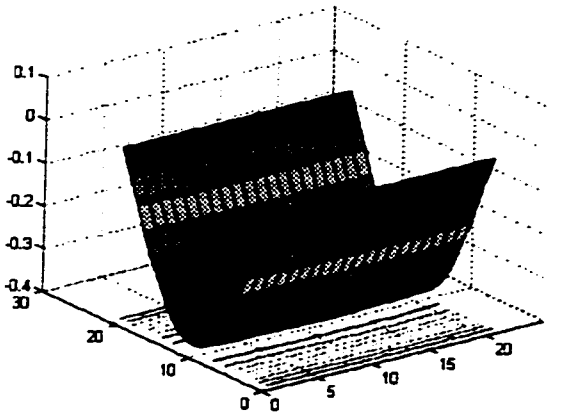

Mode 1

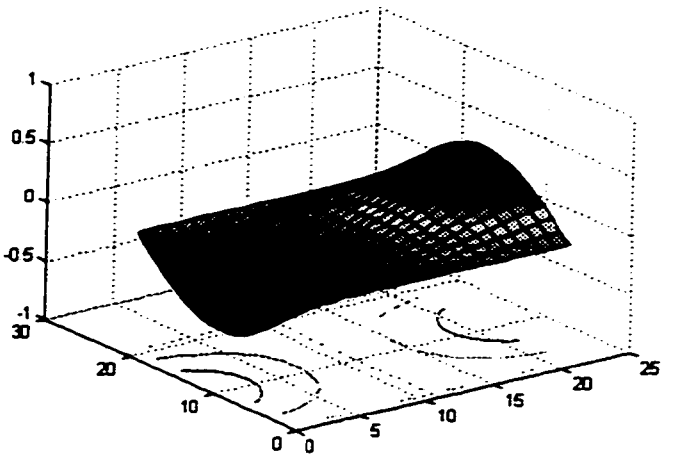

Mode 2

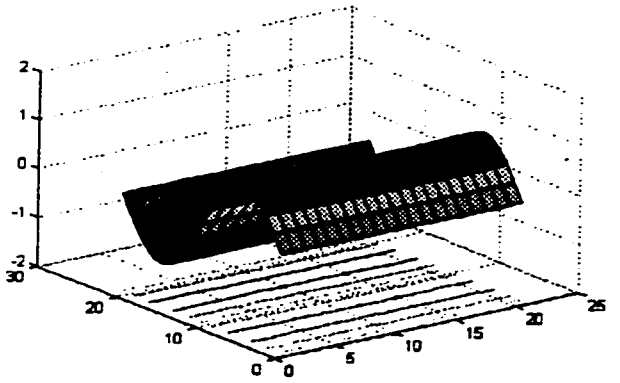

Mode 3

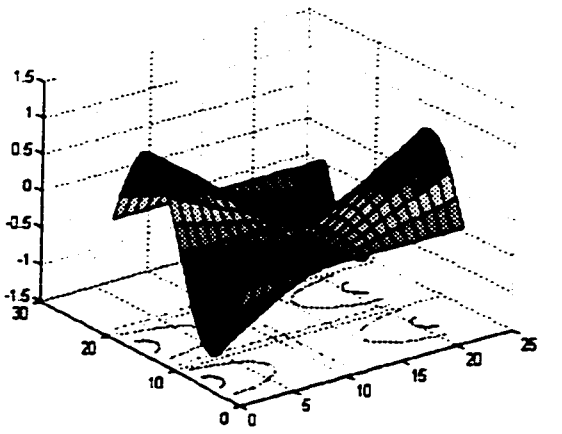

Mode 4

Table A.91 - A.95 Eigenvalues, TFTF Plate, $\phi = 1 / 2.0$

[A.91]									
Mode	-100%	-50%	0%	20%	40%	60%	80%	90%	99%
1	14.68	12.71	10.37	9.276	8.030	6.550	4.619	3.249	1.041
2	29.20	28.27	27.30	26.90	26.49	26.08	25.67	25.46	25.27
3	44.41	41.91	39.25	38.14	37.00	35.81	34.59	33.96	33.38
4	67.41	65.78	64.13	63.45	62.77	62.08	61.38	61.04	60.71

[A.92]									
Mode	-100%	-50%	0%	20%	40%	60%	80%	90%	99%
1	15.79	13.68	11.17	9.991	8.654	7.069	5.004	3.546	1.163
2	29.79	28.72	27.62	27.16	26.70	26.23	25.75	25.51	25.29
3	45.94	43.14	40.16	38.90	37.60	36.25	34.85	34.13	33.46
4	68.43	33.59	64.69	63.92	63.14	62.34	61.54	61.13	60.77

[A.93]									
Mode	-100%	-50%	0%	20%	40%	60%	80%	90%	99%
1	17.59	15.23	12.44	11.13	9.639	7.871	5.566	3.936	1.244
2	30.80	29.53	28.19	27.64	27.08	26.50	25.92	25.62	25.34
3	48.56	45.28	41.74	40.24	38.68	37.05	35.35	34.47	33.66
4	70.24	68.02	65.72	64.77	63.82	62.85	61.86	61.37	60.91

[A.94]									
Mode	-100%	-50%	0%	20%	40%	60%	80%	90%	99%
1	18.97	16.43	13.42	12.01	10.40	8.496	6.009	4.248	1.337
2	31.65	30.20	28.69	28.06	27.42	26.76	26.08	25.74	25.42
3	50.70	47.05	43.10	41.41	39.65	37.81	35.87	34.86	33.92
4	71.77	69.25	66.62	65.55	64.45	63.34	62.20	61.63	61.10

[A.95]									
Mode	-100%	-50%	0%	20%	40%	60%	80%	90%	99%
1	20.07	17.39	14.21	12.77	11.02	9.001	6.368	4.505	1.428
2	32.36	30.78	29.12	28.43	27.72	26.99	26.24	25.86	25.51
3	52.48	48.55	44.27	42.43	40.52	38.50	36.38	35.26	34.23
4	73.08	70.31	67.44	66.25	65.04	63.81	62.55	61.91	61.38

Table 4.96 - 4.100 Eigenvalues, TFTF Plate, $\phi = 1 / 2.0$

[A.96] $K_{x,o} = -5.0$, $\phi = 1/2.0$ In-plane load as a percentage of Buckling load ($K_{x,cr}$)

Mode	-100%	-50%	0%	20%	40%	60%	80%	90%	99%
1	20.98	18.18	14.86	13.30	11.52	9.413	6.655	4.701	1.444
2	32.97	31.28	29.50	28.76	27.99	27.21	26.40	25.98	25.60
3	54.00	49.84	45.29	43.34	41.29	39.14	36.86	35.66	34.55
4	74.22	71.25	68.16	66.89	65.58	64.26	62.90	62.21	61.58

[A.97] $K_{x,o} = -7.5$, $\phi = 1/2.0$ In-plane load as a percentage of Buckling load ($K_{x,cr}$)

Mode	-100%	-50%	0%	20%	40%	60%	80%	90%	99%
1	22.66	19.66	16.08	14.40	12.48	10.20	7.216	5.098	1.568
2	34.16	32.28	30.28	29.44	28.57	27.68	26.75	26.28	25.84
3	56.94	52.38	47.37	45.20	42.94	40.53	37.98	36.63	35.38
4	76.49	73.17	69.69	68.25	66.78	65.27	63.73	62.95	62.23

[A.98] $K_{x,o} = -10.0$, $\phi = 1/2.0$ In-plane load as a percentage of Buckling load ($K_{x,cr}$)

Mode	-100%	-50%	0%	20%	40%	60%	80%	90%	99%
1	23.83	20.69	16.94	15.17	13.16	10.76	7.625	5.399	1.722
2	35.04	33.03	30.88	29.97	29.04	28.07	27.06	26.55	26.07
3	59.07	54.25	48.94	46.65	44.23	41.67	38.94	37.50	36.15
4	78.20	74.65	70.91	69.36	67.78	66.15	64.49	63.64	62.86

[A.99] $K_{x,o} = -20.0$, $\phi = 1/2.0$ In-plane load as a percentage of Buckling load ($K_{x,cr}$)

Mode	-100%	-50%	0%	20%	40%	60%	80%	90%	99%
1	26.32	22.89	18.78	16.83	14.61	11.96	8.477	5.999	1.870
2	37.06	34.78	32.32	31.28	30.20	29.08	27.91	27.30	26.74
3	63.92	58.60	52.71	50.15	47.45	44.58	41.51	39.88	38.35
4	82.28	78.27	74.03	72.26	70.44	68.57	66.65	65.67	64.77

[A.100] $K_{x,o} = -25.0$, $\phi = 1/2.0$ In-plane load as a percentage of Buckling load ($K_{x,cr}$)

Mode	-100%	-50%	0%	20%	40%	60%	80%	90%	99%
1	27.47	23.90	19.63	17.60	15.28	12.51	8.874	6.279	1.948
2	38.07	35.67	33.07	31.97	30.83	29.63	28.39	27.74	27.14
3	66.30	60.76	54.63	51.97	49.15	46.15	42.93	41.23	39.63
4	84.40	80.19	75.73	73.87	71.95	69.98	67.95	66.91	65.96

Figure A.28 Eigenvalue curves, TFTF plate, $K_{2R}=K_{4R}=0.5$, $\phi = 1/2.0$,

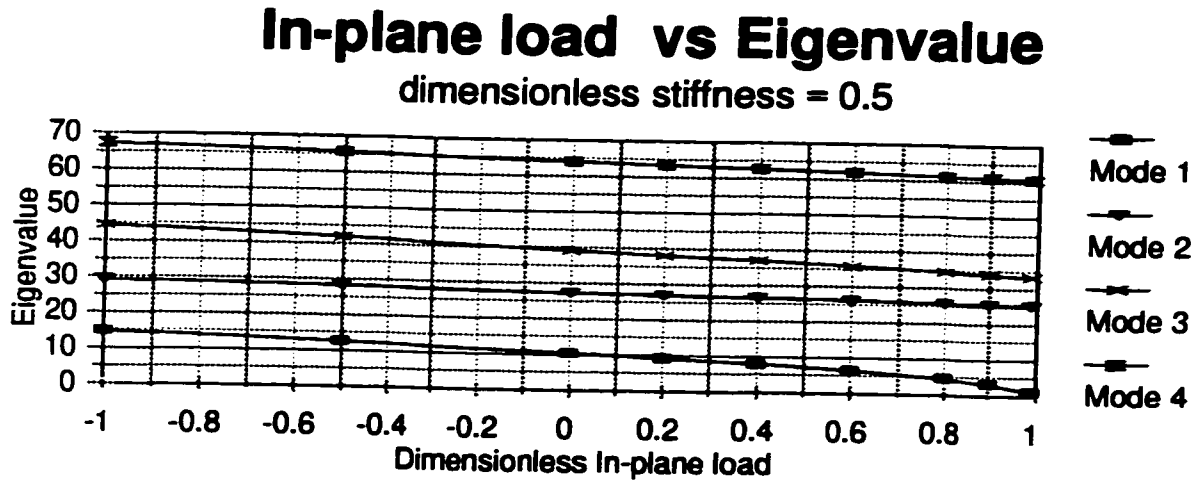

Figure A.29 Eigenvalue curves, TFTF plate, $K_{2R}=K_{4R}=30.0$, $\phi = 1/2.0$,

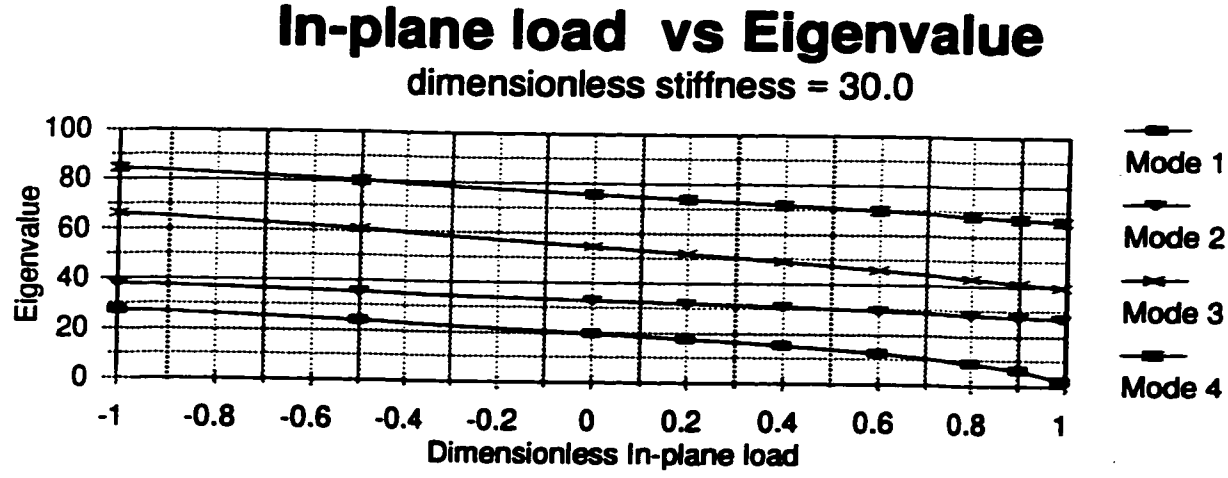

Figure A.30, **TFTF Plate,** $K_{2r/4r} = 30.0$, $\Phi = 1/2.0$

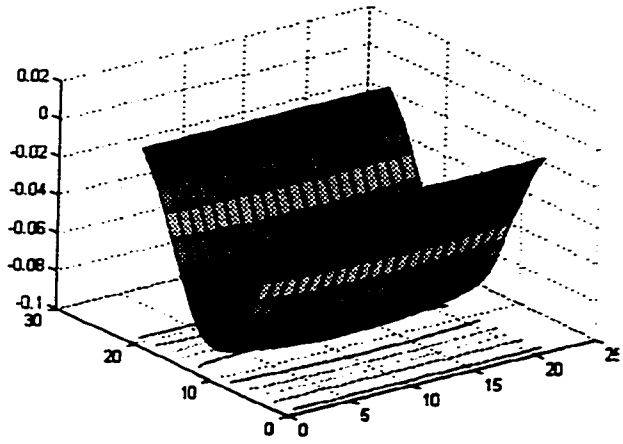

Mode 1

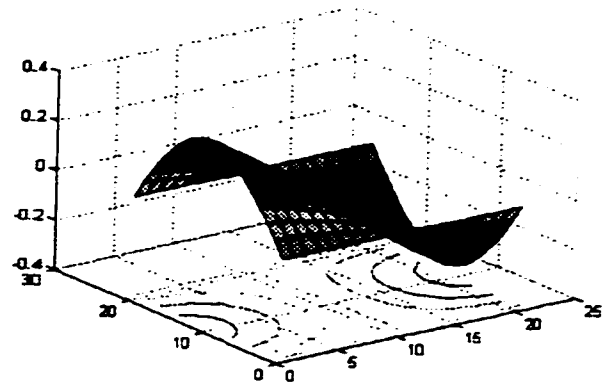

Mode 2

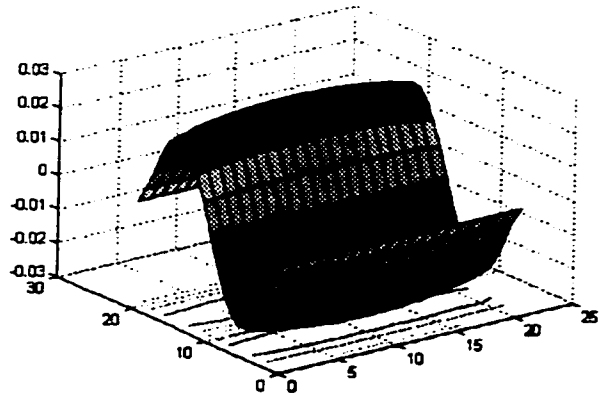

Mode 3

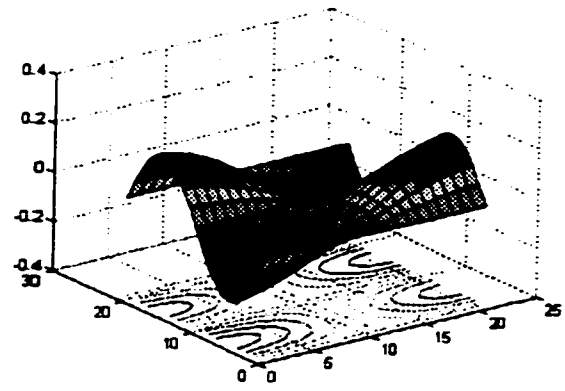

Mode 4

Table A.101 - A.105 Eigenvalues, TFTF Plate, $\phi = 1 / 1.5$

[A.101] $K_{x,y} = 0.5$, $\phi = 1/1.5$ In-plane load as a percentage of buckling load (-50%)

Mode	-100%	-50%	0%	20%	40%	60%	80%	90%	99%
1	14.74	12.77	10.42	9.324	8.074	6.592	4.661	3.295	1.036
2	24.03	22.87	21.65	21.10	20.62	20.08	19.53	19.26	19.00
3	44.657	42.15	39.49	38.378	37.228	36.04	34.82	34.18	33.61
4	58.68	56.80	54.85	54.05	53.24	52.52	51.58	51.16	50.78

[A.102] $K_{x,y} = 0.6$, $\phi = 1/1.5$ In-plane load as a percentage of buckling load (-60%)

Mode	-100%	-50%	0%	20%	40%	60%	80%	90%	99%
1	15.86	13.74	11.21	10.03	8.690	7.097	5.020	3.556	1.150
2	24.74	23.43	22.05	21.47	20.88	20.27	19.64	19.31	19.02
3	46.19	43.39	40.39	39.13	37.82	36.47	35.06	34.34	33.68
4	59.86	57.72	55.51	54.59	53.66	52.72	51.76	51.27	50.83

[A.103] $K_{x,y} = 0.8$, $\phi = 1/1.5$ In-plane load as a percentage of buckling load (-80%)

Mode	-100%	-50%	0%	20%	40%	60%	80%	90%	99%
1	17.65	15.29	12.49	11.17	9.672	7.896	5.580	3.940	1.214
2	25.94	24.40	22.75	22.05	21.34	20.60	19.83	19.43	19.07
3	48.80	45.51	41.97	40.46	38.90	37.27	35.56	34.68	33.86
4	61.91	59.36	56.68	55.58	54.45	53.30	52.12	51.52	50.98

[A.104] $K_{x,y} = 0.8$, $\phi = 1/2.0$ In-plane load as a percentage of buckling load (-80%)

Mode	-100%	-50%	0%	20%	40%	60%	80%	90%	99%
1	19.03	16.49	13.47	12.05	10.44	8.521	6.023	4.254	1.315
2	26.92	25.20	23.34	22.55	21.74	20.89	20.01	19.50	19.14
3	50.94	47.28	43.32	41.62	39.86	38.01	36.07	35.06	34.13
4	63.63	60.74	57.72	56.46	55.17	53.86	52.51	51.82	51.19

[A.105] $K_{x,y} = 0.8$, $\phi = 1/2.5$ In-plane load as a percentage of buckling load (-80%)

Mode	-100%	-50%	0%	20%	40%	60%	80%	90%	99%
1	20.13	17.45	14.26	12.76	11.05	9.029	6.389	4.521	1.442
2	27.74	25.87	23.85	22.99	22.10	21.16	20.19	19.68	19.22
3	52.71	48.77	44.48	42.65	40.73	38.71	36.58	35.47	34.44
4	65.09	61.94	58.63	57.25	55.84	54.39	52.90	52.14	51.44

Table A.106 - A.110 Eigenvalues, TFTF Plate, $\phi = 1 / 1.5$

[A.106] $K_{x/c}$ -50, ϕ = 1/1.5 In-plane load as a percentage of Buckling load (-0.07)

Mode	-100%	-50%	0%	20%	40%	60%	80%	90%	99%
1	21.04	18.24	14.91	13.34	11.56	9.446	6.685	4.730	1.504
2	28.43	26.44	24.28	23.37	22.41	21.41	20.35	19.81	19.30
3	54.22	50.06	45.50	43.55	41.50	39.35	37.07	35.80	34.76
4	66.34	62.99	59.44	57.96	56.45	54.88	53.28	52.46	51.70

[A.107] $K_{x/c}$ -75, ϕ = 1/1.5 In-plane load as a percentage of Buckling load (-0.10)

Mode	-100%	-50%	0%	20%	40%	60%	80%	90%	99%
1	22.73	19.72	16.13	14.44	12.52	10.23	7.237	5.114	1.579
2	29.77	27.57	25.16	24.13	23.05	21.92	20.72	20.09	19.51
3	57.17	52.59	47.57	45.41	43.13	40.73	38.17	36.82	35.57
4	68.80	65.10	61.13	59.47	57.76	55.99	54.17	53.24	52.38

[A.108] $K_{x/c}$ -100, ϕ = 1/1.5 In-plane load as a percentage of Buckling load (-0.13)

Mode	-100%	-50%	0%	20%	40%	60%	80%	90%	99%
1	23.90	20.75	16.99	15.21	13.20	10.79	7.644	5.412	1.719
2	30.74	28.39	25.82	24.71	23.55	22.32	21.02	20.34	19.71
3	59.30	54.47	49.15	46.85	44.43	41.86	39.13	37.68	36.33
4	69.28	66.70	62.46	60.68	58.84	56.94	54.97	53.96	53.03

[A.109] $K_{x/c}$ -200, ϕ = 1/1.5 In-plane load as a percentage of Buckling load (-0.07)

Mode	-100%	-50%	0%	20%	40%	60%	80%	90%	99%
1	26.40	22.96	18.83	16.88	14.65	12.00	8.505	6.021	1.893
2	32.91	30.27	27.35	26.09	24.75	23.34	21.82	21.02	20.26
3	64.15	58.82	52.91	50.35	47.64	44.77	41.69	40.05	38.52
4	70.49	69.33	65.76	63.74	61.65	59.48	57.22	56.06	54.99

[A.110] $K_{x/c}$ -300, ϕ = 1/1.5 In-plane load as a percentage of Buckling load (-0.07)

Mode	-100%	-50%	0%	20%	40%	60%	80%	90%	99%
1	27.55	23.97	19.68	17.65	15.33	12.56	8.909	6.313	2.008
2	33.96	31.19	28.12	26.79	25.38	23.87	22.25	21.40	20.59
3	66.54	60.99	54.84	52.17	49.35	46.34	43.12	41.41	39.80
4	71.14	69.91	67.53	65.41	63.21	60.92	58.54	57.31	56.18

Figure A.31 Eigenvalue curves, TFTF plate, $K_{2R}=K_{4R}=1.0$, $\phi = 1/1.5$,

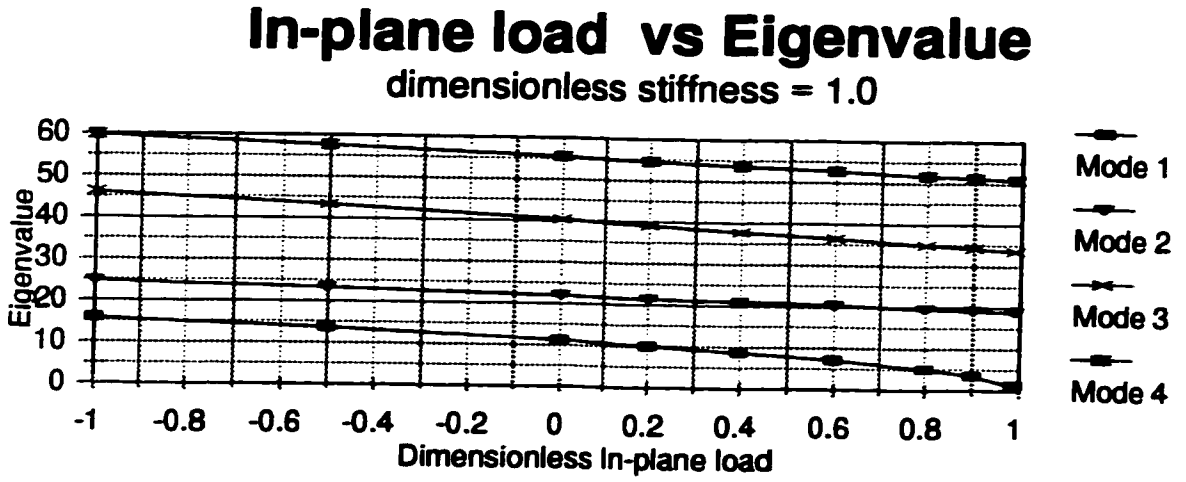

Figure A.32 Eigenvalue curves, TFTF plate, $K_{2R}=K_{4R}=7.5$, $\phi = 1/1.5$,

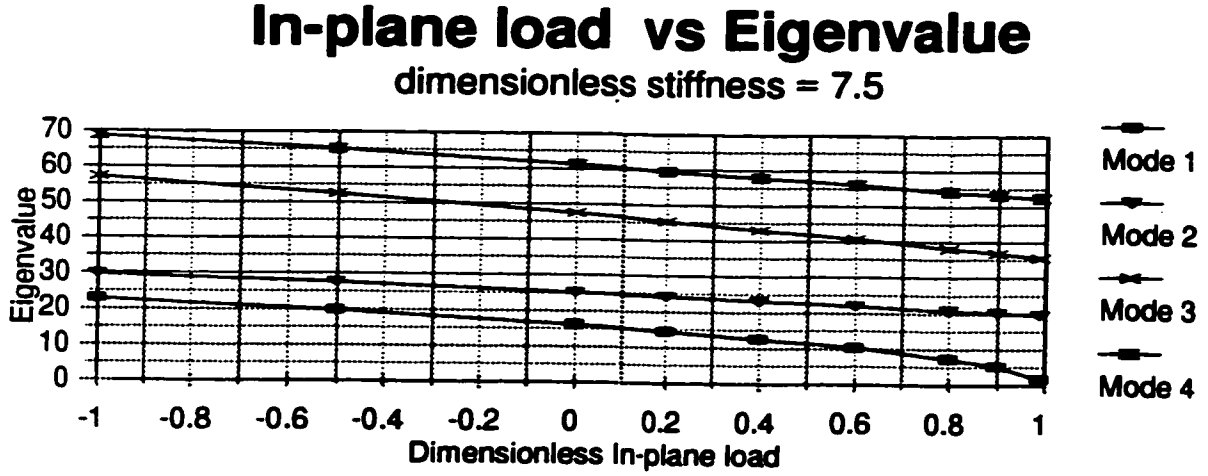

Figure A.33, TFTF Plate, $K_{2r/4r} = 1.0$, $\Phi = 1/1.5$

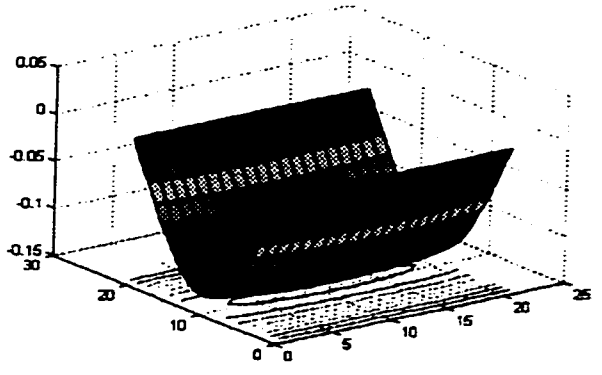

Mode 1

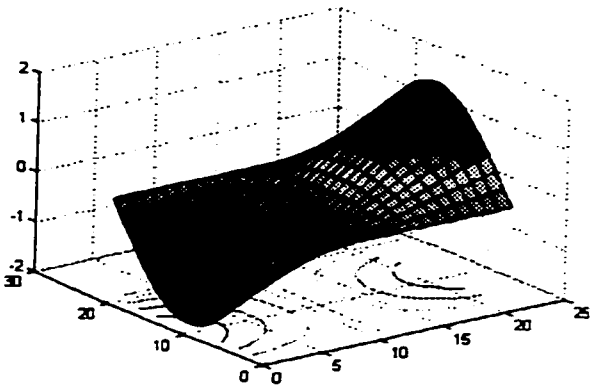

Mode 2

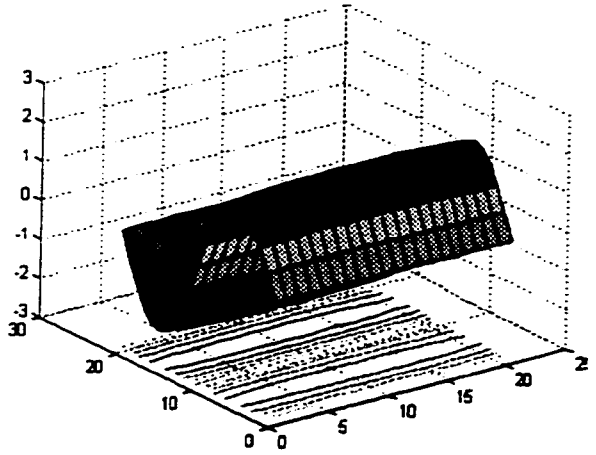

Mode 3

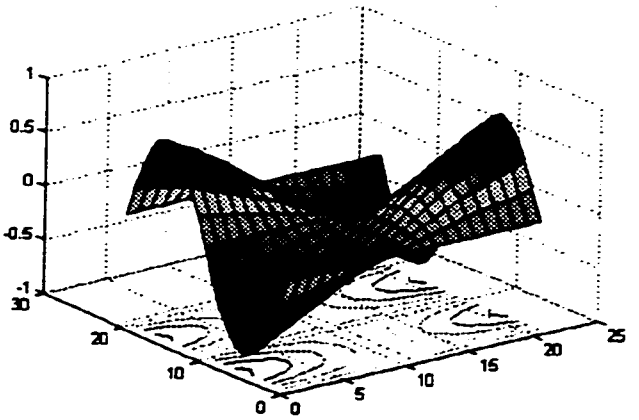

Mode 4

Table A.111 - A.115 Eigenvalues, TFTF F Plate, $\phi = 2.0 / 1$

[A.111] $K_{x/a} = 0.5$, $\Phi = 2.0/1$ In-plane load as a percentage of Buckling load(5.73)

Mode	-100%	-50%	0%	20%	40%	60%	80%	90%	99%
1	15.03	13.01	10.63	9.503	8.230	6.720	4.751	3.360	1.059
2	16.31	14.47	12.36	11.419	10.38	9.233	7.917	7.168	6.421
3	20.96	19.57	18.07	17.43	16.78	16.08	15.37	15.00	14.66
4	29.88	28.92	27.93	27.52	27.11	26.69	26.27	26.05	25.85

[A.112] $K_{x/a} = 1.0$, $\Phi = 2.0/1$ In-plane load as a percentage of Buckling load([illegible])

Mode	-100%	-50%	0%	20%	40%	60%	80%	90%	99%
1	16.13	13.97	11.40	10.20	8.835	7.214	5.101	3.607	1.142
2	17.33	15.34	13.05	12.01	10.87	9.601	8.134	7.291	6.438
3	21.77	20.22	18.54	17.83	17.09	16.31	15.49	15.06	14.67
4	30.45	29.37	28.24	27.78	27.31	26.83	26.34	26.09	25.86

[A.113] $K_{x/a} = 2.0$, $\Phi = 2.0/1$ In-plane load as a percentage of Buckling load([illegible])

Mode	-100%	-50%	0%	20%	40%	60%	80%	90%	99%
1	17.89	15.50	12.66	11.32	9.807	8.009	5.664	4.005	1.267
2	18.98	16.75	14.16	12.98	11.68	10.22	8.509	7.508	6.476
3	23.12	21.32	19.36	18.51	17.63	16.73	15.71	15.19	14.71
4	31.44	30.14	28.79	28.23	27.66	27.08	26.48	26.18	25.90

[A.114] $K_{x/a} = 3.0$, $\Phi = 2.0/1$ In-plane load as a percentage of Buckling load(7.24)

Mode	-100%	-50%	0%	20%	40%	60%	80%	90%	99%
1	19.26	16.69	13.63	12.20	10.50	8.628	6.102	4.315	1.362
2	20.28	17.86	15.04	13.76	12.33	10.72	8.821	7.695	6.516
3	24.21	22.22	20.03	19.09	18.09	17.04	15.91	15.32	14.76
4	32.26	30.80	29.26	28.62	27.97	27.30	26.62	26.27	25.95

[A.115] $K_{x/a} = 4.0$, $\Phi = 2.0/1$ In-plane load as a percentage of Buckling load([illegible])

Mode	-100%	-50%	0%	20%	40%	60%	80%	90%	99%
1	20.30	17.64	14.42	12.90	11.18	9.130	6.459	4.568	1.446
2	21.33	18.76	15.77	14.39	12.87	11.14	9.088	7.860	6.559
3	25.10	22.96	20.60	19.57	18.49	17.33	16.09	15.44	14.82
4	32.95	31.35	29.67	28.97	28.25	27.51	26.75	26.36	26.01

Table A.116 - A.120 Eigenvalues, TFTF Plate, $\phi = 2.0 / 1$

[illegible]

Mode	-100%	-50%	0%	20%	40%	60%	80%	90%	99%
1	21.26	18.43	15.07	13.48	11.68	9.546	6.755	4.778	1.514
2	22.20	19.51	16.37	14.92	13.32	11.50	9.318	8.005	6.601
3	25.86	23.59	21.08	19.99	18.83	17.59	16.26	15.55	14.88
4	33.53	31.83	30.02	29.27	28.50	27.69	26.88	26.46	26.07

[illegible]

Mode	-100%	-50%	0%	20%	40%	60%	80%	90%	99%
1	22.95	19.91	16.29	14.58	12.64	10.33	7.316	5.177	1.639
2	23.83	20.92	17.52	15.94	14.20	12.19	9.774	8.300	6.699
3	27.30	24.81	22.04	20.82	19.52	18.13	16.62	15.80	15.03
4	34.69	32.78	30.75	29.89	29.01	28.10	27.16	26.68	26.24

[illegible]

Mode	-100%	-50%	0%	20%	40%	60%	80%	90%	99%
1	24.13	20.94	17.15	15.36	13.32	10.89	7.715	5.461	1.780
2	24.97	21.92	18.33	16.67	14.82	12.70	10.11	8.528	6.784
3	28.33	25.69	22.74	21.44	20.04	18.55	16.90	16.02	15.17
4	35.33	33.49	31.30	30.37	29.42	28.43	27.41	26.88	26.39

[illegible]

Mode	-100%	-50%	0%	20%	40%	60%	80%	90%	99%
1	26.64	23.16	19.00	17.03	14.79	12.10	8.583	6.078	1.924
2	27.43	24.08	20.12	18.28	16.21	13.82	10.89	9.065	7.011
3	30.60	27.66	24.33	22.85	21.26	19.53	17.62	16.58	15.57
4	37.46	35.13	32.61	31.54	30.43	29.27	28.06	27.43	26.85

[illegible]

Mode	-100%	-50%	0%	20%	40%	60%	80%	90%	99%
1	27.81	24.19	19.86	17.81	15.47	12.67	8.987	6.366	2.015
2	28.58	25.09	20.96	19.03	16.87	14.36	11.27	9.333	7.135
3	31.68	28.61	25.11	23.55	21.87	20.04	18.00	16.88	15.80
4	38.41	35.95	33.28	32.15	30.96	29.72	28.43	27.75	27.13

Figure A.34 Eigenvalue curves, TFTF plate, $K_{2R}=K_{4R}=0.5$, $\phi = 2.0/1$,

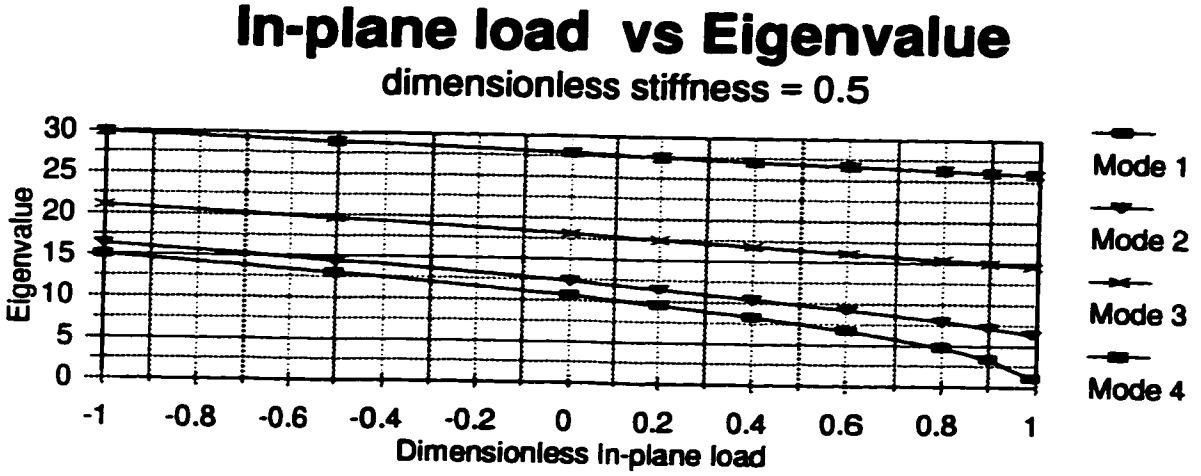

Figure A.35 Eigenvalue curves, TFTF plate, $K_{2R}=K_{4R}=30.0$, $\phi = 2.0/1$,

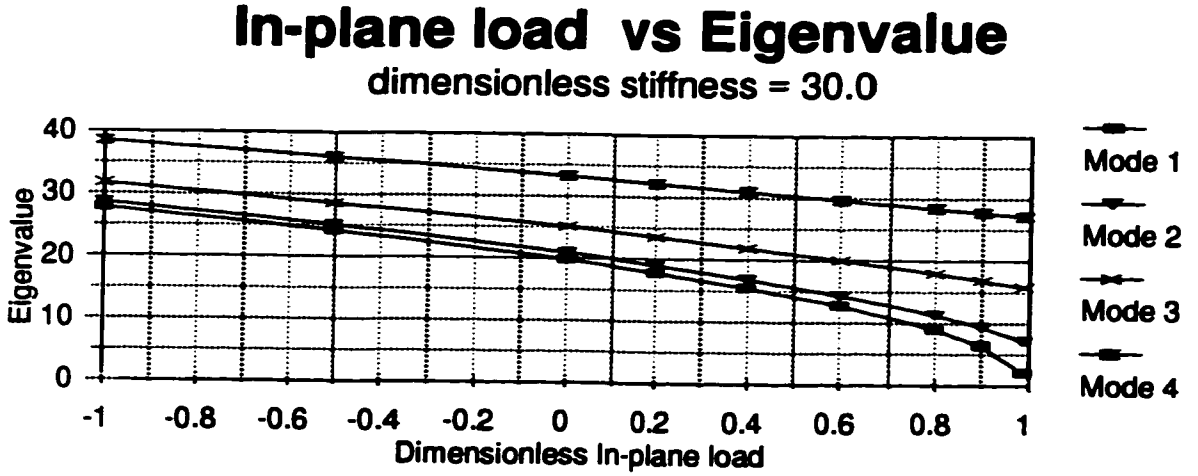

Figure A.36, TFTF Plate, $K_{2r/4r} = 0.5$, $\Phi = 2.0/1$

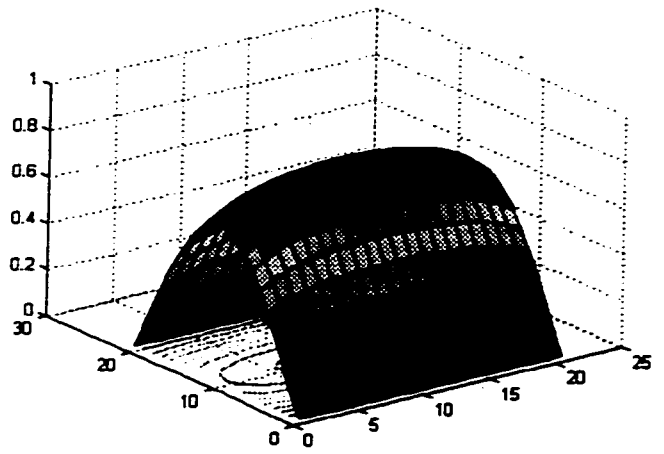

Mode 1

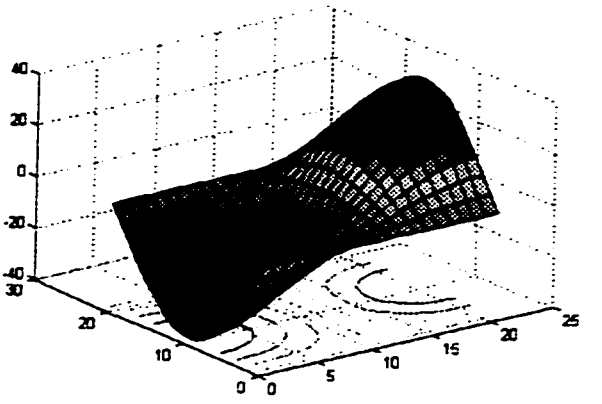

Mode 2

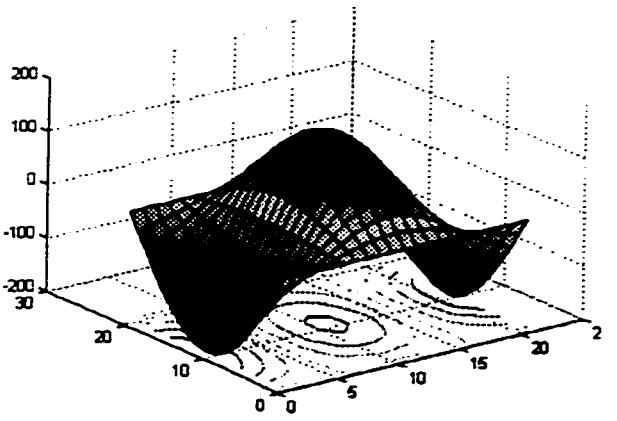

Mode 3

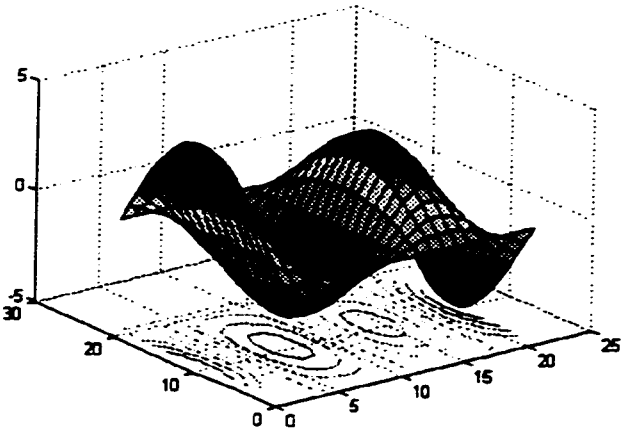

Mode 4

Table A.121 - A.125 Eigenvalues, TFTF Plate, $\phi = 2.5 / 1$

[A.121] $K_{x,cr} = 8.5$, $\Phi = 2.5/1$ In-plane load as a percentage of buckling load (71.4N)									
Mode	-100%	-50%	0%	20%	40%	60%	80%	90%	99%
1	15.00	13.05	10.65	9.528	8.251	6.737	4.763	3.368	1.062
2	15.89	13.99	11.79	10.78	9.672	8.418	6.940	6.067	5.157
3	18.87	17.30	15.57	14.83	14.04	13.21	12.32	11.85	11.41
4	24.45	23.26	22.01	21.48	20.95	20.40	19.84	19.55	19.29

[A.122] $K_{x,cr} = 8.4$, $\Phi = 2.5/1$ In-plane load as a percentage of buckling load (72.2N)									
Mode	-100%	-50%	0%	20%	40%	60%	80%	90%	99%
1	16.163	14.00	11.43	10.22	8.834	7.229	5.112	3.615	1.142
2	16.93	14.88	12.50	11.40	10.19	8.818	7.185	6.209	5.176
3	19.76	18.03	16.12	15.28	14.48	13.47	12.46	11.93	11.43
4	25.15	23.81	22.40	21.81	21.20	20.58	19.93	19.61	19.30

[A.123] $K_{x,cr} = 7.8$, $\Phi = 2.5/1$ In-plane load as a percentage of buckling load (77.0N)									
Mode	-100%	-50%	0%	20%	40%	60%	80%	90%	99%
1	17.93	15.53	12.68	11.34	9.825	8.023	5.674	4.013	1.270
2	18.63	16.33	13.65	12.42	11.05	9.484	7.601	6.457	5.216
3	21.23	19.25	17.04	16.07	15.04	13.93	12.73	12.08	11.46
4	26.32	24.75	23.08	22.37	21.64	20.89	20.11	19.70	19.33

[A.124] $K_{x,cr} = 7.3$, $\Phi = 2.5/1$ In-plane load as a percentage of buckling load (82.3N)									
Mode	-100%	-50%	0%	20%	40%	60%	80%	90%	99%
1	19.29	16.72	13.66	12.22	10.58	8.642	6.112	4.322	1.365
2	19.95	17.47	14.56	13.23	11.73	10.02	7.943	6.665	5.254
3	22.41	20.23	17.79	16.72	15.57	14.32	12.96	12.22	11.51
4	27.29	25.53	23.66	22.85	22.03	21.17	20.27	19.81	19.38

[A.125] $K_{x,cr} = 6.9$, $\Phi = 2.5/1$ In-plane load as a percentage of buckling load (87.0N)									
Mode	-100%	-50%	0%	20%	40%	60%	80%	90%	99%
1	20.39	17.67	14.44	12.92	11.19	9.143	6.468	4.575	1.447
2	21.01	18.38	15.31	13.88	12.29	10.46	8.230	6.844	5.294
3	23.37	21.04	18.42	17.26	16.01	14.66	13.16	12.35	11.56
4	28.08	26.19	24.13	23.26	22.36	21.42	20.426	19.91	19.43

Table A.126 - A.130 Eigenvalues, TFTF Plate, $\phi = 2.5 / 1$

[A.126] K_{x_1} = -3.0, ϕ = 2.5/1 In-plane load as a percentage of Buckling load (39.7)									
Mode	-100%	-50%	0%	20%	40%	60%	80%	90%	99%
1	21.29	18.46	15.08	13.50	11.69	9.559	6.764	4.785	1.516
2	21.89	19.14	15.92	14.43	12.76	10.84	8.475	7.000	5.3333
3	24.17	21.72	18.95	17.72	16.40	14.95	13.35	12.47	11.62
4	28.77	26.75	24.56	23.63	22.66	21.64	20.57	20.01	19.50

[A.127] K_{x_1} = -2.5, ϕ = 2.5/1 In-plane load as a percentage of Buckling load (33.08)									
Mode	-100%	-50%	0%	20%	40%	60%	80%	90%	99%
1	22.98	19.93	16.31	14.60	12.65	10.35	7.325	5.183	1.641
2	23.54	20.58	17.09	15.47	13.66	11.55	8.956	7.313	5.418
3	25.69	23.02	19.98	18.62	17.15	15.54	13.73	12.73	11.75
4	30.08	27.85	25.40	24.36	23.26	22.11	20.89	20.25	19.65

[A.128] K_{x_1} = -2.0, ϕ = 2.5/1 In-plane load as a percentage of Buckling load (26.46)									
Mode	-100%	-50%	0%	20%	40%	60%	80%	90%	99%
1	24.16	20.97	17.17	15.38	13.34	10.90	7.724	5.466	1.730
2	24.69	21.59	17.93	16.22	14.30	12.07	9.309	7.548	5.491
3	26.78	23.95	20.73	19.29	17.72	15.99	14.03	12.94	11.88
4	31.03	28.65	26.03	24.91	23.72	22.47	21.14	20.44	19.80

[A.129] K_{x_1} = -1.5, ϕ = 2.5/1 In-plane load as a percentage of Buckling load (19.85)									
Mode	-100%	-50%	0%	20%	40%	60%	80%	90%	99%
1	26.67	23.19	19.02	17.05	14.80	12.12	8.593	6.085	1.927
2	27.17	23.77	19.73	17.85	15.72	13.23	10.11	8.093	5.685
3	29.13	26.01	22.41	20.78	19.00	17.03	14.77	13.49	12.22
4	33.16	30.47	27.50	26.20	24.84	23.38	21.82	21.00	20.22

[A.130] K_{x_1} = -3.0, ϕ = 2.5/1 In-plane load as a percentage of Buckling load (13.23)									
Mode	-100%	-50%	0%	20%	40%	60%	80%	90%	99%
1	27.84	24.22	19.89	17.83	15.49	12.68	9.000	6.373	2.018
2	28.32	24.78	20.58	18.61	16.38	13.77	10.49	8.359	5.788
3	30.25	26.98	23.21	21.50	19.63	17.54	15.14	13.78	12.41
4	34.18	31.36	28.22	26.86	25.41	23.86	22.19	21.30	20.47

Figure A.37 Eigenvalue curves, TFTF plate, $K_{2R}=K_{4R}=0.5$, $\phi = 2.5/1$,

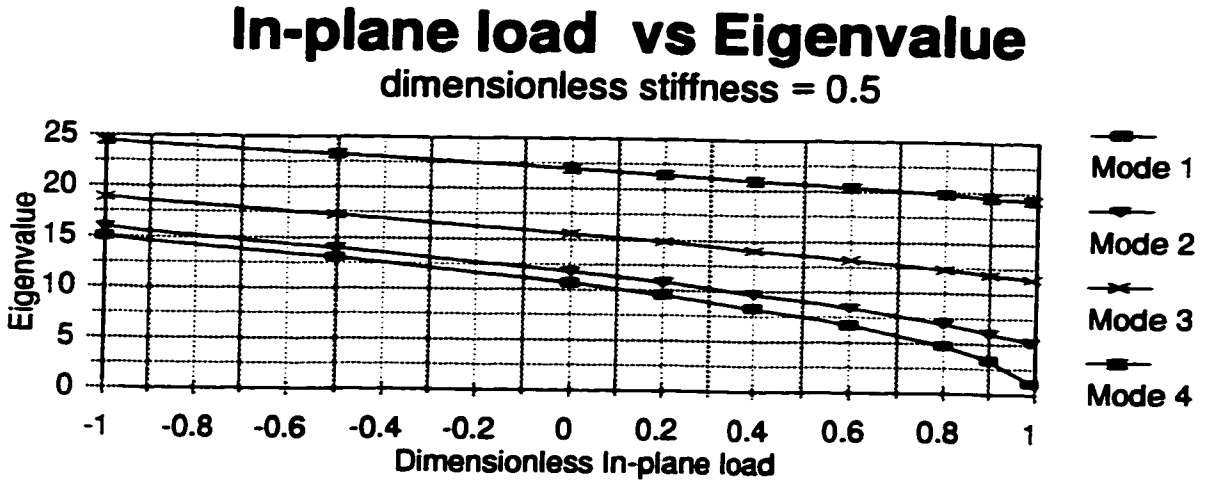

Figure A.38 Eigenvalue curves, TFTF plate, $K_{2R}=K_{4R}=30.0$, $\phi = 2.5/1$,

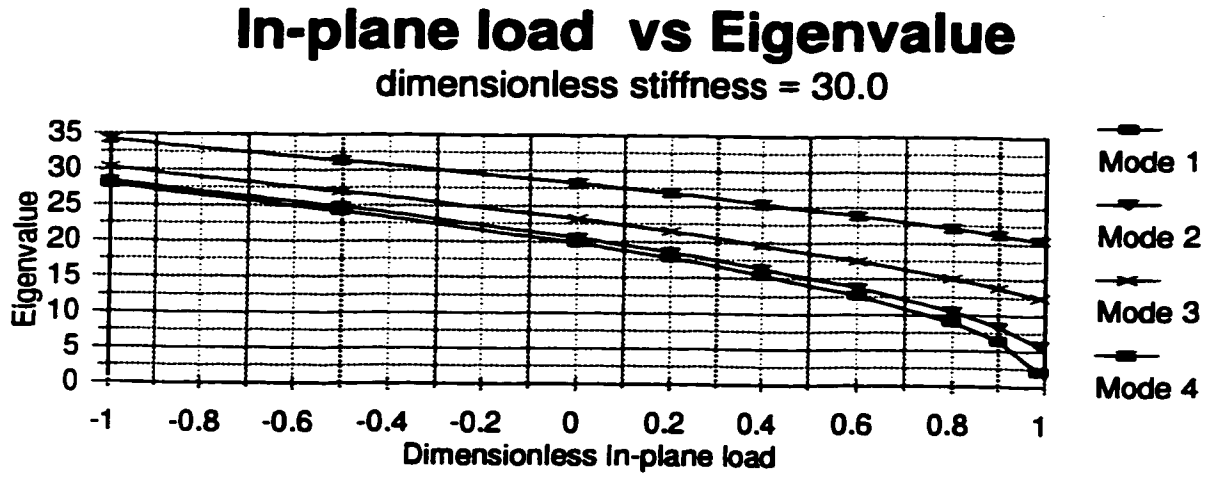

Figure 4.39, TFTF Plate, $K_{2r/4r} = 0.5$, $\Phi = 2.5/1$

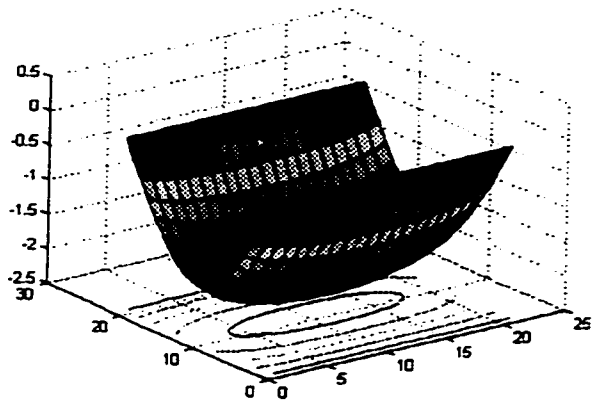

Mode 1

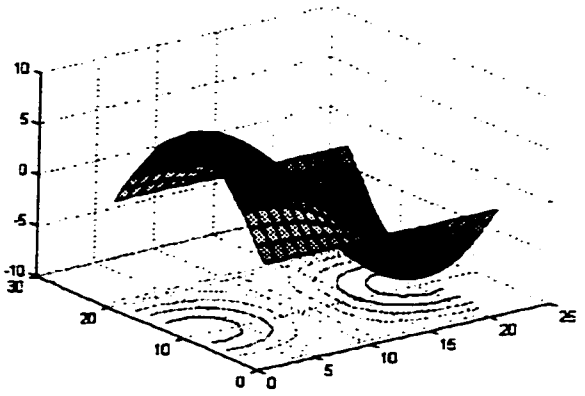

Mode 2

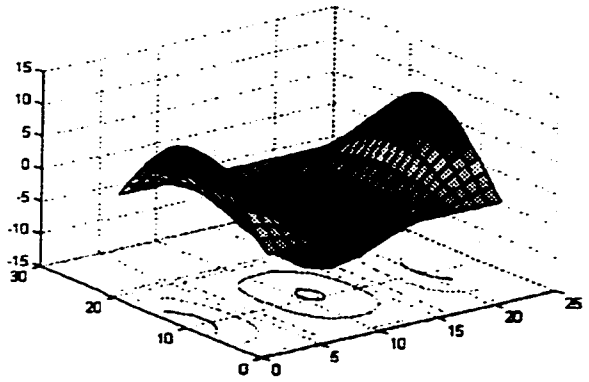

Mode 3

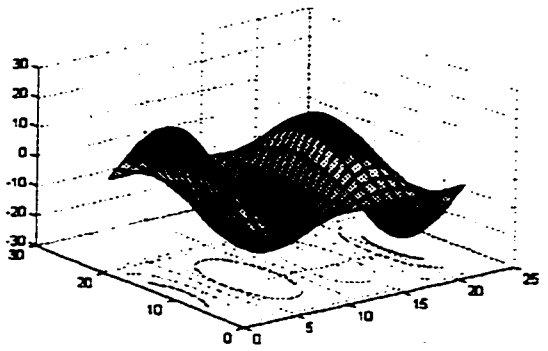

Mode 4

Table A.131 - 4.135 Eigenvalues, TFTF Plate, $\phi = 3.0 / 1$

[A.131] $K_{y,x} = 0.5$, $\phi = 3.0/1$ In-plane load as a percentage of buckling load (16.78)

Mode	-100%	-50%	0%	20%	40%	60%	80%	90%	99%
1	15.09	13.07	10.67	9.544	8.266	6.749	4.772	3.374	1.065
2	15.66	13.72	11.46	10.42	9.264	7.940	6.346	5.375	4.317
3	17.73	16.04	14.16	13.33	12.45	11.50	10.46	9.901	9.369
4	21.54	20.17	18.71	18.09	17.45	16.78	16.09	15.73	15.40

[A.132] $K_{y,x} = 1.0$, $\phi = 3.0/1$ In-plane load as a percentage of buckling load (16.78)

Mode	-100%	-50%	0%	20%	40%	60%	80%	90%	99%
1	16.19	14.02	11.45	10.24	8.868	7.240	5.120	3.620	1.143
2	16.72	14.63	12.19	11.06	9.805	8.362	6.612	5.533	4.338
3	18.67	16.83	14.76	13.84	12.86	11.80	10.63	9.992	9.383
4	22.32	20.80	19.16	18.47	17.74	16.99	16.20	15.79	15.41

[A.133] $K_{y,x} = 2.0$, $\phi = 3.0/1$ In-plane load as a percentage of buckling load (16.78)

Mode	-100%	-50%	0%	20%	40%	60%	80%	90%	99%
1	17.95	15.55	12.70	11.36	9.838	8.033	5.681	4.017	1.270
2	18.43	16.10	13.37	12.11	10.69	9.060	7.059	5.805	4.399
3	20.23	18.13	15.75	14.70	13.56	12.31	10.93	10.16	9.421
4	23.63	21.87	19.95	19.12	18.26	17.36	16.41	15.91	15.45

[A.134] $K_{y,x} = 4.0$, $\phi = 3.0/1$ In-plane load as a percentage of buckling load (16.78)

Mode	-100%	-50%	0%	20%	40%	60%	80%	90%	99%
1	19.31	16.73	13.67	12.23	10.59	8.652	6.120	4.328	1.371
2	19.76	17.25	14.29	12.93	11.395	9.617	7.422	6.031	4.419
3	21.45	19.16	16.56	15.40	14.13	12.74	11.18	10.32	9.465
4	24.70	22.74	20.60	19.67	18.70	17.68	16.59	16.02	15.49

[A.135] $K_{y,x} = 8.0$, $\phi = 3.0/1$ In-plane load as a percentage of buckling load (16.78)

Mode	-100%	-50%	0%	20%	40%	60%	80%	90%	99%
1	20.41	17.69	14.45	12.93	11.20	9.152	6.475	4.579	1.448
2	20.84	18.18	15.05	13.60	11.97	10.07	7.724	6.222	4.456
3	22.45	20.01	17.23	15.97	14.61	13.11	11.41	10.45	9.513
4	25.58	23.47	21.15	20.14	19.09	17.96	16.77	16.14	15.54

Table A.136 - A.140 Eigenvalues, TFTF Plate, $\phi = 3.0 / 1$

[A.136] $K_{x,c}$=[illegible], ϕ = 3.0/1 In-plane load as a percentage of Buckling load (81.61)

Mode	-100%	-50%	0%	20%	40%	60%	80%	90%	99%
1	21.31	18.47	15.10	13.51	11.71	9.568	6.770	4.789	1.515
2	21.72	18.95	15.68	14.16	12.45	10.46	7.980	6.387	4.492
3	23.28	20.72	17.79	16.47	15.02	13.43	11.61	10.58	9.563
4	26.31	24.08	21.62	20.55	19.42	18.22	16.93	16.24	15.60

[A.137] $K_{x,c}$=[illegible], ϕ = 3.0/1 In-plane load as a percentage of Buckling load (79.99)

Mode	-100%	-50%	0%	20%	40%	60%	80%	90%	99%
1	23.00	19.95	16.32	14.61	12.67	10.35	7.331	5.187	1.640
2	23.38	20.39	16.86	15.22	13.36	11.19	8.478	6.714	4.572
3	24.85	22.07	18.87	17.42	15.83	14.06	12.02	10.85	9.683
4	27.73	25.28	22.55	21.35	20.09	18.73	17.26	16.48	15.74

[A.138] $K_{x,c}$=[illegible], ϕ = 3.0/1 In-plane load as a percentage of Buckling load (78.38)

Mode	-100%	-50%	0%	20%	40%	60%	80%	90%	99%
1	24.18	20.99	17.18	15.39	13.35	10.91	7.729	5.470	1.729
2	24.54	21.41	17.70	15.97	14.01	11.72	8.841	6.957	4.638
3	25.96	23.03	19.65	18.11	16.42	14.52	12.33	11.07	9.792
4	28.75	26.14	23.23	21.95	20.59	19.13	17.54	16.69	15.87

[A.139] $K_{x,c}$=[illegible], ϕ = 3.0/1 In-plane load as a percentage of Buckling load (76.90)

Mode	-100%	-50%	0%	20%	40%	60%	80%	90%	99%
1	26.69	23.21	19.04	17.07	14.81	12.13	8.600	6.090	1.929
2	27.03	23.60	19.52	17.61	15.44	12.89	9.654	7.512	4.812
3	28.36	25.13	21.37	19.65	17.75	15.60	13.08	11.61	10.06
4	30.98	28.07	24.79	23.34	21.78	20.09	18.23	17.22	16.26

[A.140] $K_{x,c}$=[illegible], ϕ = 3.0/1 In-plane load as a percentage of Buckling load (75.42)

Mode	-100%	-50%	0%	20%	40%	60%	80%	90%	99%
1	27.86	24.24	19.90	17.84	15.50	12.69	9.004	6.377	2.017
2	28.19	24.62	20.37	18.37	16.11	13.44	10.03	7.779	4.901
3	29.50	26.13	22.19	20.39	18.39	16.13	13.46	11.89	10.26
4	32.05	29.01	25.56	24.02	22.30	20.58	18.60	17.52	16.48

Figure A.40 Eigenvalue curves, TFTF plate, $K_{2R}=K_{4R}=0.5$, $\phi = 3.0/1$,

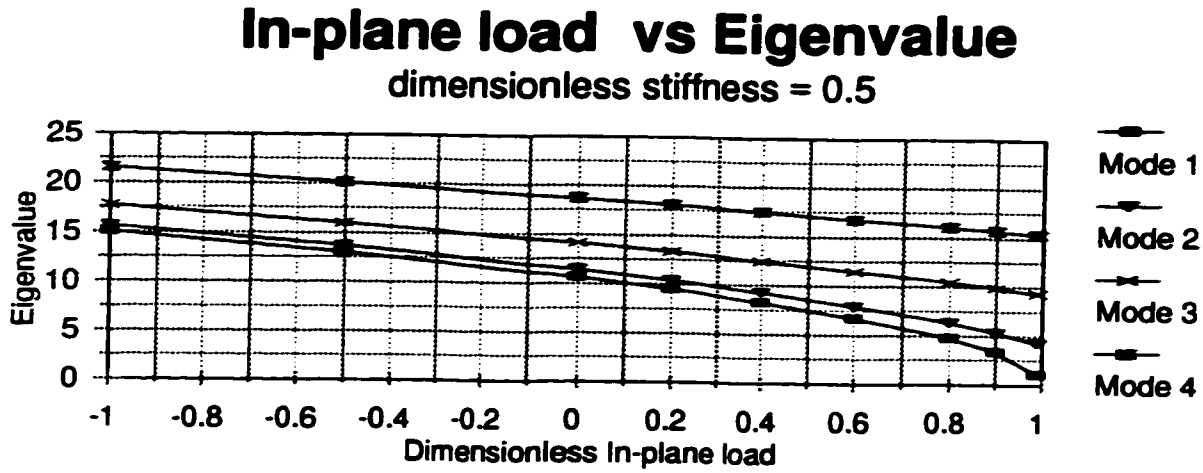

Figure A.41 Eigenvalue curves, TFTF plate, $K_{2R}=K_{4R}=30.0$, $\phi = 3.0/1$,

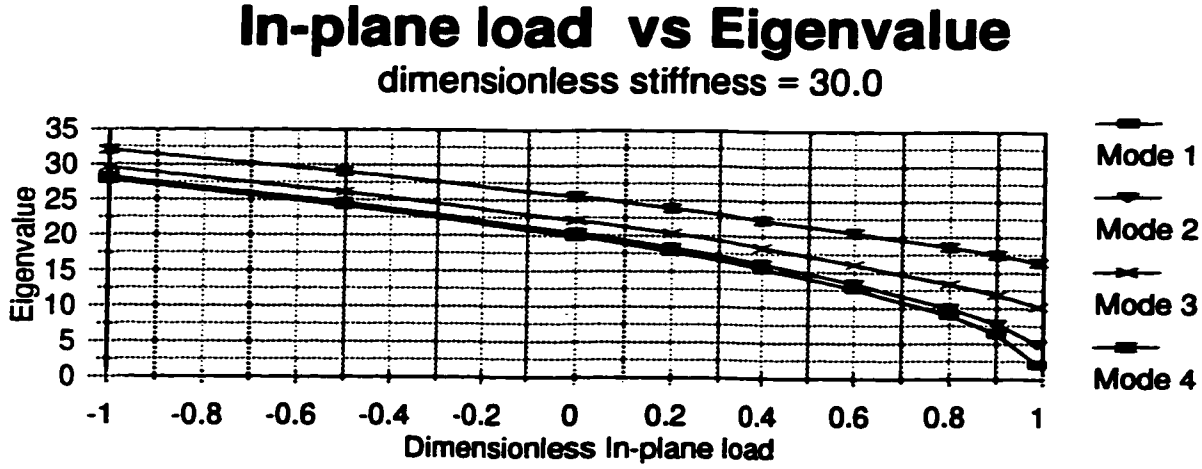

Figure 4.42, TFTF Plate, $K_{2r/4r} = 30.0$, $\Phi = 3.0/1$

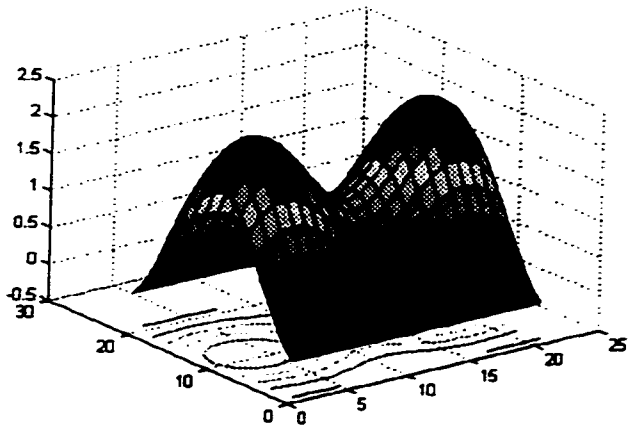

Mode 1

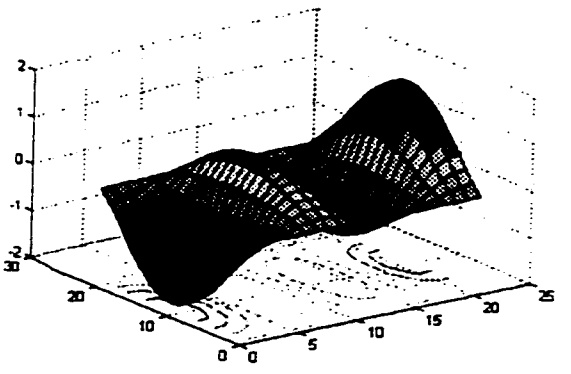

Mode 2

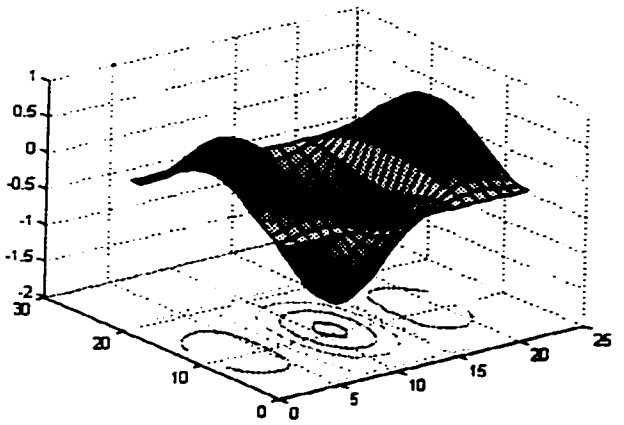

Mode 3

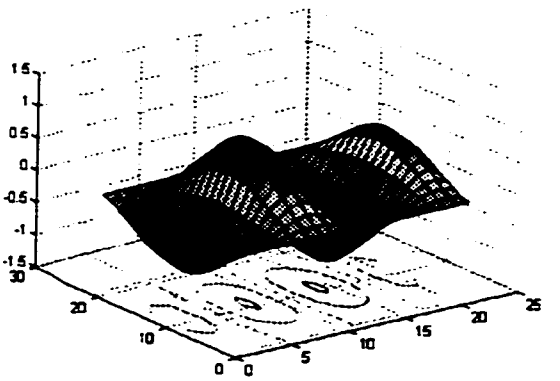

Mode 4

Appendix B

Appendix B lists the contributions of each building block towards enforcing a particular boundary condition in the superimposed solution, while, Appendix C lists the integrals solved in the following equations.

It should be noted that amplitude factors should be excluded from the following coefficients since block amplitudes are unknown. Therefore, treat building block coefficients A, B, C, and D as A/E, B/E, C/E, and D/E respectively.

B.1 SRSV Building Block Contributions

B.1.1 Bending Moment at $\eta = 1$.

General Equation

$$a_m = Y_m''(1) - \upsilon(m\pi\phi)^2 Y_m(1)$$

Case 1 Equation

$$a_m = \left[\left(\beta_m^2 - \gamma_m^2 - \upsilon(m\pi\phi)^2\right)A_m - 2\beta_m\gamma_m D_m\right]\sinh(\beta_m)\sin(\gamma_m) + \left[\left(\beta_m^2 - \gamma_m^2 - \upsilon(m\pi\phi)^2\right)D_m + 2\beta_m\gamma_m A_m\right]\cosh(\beta_m)\cos(\gamma_m)$$

Case 2 Equation

$$a_m = \left(\beta_m^2 - \upsilon(m\pi\phi)^2\right)B_m\cosh(\beta_m) - \left(\gamma_m^2 + \upsilon(m\pi\phi)^2\right)D_m\cos(\gamma_m)$$

Case 3 Equation

$$a_m = \left(\beta_m^2 - \upsilon(m\pi\phi)^2\right)B_m\cosh(\beta_m) + \left(\gamma_m^2 - \upsilon(m\pi\phi)^2\right)D_m\cosh(\gamma_m)$$

B.1.2 Slope at $\xi = 1$.

General Equation

$$e_{mo} = m\pi(-1)^m \int_0^1 Y_m(\eta)d\eta$$

$$e_{mn} = 2m\pi(-1)^m \int_0^1 Y_m(\eta)\cos(n\pi\eta)d\eta$$

Case 1 Equation

$$e_{mo} = m\pi(-1)^m \left[A_n \int_0^1 \sinh(\beta_n\eta)\sin(\gamma_n\eta)d\eta + D_n \int_0^1 \cosh(\beta_n\eta)\cos(\gamma_n\eta)d\eta \right]$$

$$e_{mn} = 2m\pi(-1)^m \left[A_n \int_0^1 \sinh(\beta_n\eta)\sin(\gamma_n\eta)\cos(n\pi\eta)d\eta + D_n \int_0^1 \cosh(\beta_n\eta)\cos(\gamma_n\eta)\cos(n\pi\eta)d\eta \right]$$

Case 2 Equation

$$e_{mo} = m\pi(-1)^m \left[B_n \int_0^1 \cosh(\beta_n\eta)d\eta + D_n \int_0^1 \cos(\gamma_n\eta)d\eta \right]$$

$$e_{mn} = 2m\pi(-1)^m \left[B_n \int_0^1 \cosh(\beta_n\eta)\cos(n\pi\eta)d\eta + D_n \int_0^1 \cos(\gamma_n\eta)\cos(n\pi\eta)d\eta \right]$$

Case 3 Equation

$$e_{mo} = m\pi(-1)^m \left[B_n \int_0^1 \cosh(\beta_n\eta)d\eta + D_n \int_0^1 \cosh(\gamma_n\eta)d\eta \right]$$

$$e_{mn} = 2m\pi(-1)^m\left[B_n\int_0^1 \cosh(\beta_n\eta)\cos(n\pi\eta)d\eta + D_n\int_0^1 \cosh(\gamma_n\eta)\cos(n\pi\eta)d\eta\right]$$

B.1.3 Bending Moment at $\eta = 0$

General Equation

$$i_m = Y_m''(0) - \upsilon(m\pi\phi)^2 Y_m(0)$$

Case 1 Equation

$$i_m = \left(\beta_m^2 - \gamma_m^2 - \upsilon(m\pi\phi)^2\right)D_n + 2\beta_n\gamma_n A_n$$

Case 2 Equation

$$i_m = \left(\beta_m^2 - \upsilon(m\pi\phi)^2\right)B_n - \left(\gamma_m^2 + \upsilon(m\pi\phi)^2\right)D_n$$

Case 3 Equation

$$i_m = \left(\beta_m^2 - \upsilon(m\pi\phi)^2\right)B_n + \left(\gamma_m^2 - \upsilon(m\pi\phi)^2\right)D_n$$

B.1.4 Slope at $\xi = 0$.

General Equation

$$S_{mo} = m\pi\int_0^1 Y_m(\eta)d\eta$$

$$S_{mn} = 2m\pi\int_0^1 Y_m(\eta)\cos(n\pi\eta)d\eta$$

Case 1 Equation

$$S_{mo} = m\pi\left[A_m\int_0^1 \sinh(\beta_m\eta)\sin(\gamma_m\eta)d\eta + D_m\int_0^1 \cosh(\beta_m\eta)\cos(\gamma_m\eta)d\eta\right]$$

$$S_{mn} = 2m\pi\left[A_m\int_0^1 \sinh(\beta_m\eta)\sin(\gamma_m\eta)\cos(n\pi\eta)d\eta + D_m\int_0^1 \cosh(\beta_m\eta)\cos(\gamma_m\eta)\cos(n\pi\eta)d\eta\right]$$

Case 2 Equation

$$S_{mo} = m\pi\left[B_m\int_0^1 \cosh(\beta_m\eta)d\eta + D_m\int_0^1 \cos(\gamma_m\eta)d\eta\right]$$

$$S_{mn} = 2m\pi\left[B_m\int_0^1 \cosh(\beta_m\eta)\cos(n\pi\eta)d\eta + D_m\int_0^1 \cos(\gamma_m\eta)\cos(n\pi\eta)d\eta\right]$$

Case 3 Equation

$$S_{mo} = m\pi\left[B_m\int_0^1 \cosh(\beta_m\eta)d\eta + D_m\int_0^1 \cosh(\gamma_m\eta)d\eta\right]$$

$$S_{mn} = 2m\pi\left[B_m\int_0^1 \cosh(\beta_m\eta)\cos(n\pi\eta)d\eta + D_m\int_0^1 \cosh(\gamma_m\eta)\cos(n\pi\eta)d\eta\right]$$

B.2 SRWR Building Block Contributions

B.2.1 Bending Moment at $\eta = 1$

General Equation

$$b_{mn} = 2\upsilon\phi^2(-1)^n\int_0^1 \ddot{Y}_n(\xi)\sin(m\pi\xi)d\xi - 2(n\pi)^2(-1)^n\int_0^1 Y_n(\xi)\sin(m\pi\xi)d\xi$$

Case 1 Equation

$$b_{mn} = 2(-1)^n\left[\left(\upsilon\phi^2\left(\beta_n^2-\gamma_n^2\right)-(n\pi)^2\right)B_n+2\upsilon\phi^2\beta_n\gamma_nC_n\right]\int_0^1 \sin(\beta_n\xi)\cos(\gamma_n\xi)\sin(m\pi\xi)d\xi$$

$$+2(-1)^n\left[\left(\upsilon\phi^2\left(\beta_n^2-\gamma_n^2\right)-(n\pi)^2\right)C_n-2\upsilon\phi^2\beta_n\gamma_nB_n\right]\int_0^1 \cosh(\beta_n\xi)\sin(\gamma_n\xi)\sin(m\pi\xi)d\xi$$

Case 2 Equation

$$b_{mn} = 2(-1)^n\left(\upsilon\phi^2\beta_n^2-(n\pi)^2\right)A_n\int_0^1 \sinh(\beta_n\xi)\sin(m\pi\xi)d\xi$$

$$-2(-1)^n\left(\upsilon\phi^2\gamma_n^2+(n\pi)^2\right)C_n\int_0^1 \sin(\gamma_n\xi)\sin(m\pi\xi)d\xi$$

Case 3 Equation

$$b_{mn} = 2(-1)^n\left(\upsilon\phi^2\beta_n^2-(n\pi)^2\right)A_n\int_0^1 \sinh(\beta_n\xi)\sin(m\pi\xi)d\xi$$

$$+2(-1)^n\left(\upsilon\phi^2\gamma_n^2-(n\pi)^2\right)C_n\int_0^1 \sinh(\gamma_n\xi)\sin(m\pi\xi)d\xi$$

Case 4 Equation

$$b_{mn} = -2(-1)^n\left(\upsilon\phi^2\beta_n^2+(n\pi)^2\right)A_n\int_0^1 \sin(\beta_n\xi)\sin(m\pi\xi)d\xi$$

$$-2(-1)^n\left(\upsilon\phi^2\gamma_n^2+(n\pi)^2\right)C_n\int_0^1 \sin(\gamma_n\xi)\sin(m\pi\xi)d\xi$$

B.2.2 Slope at $\xi = 1$.

General Equation

$$f_n = Y_n'(1)$$

Case 1 Equation

$$f_n = (C_n\beta_n - B_n\gamma_n)\sinh(\beta_n)\sin(\gamma_n) + (B_n\beta_n + C_n\gamma_n)\cosh(\beta_n)\cos(\gamma_n)$$

Case 2 Equation

$$f_n = A_n\beta_n\cosh(\beta_n) + C_n\gamma_n\cos(\gamma_n)$$

Case 3 Equation

$$f_n = A_n\beta_n\cosh(\beta_n) + C_n\gamma_n\cosh(\gamma_n)$$

Case 4 Equation

$$f_n = A_n\beta_n\cos(\beta_n) + C_n\gamma_n\cos(\gamma_n)$$

B.2.3 Bending Moment at $\eta = 0$

General Equation

$$j_{mn} = 2\upsilon\phi^2\int_0^1 Y_n''(\xi)\sin(m\pi\xi)d\xi - 2(n\pi)^2\int_0^1 Y_n(\xi)\sin(m\pi\xi)d\xi$$

Case 1 Equation

$$j_{mn} = 2\left[\left(\upsilon\phi^2\left(\beta_n^2 - \gamma_n^2\right) - (n\pi)^2\right)B_n + 2\upsilon\phi^2\beta_n\gamma_n C_n\right]\int_0^1 \sin(\beta_n\xi)\cos(\gamma_n\xi)\sin(m\pi\xi)d\xi$$

$$+2\left[\left(\upsilon\phi^2\left(\beta_n^2 - \gamma_n^2\right) - (n\pi)^2\right)C_n - 2\upsilon\phi^2\beta_n\gamma_n B_n\right]\int_0^1 \cosh(\beta_n\xi)\sin(\gamma_n\xi)\sin(m\pi\xi)d\xi$$

Case 2 Equation

$$j_{mn} = 2\left(\upsilon\phi^2\beta_n^2 - (n\pi)^2\right)A_n\int_0^1 \sinh(\beta_n\xi)\sin(m\pi\xi)d\xi$$
$$-2\left(\upsilon\phi^2\gamma_n^2 + (n\pi)^2\right)C_n\int_0^1 \sin(\gamma_n\xi)\sin(m\pi\xi)d\xi$$

Case 3 Equation

$$j_{mn} = 2\left(\upsilon\phi^2\beta_n^2 - (n\pi)^2\right)A_n\int_0^1 \sinh(\beta_n\xi)\sin(m\pi\xi)d\xi$$
$$+2\left(\upsilon\phi^2\gamma_n^2 - (n\pi)^2\right)C_n\int_0^1 \sinh(\gamma_n\xi)\sin(m\pi\xi)d\xi$$

Case 4 Equation

$$j_{mn} = -2\left(\upsilon\phi^2\beta_n^2 + (n\pi)^2\right)A_n\int_0^1 \sin(\beta_n\xi)\sin(m\pi\xi)d\xi$$
$$-2\left(\upsilon\phi^2\gamma_n^2 + (n\pi)^2\right)C_n\int_0^1 \sin(\gamma_n\xi)\sin(m\pi\xi)d\xi$$

B.2.4 Slope at $\xi = 0$.

General Equation

$$t_n = Y_n'(0)$$

Case 1 Equation

$$t_n = B_n\beta_n + C_n\gamma_n$$

Case 2 Equation

$$t_n = A_n\beta_n + C_n\gamma_n$$

Case 3 Equation

$$t_n = A_n\beta_n + C_n\gamma_n$$

Case 4 Equation

$$f_n = A_n\beta_n + C_n\gamma_n$$

B.3 SVSR Building Block Contributions

B.3.1 Bending Moment at $\eta = 1$

General Equation

$$C_p = Y_p''(0) - \upsilon(p\pi\phi)^2 Y_p(0)$$

Case 1 Equation

$$C_p = \left(\beta_p^2 - \gamma_p^2 - \upsilon(p\pi\phi)^2\right)D_p + 2\beta_p\gamma_p A_p$$

Case 2 Equation

$$C_p = \left(\beta_p^2 - \upsilon(p\pi\phi)^2\right)B_p - \left(\gamma_p^2 + \upsilon(p\pi\phi)^2\right)D_p$$

Case 3 Equation

$$C_p = \left(\beta_p^2 - \upsilon(p\pi\phi)^2\right)B_p + \left(\gamma_p^2 - \upsilon(p\pi\phi)^2\right)D_p$$

B.3.2 Slope at $\xi = 1$.

General Equation

$$g_{po} = p\pi(-1)^p \int_0^1 Y_p(1-\eta)d\eta$$

$$g_{pn} = 2p\pi(-1)^p \int_0^1 Y_p(1-\eta)\cos(n\pi\eta)d\eta$$

Case 1 Equation

$$g_{po} = p\pi(-1)^p \left[A_p \int_0^1 \sinh(\beta_p(1-\eta))\sin(\gamma_p(1-\eta))d\eta + D_p \int_0^1 \cosh(\beta_p(1-\eta))\cos(\gamma_p(1-\eta))d\eta \right]$$

$$g_{pn} = 2p\pi(-1)^p \left[A_p \int_0^1 \sinh(\beta_p(1-\eta))\sin(\gamma_p(1-\eta))\cos(n\pi\eta)d\eta + D_p \int_0^1 \cosh(\beta_p(1-\eta))\cos(\gamma_p(1-\eta))\cos(n\pi\eta)d\eta \right]$$

Case 2 Equation

$$g_{po} = p\pi(-1)^p \left[B_p \int_0^1 \cosh(\beta_p(1-\eta))d\eta + D_p \int_0^1 \cos(\gamma_p(1-\eta))d\eta \right]$$

$$g_{pn} = 2p\pi(-1)^p \left[B_p \int_0^1 \cosh(\beta_p(1-\eta))\cos(n\pi\eta)d\eta + D_p \int_0^1 \cos(\gamma_p(1-\eta))\cos(n\pi\eta)d\eta \right]$$

Case 3 Equation

$$g_{po} = p\pi(-1)^p\left[B_r\int_0^1 \cosh(\beta_r(1-\eta))d\eta + D_r\int_0^1 \cosh(\gamma_r(1-\eta))d\eta\right]$$

$$g_{pn} = 2p\pi(-1)^p\left[B_r\int_0^1 \cosh(\beta_r(1-\eta))\cos(n\pi\eta)d\eta + D_r\int_0^1 \cosh(\gamma_r(1-\eta))\cos(n\pi\eta)d\eta\right]$$

B.3.3 Bending Moment at $\eta = 0$

General Equation

$$k_p = Y_p''(1) - \upsilon(p\pi\phi)^2 Y_p(1)$$

Case 1 Equation

$$k_p = \left[\left(\beta_p^2 - \gamma_p^2 - \upsilon(p\pi\phi)^2\right)A_r - 2\beta_r\gamma_r D_r\right]\sinh(\beta_r)\sin(\gamma_r) + \left[\left(\beta_p^2 - \gamma_p^2 - \upsilon(p\pi\phi)^2\right)D_r + 2\beta_r\gamma_r A_r\right]\cosh(\beta_r)\cos(\gamma_r)$$

Case 2 Equation

$$k_p = \left(\beta_p^2 - \upsilon(p\pi\phi)^2\right)B_r\cosh(\beta_r) - \left(\gamma_p^2 + \upsilon(p\pi\phi)^2\right)D_r\cos(\gamma_r)$$

Case 3 Equation

$$k_p = \left(\beta_p^2 - \upsilon(p\pi\phi)^2\right)B_r\cosh(\beta_r) + \left(\gamma_p^2 - \upsilon(p\pi\phi)^2\right)D_r\cosh(\gamma_r)$$

B.3.4 Slope at $\xi = 0$.

General Equation

$$u_{po} = p\pi \int_0^1 Y_p(1-\eta)d\eta$$

$$u_{pn} = 2p\pi \int_0^1 Y_p(1-\eta)\cos(n\pi\eta)d\eta$$

Case 1 Equation

$$u_{po} = p\pi\left[A_p \int_0^1 \sinh(\beta_p(1-\eta))\sin(\gamma_p(1-\eta))d\eta + D_p \int_0^1 \cosh(\beta_p(1-\eta))\cos(\gamma_p(1-\eta))d\eta\right]$$

$$u_{pn} = 2p\pi\left[A_p \int_0^1 \sinh(\beta_p(1-\eta))\sin(\gamma_p(1-\eta))\cos(n\pi\eta)d\eta + D_p \int_0^1 \cosh(\beta_p(1-\eta))\cos(\gamma_p(1-\eta))\cos(n\pi\eta)d\eta\right]$$

Case 2 Equation

$$u_{po} = p\pi\left[B_p \int_0^1 \cosh(\beta_p(1-\eta))d\eta + D_p \int_0^1 \cos(\gamma_p(1-\eta))d\eta\right]$$

$$u_{pn} = 2p\pi\left[B_p \int_0^1 \cosh(\beta_p(1-\eta))\cos(n\pi\eta)d\eta + D_p \int_0^1 \cos(\gamma_p(1-\eta))\cos(n\pi\eta)d\eta\right]$$

Case 3 Equation

$$u_{po} = p\pi\left[B_p\int_0^1 \cosh(\beta_p(1-\eta))d\eta + D_p\int_0^1 \cosh(\gamma_p(1-\eta))d\eta\right]$$

$$u_{pn} = 2p\pi\left[B_p\int_0^1 \cosh(\beta_p(1-\eta))\cos(n\pi\eta)d\eta + D_p\int_0^1 \cosh(\gamma_p(1-\eta))\cos(n\pi\eta)d\eta\right]$$

B.4 WRSR Building Block Contributions

B.4.1 Bending Moment at $\eta = 1$

General Equation

$$d_{mq} = 2\upsilon\phi^2(-1)^q\int_0^1 \ddot{Y}_q(1-\xi)\sin(m\pi\xi)d\xi - 2(q\pi)^2(-1)^q\int_0^1 Y_q(1-\xi)\sin(m\pi\xi)d\xi$$

Case 1 Equation

$$d_{mq} = 2(-1)^q\left[\left(\upsilon\phi^2\left(\beta_q^2-\gamma_q^2\right)-(q\pi)^2\right)B_r + 2\upsilon\phi^2\beta_r\gamma_r C_r\right]\int_0^1 \sinh(\beta_r(1-\xi))\cos(\gamma_r(1-\xi))\sin(m\pi\xi)d\xi$$
$$+2(-1)^q\left[\left(\upsilon\phi^2\left(\beta_q^2-\gamma_q^2\right)-(q\pi)^2\right)C_r - 2\upsilon\phi^2\beta_r\gamma_r B_r\right]\int_0^1 \cosh(\beta_r(1-\xi))\sin(\gamma_r(1-\xi))\sin(m\pi\xi)d\xi$$

Case 2 Equation

$$d_{mq} = 2(-1)^q\left(\upsilon\phi^2\beta_q^2 - (q\pi)^2\right)A_q\int_0^1 \sinh(\beta_q(1-\xi))\sin(m\pi\xi)d\xi$$
$$-2(-1)^q\left(\upsilon\phi^2\gamma_q^2 + (q\pi)^2\right)C_q\int_0^1 \sin(\gamma_q(1-\xi))\sin(m\pi\xi)d\xi$$

Case 3 Equation

$$d_{mq} = 2(-1)^q\left(\upsilon\phi^2\beta_q^2 - (q\pi)^2\right)A_q\int_0^1 \sinh(\beta_q(1-\xi))\sin(m\pi\xi)d\xi$$
$$+2(-1)^q\left(\upsilon\phi^2\gamma_q^2 - (q\pi)^2\right)C_q\int_0^1 \sinh(\gamma_q(1-\xi))\sin(m\pi\xi)d\xi$$

Case 4 Equation

$$d_{mq} = -2(-1)^q\left(\upsilon\phi^2\beta_q^2 + (q\pi)^2\right)A_q\int_0^1 \sin(\beta_q(1-\xi))\sin(m\pi\xi)d\xi$$
$$-2(-1)^q\left(\upsilon\phi^2\gamma_q^2 + (q\pi)^2\right)C_q\int_0^1 \sin(\gamma_q(1-\xi))\sin(m\pi\xi)d\xi$$

B.4.2 Slope at $\xi = 1$.

General Equation

$$h_q = -Y_q'(0)$$

Case 1 Equation

$$h_q = -B_q\beta_q - C_q\gamma_q$$

Case 2 Equation

$$h_q = -A_q\beta_q - C_q\gamma_q$$

Case 3 Equation

$$h_q = -A_q\beta_q - C_q\gamma_q$$

Case 4 Equation

$$h_q = -A_q\beta_q - C_q\gamma_q$$

B.4.3 Bending Moment at $\eta = 0$

General Equation

$$l_{mq} = 2\upsilon\phi^2\int_0^1 \ddot{Y}_q(1-\xi)\sin(m\pi\xi)d\xi - 2(q\pi)^2\int_0^1 Y_q(1-\xi)\sin(m\pi\xi)d\xi$$

Case 1 Equation

$$l_{mq} = 2\left[\left(\upsilon\phi^2\left(\beta_q^2-\gamma_q^2\right)-(q\pi)^2\right)B_q + 2\upsilon\phi^2\beta_q\gamma_q C_q\right]\int_0^1 \sinh(\beta_q(1-\xi))\cos(\gamma_q(1-\xi))\sin(m\pi\xi)d\xi$$
$$+2\left[\left(\upsilon\phi^2\left(\beta_q^2-\gamma_q^2\right)-(q\pi)^2\right)C_q - 2\upsilon\phi^2\beta_q\gamma_q B_q\right]\int_0^1 \cosh(\beta_q(1-\xi))\sin(\gamma_q(1-\xi))\sin(m\pi\xi)d\xi$$

Case 2 Equation

$$l_{mq} = 2\left(\upsilon\phi^2\beta_q^2-(q\pi)^2\right)A_q\int_0^1 \sinh(\beta_q(1-\xi))\sin(m\pi\xi)d\xi$$
$$-2\left(\upsilon\phi^2\gamma_q^2+(q\pi)^2\right)C_q\int_0^1 \sin(\gamma_q(1-\xi))\sin(m\pi\xi)d\xi$$

Case 3 Equation

$$l_{mq} = 2\left(\upsilon\phi^2\beta_q^2 - (q\pi)^2\right)A_q\int_0^1 \sinh(\beta_q(1-\xi))\sin(m\pi\xi)d\xi$$
$$+2\left(\upsilon\phi^2\gamma_q^2 - (q\pi)^2\right)C_q\int_0^1 \sinh(\gamma_q(1-\xi))\sin(m\pi\xi)d\xi$$

Case 4 Equation

$$l_{mq} = -2\left(\upsilon\phi^2\beta_q^2 + (q\pi)^2\right)A_q\int_0^1 \sin(\beta_q(1-\xi))\sin(m\pi\xi)d\xi$$
$$-2\left(\upsilon\phi^2\gamma_q^2 + (q\pi)^2\right)C_q\int_0^1 \sin(\gamma_q(1-\xi))\sin(m\pi\xi)d\xi$$

B.4.4 Slope at $\xi = 1$.

General Equation

$$V_q = -Y_q'(1)$$

Case 1 Equation

$$V_q = -(C_q\beta_q - B_q\gamma_q)\sinh(\beta_q)\sin(\gamma_q) - (B_q\beta_q + C_q\gamma_q)\cosh(\beta_q)\cos(\gamma_q)$$

Case 2 Equation

$$V_q = -A_q\beta_q\cosh(\beta_q) - C_q\gamma_q\cos(\gamma_q)$$

Case 3 Equation

$$V_q = -A_q\beta_q\cosh(\beta_q) - C_q\gamma_q\cosh(\gamma_q)$$

Case 4 Equation

$$V_q = -A_q\beta_q\cos(\beta_q) - C_q\gamma_q\cos(\gamma_q)$$

Appendix C

List of Solved Integrals

Appendix C contains the integrals which are used to solve the terms in building block contributions in appendix B. These mathematical contributions are given by D. J. Michelussi[4]. These integrals enter superimposed solution when building block solutions must be expanded in Fourier series.

$$\int_0^1 \cos(Ax)dx = \frac{\sin(A)}{A}$$

$$\int_0^1 \cosh(Ax)dx = \frac{\sinh(A)}{A}$$

$$\int_0^1 \cos(A(1-x))dx = \int_0^1 \cos(Ax)dx$$

$$\int_0^1 \cosh(A(1-x))dx = \int_0^1 \cosh(Ax)dx$$

$$\int_0^1 \sin(Ax)\sin(Bx)dx = \frac{A\cos(A)\sin(B) - B\sin(A)\cos(B)}{B^2 - A^2}$$

$$\int_0^1 \sin(Ax)\cos(Bx)dx = \frac{A\cos(A)\cos(B) + B\sin(A)\sin(B) - A}{B^2 - A^2}$$

$$\int_0^1 \cos(Ax)\cos(Bx)dx = \frac{1}{2}\int_0^1 \cos((A+B)x)dx + \frac{1}{2}\int_0^1 \cos((A-B)x)dx$$

$$\int_0^1 \sin(Ax)\sin(Bx)dx = \frac{A\cosh(A)\sin(B) - B\sinh(A)\cos(B)}{A^2+B^2}$$

$$\int_0^1 \sinh(Ax)\cos(Bx)dx = \frac{A\cosh(A)\cos(B) + B\sinh(A)\sin(B) - A}{A^2+B^2}$$

$$\int_0^1 \cosh(Ax)\sin(Bx)dx = \frac{A\sinh(A)\sin(B) - B\cosh(A)\cos(B) + B}{A^2+B^2}$$

$$\int_0^1 \cosh(Ax)\cos(Bx)dx = \frac{A\sinh(A)\cos(B) + B\cosh(A)\sin(B)}{A^2+B^2}$$

$$\int_0^1 \sinh(Ax)\sin(Bx)\sin(Cx)dx = \frac{1}{2}\int_0^1 \sinh(Ax)\cos((B-C)x)dx - \frac{1}{2}\int_0^1 \sinh(Ax)\cos((B+C)x)dx$$

$$\int_0^1 \sinh(Ax)\sin(Bx)\cos(Cx)dx = \frac{1}{2}\int_0^1 \sinh(Ax)\sin((B+C)x)dx + \frac{1}{2}\int_0^1 \sinh(Ax)\sin((B-C)x)dx$$

$$\int_0^1 \sinh(Ax)\cos(Bx)\cos(Cx)dx = \frac{1}{2}\int_0^1 \sinh(Ax)\cos((B+C)x)dx + \frac{1}{2}\int_0^1 \sinh(Ax)\cos((B-C)x)dx$$

$$\int_0^1 \cosh(Ax)\sin(Bx)\sin(Cx)dx = \frac{1}{2}\int_0^1 \cosh(Ax)\cos((B-C)x)dx - \frac{1}{2}\int_0^1 \cosh(Ax)\cos((B+C)x)dx$$

$$\int_0^1 \cosh(Ax)\sin(Bx)\cos(Cx)dx = \frac{1}{2}\int_0^1 \cosh(Ax)\sin((C+B)x)dx - \frac{1}{2}\int_0^1 \cosh(Ax)\sin((C-B)x)dx$$

$$\int_0^1 \cosh(Ax)\cos(Bx)\cos(Cx)dx = \frac{1}{2}\int_0^1 \cosh(Ax)\cos((B+C)x)dx + \frac{1}{2}\int_0^1 \cosh(Ax)\cos((B-C)x)dx$$

$$\int_0^1 \sin(A(1-x))\sin(Bx)dx = \sin(A)\int_0^1 \sin(Bx)\cos(Ax)dx - \cos(A)\int_0^1 \sin(Ax)\sin(Bx)dx$$

$$\int_0^1 \cos(A(1-x))\sin(Bx)dx = \cos(A)\int_0^1 \sin(Bx)\cos(Ax)dx + \sin(A)\int_0^1 \sin(Ax)\sin(Bx)dx$$

$$\int_0^1 \cos(A(1-x))\cos(Bx)dx = \cos(A)\int_0^1 \cos(Ax)\cos(Bx)dx + \sin(A)\int_0^1 \sin(Ax)\cos(Bx)dx$$

$$\int_0^1 \sinh(A(1-x))\sin(Bx)dx = \sin(B)\int_0^1 \sinh(Ax)\cos(Bx)dx - \cos(B)\int_0^1 \sinh(Ax)\sin(Bx)dx$$

$$\int_0^1 \cosh(A(1-x))\sin(Bx)dx = \sin(B)\int_0^1 \cosh(Ax)\cos(Bx)dx - \cos(B)\int_0^1 \cosh(Ax)\sin(Bx)dx$$

$$\int_0^1 \cosh(A(1-x))\cos(Bx)dx = \sin(B)\int_0^1 \cosh(Ax)\sin(Bx)dx + \cos(B)\int_0^1 \cosh(Ax)\cos(Bx)dx$$

$$\int_0^1 \sinh(A(1-x))\sin(B(1-x))dx = \int_0^1 \sinh(Ax)\sin(Bx)dx$$

$$\int_0^1 \cosh(A(1-x))\cos(B(1-x))dx = \int_0^1 \cosh(Ax)\cos(Bx)dx$$

$$\int_0^1 \sinh(A(1-x))\sin(B(1-x))\sin(Cx)dx =$$

$$\sin(C)\int_0^1 \sinh(Ax)\sin(Bx)\cos(Cx)dx - \cos(C)\int_0^1 \sinh(Ax)\sin(Bx)\sin(Cx)dx$$

$$\int_0^1 \sinh(A(1-x))\sin(B(1-x))\cos(Cx)dx =$$

$$\cos(C)\int_0^1 \sinh(Ax)\sin(Bx)\cos(Cx)dx + \sin(C)\int_0^1 \sinh(Ax)\sin(Bx)\sin(Cx)dx$$

$$\int_0^1 \sinh(A(1-x))\cos(B(1-x))\sin(Cx)dx =$$

$$\sin(C)\int_0^1 \sinh(Ax)\cos(Bx)\cos(Cx)dx - \cos(C)\int_0^1 \sinh(Ax)\cos(Bx)\sin(Cx)dx$$

$$\int_0^1 \cosh(A(1-x))\sin(B(1-x))\sin(Cx)dx =$$

$$\sin(C)\int_0^1 \cosh(Ax)\sin(Bx)\cos(Cx)dx - \cos(C)\int_0^1 \cosh(Ax)\sin(Bx)\sin(Cx)dx$$

$$\int_0^1 \cosh(A(1-x))\cos(B(1-x))\sin(Cx)dx =$$

$$\sin(C)\int_0^1 \cosh(Ax)\cos(Bx)\cos(Cx)dx - \cos(C)\int_0^1 \cosh(Ax)\cos(Bx)\sin(Cx)dx$$

$$\int_0^1 \cosh(A(1-x))\cos(B(1-x))\cos(Cx)dx =$$

$$\cos(C)\int_0^1 \cosh(Ax)\cos(Bx)\cos(Cx)dx + \sin(C)\int_0^1 \cosh(Ax)\cos(Bx)\sin(Cx)dx$$

Appendix D

Fortran Program Listing

```
C THIS PROGRAM IS TO FIND CRITICAL LOADS AND EIGENVALUES
C  PRESENT PROGRAM ANALYSES TORSIONAL-FREE-TORSIONAL-FREE
C   AND SIMPLE-FREE-TORSIONAL-FREE(WITH SOME MODIFICATIONS) PLATES.
C YOU NEED TO MODIFY THIS PROGRAM TO ANALYSE SIMPLE-FREE-TORSIONAL-C FREE PLATES- THESE MODIFICATIONS
ARE SIMPLY ELIMINATING SOME CUNNECESSARY EQUATIONS, WHICH ARE EASILY RECOGNISED.

      IMPLICIT DOUBLE PRECISION (A-H,O-Z)

C     DIMENSION ARRAYS

      DIMENSION A(60,60),EM(30),EN(30),W(61,61),WMX(61,61),WMY(61,61)
      DIMENSION ANS(71),EM1(30),WS(61,61)

      COMMON  POI,PHI,PHIS,WMX,WMY,POIS,EM,EN,PI,ALMDS,W,NXX,K,K2,K3,
     C K4,EM1,PS2,WS

    1 FORMAT (7(E13.6,3X))

      C=1.
      PI=4.*DATAN(C)

      xx1=102.0
      xx2=0.010
      xx3=30.0
      ll1=7
      NN = 10
      RAT =-1.0
      CRIT = 3.66
      ASP = 1/3.0



      K=LL1
      K2=2*K
      K3=3*K
      K4=4*K
      POI=0.333
      POIS=2.-POI
      PHI11=ASP
CCH     PHI11=2.5
      PS2=RAT*CRIT
CCH     PS2=-1.0*214.58
CCH     PS2=XX1
      AKR2=XX3
      ALMDS=XX1
CCH     ALMDS=0.0001
      DEL=XX2
      DLIM=ALMDS +NN*DEL
CCH     DLIM=PS2+NN*DEL
      PHI=PHI11
      PHIS=PHI*PHI

C     MATRIX INITIALIZING OPERATION

    9 DO 17 M=1,K4
      DO 17 N=1,K4
   17 A(M,N)=0.

      ALMDS=ALMDS+DEL
CCH     PS2=PS2+DEL
      DO 54 M=1,K
      AMM=M
      DO 54 N=1,K

C     SET UP DIVISOR DIV REQUIRED FOR COSINE EXPANSION TERMS AND
C     CONTINUE WITH COMPUTATIONS.
```

```
      DIV=2.
      IF(N.LT.2) GO TO 600
      DIV=1.

  600 CONTINUE
      EMP=M*PI
      EMPS=EMP*EMP
      ENP=(N-1)*PI

      DELMS=EMPS
      DELML=EMPS*EMPS-ALMDS*ALMDS-PS2*EMPS/PHIS
      CASE=1.
      XX=DELMS*DELMS-DELML
      IF (XX.LT.0.) GO TO 700
      CASE=2.
      IF (DELML.LT.0.) GO TO 750
      CASE=3.
      GO TO 800
  700 XX=(DSQRT(DELML)+DELMS)/2.
      BM=PHI*DSQRT(XX)
      XX=(DSQRT(DELML)-DELMS)/2.
      GM=PHI*DSQRT(XX)
      BMS=BM*BM
      GMS=GM*GM
      X1=BM*(BMS-3.*GMS)*DSINH(BM)*DCOS(GM)-GM*(3.*BMS-GMS)*DCOSH(BM)
     1 *DSIN(GM)
      Y1=-2.*BM*GM*(BMS+GMS)*(SINH(BM)*DSINH(BM)+DSIN(GM)*DSIN(GM))
      X2=POIS*EMPS*PHIS*(BM*DSINH(BM)*DCOS(GM)-GM*DCOSH(BM)*DSIN(GM))
      TD11M=X1/Y1-X2/Y1
      X2=BM*(BMS-3.*GMS)*DCOSH(BM)*DSIN(GM)+GM*(3.*BMS-GMS)*DSINH(BM)
     1 *DCOS(GM)
      Y1=-2.*BM*GM*(BMS+GMS)*(SINH(BM)*DSINH(BM)+DSIN(GM)*DSIN(GM))
      X1=POIS*EMPS*PHIS*(BM*DCOSH(BM)*DSIN(GM)+GM*DSINH(BM)*DCOS(GM))
      TD14M= (X1/Y1-X2/Y1)
      IF(N.GT.1.) GO TO 701
CCH     WRITE (6,1) AMM,CASE
      ZZ1=TD11M*BM-TD14M*GM
      ZZ2=TD11M*GM+TD14M*BM
      ZZ3=ZZ1*BM-ZZ2*GM
      ZZ4=ZZ1*GM+ZZ2*BM
      A(M,M)=-((ZZ3-POI*PHIS*TD11M*EMPS)*DSINH(BM)*DSIN(GM)+(ZZ4-POI*
     1 PHIS*TD14M*EMPS)*DCOSH(BM)*DCOS(GM))
      A(M+K,M)=-(ZZ4-POI*PHIS*TD14M*EMPS)
  701 Z1=0.
      CALL SCS11(BM,Z1,ENP,GM,X1,X3)
      CALL SCC11(BM,Z1,ENP,GM,X3,X2)
      A(N+K2,M)=2.*EMP*(TD11M*X1+TD14M*X2)*DCOS(EMP)/DIV
      A(N+K3,M)=A(N+K2,M)/DCOS(EMP)
      GO TO 54

  750 X1= DELMS*DELMS-DELML
      X1=DSQRT(X1)
      XX=X1+DELMS
      BM=PHI*DSQRT(XX)
      XX=X1-DELMS
      GM=PHI*DSQRT(XX)
      BMS=BM*BM
      GMS=GM*GM
      TD22M=(GMS+POIS*EMPS*PHIS)/(BM*(BMS+GMS)*DSINH(BM))
      TD24M=-(BMS-POIS*EMPS*PHIS)/(GM*(BMS+GMS)*DSIN(GM))
      IF(N.GT.1) GO TO 751
C     WRITE (6,1) AMM,CASE
      A(M,M)=-(TD22M*(BMS-POI*PHIS*EMPS)*DCOSH(BM)-TD24M*(GMS+POI*PHIS
     1 *EMPS)*DCOS(GM))
      A(M+K,M)=-(TD22M*(BMS-POI*PHIS*EMPS)-TD24M*(GMS+POI*PHIS*EMPS))
  751 Z1=0.
      Z2=0.
      CALL SCC11(BM,Z1,Z2,ENP,X3,X1)
```

```
      CALL SCC2(GM,Z1,Z2,ENP,X3,X2)
      A(N+K2,M)=2.*EMP*(TD22M*X1+TD24M*X2)*DCOS(EMP)/DIV
      A(N+K3,M)=A(N+K2,M)/DCOS(EMP)
      GO TO 54

  800 X1=DELMS*DELMS-DELML
      X1=DSQRT(X1)
      XX=DELMS+X1
      BM=PHI*DSQRT(XX)
      XX=DELMS-X1
      GM=PHI*DSQRT(XX)
      BMS=BM*BM
      GMS=GM*GM
      TD33M=(POIS*EMPS*PHIS-GMS)/(BM*(BMS-GMS)*DSINH(BM))
      TD34M= (BMS-POIS*EMPS*PHIS)/(GM*(BMS-GMS)*DSINH(GM))
      IF(N.GT.1) GO TO 801
C     WRITE (6,1) AMM,CASE
      A(M,M)=-(TD33M*(BMS-POI*PHIS*EMPS)*DCOSH(BM)+TD34M*(GMS-POI*PHIS
     1 *EMPS)*DCOSH(GM))
      A(M+K,M)=-(TD33M*(BMS-POI*PHIS*EMPS)+TD34M*(GMS-POI*PHIS*EMPS))
  801 Z1=0.
      Z2=0.
      CALL SCC11(BM,Z1,Z2,ENP,X3,X1)
      CALL SCC11(GM,Z1,Z2,ENP,X3,X2)
      A(N+K2,M)=2.*EMP*(TD33M*X1+TD34M*X2)*DCOS(EMP)/DIV
      A(N+K3,M)=A(N+K2,M)/DCOS(EMP)
   54 CONTINUE

      DO 53 I=1,K
      A(I+K,I+K)=A(I,I)
      A(I,I+K)=A(I+K,I)
      DO 53 J=1,K
      AII=(I-1)*PI
      FAC=DCOS(AII)
      A(I+K2,J+K)=A(I+K2,J)*FAC
      A(I+K3,J+K)=A(I+K3,J)*FAC
   53 CONTINUE

      ALMDSS=ALMDS
      ALMDS=ALMDS
      DO 74 N=1,K
       ANN=N
      DO 74 M=1,K

C     SET UP DIVISOR DIV REQUIRED FOR COSINE TERM EXPANSION.

      DIV=2.
      IF(M.LT.2) GO TO 601
      DIV=1.

  601 CONTINUE

      EMP=M*PI
      ENP=(N-1)*PI
      ENPS=ENP*ENP

      DELNS=ENPS-PS2/2.
      DELNL=ENPS*ENPS-ALMDS*ALMDS*PHIS*PHIS
      CASE=1.
      XX=DELNS*DELNS-DELNL
      IF (XX.LT.0.) GO TO 900
      CASE=2.
      IF (DELNL.LT.0.) GO TO 950
      CASE=3.
      IF(DELNS.GT.0.) GO TO 1000
      CASE=4.
      GO TO 1050
  900 XX=(SQRT(DELNL)+DELNS)/2.
```

```
      BN=DSQRT(XX)/PHI
      XX=(DSQRT(DELNL)-DELNS)/2.
      GN=DSQRT(XX)/PHI
      TD11N=-DCOSH(BN)*DSIN(GN)/(2.*BN*GN*(DCOS(GN)*DCOS(GN)-DCOSH(BN)*
     1 DCOSH(BN)))
      TD15N=DSINH(BN)*DCOS(GN)/(2.*BN*GN*(DCOS(GN)*DCOS(GN)-DCOSH(BN)*
     1 DCOSH(BN)))
      IF(M.GT.1) GO TO 901
CCH     WRITE (6,1) ANN,CASE
      A(K2+N,K2+N)=TD11N*(BN*DCOSH(BN)*DCOS(GN)-GN*DSINH(BN)*DSIN(GN))
     1 +TD15N*(BN*DSINH(BN)*DSIN(GN)+GN*DCOSH(BN)*DCOS(GN))
      A(K3+N,K2+N)=TD11N*BN+TD15N*GN
  901 ZZ1=TD11N*BN+TD15N*GN
      ZZ2=TD11N*GN-TD15N*BN
      ZZ3=ZZ1*BN-ZZ2*GN
      ZZ4=-(ZZ1*GN+ZZ2*BN)
      Z1=0.
      CALL SCS11(BN,Z1,GN,EMP,X1,X3)
      CALL SSS11(BN,Z1,GN,EMP,X3,X2)
      A(M,N+K2)=-2.*(POI*PHIS*ZZ3-TD11N*ENPS)*X1*DCOS(ENP)+2.*(TD15N*
     1 ENPS-POI*PHIS*ZZ4)*X2*DCOS(ENP)
      A(M+K,N+K2)=-2.*(POI*PHIS*ZZ3-TD11N*ENPS)*X1+2.*(TD15N*
     1 ENPS-POI*PHIS*ZZ4)*X2
      GO TO 74
  950 X1=DELNS*DELNS-DELNL
      XX=DSQRT(X1)+DELNS
      BN=DSQRT(XX)/PHI
      XX=DSQRT(X1)-DELNS
      GN=DSQRT(XX)/PHI
      BNS=BN*BN
      GNS=GN*GN
      TD22N=-1./((BNS+GNS)*DSINH(BN))
      TD25N=1./((BNS+GNS)*DSIN(GN))
      IF(M.GT.1) GO TO 951
C     WRITE (6,1) ANN,CASE
      A(N+K2,N+K2)=BN*TD22N*DCOSH(BN)+GN*TD25N*DCOS(GN)
      A(N+K3,N+K2)=BN*TD22N+GN*TD25N
  951 Z1=0.
      Z2=0.
      CALL SCS11(BN,Z1,Z2,EMP,X1,X3)
      CALL SCS2(GN,Z1,Z2,EMP,X2,X3)
      A(M,N+K2)=-2.*TD22N*(POI*PHIS*BNS-ENPS)*X1*DCOS(ENP)+2.*TD25N*(
     1 ENPS+POI*PHIS*GNS)*X2*DCOS(ENP)
      A(M+K,N+K2)=-2.*TD22N*(POI*PHIS*BNS-ENPS)*X1+2.*TD25N*(
     1 ENPS+POI*PHIS*GNS)*X2
      GO TO 74
 1000 X1=DELNS*DELNS-DELNL
      XX=DELNS+DSQRT(X1)
      BN=DSQRT(XX)/PHI
      XX=DELNS-DSQRT(X1)
      GN=DSQRT(XX)/PHI
      BNS=BN*BN
      GNS=GN*GN
      TD33N=-1./((BNS-GNS)*DSINH(BN))
      TD35N= 1./((BNS-GNS)*DSINH(GN))
      IF(M.GT.1) GO TO 1001
C     WRITE (6,1) ANN,CASE
      A(N+K2,N+K2)=TD33N*BN*DCOSH(BN)+TD35N*GN*DCOSH(GN)
      A(N+K3,N+K2)=TD33N*BN+TD35N*GN
 1001 Z1=0.
      Z2=0.
      CALL SCS11(BN,Z1,Z2,EMP,X1,X3)
      CALL SCS11(GN,Z1,Z2,EMP,X2,X3)
      A(M,N+K2)=-2.*TD33N*(POI*PHIS*BNS-ENPS)*X1*DCOS(ENP)-2.*TD35N*(
     1    POI*PHIS*GNS-ENPS)*X2*DCOS(ENP)
      A(M+K,N+K2)=-2.*TD33N*(POI*PHIS*BNS-ENPS)*X1-2.*TD35N*(
     1    POI*PHIS*GNS-ENPS)*X2
      GO TO 74
```

```
 1050 X1=DELNS*DELNS-DELNL
      IF(DELNL.EQ.0.) GO TO 1100
      XX=-DELNS-DSQRT(X1)
      BN=DSQRT(XX)/PHI
      XX=-DELNS+DSQRT(X1)
      GN=DSQRT(XX)/PHI
      BNS=BN*BN
      GNS=GN*GN
      TD44N=-1./((GNS-BNS)*DSIN(BN))
      TD45N= 1./((GNS-BNS)*DSIN(GN))
      IF(M.GT.1) GO TO 1051
CCH     WRITE (6,1) ANN,CASE
      A(N+K2,N+K2)=BN*TD44N*DCOS(BN)+GN*TD45N*DCOS(GN)
      A(N+K3,N+K2)=BN*TD44N+GN*TD45N
 1051 Z1=0.
      Z2=0.
      CALL SCS2(BN,Z1,Z2,EMP,X1,X3)
      CALL SCS2(GN,Z1,Z2,EMP,X2,X3)
      A(M,N+K2)=2.*TD44N*(POI*PHIS*BNS+ENPS)*X1*DCOS(ENP)+2.*TD45N*(
     1    POI*PHIS*GNS+ENPS)*X2*DCOS(ENP)
      A(M+K,N+K2)=2.*TD44N*(POI*PHIS*BNS+ENPS)*X1+2.*TD45N*(
     1    POI*PHIS*GNS+ENPS)*X2
      GO TO 74

 1100 ALFS=PS2/PHIS
      ALFA=DSQRT(ALFS)
      Z1=0.
      Z2=0.
      IF(M.GT.1.) GO TO 1101
CCH     WRITE (6,1) CASE
      A(N+K2,N+K2)=(ALFA*DCOS(ALFA)-DSIN(ALFA))/(ALFS*DSIN(ALFA))
 1101 CALL SCS2(ALFA,Z1,Z2,EMP,X1,X2)
      A(M,N+K2)=-2.*X1/DSIN(ALFA)
      A(M+K,N+K2)=-2.*X1/DSIN(ALFA)
   74 CONTINUE

      ALMDS=ALMDSS

      DO 73 I=1,K
      A(I+K3,I+K3)=-A(I+K2,I+K2)
      A(I+K2,I+K3)=-A(I+K3,I+K2)
      DO 73 J=1,K
      AII = I*PI
      FAC = (-1*DCOS(AII))
      A(I,J+K3)=A(I,J+K2)*FAC
      A(I+K,J+K3)=A(I+K,J+K2)*FAC
   73 CONTINUE


C     BY-PASS NEXT 7 LINES IF YOU DO NOT WANT ELASTIC EDGE SUPPORT
C     ON EDGE PSI=0 AND PSI=1.


      DO 7400 I=1,K
      DO 7400 J=1,K4
      A(I+K2,J)=A(I+K2,J)*AKR2
 7400 A(I+K3,J)=A(I+K3,J)*AKR2
C     PRINT *, A(I+K2,J), A(I+K3,J)
C7400 PAUSE
      DO 7401 I=1,K
      A(I+K2,I+K2)=A(I+K2,I+K2)-1.
 7401 A(I+K3,I+K3)=A(I+K3,I+K3)+1.
C     PRINT *, A(I+K2,I+K2), A(I+K3,I+K3)
C7401 PAUSE
```

```
      IF(DEL.EQ.0.) GO TO 93

      KK=K4

 2117 CALL DETERM1(A,KK,Y)


      WRITE (6,1) ALMDS,Y
CCH   WRITE (6,1) PS2,Y


      IF(ALMDS.LT.DLIM) GO TO 9
CCH   IF(PS2.LT.DLIM) GO TO 9
      GO TO 118

  93 CONTINUE


      DO 810 I=1,K2
      EM(I)=0.
      EM1(I)=0.
      EN(I)=0.
  810 ANS(I)=0.
      SUM=0.
      DO 815 I=K2+1,K2+1
  815 SUM=SUM+A(1,I)


C     WRITE (6,1) SUM,PI,PI

      CALL DETR(A,K3 ,ANS)

      DO 95 I=1,K
      EN(I)=ANS(I+K2)
      EM1(I)=ANS(I+K)
   95 EM(I)=ANS(I)

C     EN (1)=1.

      IF(PI.GT.0.)GOTO 100

      DO 99 L=1,K
      ALL=L
      WRITE(6,1) ALL, EM(L),EM1(L),EN(L)
   99 CONTINUE

      PAUSE
      IF(PI.GT.0.) GO TO 118
  100 NXX=61


      DO 101 N=1,61
      DO 101 M=1,61
      WMX(N,M)=0.
      WMY(N,M)=0.
      WS(N,M)=0.
  101 W(N,M)=0.0
      CALL SHAPE1
      IF(PI.GT.0.) GO TO 1214

      SUMM=0.
      DO 819 J=1,61
      XX=PI*(J-1)/60.
  819 SUMM=SUMM*WMY(61,J)*DSIN(XX)
      SUMM=2.*SUMM/61.
      WRITE (6,1) SUMM,SUMM
      PAUSE
      IF(PI.GT.0.) GO TO 118
```

```
1214    CONTINUE
        DO 1241 I= 1,61,3
        AII=I
        WRITE (6,1) PI
        DO 1240 J= 1,61,3
        AJJ=J
1240    WRITE (6,1) AII,AJJ,W(I,J)
        PAUSE
1241    CONTINUE
        PAUSE
118     CONTINUE
        STOP
        END


        SUBROUTINE SHAPE1
        IMPLICIT DOUBLE PRECISION (A-H,O-Z)

        DIMENSION       EM(15),EN(15),W(61,61),WMX(61,61),WMY(61,61)        ZZ200220
        DIMENSION   EM1(15),WS(61,61)

        COMMON  POI,PHI,PHIS,WMX,WMY,POIS,EM,EN,PI,ALMDS,W,NXX,K,K2,K3,   Z200280
       C K4,EM1,PS2,WS

       1 FORMAT(7(E13.6,3X))

        DO 47 L= 1,61,3
        ETA=(L-1)/ FLOAT(NXX-1)
        ET1=1.-ETA
        DO 47 J= 1,61,3
        PSI=(J-1)/ FLOAT(NXX-1)
        PSA=1.-PSI

        DO 54 M=1,K
        EMP=M*PI
        EMPS=EMP*EMP

        DELMS=EMPS
        DELML=EMPS*EMPS-ALMDS*ALMDS-PS2*EMPS/PHIS
        CASE=1.
        XX=DELMS*DELMS-DELML
        IF (XX.LT.0.) GO TO 700
        CASE=2.
        IF (DELML.LT.0.) GO TO 750
        CASE=3.
        GO TO 800
      700 XX=(DSQRT(DELML)+DELMS)/2.
        BM=PHI*DSQRT(XX)
        XX=(DSQRT(DELML)-DELMS)/2.
        GM=PHI*DSQRT(XX)
        BMS=BM*BM
        GMS=GM*GM
        X1=BM*(BMS-3.*GMS)*DSINH(BM)*DCOS(GM)-GM*(3.*BMS-GMS)*DCOSH(BM)
       1 *DSIN(GM)
        Y1=-2.*BM*GM*(BMS+GMS)*(SINH(BM)*DSINH(BM)+DSIN(GM)*DSIN(GM))
        X2=POIS*EMPS*PHIS*(BM*DSINH(BM)*DCOS(GM)-GM*DCOSH(BM)*DSIN(GM))
        TD11M=X1/Y1-X2/Y1
        X2=BM*(BMS-3.*GMS)*DCOSH(BM)*DSIN(GM)+GM*(3.*BMS-GMS)*DSINH(BM)
       1 *DCOS(GM)
        Y1=-2.*BM*GM*(BMS+GMS)*(SINH(BM)*DSINH(BM)+DSIN(GM)*DSIN(GM))
        X1=POIS*EMPS*PHIS*(BM*DCOSH(BM)*DSIN(GM)+GM*DSINH(BM)*DCOS(GM))
        TD14M= (X1/Y1-X2/Y1)
        W(L,J)=W(L,J)+EM(M)*(TD11M*DSINH(BM*ETA)*DSIN(GM*ETA)+TD14M*
       1 DCOSH(BM*ETA)*DCOS(GM*ETA))*DSIN(EMP*PSI)
        W(L,J)=W(L,J)+EM1(M)*(TD11M*DSINH(BM*ET1)*DSIN(GM*ET1)+TD14M*
       1 DCOSH(BM*ET1)*DCOS(GM*ET1))*DSIN(EMP*PSI)
```

```
      ZZ1=TD11M*BM-TD14M*GM
      ZZ2=TD11M*GM+TD14M*BM
      ZZ3=ZZ1*BM-ZZ2*GM
      ZZ4=ZZ1*GM+ZZ2*BM
      WMY(L,J)=WMY(L,J)-EM(M)*((ZZ3-POI*PHIS*TD11M*EMPS)*DSINH(BM*ETA)*
     1DSIN(GM*ETA)+(ZZ4-POI*PHIS*TD14M*EMPS)*DCOSH(BM*ETA)*DCOS(GM*ETA))
     1*DSIN(EMP*PSI)
      WMY(L,J)=WMY(L,J)-EM1(M)*((ZZ3-POI*PHIS*TD11M*EMPS)*DSINH(BM*ET1)*
     1DSIN(GM*ET1)+(ZZ4-POI*PHIS*TD14M*EMPS)*DCOSH(BM*ET1)*DCOS(GM*ET1))
     1*DSIN(EMP*PSI)

      WS(L,J)=WS(L,J)+EM(M)*EMP*(TD11M*DSINH(BM*ETA)*DSIN(GM*ETA)+
     1 TD14M*DCOSH(BM*ETA)*DCOS(GM*ETA))*DCOS(EMP*PSI)
      WS(L,J)=WS(L,J)+EM1(M)*EMP*(TD11M*DSINH(BM*ET1)*DSIN(GM*ET1)+
     1 TD14M*DCOSH(BM*ET1)*DCOS(GM*ET1))*DCOS(EMP*PSI)
      GO TO 54

  750 X1= DELMS*DELMS-DELML
      X1=DSQRT(X1)
      XX=X1+DELMS
      BM=PHI*DSQRT(XX)
      XX=X1-DELMS
      GM=PHI*DSQRT(XX)
      BMS=BM*BM
      GMS=GM*GM
      TD22M=(GMS+POIS*EMPS*PHIS)/(BM*(BMS+GMS)*DSINH(BM))
      TD24M=-(BMS-POIS*EMPS*PHIS)/(GM*(BMS+GMS)*DSIN(GM))

      W(L,J)=W(L,J)+EM(M)*(TD22M*DCOSH(BM*ETA)+TD24M*DCOS(GM*ETA))*
     1 DSIN(EMP*PSI)
      W(L,J)=W(L,J)+EM1(M)*(TD22M*DCOSH(BM*ET1)+TD24M*DCOS(GM*ET1))*
     1 DSIN(EMP*PSI)
      WMY(L,J)=WMY(L,J)-EM(M)*(TD22M*(BMS-POI*PHIS*EMPS)*DCOSH(BM*ETA)-
     1 TD24M*(GMS+POI*PHIS*EMPS)*DCOS(GM*ETA))*DSIN(EMP*PSI)
      WMY(L,J)=WMY(L,J)-EM1(M)*(TD22M*(BMS-POI*PHIS*EMPS)*DCOSH(BM*ET1)-
     1 TD24M*(GMS+POI*PHIS*EMPS)*DCOS(GM*ET1))*DSIN(EMP*PSI)

      WS(L,J)=WS(L,J)+EM(M)*EMP*(TD22M*DCOSH(BM*ETA)+TD24M*DCOS(GM*ETA)
    =WS(L,J)+EM(M)*EMP*(TD22M*DCOSH(BM*ETA)+TD24M*DCOS(GM*ETA)
     1 )*DCOS(EMP*PSI)

      WS(L,J)=WS(L,J)+EM1(M)*EMP*(TD22M*DCOSH(BM*ET1)+TD24M*DCOS(GM*ET1)
     1 )*DCOS(EMP*PSI)
      GO TO 54

  800 X1=DELMS*DELMS-DELML
      X1=DSQRT(X1)
      XX=DELMS+X1
      BM=PHI*DSQRT(XX)
      XX=DELMS-X1
      GM=PHI*DSQRT(XX)
      BMS=BM*BM
      GMS=GM*GM
      TD33M=(POIS*EMPS*PHIS-GMS)/(BM*(BMS-GMS)*DSINH(BM))
      TD34M= (BMS-POIS*EMPS*PHIS)/(GM*(BMS-GMS)*DSINH(GM))

      W(L,J)=W(L,J)+EM(M)*(TD33M*DCOSH(BM*ETA)+TD34M*DCOSH(GM*ETA))*
     1 DSIN(EMP*PSI)
      W(L,J)=W(L,J)+EM1(M)*(TD33M*DCOSH(BM*ET1)+TD34M*DCOSH(GM*ET1))*
     1 DSIN(EMP*PSI)

      WMY(L,J)=WMY(L,J)-EM(M)*(TD33M*(BMS-POI*PHIS*EMPS)*DCOSH(BM*ETA)+
     1 TD34M*(GMS-POI*PHIS*EMPS)*DCOSH(GM*ETA))*DSIN(EMP*PSI)
      WMY(L,J)=WMY(L,J)-EM1(M)*(TD33M*(BMS-POI*PHIS*EMPS)*DCOSH(BM*ET1)+
     1 TD34M*(GMS-POI*PHIS*EMPS)*DCOSH(GM*ET1))*DSIN(EMP*PSI)

      WS(L,J)=WS(L,J)+EM(M)*EMP*(TD33M*DCOSH(BM*ETA)+TD34M*DCOSH(GM*ETA)
     1 )*DCOS(EMP*PSI)
```

```
      WS(L,J)=WS(L,J)+EM1(M)*EMP*(TD33M*DCOSH(BM*ET1)+TD34M*DCOSH(GM*ET1
     1))*DCOS(EMP*PSI)

   54 CONTINUE
      ALMDSS=ALMDS
      ALMDS=ALMDS*PHIS
      DO 74 N=1,K

      ENP=(N-1)*PI
      ENPS=ENP*ENP

      DELNS=ENPS-PS2/2.
      DELNL=ENPS*ENPS-ALMDS*ALMDS*PHIS*PHIS
      CASE=1.
      XX=DELNS*DELNS-DELNL
      IF (XX.LT.0.) GO TO 900
      CASE=2.
      IF (DELNL.LT.0.) GO TO 950
      CASE=3.
      IF(DELNS.GT.0.) GO TO 1000
      CASE=4.
      GO TO 1050
  900 XX=(SQRT(DELNL)+DELNS)/2.
      BN=DSQRT(XX)/PHI
      XX=(DSQRT(DELNL)-DELNS)/2.
      GN=DSQRT(XX)/PHI
      TD11N=DCOSH(BN)*DSIN(GN)/(2.*BN*GN*(DCOS(GN)*DCOS(GN)-DCOSH(BN)*
     1 DCOSH(BN)))
      TD15N=-DSINH(BN)*DCOS(GN)/(2.*BN*GN*(DCOS(GN)*DCOS(GN)-DCOSH(BN)*
     1 DCOSH(BN)))
      W(L,J)=W(L,J)+EN(N)*(TD11N*DSINH(BN*PSI)*DCOS(GN*PSI)+TD15N*
     1 DCOSH(BN*PSI)*DSIN(GN*PSI))*DCOS(ENP*ETA)
      ZZ1=TD11N*BN+TD15N*GN
      ZZ2=TD11N*GN-TD15N*BN
      ZZ3=ZZ1*BN-ZZ2*GN
      ZZ4=-(ZZ1*GN+ZZ2*BN)
      WMY(L,J)=WMY(L,J)-EN(N)*((-TD11N*ENPS+POI*PHIS*ZZ3)*DSINH(BN*PSI)      PSI)
     1 *DCOS(GN*PSI)-(TD15N*ENPS-POI*PHIS*ZZ4)*DCOSH(BN*PSI)
     1 *DSIN(GN*PSI))*DCOS(ENP*ETA)
      WS(L,J)=WS(L,J)+EN(N)*(ZZ1*DCOSH(BN*PSI)*DCOS(GN*PSI)-ZZ2*DSINH(
     1 BN*PSI)*DSIN(GN*PSI))*DCOS(ENP*ETA)
      GO TO 74
  950 X1=DELNS*DELNS-DELNL
      XX=DSQRT(X1)+DELNS
      BN=DSQRT(XX)/PHI
      XX=DSQRT(X1)-DELNS
      GN=DSQRT(XX)/PHI
      BNS=BN*BN
      GNS=GN*GN
      TD22N=1./((BNS+GNS)*DSINH(BN))
      TD25N=-1./((BNS+GNS)*DSIN(GN))

      W(L,J)=W(L,J)+EN(N)*(TD22N*DSINH(BN*PSI)+TD25N*DSIN(GN*PSI))*
     1 DCOS(ENP*ETA)

      WMY(L,J)=WMY(L,J)-EN(N)*(TD22N*(POI*PHIS*BNS-ENPS)*DSINH(BN*PSI)
     1 -TD25N*(ENPS+POI*PHIS*GNS)*DSIN(GN*PSI))*DCOS(ENP*ETA)

      WS(L,J)=WS(L,J)+EN(N)*(TD22N*BN*DCOSH(BN*PSI)+TD25N*GN*DCOS(GN*
     1 PSI))*DCOS(ENP*ETA)

      GO TO 74
 1000 X1=DELNS*DELNS-DELNL
      XX=DELNS+DSQRT(X1)
      BN=DSQRT(XX)/PHI
      XX=DELNS-DSQRT(X1)
      GN=DSQRT(XX)/PHI
      BNS=BN*BN
```

```
      GNS=GN*GN
      TD33N=1./((BNS-GNS)*DSINH(BN))
      TD35N=-1./((BNS-GNS)*DSINH(GN))
      W(L,J)=W(L,J)+EN(N)*(TD33N*DSINH(BN*PSI)+TD35N*DSINH(GN*PSI))*
     1 DCOS(ENP*ETA)

      WMY(L,J)=WMY(L,J)-EN(N)*(TD33N*(POI*PHIS*BNS-ENPS)*DSINH(BN*PSI)
     1 +TD35N*(-ENPS+POI*PHIS*GNS)*DSINH(GN*PSI))*DCOS(ENP*ETA)

      WS(L,J)=WS(L,J)+EN(N)*(TD33N*BN*DCOSH(BN*PSI)+TD35N*GN*DCOSH(GN*
     1 PSI))*DCOS(ENP*ETA)

      GO TO 74


 1050 X1=DELNS*DELNS-DELNL
      XX=-DELNS-DSQRT(X1)
      BN=DSQRT(XX)/PHI
      XX=-DELNS+DSQRT(X1)
      GN=DSQRT(XX)/PHI
      BNS=BN*BN
      GNS=GN*GN
      TD44N=1./((GNS-BNS)*DSIN(BN))
      TD45N=-1./((GNS-BNS)*DSIN(GN))
      W(L,J)=W(L,J)+EN(N)*(TD44N*DSIN(BN*PSI)+TD45N*DSIN(GN*PSI))*
     1 DCOS(ENP*ETA)

      WMY(L,J)=WMY(L,J)+EN(N)*(TD44N*(POI*PHIS*BNS+ENPS)*DSIN(BN*PSI)
     1 +TD45N*(ENPS+POI*PHIS*GNS)*DSIN(GN*PSI))*DCOS(ENP*ETA)

      WS(L,J)=WS(L,J)+EN(N)*(TD44N*BN*DCOS(BN*PSI)+TD45N*GN*DCOS(GN*
     1 PSI))*DCOS(ENP*ETA)

 74 CONTINUE

 46 CONTINUE
 47 CONTINUE
      RETURN
      END
```

Standard Programs used for matrix manipulation and integral calculation

```
      SUBROUTINE DETERM1(A,N,DET)
C
C     THIS IS A STANDARD SUBPROGRAM FOR FINDING THE DETERMINANT OF A
C     SQUARE N BY N MATRIX.THE DETERMINANT IS STORED AS DET.
C
      IMPLICIT DOUBLE PRECISION(A-H,O-Z)                    ZZ207280
      DIMENSION A(60,60)                                    ZZ207290
      SIGN=1.                                               ZZ207300
      LAST=N-1                                              ZZ207310
C                                                           ZZ207320
C     START OVERALL LOOP FOR(N-1) PIVOTS                    ZZ207330
C                                                           ZZ207340
      DO 200 I=1,LAST                                       ZZ207350
C                                                           ZZ207360
C     FIND THE LARGEST REMAINING TERM IN I-TH COLUMN FOR PIVOT      ZZ207370
C                                                           ZZ207380
      BIG=0.                                                ZZ207390
      DO 50 K=I,N                                           ZZ207400
      TERM=DABS(A(K,I))                                     ZZ207410
      IF (TERM-BIG)50,50,30                                 ZZ207420
   30 BIG=TERM                                              ZZ207430
      L=K                                                   ZZ207440
   50 CONTINUE                                              ZZ207450
C                                                           ZZ207460
C     CHECK WHETHER A NON-ZERO TERM HAS BEEN FOUND          ZZ207470
C                                                           ZZ207480
      IF (BIG)80,60,80                                      ZZ207490
C                                                           ZZ207500
C     L-TH ROW HAS THE BIGGEST TERM---IS I=L                ZZ207510
C                                                           ZZ207520
   80 IF (I-L)90,120,90                                     ZZ207530
C                                                           ZZ207540
C     I IS NOT EQUAL TO L,SWITCH ROWS I AND L               ZZ207550
   90 SIGN=-SIGN                                            ZZ207560
      DO 100 J=1,N                                          ZZ207570
      TEMP=A(I,J)                                           ZZ207580
      A(I,J)=A(L,J)                                         ZZ207590
  100 A(L,J)=TEMP                                           ZZ207600
C                                                           ZZ207610
C     NOW START PIVOTAL REDUCTION                           ZZ207620
C                                                           ZZ207630
  120 PIVOT=A(I,I)                                          ZZ207640
      NEXTR=I+1                                             ZZ207650
C                                                           ZZ207660
C     FOR EACH OF THE ROWS AFTER THE I-TH                   ZZ207670
      DO 200 J=NEXTR,N                                      ZZ207680
C                                                           ZZ207690
C     MULTIPLYING CONSTANT FOR THE J-TH ROW IS              ZZ207700
C                                                           ZZ207710
      CONST=A(J,I)/PIVOT                                    ZZ207720
C                                                           ZZ207730
C     NOW REDUCE EACH TERM OF THE J-TH ROW                  ZZ207740
C                                                           ZZ207750
      DO 200 K=I,N                                          ZZ207760
  200 A(J,K)=A(J,K)-CONST*A(I,K)                            ZZ207770
C                                                           ZZ207780
C     END OF PIVOTAL REDUCTION---NOW COMPUTE DETERMINANT    ZZ207790
      DET=SIGN                                              ZZ207800
      DO 300 I=1,N                                          ZZ207810
  300 DET=DET*A(I,I)*10.                                    ZZ207820
```

```
      GO TO 61                                          ZZ207830
     60 DET=0.                                          ZZ207840
     61 RETURN                                          ZZ207850
      END                                              ZZ207860

      SUBROUTINE EXP1(A,N)
      IMPLICIT DOUBLE PRECISION (A-H,O-Z)
      IFLAG=1
C
C  CHECK IF NUMBER IS NEGATIVE
C
      IF(A.LT.0.0) IFLAG=-1
      A=ABS(A)
C
C  CHECK IF NUMBER IS LESS OR GREATER THAN 1.0
C
      IF(A.EQ.1.) GO TO 100
      IF(A.LT.1.0) GO TO 101
      N=0
   20  A=A/10.
      N=N+1
      IF(A.LT.1.) THEN
      A=A*FLOAT(IFLAG)
      A=A
      N=N
      RETURN
      ELSE
      GO TO 20
      ENDIF
  101  N=0
   30  A=A*10.
      N=N-1
      IF(A.GT.1.) THEN
      A=A*FLOAT(IFLAG)/10.
      N=N+1
      RETURN
      ELSE
      GO TO 30
      ENDIF
  100  N=1
      A=A*FLOAT(IFLAG)/10.
      RETURN
      END

      SUBROUTINE DETERM (A,N,DET,SUM1,SUM2)
      IMPLICIT DOUBLE PRECISION (A-H,O-Z)
      DIMENSION A(90,90)
    1 FORMAT (7(E13.6,3X))
      XXX=1.
      SIGN=1.
      LAST=N-1
C
C   START OVERALL LOOP FOR(N-1) PIVOTS
C
      DO 200 I=1,LAST
C
C   FIND THE LARGEST REMAINING TERM IN I-TH COLUMN FOR PIVOT
C
      BIG=0.
      DO 50 K=I,N
      TERM=DABS(A(K,I))
      IF (TERM-BIG)50,50,30
   30 BIG=TERM
      L=K
   50 CONTINUE
C
C   CHECK WHETHER A NON-ZERO TERM HAS BEEN FOUND
C
```

```
      IF (BIG)80,60,80
C
C     L-TH ROW HAS THE BIGGEST TERM---IS I=L
C
   80 IF (I-L)90,120,90
C
C     I IS NOT EQUAL TO L,SWITCH ROWS I AND L
   90 SIGN=-SIGN
      DO 100 J=1,N
      TEMP=A(I,J)
      A(I,J)=A(L,J)
  100 A(L,J)=TEMP
C
C     NOW START PIVOTAL REDUCTION
C
  120 PIVOT=A(I,I)
      NEXTR=I+1
C
C     FOR EACH OF THE ROWS AFTER THE I-TH
      DO 200 J=NEXTR,N
C
C     MULTIPLYING CONSTANT FOR THE J-TH ROW IS
C
      CONST=A(J,I)/PIVOT
C
C     NOW REDUCE EACH TERM OF THE J-TH ROW
C
      DO 200 K=I,N
  200 A(J,K)=A(J,K)-CONST*A(I,K)
C
C     END OF PIVOTAL REDUCTION---NOW COMPUTE DETERMINANT
      DET=SIGN
      ZZ=4444.
      IF(ZZ.GT.1) GO TO 61
      TOPL=1.D60
      BOTL=1./TOPL
      DO 300 I=1,1
      DET=DET*A(I,I)
      TEST=DABS(DET)
      IF (TEST.  GT. TOPL) GO TO 301
      IF (TEST.  LT. BOTL) GO TO 301
      IF(XXX.LT.0.) GO TO 301
      GO TO 300
  301 ZZ=0.
      WRITE(6,302) ZZ, ZZ  , DET
  302 FORMAT(' ',5X,F8.2,5X,F10.6,5X,D15.8)
      DET=1.
  300 CONTINUE
CC    WRITE(6,303) ZZ, ALMDS, DET, ZZ
  303 FORMAT(' ',5X,F8.2,5X,F10.6,5X,D15.8,5X,F8.2)
      GO TO 61
   60 DET=0.
      WRITE (6,1) DET
      GO TO 3002
   61 CONTINUE
      SUM1=1.
      SUM2=0.
      DO 3000 I=1,N
      XX=A(I,I)
      CALL EXP1(XX,M)
      SUM1=SUM1*XX
      SUM2=SUM2+FLOAT(M)
      YY=DABS(SUM1)
      IF(YY.GT.0.1) GO TO 3000
      SUM1=SUM1*10.
      SUM2=SUM2-1.
 3000 CONTINUE
      SUM1=SUM1*SIGN
```

```
3002  CONTINUE
      RETURN
      END

      SUBROUTINE DETR(A,N,X)
      IMPLICIT DOUBLE PRECISION (A-H,O-Z)
      DIMENSION A(45,45) ,X(46)
      SIGN=1.
      M=N-1
      LAST=M-1
C
C     START OVERALL LOOP FOR(N-1) PIVOTS
C
      DO 7 I=1,LAST
C
C     FIND THE LARGEST REMAINING TERM IN I-TH COLUMN FOR PIVOT
C
      BIG=0.
      DO 2 K=I,M
      TERM=DABS(A(K,I))
      IF(TERM-BIG)2,2,1
    1 BIG=TERM
      L=K
    2 CONTINUE
C
C     CHECK WHETHER A NON-ZERO TERM HAS BEEN FOUND
C
      IF(BIG)3,11,3
C
C     L-TH ROW HAS THE BIGEST TERM---IS I=L
C
    3 IF(I-L)4,6,4
C
C     I IS NOT EQUAL TO L, SWITCH ROWS I AND L
C
    4 DO 5 J=1,N
      TEMP=A(I,J)
      A(I,J)=A(L,J)
    5 A(L,J)=TEMP
C
C     NOW START PIVOTAL REDUCTION
C
    6 PIVOT=A(I,I)
      NEXTR=I+1
C
C     FOR EACH OF THE ROWS AFTER THE I-TH
C
      DO 7 J=NEXTR,M
C
C     MULTIPLYING CONSTANT FOR THE J-TH ROW IS:
C
      CONST=A(J,I)/PIVOT
C
C     NOW REDUCE EACH TERM OF THE J-TH ROW
C
      DO 7 K=I,N
    7 A(J,K)=A(J,K)-CONST*A(I,K)
C
C     END OF PIVOTAL REDUCTION-- PERFORM BACK SUBSTITUTION
C
      M=N-1
      DO 10 I=1,M
C
C     IREV IS THE BACKWARD INDEX,GOING FROM M BACK TO 1
C
      IREV=M+1-I
C
C     GET Y(IREV) IN PREPARATION
```

```
C
      Y=A(IREV,N)
      IF(IREV-M)8,10,8
C
C     NOT WORKING ON LAST ROW,I IS 2 OR GREATER
C
    8 DO 9 J=2,I
C
C     WORK BACKWARD FOR X(N),X(N-1)----SUBSTITUTING PREVIOUSLY
C     FOUND VALUES
C
      K=N+1-J
    9 Y=Y-A(IREV,K)*X(K)
C
C     FINALLY,COMPUTE X(IREV)
C
   10 X(IREV)=Y/A(IREV,IREV)
      X(N)=-1
   11 RETURN
      END

      SUBROUTINE SSS11(BM,A0,EMP,ENP,X1,X2)
      IMPLICIT DOUBLE PRECISION (A-H,O-Z)
      QLIM=240.
      BMS=BM*BM
      BM0=BM*A0
      EMMP=EMP-ENP
      EMPP=EMP+ENP
      EMMPS=EMMP*EMMP
      EMPPS=EMPP*EMPP
      IF(BM.GT.QLIM) GO TO 8
      IF(A0.NE.0.) GO TO 2
      X11=(BM*DCOS(EMMP)*DSINH(BM)+EMMP*DSIN(EMMP)*DCOSH(BM))/(BMS+EMMPS
     C)-(BM*DCOS(EMPP)*DSINH(BM)+EMPP*DSIN(EMPP)*DCOSH(BM))/(BMS+EMPPS)
      X22=(BM*(DCOS(EMMP)*DCOSH(BM)-1.)+EMMP*DSIN(EMMP)*DSINH(BM))/(BMS+
     CEMMPS)-(BM*(DCOS(EMPP)*DCOSH(BM)-1.)+EMPP*DSIN(EMPP)*DSINH(BM))/(B
     CMS+EMPPS)
      X1=-X22/(2.       )
      X2=X11/(2.        )
      GO TO 3
    2 X1=-(BM*DCOS(EMMP)-BM*DCOSH(BM))/(BMS+EMMPS)+(BM*DCOS(EMPP)-BM*
     1 DCOSH(BM))/(BMS+EMPPS)
      X1=X1/(2.         )
      X2=(EMMP*DSIN(EMMP)+BM*DSINH(BM))/(BMS+EMMPS)-(EMPP*DSIN(EMPP)+BM*
     1 DSINH(BM))/(BMS+EMPPS)
      X2=X2/(2.         )
      GO TO 3
    8 CONTINUE
      IF(A0.NE.0.) GO TO 9
      X2=-(BM*DCOS(EMMP)+EMMP*DSIN(EMMP))/(2.*(BMS+EMMPS))+(BM*
     1 DCOS(EMPP)+EMPP*DSIN(EMPP))/(2.*(BMS+EMPPS))
      X2=X2*DSINH(BM)
      X1=X2
      X2=-X2
      GO TO 3
    9 CONTINUE
      X1=(BM/2.)*(1./(BMS+EMMPS)-1./(BMS+EMPPS))
      X1=X1*DSINH(BM)
      X2=X1
    3 IF(A0.NE.0.)GOTO 1
      X1=-X1
    1 CONTINUE
      RETURN
      END
      SUBROUTINE SSS2(GM,A0,EMP,ENP,X1,X2)
      IMPLICIT DOUBLE PRECISION (A-H,O-Z)
      GM0=GM*A0
      CALL CSS(GM,EMP,ENP,X11)
```

```
      CALL SSS(GM,EMP,ENP,X22)
      X1=DSIN(GM0)*X11-DCOS(GM0)*X22
      X2=DCOS(GM0)*X11+DSIN(GM0)*X22
      IF(A0.NE.0.)GOTO 1
      X1=-X1
    1 CONTINUE
      X1=X1/DSIN(GM)
      X2=X2/DSIN(GM)
      RETURN
      END

      SUBROUTINE SCS11(BM,A0,EMP,ENP,X1,X2)
      IMPLICIT DOUBLE PRECISION (A-H,O-Z)
      QLIM=240.
      BMS=BM*BM
      BM0=BM*A0
      EMMP=EMP-ENP
      EMPP=EMP+ENP
      EMMPS=EMMP*EMMP
      EMPPS=EMPP*EMPP
      IF(BM.GT.QLIM) GO TO 8
      IF(A0.NE.0.) GO TO 2
      X11=(BM*DSIN(EMPP)*DSINH(BM)-EMPP*(DCOS(EMPP)*DCOSH(BM)-1.))/(BMS+
     CEMPPS)-(BM*DSIN(EMMP)*DSINH(BM)-EMMP*(DCOS(EMMP)*DCOSH(BM)-1.))/(B
     CMS+EMMPS)
      X22=(BM*DSIN(EMPP)*DCOSH(BM)-EMPP*DCOS(EMPP)*DSINH(BM))/(BMS+EMPPS
     C)-(BM*DSIN(EMMP)*DCOSH(BM)-EMMP*DCOS(EMMP)*DSINH(BM))/(BMS+EMMPS)
      X1=-X22/(2.)
      X2=X11/(2.)
      GO TO 3
    2 X1=-(BM*DSIN(EMPP)-EMPP*DSINH(BM))/(BMS+EMPPS)+(BM*DSIN(EMMP)-EMMP
     1 *DSINH(BM))/(BMS+EMMPS)
      X1=X1/(2.       )
      X2=-(EMPP*DCOS(EMPP)-EMPP*DCOSH(BM))/(BMS+EMPPS)+(EMMP*DCOS(EMMP)-
     1 EMMP*DCOSH(BM))/(BMS+EMMPS)
      X2=X2/(2.       )
      GO TO 3
    8 IF(A0.NE.0.) GO TO 9
      X1=-(BM*DSIN(EMPP)-EMPP*DCOS(EMPP))/(2.*(BMS+EMPPS))+(BM*
     1 DSIN(EMMP)-EMMP*DCOS(EMMP))/(2.*(BMS+EMMPS))
      X1=X1*DSINH(BM)
      X2=-X1
      GO TO 3
    9 X1=EMPP/(2.*(BMS+EMPPS))-EMMP/(2.*(BMS+EMMPS))
      X1=X1*DSINH(BM)
      X2=X1
    3 IF(A0.NE.0.)GOTO 1
      X1=-X1
    1 CONTINUE
      RETURN
      END
      SUBROUTINE SCS2(GM,A0,EMP,ENP,X1,X2)
      IMPLICIT DOUBLE PRECISION (A-H,O-Z)
      GM0=GM*A0
      CALL CCS(GM,EMP,ENP,X11)
      CALL CSS(EMP,GM,ENP,X22)
      X1=DSIN(GM0)*X11-DCOS(GM0)*X22
      X2=DCOS(GM0)*X11+DSIN(GM0)*X22
      X1=X1
      X2=X2
      IF(A0.NE.0.)GOTO 1
      X1=-X1
    1 CONTINUE
      RETURN
      END

SUBROUTINE SCC11(BM,A0,EMP,ENP,X1,X2)
      IMPLICIT DOUBLE PRECISION (A-H,O-Z)
```

```
      QLIM=240.
      BMS=BM*BM
      BM0=BM*A0
      EMMP=EMP-ENP
      EMPP=EMP+ENP
      EMMPS=EMMP*EMMP
      EMPPS=EMPP*EMPP
      IF(BM.GT.QLIM) GO TO 8
      IF(A0.EQ.0.) GO TO 2
      X1=-(BM*DCOS(EMMP)-BM*DCOSH(BM))/(BMS+EMMPS)+(BM*DCOSH(BM)-BM*
     1 DCOS(EMPP))/(BMS+EMPPS)
      X2=(BM*DSINH(BM)+EMMP*DSIN(EMMP))/(BMS+EMMPS)+(BM*DSINH(BM)+EMPP*
     1 DSIN(EMPP))/(BMS+EMPPS)
      X1= X1 /(2.       )
      X2=X2 /(2.       )
      GO TO 3
    2 X1=-(BM*(DCOS(EMMP)*DCOSH(BM)-1.)+EMMP*DSIN(EMMP)*DSINH(BM))/(BMS
     1 +EMMPS)-(BM*(DCOS(EMPP)*DCOSH(BM)-1.)+EMPP*DSIN(EMPP)*DSINH(BM))/
     1 (BMS+EMPPS)
      X1=X1/(2.       )
      X2=(BM*DCOS(EMMP)*DSINH(BM)+EMMP*DSIN(EMMP)*DCOSH(BM))/(BMS+EMMPS)
     1 +(BM*DCOS(EMPP)*DSINH(BM)+EMPP*DSIN(EMPP)*DCOSH(BM))/(BMS+EMPPS)
      X2=X2/(2.       )
      GO TO 3
    8 CONTINUE
      IF(A0.NE.0.) GO TO 9
      X1=-(BM*DCOS(EMMP)+EMMP*DSIN(EMMP))/(2.*(BMS+EMMPS))-(BM*
     1 DCOS(EMPP)+EMPP*DSIN(EMPP))/(2.*(BMS+EMPPS))
      X1=X1*DSINH(BM)
      X2=-X1
      GO TO 3
    9 CONTINUE
      X1=(BM/2.)*(1./(BMS+EMMPS)+1./(BMS+EMPPS))
      X2=X1*DSINH(BM)
    3 IF(A0.NE.0.)GOTO 1
      X1=-X1
    1 CONTINUE
      RETURN
      END
```